Variations of southeast Vatnajökull past, present and future

Hrafnhildur Hannesdóttir

Variations of southeast Vatnajökull past, present and future

Hrafnhildur Hannesdóttir

Dissertation submitted in partial fulfillment of a
Philosophiae Doctor degree in Geology

Advisors
Helgi Björnsson
Research Professor Emeritus, University of Iceland
Dr. Guðfinna Aðalgeirsdóttir

PhD Committee
Dr. Helgi Björnsson
Research Professor, University of Iceland

Dr. Guðfinna Aðalgeirsdóttir
Associate Professor at the Faculty of Earth Sciences
University of Iceland

Dr. Jón Eiríksson
Research Professor Emeritus, University of Iceland

Opponents
Dr. Per Holmlund
Department of Physical Geography and Quaternary Geology
Stockholm University

Dr. Astrid Ogilvie
Visiting Nansen Professor, University of Akureyri
Stefansson Arctic Institute, Akureyri
Fellow of the Institute of Arctic and Alpine Research (INSTAAR)

Faculty of Earth Sciences
School of Engineering and Natural Sciences
University of Iceland
Reykjavík, November 2014

Variations of southeast Vatnajökull- past, present and future
Dissertation submitted in partial fulfillment of a *Philosophiae Doctor* degree in Geology

Faculty of Earth Sciences
School of Engineering and Natural Sciences
University of Iceland
Sturlugata 7
101, Reykjavík
Iceland

Telephone: 525 4000

Bibliographic information:
Hrafnhildur Hannesdóttir, 2014, V*ariations of southeast Vatnajökull- past, present and future,* PhD dissertation, Faculty of Earth Sciences, University of Iceland, 197 pp.

ISBN 978-9935-9038-7-7
Printing: Háskólaprent
Reykjavík, Iceland, November 2014

Heinabergsjökull 24th of July 1902 (Archives of the National Survey of Iceland).

Abstract

The temperate outlet glaciers of SE-Vatnajökull are sensitive to climate change, and provide important climatic and glaciologic information through their recorded variations in mass balance and extent. They descend to the coast from an elevation of 1500–2100 m a.s.l., are located in one of the warmest and wettest area in Iceland and have among the highest mass turnover rates worldwide. The area was settled in the 9th century, and people have lived in close proximity to the glaciers, which has led to numerous contemporary written documents, also provided by the travelers and explorers of the 18th and 19th centuries. According to the unique local historical records, the outlet glaciers advanced in the latter half of the 17th century and extended far out on the lowlands in the mid-18th century. The glaciers were at their LIA terminal moraines around 1880–1890 and soon thereafter started retreating. The well-preserved glacial geomorphological features (including lateral moraines, trimlines and erratics) outlining the LIA maximum extent of the glaciers, have been mapped in this study. A reconstruction of the LIA glacier surface geometry was made, based on the geomorphological data, historical photographs, and information from the oldest reliable topographic maps of 1904. A LiDAR (laser scanning) digital elevation model (DEM) from 2010/2011 provided a reference topography for the reconstruction. From the elevation of the uppermost LIA lateral moraines, the equilibrium line altitude (ELA) was estimated to have been ~300 m lower during the LIA than around 2010. Various datasets on glacier extent and geometry since the end of the 19th century have been used to derive area and volume changes for the period 1890–2010. DEMs have been created from maps, aerial images, DGPS measurements and airborne surveys. In the period 1890–2010 the glacierized area shrunk by 164 km^2, the outlet glaciers lowered by 150–270 m near the terminus and collectively lost 60±8 km^3 of ice, equal to a global mean sea level rise of 0.15±0.02 mm. The bedrock topography of SE-Vatnajökull has previously been surveyed with radio echo sounding (RES) measurements, allowing relative volume change estimates, indicating that they have lost 15–50% of their LIA maximum volume. The geodetic mass balance has been estimated by subtracting the DEMs from each other. The most negative balance was observed between 2002 and 2010, when the glaciers lost on average –1.34±0.12 m w.e. a^{-1}, which is among the highest rates of mass loss worldwide in the early 21st century. The variable dynamic response of the glaciers to similar climate forcing is related to their

different hypsometry, bedrock topography, and the presence of proglacial lakes. The time series of area and volume changes of the entire post-LIA period created in this thesis provided an opportunity to evaluate the empirical volume-area scaling relation, indicating that ice volume may be underestimated by 50% if applying the commonly proposed constants of the power law. A vertically integrated Shallow Ice Approximation ice-flow model, coupled with a positive degree–day surface mass balance model, is used to simulate the evolution of the three outlet glaciers descending from the dome of Breiðabunga, constrained with the observed history of volume change. The degree–day model uses downscaled daily precipitation derived from an orographic precipitation model, that simulates well the observed pattern of winter mass balance variance. Simulations imply that the LIA maximum ice volume is reached with 1°C lower temperatures than the average of the 1980–2000 baseline period and a 20% decrease in annual precipitation, which is in line with meteorological data from nearby lowland stations. Applying a step change in temperature of +3°C, as predicted by some future scenarios will be reached by 2100, the model simulations indicate that the glaciers would loose 80–90% of their present volume.

Útdráttur

Gögn um jöklabreytingar á Íslandi eru mikilvægar vísbendingar um hnattrænar loftslagsbreytingar. Skriðjöklar í Austur-Skaftafellssýslu eru á einu hlýjasta og úrkomumesta svæði landsins, bregðast hratt við breytingum í afkomu og velta í búskap er með því mesta sem gerist á jörðinni. Stafræn kort af yfirborði og botni jöklanna, afkomumælingar og veðurgögn veita einstakt tækifæri til rannsókna á viðbrögðum jökla við loftslagsbreytingum. Hvergi hefur sambúð manns og jökuls verið eins náin og saga jöklabreytinga á fyrri öldum á þessu svæði er vel skráð. Skrif ferðalanga og fræðimanna sem lögðu leið sína um sveitirnar á 17., 18. og 19. öld, ásamt sýslu- og sóknalýsingum, veita innsýn í þær breytingar sem urðu á seinni hluta Litlu ísaldar, er jöklar tóku að ganga fram niður á láglendi. Samkvæmt samtímaheimildum lágu allflestir jöklar fram á fremstu öldum á árunum 1880–1890 og tóku að hörfa upp frá því. Vel varðveittar jökulmenjar (þ.m.t. jaðarurðir, grettistök, roflínur og strandlínur fyrrum jökulstíflaðra lóna) er vitna um mestu útbreiðslu þeirra á Litlu ísöld, hafa verið kortlagðar. Yfirborð skriðjöklanna í hámarksstöðu hefur verið endurgert samkvæmt hæð þessara ummerkja, sögulegum ljósmyndum, kortum frá 1904 ásamt upplýsingum úr skrifuðum heimildum. Háupplausnar LiDAR (leysigeisla) hæðarlíkan af yfirborði jöklanna og næsta nágrenni þeirra hefur notast sem grunnur fyrir endurgerðina. Jafnvægislína á Litlu ísöld hefur verið áætluð um 300 m lægri en nú á dögum út frá hæð efstu jaðarurða. Stafræn hæðarlíkön eru gerð út frá kortum, loftmyndum, GPS-sniðmælingum og fjarkönnunargögnum, svo sem LiDAR mælingunum. Út frá þeim eru flatarmáls- og rúmmálsbreytingar áætlaðar, ásamt meðalafkomu jöklanna á mismunandi tímabilum frá ~1890 til 2010. Flatarmál jöklanna hefur minnkað um 164 km^2, yfirborð þeirra lækkað um 150–270 m nálægt sporði og rýrnun allra samsvarar 60±8 km^3 af ís, en það jafngildir ~0,15±0,02 mm hækkun í heimshöfunum. Botn jöklanna hefur áður verið kortlagður með íssjármælingum og því er hægt að meta hlutfallslegt rúmmálstap jöklanna, en þeir hafa rýrnað um 15–50% síðan ~1890. Á árunum 2002–2010 var afkoman neikvæðust eða –1,34±0,12 m að vatnsgildi á ári, sem er með því mesta sem þekkist í heiminum í byrjun 21. aldar. Ólík viðbrögð jöklanna við svipuðum breytingum í afkomu er háð mismunandi flatarmálsdreifingu þeirra með hæð, botnlögun, og tilvist sporðalóna sem auka leysingu. Lagt er mat á reynslulögmál sem metur rúmmál út frá flatarmáli jökla með þeirri tímaröð flatarmáls- og rúmmálsbreytinga frá lokum Litlu ísaldar sem búin var til. Samanburðurinn gefur til kynna að ísrúmmál geti verið vanmetið um allt að

50% ef notaðir eru hefðbundnir stuðlar reynslulögmálsins. Saga þekktra jöklabreytinga er einnig notuð til þess að stilla af afkomu- og ísflæðilíkön sem lýsa viðbrögðum þriggja skriðjökla Breiðubungu við breytingum í veðurfari. Dreifð úrkoma er í fyrsta skipti notuð til þess að reikna afkomu fyrir íslenska jökla, en strjálar stikur á safnsvæði þessarra jökla hafa ekki lýst breytileika vetrarafkomunar nægilega vel, sem upphaflegt afkomulíkan var stillt af með. Til að herma rúmmál jöklanna við hámark Litlu ísaldar þurfti að lækka hita um 1°C og úrkomu um 20% miðað við viðmiðunartímabilið 1980–2000. Framtíðarspár um loftslagsbreytingar gera sumar hverjar ráð fyrir að hitastig muni hækka um 3°C fyrir lok 21. aldar. Ef líkanið er keyrt með þeirri hitastigsbreytingu myndi það leiða til þess að jöklarnir hyrfu nánast alveg, eða tapa 80–90% af rúmmáli sínu.

Preface

This PhD project has been carried out at the Institute of Earth Sciences, University of Iceland. Variations of the outlet glaciers of SE-Vatnajökull since ~1650–2010 are deduced from historical data, maps, in situ surface measurements and airborne data. The record of volume and area changes since the end of the 19th century are used to calibrate a mass balance-ice flow model, which is used to simulate the response of selected outlet glaciers to changes in temperature and precipitation. The results are presented in papers I–IV, which are published, in review or to be submitted.

Paper I
Hannesdóttir, H., Björnsson, H., Pálsson, F., Aðalgeirsdóttir, G., Guðmundsson, Sn. (2014). Variations of southeast Vatnajökull ice cap (Iceland) 1650-1900 and reconstruction of the glacier surface geometry at the Little Ice Age maximum. *Geografiska Annaler: Series A, Physical Geography. doi:10.1111/geoa.12064.*

Paper II

Guðmundsson, Sn., **Hannesdóttir, H**., Björnsson, H. (2012). Post-Little Ice Age (1891-2011 AD) volume loss of Kotárjökull glacier, SE-Iceland, as established from historical photography. *Jökull 62, 97-110.*

Paper III
Hannesdóttir, H., Björnsson, H., Pálsson, F., Aðalgeirsdóttir, G., and Guðmundsson, Sv. (2014). Area, volume and mass changes of SE-Vatnajökull ice cap, Iceland, from the Little Ice Age maximum in the late 19th century to 2010. *The Cryosphere Discussion 8, 1-55.doi:10.5194/tcd-8-1-2014.*

Paper IV
Hannesdóttir, H., Aðalgeirsdóttir, G., Jóhannesson, T., Guðmundsson, Sv., Crochet, P., Ágústsson, H., Pálsson, F., Magnússon, E., Sigurðsson, S.Þ., Björnsson, H. Mass balance modelling and simulation of the evolution of the outlets of SE-Vatnajökull ice cap, Iceland, using downscaled orographic precipitation. *To be submitted.*

Other related co-authored papers:

Aðalgeirsdóttir, G., Guðmundsson, S., Björnsson, H., Pálsson, F., Jóhannesson, T., **Hannesdóttir, H**., Sigurðsson, S.Þ., Berthier, E. (2011). Modelling the 20th and 21st century evolution of Hoffellsjökull glacier, SE-Vatnajökull, Iceland, *The Cryosphere, 5, 961-975. doi: 10.5194/tc-5-961-2011*.

Ágústsson, H., **Hannesdóttir, H**., Þorsteinsson, Þ., Pálsson, F., Oddsson, B. (2013). Mass balance of Mýrdalsjökull ice cap accumulation area and comparison of observed winter balance with simulated precipitation. *Jökull 63, 91-104.*

Table of Contents

List of Figures ..... **xii**
Abbreviations ..... **xiv**
Acknowledgements ..... **xv**
1 Introduction **1**
1.1 Background and previous work 2
1.2 Research aims 5
1.3 Study area 6

2 Data and Methods **9**
2.1 Historical data 9
2.2 LIA glacial geomorphological features and reconstruction of glacier surface geometry 10
2.3 Bedrock topography 11
2.4 Glacier outlines and surface DEMs 12
2.5 Mass balance data 14
2.6 Meteorological data and modelled precipitation 14
2.7 Glacier models 15

3 Summary of papers **17**
3.1 Paper I 17
3.2 Paper II 19
3.3 Paper III 20
3.4 Paper IV 23

4 General conclusions and outlook **26**
References **31**
Paper I **39**
Paper II **73**
Paper III **89**
Paper IV **147**

List of Figures

Figure 1. Iceland in the North Atlantic Ocean and modern ocean surface circulation patterns (on the left); NAC=North Atlantic Current, IC=Irminger Current, EGC=East Greenland Current, EIC=East Icelandic Current, modified from Knudsen et al.(2012). The bathymetric data is modified from the ETOPO1 data base of NOAA (NGDC), copyright: IMO. MODIS image of Iceland from the 9th of September 2009 (http://rapidfire.sci.gsfc.nasa. gov/ gallery/) showing the major ice caps in Iceland (on the right)................. 1

Figure 2. (a) Iceland and the largest ice caps in Iceland, Vatnajökull (V) on the SE-coast and the dark coloured area is the county of East-Skaftafellssýsla. (b) Vatnajökull, the boxes show the outline of c and d, Öræfajökull (Ö), Breiðabunga (B) and Goðahnjúkar (G). (c) The outlet glaciers descending from Öræfajökull ice cap and Morsárjökull and (d) the eastern outlet glaciers. The surface topography is from the 2010 LiDAR DEMs, with 100 m contour lines, and ice divides are delineated in black. Note the different scale of the two figures. Proglacial lakes and rivers are shown in blue and the main road in black. 6

Figure 3. SE-Iceland on the map of Abraham Ortelius from 1590 (on the left) and Björn Gunnlaugsson from 1844 (on the right), from http://islandskort.is... 9

Figure 4. Moraine fragments with a dense vegetation cover found outside the LIA terminal moraines of Skálafellsjökull (photo: Hrafnhildur Hannesdóttir). 11

Figure 5. LIA lateral moraines west of Skaftafellsjökull on the left (photo: Hrafnhildur Hannesdóttir). The forefield of Fláajökull on the right (photo: Snævarr Guðmundsson). 18

Figure 6. Rótarfjallshnúkur and the upper reaches of Kotárjökull by Howell (on the left) and a 3-D image from the 2010 LiDAR DEM of the same area (on the right). The crevassed areas (marked c1–c9) were used to calculate surface elevation changes in the accumulation area. 19

Figure 7. Surface lowering (in m) of the SE-outlet glaciers 1890-2010. Note the different scale on the two figures. 21

Figure 8. Geodetic mass balance of the SE-outlet glaciers during different time periods. 22

Figure 9. (a) Manually interpolated winter mass balance map showing the average of the time period 1996-2009 (b) and in 2010-2013 when the two stakes, Skf01 and Fl01, had been added to the mass balance network. The measurements of individual years are shown; 2010 (yellow), 2011 (turquoise), 2012 (white), 2013 (red). 23

Figure 10. Longitudinal profiles down the central flowline of Skálafellsjökull showing the thickness and location of the terminus at different times according to observations and at the end of various simulations. The white horizontal line indicates the elevation range of the ELA, derived from a set of MODIS images 2007-2011. 24

Figure 11. (a) The simulated LIA glacier geometry obtained with a step change in temperature equal to 1°C cooling and 20% decrease of annual precipitation, relative to the climate of the baseline period 1980-2000. (b) The glacier geometry at the end of a simulation forced with step change of +3°C and 10% increase in annual precipitation compared to the baseline period. 25

Abbreviations

AAR	Accumulation Area Ratio
CES	Climate and Energy Systems
CWE	Climate, Water and Energy
DEM	Digital Elevation Model
DGPS	Differential Global Positioning System
ELA	Equilibrium Line Altitude
GPS	Global Positioning System
IES	Institute of Earth Sciences
IMO	Icelandic Meteorological Office
LANDSAT	Land Remote Sensing Satellite
LIA	Little Ice Age
LiDAR	Light Detection and Ranging
MBT	Mass balance model for temperate glaciers
MODIS	Moderate Resolution Imaging Spectroradiometer
PDD	Positive Degree–Day
RES	Radio Echo Sounding
SIA	Shallow Ice Approximation
SPOT	Systéme Pour l´Observation de la Terre
SVALI	Stability and Variations of Arctic Land Ice
WRF	Weather Research and Forecasting
w.e.	Water Equivalent

Acknowledgements

Several people have provided invaluable support during my PhD studies. My supervisor Helgi Björnsson has been very supportive and patient, an excellent (and quick!) manuscript reviewer at every stage, and his doors always open for dicussions on glaciology as well as other important subjects. The strong support and guidance of my other supervisor, Guðfinna (Tollý) Aðalgeirsdóttir, has been important through the second half of this work, including critically reading manuscripts, providing help with the model codes and applying for extra funding. Both of them encouraged me and provided several opportunities to participate in international conferences and meetings. Two other members of the Glaciology Group of the University of Iceland served as very important co-supervisors, namely Finnur Pálsson and Sverrir Guðmundsson, guiding me through the hidden corridors of Surfer and Matlab and helping with several other problems. Eyjólfur Magnússon has also answered countless questions regarding the two programs. Tómas Jóhannesson at the Meteorological Office made the last part of the project possible, modifying the mass balance model, gave good comments on manuscripts, and assisted in several other ways. Stimulating discussions with Alexander Jarosch in the last year of the studies were encouraging in the final phase. This project would not have been possible without the comprehensive dataset of the Glaciology Group at the Institute of Earth Sciences, that has been gathered in the last few decades or the existing mass balance and ice flow models that have been used to predict future response of Icelandic glaciers to climate change. I acknowledge the help of Trausti Jónsson at the Icelandic Meteorological Office with the meteorological data, and Philippe Crochet and Hálfdán Ágústsson for downscaled precipitation data. I thank Jón Eiríksson for being part of the doctoral committee.

The help of the numerous people who accompanied me during fieldwork is highly appreciated, including Hálfdán Ágústsson, Sveinbjörn Steinþórsson, Rannveig Einarsdóttir, Jóhanna Katrín Þórhallsdóttir, Eiríkur Lárusson, Katrín Auðunardóttir, and Bergrún Arna Óladóttir. I thank the Icelandic Glaciological Society (JÖRFÍ), Vatnajökull National Park, Ágúst Hálfdánsson, Björn Oddsson, Þóra Karlsdóttir and Þorsteinn Jónsson for logistical support during fieldwork. I was privileged to get the opportunity to visit and discuss with the brothers of Kvísker (Sigurður, Helgi and Hálfdán) and explore their photo albums. Svavar Sigurjónsson is credited for access to his archives of scanned historical photographs from Austur-Skaftafellssýsla. Attending the summerschool in Karthaus and the Glaciology course at UNIS in 2008 provided opportunities to expand the professional network, get aquinted with students working on similar projects, including Jakob Abermann, Samuel Nussbaumer, and Anne Chapius. Being an associated graduate student of the SVALI Nordic Centre of Excellence has further helped to connect with enthusiastic glaciologists and geoscientists. The open online course *Writing in the Sciences* offered by Stanford University, provided excellent tools for writing manuscript for scientific journals and for construction of the thesis.

This work was funded by a doctoral grant of the Research Fund of the University of Iceland, the Icelandic Road Administration, the Fund of the Kvísker siblings, the University of Iceland´s Research Center in Hornafjörður, SVALI Nordic Centre of Excellence, the University of Iceland Research Fund and the Directorate of Labour. Working at the University of Iceland´s Research Centre in Hornafjörður in 2006–2007, facilitated organizing the fieldwork and I acknowledge the support of Þorvarður Árnason, the director of the Centre. I was fortunate to receive a grant from the European Science Foundation Student sponsorship to attend the IGS meeting in Chamonix in May 2014. The Institute of Earth Sciences is thanked for the office space (which they are running out of) and other facilities. This study has relied heavily on the recent LiDAR maps of the glaciers in Iceland that were funded by the Icelandic Research Fund, the Landsvirkjun (the National Power Company of Iceland) Research Fund, the Icelandic Road Administration, the Reykjavík Energy Environmental and Energy Research Fund, the Klima- og Luftgruppen (KoL) reseach fund of the Nordic Council of Ministers, the Vatnajökull National Park, the organisation Friends of Vatnajökull, the National Land Survey of Iceland and the Icelandic Meteorological Office.

I was lucky to move to the office on the hallway, away from the kitchen and toilet traffic on the north side in Askja, and join the excellent company of Þórdís Högnadóttir and Snævarr Guðmundsson (and the rest of the crew), keeping up the good spirit, going out for lunch and ice cream whenever needed. The company of fellow students and staff in Askja lightened up the day during lunch and coffee breaks in the last few years, including Björn Oddsson, Sædís, Amandine, Bergrún Arna, Erik Sturkell, Sófus, Olga Kolbrún, Ágúst Þór, Halldóra Björk, Sigga, Ásta Rut, Tobba, Jón Bjarni, Gro, Sigurlaug Hjaltadóttir, Esther Ruth, Eydís Salóme, Joachin, Þóra Árnadóttir … and many more. Magnús Tumi Guðmundsson has been supportive in various ways along the way.

I thank Guðfinna Ragnarsdóttir for introducing me to the fascinating world of Icelandic geology during my high-school studies. Participating in my first spring expedition to Vatnajökull in 2004 probably gave me the glacier sickness. It has been a life rewarding experience to get to know the people, who make those trips inspiring, successful and enjoyable, and be exposed to the vast nature of the ice cap and participate in the measurements and the variable scientific work. Hálfdán Ágústsson has been ready to assist with everything- always, including computer problems, providing meteorological data, taking care of the household and the boys, and being field assistant number 1. Thank you – thank you – THANK YOU. Although my two boys have kept me occupied with other things than writing the thesis, they have kept my mental health in good shape (most of the time…) – reminding me that there is life after office hours, and before. I am indebted to my parents for countless trips around the country, promoting the appreciation for Icelandic nature, and for their unmeasurable support in every possible way.

1 Introduction

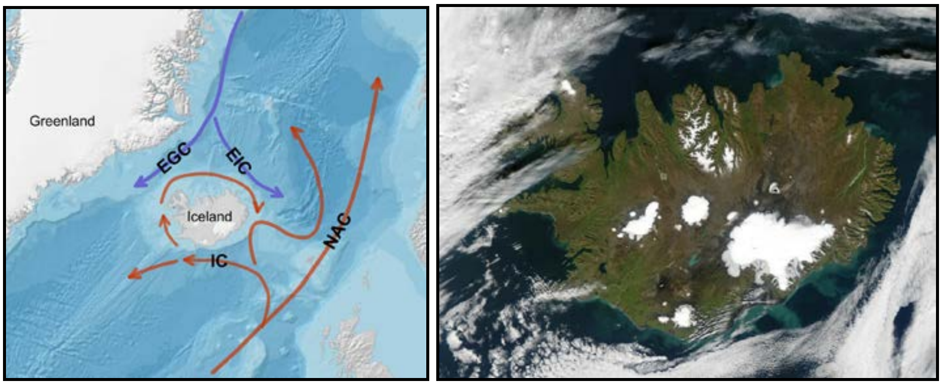

Figure 1. Iceland in the North Atlantic Ocean and modern ocean surface circulation patterns (on the left); NAC=North Atlantic Current, IC=Irminger Current, EGC=East Greenland Current, EIC=East Icelandic Current, modified from Knudsen et al.(2012). The bathymetric data is modified from the ETOPO1 data base of NOAA (NGDC), copyright: IMO. MODIS image of Iceland from the 9th of September 2009 (http://rapidfire.sci.gsfc.nasa.gov/ gallery/) showing the major ice caps in Iceland (on the right).

Iceland is located at major climatic boundaries in the North Atlantic Ocean, influenced by changes in the atmospheric circulation and warm and cold ocean surface currents (Fig. 1). The climate is relatively mild, with small seasonal variations in temperature, close to 0°C in winter and 11°C during summer in the lowlands (e.g. Einarsson, 1984; Ólafsson, *et al*., 2007). The temperate glaciers and ice caps cover ~11% of the country and have high mass turnover rates in the range of 1.5–3.0 m w.e. (water equivalent) a^{-1} (Björnsson *et al*., 2013). The mass balance sensitivity of Icelandic glaciers is among the highest worldwide (De Woul and Hock, 2005), and the glaciers provide important climatic information through variations in mass balance and extent. The highest rate of meltwater input to the North Atlantic Ocean, apart from Greenland, comes from the Icelandic glaciers, contributing ~0.03 mm a^{-1} to global sea level rise since the mid-1990s (Björnsson *et al*., 2013). The Little Ice Age (LIA) in Iceland was characterized by cold but variable climate, evidenced in the historical documents (Ogilvie and Jónsson, 2001 and references therein), marine (Knudsen *et al.*, 2012 and references therein) and lacustrine sedimentary records (Geirsdóttir *et al.*, 2009 and references therein) and widespread glacier advances (e.g. Sigurðsson, 2005). The high-resolution terrestrial records have dated the transition into the LIA to around 1250–1300 (Striberger *et al.*, 2010; Larsen *et al.*, 2011; Geirsdóttir *et al.*, 2013), which is in accordance with the written sources (Þórarinsson, 1960; Ogilvie, 2005). The majority of glaciers in Iceland reached their Holocene maximum extent either in the 18th or 19th century and some advanced during both periods (e.g. Þórarinsson, 1943; Guðmundsson, 1997; Evans, 1999; Sigurðsson, 2005; Kirkbride and Dugmore, 2008; Björnsson, 2009; Geirsdóttir *et al.*,2009; Larsen *et al.*,2011).

Vatnajökull (8100 km^2) is the largest ice cap in Europe by volume (3100 km^3), it rises 2100 m a.s.l. and the SE-outlet glaciers descend to sea level. The historical record of glacier variations during the latter part of the LIA and the detailed record of glacier changes, compiled in this study, is unique for studying the response of the glaciers to climate change. Data on the extent, and surface topography of the outlet glaciers of SE-Vatnajökull at various times, bedrock and meteorological data, are used in this work to study the relationship between glacier variations and climate forcing. Only a few quantitative estimates exist on areal and volume changes of the entire post-LIA time period for Icelandic glaciers (Aðalgeirsdóttir *et al.*, 2011; Pálsson *et al.*, 2012; Guðmundsson, 2014). The glacier inventory created in this thesis provides a basic dataset that is used to constrain a mass balance-ice flow model that simulates the response of three of the SE-outlet glaciers to climate.

1.1 Background and previous work

The outlet glaciers of SE-Vatnajökull flow down to the lowlands and have influenced the livelihood of the inhabitants of Austur-Skaftafellssýsla and nowhere in Iceland have people lived in such proximity to glaciers (Fig. 2). Due to the travels of the early explorers of the 18th and 19th centuries, the official county and parish descriptions, and the writings of Icelandic naturalists (Sveinn Pálsson, Eggert Ólafsson, Bjarni Pálsson, Þorvaldur Thoroddsen), considerable information on the oscillations of these glaciers during the latter part of the LIA is available. The historical records on the variations of the outlet glaciers of SE-Vatnajökull have been collected, analyzed and interpreted by Sigurður Þórarinsson (e.g. Þórarinsson 1939, 1943, 1964, 1974), by Guðmundur Bárðarson before him (Bárðarson, 1934), and by Flosi Björnsson the late farmer of Kvísker (Björnsson, 1956, 1993, 1996, 1998) to name a few. The LIA terminal moraines in the forefield of the SE-outlets of Vatnajökull have been mapped and dated to the 18th or 19th

century by lichenometry and a few by tephrochronology (e.g. Gordon and Sharp, 1983; Snorrason, 1984; Thompson and Jones, 1986; Thompson, 1988; Guðmundsson 1998; Evans *et al.*, 1999; Dabski, 2002; McKinzey *et al.*, 2004, 2005; Bradwell, 2004; Bradwell *et al*,. 2006; Chenet *et al.*, 2010), whereas Þórarinsson (1943) used the historical documents to infer about the maximum LIA stand of the glaciers.

The Swedish-Icelandic expedition on Hoffellsjökull and Heinabergsjökull in 1935–1938 carried out glaciological measurements, and was led by Hans W:son Ahlmann and Jón Eyþórsson, accompanied by Sigurður Þórarinsson and Carl Mannerfelt, who were students at Stockholm University at the time (Ahlmann and Þórarinsson, 1943). They measured ice flow, surface mass balance and surveyed the glacier surface topography. The main work was done on Hoffellsjökull, but for ablation measurements, the upper part of Heinabergsjökull was more accessible and not as dangerous as Hoffellsjökull, and gave comparable results. A relation between temperature measured at nearby meteorological stations outside the glaciers and the ablation was found. They observed fluctuations of the elevation of the firnline during the 3 year long survey period, ranging from 1000 m to 1200 m, and concluded that the glacier morphology (hypsometry, area distribution with altitude) would have the largest affect on the glacier regime. The lower mass balance values on the plateau were related to decreased orographic precipitation with elevation and snowdrift (Ahlmann and Þórarinsson, 1943). Their measurements are in line with modern surface mass balance values; winter balance in the accumulation area around 2 m water w.e. a^{-1}, and annual balance of –12 to –10 m w.e. a^{-1} at the terminus and even melting in the ablation area during winter (Ahlmann and Þórarinsson, 1943; Aðalgeirsdóttir *et al.*, 2011).

The glacier margins of some of the outlets of this study have previously been digitized from maps, as well as the contour lines of the glacier surface topograhy, but without correcting for horizontal distortion or estimating the vertical accuracy (Björnsson and Eydal, 1998). Due to the errors in the old trigonometric network for Iceland, the 1904 maps in particular, and the 1945 maps, are somewhat distorted horizontally. Initiated by Jón Eyþórsson in the early 1930s, regular monitoring of glacier frontal variations have been carried out by volunteers of the Icelandic Glaciological Society, providing annual records of advance and retreat (Eyþórsson, 1963; Sigurðsson *et al.*, 2007; http://spordakost.jorfi.is). Most glaciers retreated fast after the 1930s following the warm temperatures between 1930 and 1940, but glacier recession slowed down in the following decades, and some glaciers advanced in the time period 1970–1995 (Jóhannesson and Sigurðsson, 1998). After

1995, the climate warmed again and glacier retreat accelerated (Sigurðsson, 2005; Björnsson and Pálsson, 2008; Björnsson *et al*., 2013).

The scientific work carried out on Vatnajökull in the last few decades by the Glaciology Group at the Institute of Earth Sciences, University of Iceland, has provided the necessary framework for this thesis. The bedrock topography of Vatnajökull has been constructed from Differential Global Positioning System (DGPS) and radio echo sounding (RES) surveys in the last three decades (Björnsson, 1986, 1988, 2009; Björnsson and Pálsson, 2008; Magnússon *et al.*, 2012). Mass balance measurements have been carried out on Vatnajökull since 1991, with positive net mass balance during the first 3 years of measurements, and negative after 1995, showing considerable variation of the mean specific mass balance, ranging from –2.1 to –0.3 m w.e. a^{-1} (Björnsson *et al.*, 2013 and references therein). The concentration of observation sites is highest on the northern and western outlets of Vatnajökull, but a number of stakes are located on the southeastern outlets. The mass balance at the plateau of Öræfajökull ice cap (1700–2000 m a.s.l.) was measured in 1993–1998 (Guðmundsson, 2000). A number of automatic weather stations have been operating on Vatnajökull since 1994 (Björnsson *et al.*, 2005) and the observed weather parameters have been used to calculate the full energy balance (Guðmundsson *et al.*, 2009b). Furthermore, physical budget calculations of energy have been compared with empirical degree–day models describing melting (Guðmundsson *et al.*, 2009b). The average equilibrium line altitude (ELA) of SE-Vatnajökull has been estimated to be around 1100–1200 m, with considerable interannual variability, based on in situ mass balance measurements, satellite imagery and model simulations, (Björnsson, 1979; Aðalgeirsdóttir *et al.*, 2005, 2006; Björnsson and Pálsson, 2008; Aðalgeirsdóttir *et al.*, 2011).

Positive degree–day (PDD) mass balance models have been developed that describe the correlation between the balance and meteorological parameters and the energy budget (Jóhannesson, 1997; Jóhannesson *et al.*, 1995, 2007; Guðmundsson *et al.*, 2006, 2009a). Numerical ice flow models simulating the larger ice caps in Iceland have been developed in the last decade, modelling their response to changes in mass balance (Aðalgeirsdóttir *et al.*, 2003, 2005, 2006; Flowers *et al.*, 2005; Marshall *et al.*, 2005). Results of the spatially distributed coupled models of ice dynamics and hydrology, indicate that the SE-outlet glaciers are the most sensitive to future warming of all outlets of Vatnajökull (Flowers *et al.*, 2005). They are particularly vulnerable to warming climate conditions, since their beds lie below the elevation of the current terminus and they terminate in proglacial lakes (Björnsson and Pálsson, 2008). Simulations with a coupled mass balance-ice flow model reveal that southern Vatnajökull has a mass balance sensitivity in the range of

0.8–1.3 m w.e. a^{-1} $°C^{-1}$ (Aðalgeirsdóttir *et al.*, 2006). The simulations indicate that the southern part of Vatnajökull will disappear within the next 200 years according to future climate scenarios (Aðalgeirsdóttir *et al.*, 2006; Guðmundsson *et al.*, 2006; Jóhannesson *et al.*, 2007). The first simulation of a single outlet (Hoffellsjökull, Fig. 2) was carried out on a finer resolution than used in previous studies, for the whole post-LIA time period (Aðalgeirsdóttir *et al.*, 2011). The model successfully simulates the 20% volume loss of the glacier ~1890–2010, and after calibrating the model with past changes, the future response of the glacier 2000–2100 was modelled.

1.2 Research aims

The main objectives of this study were the following:

- To derive information on the variations of the outlet glaciers of SE-Vatnajökull from historical documents during the 16th to the 19th century, and explore other historical data, including maps, paintings, and photographs, that shed light on the ice extent of the outlets during the LIA and time the LIA maximum.

- To map the LIA maximum glacial geomorphological features along the glacier margin, including lateral and terminal moraines, trimlines, and glacier erratics, from measurements in the field and a selection of airborne images, in order to deduce surface elevation changes since the LIA maximum and reconstruct the glacier surface geometry at that time.

- To delineate the glacier margin from maps, aerial and satellite images, and create glacier surface DEMs, from contour lines of maps and DGPS surveys from various years since the early 20th century. To obtain area and volume change and the geodetic mass balance from this multi-temporal glacier inventory for the whole post-LIA period.

- To use the history of area and volume changes of three of the larger outlet glaciers of Breiðabunga to constrain a numerical mass balance-ice flow model, simulating the evolution of the outlets.

- To assess the sensitivity of the three outlets to changes in temperature and precipitation with the model, and simulate their response to possible climate scenarios.

1.3 Study area

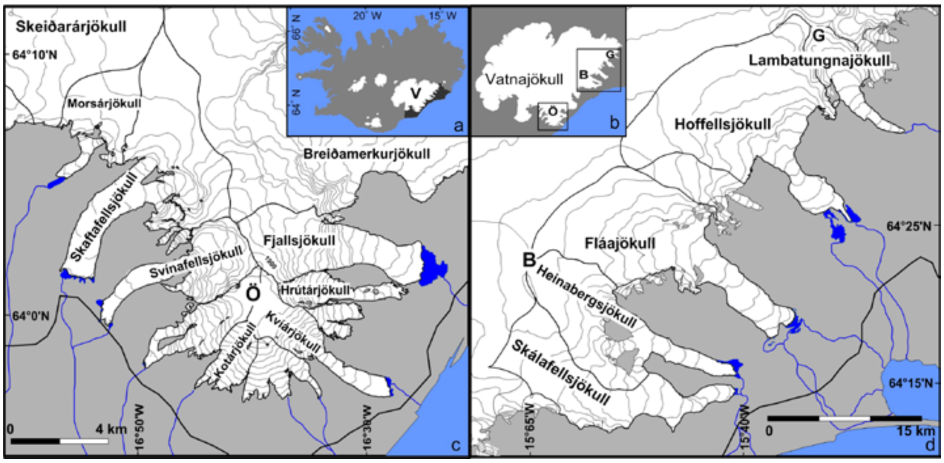

Figure 2. (a) Iceland and the largest ice caps in Iceland, Vatnajökull (V) on the SE-coast and the dark coloured area is the county of East-Skaftafellssýsla. (b) Vatnajökull, the boxes show the outline of c and d, Öræfajökull (Ö), Breiðabunga (B) and Goðahnjúkar (G). (c) The outlet glaciers descending from Öræfajökull ice cap and Morsárjökull and (d) the eastern outlet glaciers. The surface topography is from the 2010 LiDAR DEMs, with 100 m contour lines, and ice divides are delineated in black. Note the different scale of the two figures. Proglacial lakes and rivers are shown in blue and the main road in black.

The SE-outlet glaciers of Vatnajökull are located in one of the warmest and wettest area of Iceland. Seasonal variations in temperature on the south coast are small; the average winter temperature is around 0°C and average July temperature close to 11°C (Einarsson, 1984; Ólafsson *et al.*, 2007). The maritime climate is characterized by heavy winter precipitation in the range of 1000–2000 mm at the lowland meteorological stations. The ice cap receives high amounts of precipitation, due to the cyclonic westerlies crossing the North Atlantic. The outlets of SE-Vatnajökull analyzed in this study are non-surging glaciers, the distance between the westernmost and easternmost outlet is less than 100 km and most of them reach down to 20–100 m a.s.l. (Fig. 2). The glaciers vary in size from 10–200 km^2, range in thickness from 80 to 330 m, and have a variable area distribution with altitude (hypsometry). Morsárjökull, the westernmost outlet, flows down from an ice divide of 1350 m. Öræfajökull (2100 m a.s.l.) feeds several outlet glaciers: the eastern part of Skaftafellsjökull, Svínafellsjökull, Kotárjökull, Kvíárjökull, Hrútárjökull and Fjallsjökull. East of Breiðamerkurjökull, three outlet glaciers descend from the 1500 m high plateau of the Breiðabunga dome, Skálafellsjökull, Heinabergsjökull, and Fláajökull. Further east is Hoffellsjökull, and its accumulation area lies between Breiðabunga and Goðahnúkar (1500 m), which feeds Lambatungnajökull. The outlet glaciers east of Breiðamerkurjökull are referred to as the eastern outlet glaciers. The measurements of the bedrock topography of the outlet glaciers reveal that the outlets have carved into soft glacial and glaciofluvial sediments, forming depressions that are or will be occupied by ice-marginal lakes as a result of future warming (Björnsson, 2009; Magnússon *et al.*, 2012).

2 Data and Methods

2.1 Historical data

Figure 3. SE-Iceland on the map of Abraham Ortelius from 1590 (on the left) and Björn Gunnlaugsson from 1844 (on the right), from http://islandskort.is.

The historical sources providing information on the extent and variations of the outlet glaciers of SE-Vatnajökull used in this study include a) the official county (or sheriffs´ letters) and parish descriptions (1700–1900) and land registers since the early 18th century, b) travel diaries of Icelandic naturalists, c) descriptions of foreign travelers and, d) local accounts and oral tradition, which are all listed and cited in paper I. Interviews with old farmers living in the area were conducted in the summer of 2007, to collect local knowledge on glacier changes and gather historical photographs. A number of photographs are preserved from the last decade of the 19th century and the first years of the 20th century. The photographs taken by Frederick Howell in 1891 of a number of Öræfajökull´s outlet glaciers (Fiske Icelandic collection, Cornell University, http://cidc.library.cornell. edu/howell/; Ponzi, 2004) are the oldest known set of photographs of Icelandic glaciers. A number of photographs are preserved from the time of the surveys of the Danish General Staff in 1902–1904 (archives of the National Land Survey of Iceland, http://atlas.lmi.is/islandskort-dana/ljosmyndir.php). Historical maps as early as from the 16th century are preserved, but it is not until the 1830s and 1840s with the the maps of Björn Gunnlaugsson, that reliable information on the glacial extent can be extracted (Fig. 3). Mountains enclosed in ice by merging outlets can be observed on his maps, but terminus position and glacier margins can only be determined with certainty from the Danish General Staff maps of 1904.

2.2 LIA glacial geomorphological features and reconstruction of glacier surface geometry

Extensive field mapping of the well-preserved glacial geomorphological features, including lateral and terminal moraines, trimlines, glacier erratics, and shorelines of former ice-dammed lakes, which delineate the LIA maximum extent of the outlet glaciers of SE-Vatnajökull, was carried out. The field surveys were carried out in the summers of 2007 and 2008 during several excursions, altogether approximately 50 days. A laser rangefinder (Laser Technology TruPulse 200 Laser Rangefinders 7005030), with accuracy of 0.3 m, was used to target lateral moraines and erratics in unreachable areas. The fieldwork was confined to the ablation area of the glaciers, since lateral moraines are only deposited below the ELA where glaciers transport ice and rocks to the surface (e.g. Paterson, 1994). The field sites were usually reached from the termini, however snowscooters were also used to access some of the high-elevation sites of Lambatungnajökull and Fláajökull. During traverses of the glaciers (on snowscooter and on foot), the elevation was registered with a GPS instrument. The LIA terminal moraines and highest lateral moraines are assumed to be contemporaneous due to the lack of plausible dating methods, although lateral moraines may be formed by repeated glacier advances.

Airborne imagery was also used to map the glacial geomorphological features, including oblique aerial photographs taken from airplanes, aerial photographs of the National Land Survey of Iceland, SPOT5 satellite images and the high-resolution images of Loftmyndir ehf. The extent of the outlet glaciers at the LIA maximum was also assessed from the historical photographs and written documents. The reconstruction of the LIA maximum glacier surface geometry was based on the glacial geomorphological features, historical photographs, the elevation of trigonometrical points on maps from 1904, and 2010 LiDAR DEMs used as reference topography. Nunataks depicted on the historical photographs from the turn of the 19th century were compared with duplicate modern photographs to estimate changes of the glacier surface in the accumulation areas, where geomorphological evidence is sparse. The crests of the LIA lateral moraines were used to determine the previous glacier surface level at their maximum extent. Convex contour lines were drawn by hand from the elevation of the geomorphological features. The surface profiles and final ice volume of the reconstructed LIA glaciers were compared to two different models; a simple glacier model by Benn and Hulton (2010), which provides estimates of the surface profile of former glaciers using a solution for ‘perfectly plastic’ ice, and the results from the mass balance-ice flow model used in this study to simulate the three outlets of Breiðabunga.

Moraine remnants are found in a few locations, some tens of metres outside the LIA limit of the glaciers. Stóralda moraine in front of Svínafellsjökull is one of them, which has been dated to be approximately 2500 years old (Þórarinsson, 1964). Furthermore, tens of m outside the LIA moraines of Fjallsjökull and Kvíárjökull are older moraines with dense vegetation cover (Björnsson, 1998). During fieldwork, a moraine was found in front of Skálafellsjökull´s LIA terminal moraines (Fig. 4). This illustrates that some of the glaciers had reached similar positions previous to the LIA.

Figure 4. Moraine fragments with a dense vegetation cover found outside the LIA terminal moraines of Skálafellsjökull (photo: Hrafnhildur Hannesdóttir).

2.3 Bedrock topography

The bedrock topography of the outlet glaciers has been derived from RES measurements and DGPS in the last two decades (Björnsson and Pálsson, 2004; Magnússon *et al.*, 2007; Björnsson and Pálsson, 2008; Björnsson, 2009; Magnússon *et al.*, 2012, data base of the Glaciology Group of the Institute of Earth Sciences, University of Iceland). Point measurements have been carried out in the ablation area, whereas continuous profiles surveyed in the accumulation area. The vertical accuracy of the bedrock measurements is 5–20 m, depending on location. Some of the glaciers have eroded their bed 100–300 m below sea level. From the bedrock DEM, the relative ice volume changes are estimated.

2.4 Glacier outlines and surface DEMs

The areal extent and the surface topography of the outlet glaciers at different times during the period 1890–2010, were derived from various datasets of variable horizontal and vertical accuracy. The most accurate DEMs of SE-Vatnajökull were produced with airborne LiDAR technology in late August–September 2010 and 2011 (Jóhannesson et al., 2013; Icelandic Meteorological Office and Institute of Earth Sciences, University of Iceland, 2013). The high-resolution DEMs are 5 m × 5 m in pixel size with a < 0.5 m vertical and horizontal accuracy (Jóhannesson et al., 2013). The LiDAR DEMs provide a reference topography, used for improving other glacier surface DEMs, for example in areas where corrections of contour lines on old paper maps have been necessary.

The glacier margins were digitized from maps and aerial and satellite images at various times for different glaciers (Table 1), including maps from 1904, 1945 and 1989 (Danish General Staff, 1904; Army Map Service, 1950–1951; Defense Mapping Agency, 1997), the aerial photographs of the National Land Survey from 1945, 1946, 1960, 1982, 1989, Landsat satelite images of 2000, aerial images of Loftmyndir ehf from 2002, and shaded relief images of the 2010 LiDAR DEMs. The glacier margin on the maps was revised by analyzing the original aerial images (on which the maps are based), since often snow-covered areas have been mis-interpreted as glacial ice, and shadows on the glacier surface as bedrock. Glacier surface DEMs are created from contour lines of the paper maps, which are corrected in the accumulation area by analyzing the size of nunataks (method that has been deployed elsewhere, e.g. Berthier *et al.*, 2009). A 20 m × 20 m DEM of Loftmyndir ehf. is available of parts of the outlets of Öræfajökull, excluding most of their accumulation areas. DGPS surface elevation measurements have been carried out during repeated mass balance surveys and RES profiling in spring during the time period 2000–2003, and are used for DEM construction. Area and volume changes of Hoffellsjökull since the end of the LIA have previously been determined (Björnsson and Pálsson, 2004).

Table 1. Data used to obtain glacier outlines and to construct glacier surface DEMs. NLS = National Land Survey of Iceland, IMO = Icelandic Meteorological Office, IES = Institute of Earth Sciences.

airborne imagery	**time period/details**	**reference/photographer**
Aerial images	2002-2004	Loftmyndir ehf (www.loftmyndir.is)
Oblique photographs	2000-2012	Helgi Björnss, Snævarr Guðmundss, Víðir Reyniss
Aerial photographs	1945, ´60, ´82, ´89	NLS (www.lmi.is/loftmyndasafn)
SPOT5	2005	SPOT5 (SpotImage©)
Landsat	2000	http://landsat.usgs.gov
MODIS	2007-2011	http://rapidfire.sci.gsfc.nasa.gov/gallery/
LiDAR	2010-2011	IMO and IES
maps		
Danish General Staff-sheets:	1904	Danish General Staff, 1904
87 SA Öræfajökull	Öræfajökull and the upper part of acc. area of Skaftafellsj. and Svínafellsj.	
87 SV Öræfajökull	The lower ablatoin area of Morsárj., Skaftafellsj. and Svínafellsj.	
87 NV Öræfajökull	Morsárjökull and part of the upper accumulation area of Skaftafellsjökull	
96 NA Heinaberg	Part of abl. area of Skálafellsj. and Heinabergsj., Fláaj., snout of Hoffellsj.	
97 NA Kálfafellsstaður	Sultartungnajökull, outlet of Skálafellsjökull	
97 NV Kálfafellsstaður	Part of the western rim of Skálafellsjökull	
AMS (Series C762)-sheets:	1945	Army Map Service, 1950-1951
6018-I	Kvísker	
6018-IV	Svínafell	
6019-I	Veðurárdalsfjöll	
6019-II	Breiðamerkurjökull	
6019-III	Öræfajökull	
6019-IV	Esjufjöll	
6020-I	Vatnajökull I	
6020-II	Vatnajökull II	
6020-III	Vatnajökull III	
6119-IV	Kálfafellsstaður	
6120-I	Lambatungnajökull	
6120-II	Hoffell	
6120-III	Hoffellsjökull syðri	
DMA (Series C761)-sheets:	1989	Defense Mapping Agency, 1997
2213-I	Hornafjörður	
2213-III	Hestgerðislón	
2213-IV	Heinabergsjökull	
2214-II	Kollumúli	
2214-III	Eyjabakkajökull	
DGPS surveys	2000-2005	IES data base

2.5 Mass balance data

Mass balance measurements have been carried out on the studied glaciers and their neighbouring outlets since 1991 (Björnsson and Pálsson, 2008). Stakes are measured on a profile from the terminus up to the ice divide of Breiðamerkurjökull, three stakes on Hoffellsjökull, and a few survey sites are located in the accumulation area of the studied glaciers. Two new stakes in the accumulation area of Skálafellsjökull and Fláajökull were added to the mass balance survey network in 2009, as deemed necessary by the preliminary results of the model simulations from the current study. Cores are drilled through the winter snow layer using an engine driven drill in spring (April–May), and the density measured to calculate the water equivalent of the layer. Visual inspection of the dust content as well as observations of the coarseness of the snow grains is used to identify the previous year´s summer surface, i.e. to determine the thickness of the winter layer. Stakes or wires are left in the core holes or drilled into the ice in the ablation zone with a steam drill. The summer balance is measured from the extension of the stakes or wires in the spring and late autumn (September–October; Björnsson *et al.*, 1998, 2002). Manually interpolated digital mass balance maps are generated for every year since 1996, using the in situ mass balance measurements and the observed mass balance gradient (see e.g. Björnsson *et al.*, 2002 for details).

2.6 Meteorological data and modelled precipitation

Temperature and precipitation records are available from two lowland stations, Fagurhólsmýri (16 m a.s.l., 8 km south of Öræfajökull) and Hólar in Hornafjörður (16 m a.s.l., 15 km south of Hoffellsjökull). The temperature record at Hólar is available for the period 1884–1890 and since 1921, whereas the precipitation measurements started in 1931. The temperature record from Fagurhólsmýri goes back to 1898, and precipitation has been measured since 1921 until 2008. Precipitation data is available from two different models, and used in the PDD mass balance modelling. Dynamically downscaled precipitation in Iceland is available from the RÁV dataset (Rögnvaldsson *et al.*, 2011), from the non-hydrostatic mesoscale Weather Research Forecasting (WRF) model (Skamarock *et al.*, 2008), on a 3 km grid since 1995 and 9 km resolution from 1958. A linear theory (LT) model of orographic precipitation (Smith, 2003), which includes airflow dynamics, condensed water advection, and downslope evaporation provides downscaled precipitation on a 1 km grid for the time period 1959–2010 (Crochet *et al.*, 2007, 2013; Jóhannesson *et al.*, 2007).

2.7 Glacier models

The mass balance of Skálafellsjökull, Heinabergsjökull and Fláajökull is simulated with a PDD model, that has been applied on Icelandic ice caps and glaciers (Jóhannesson, 1997; Jóhannesson *et al.*, 1995, 2006) and also coupled with an ice flow model in previous studies (Aðalgeirsdóttir 2003; Aðalgeirsdóttir *et al.*, 2006, 2011; Guðmundsson *et al*., 2009a). Precipitation on the glacier is assumed to fall as snow, if the temperature at the altitude in question is below 1°C (Jóhannesson, 1997). Melting of snow and ice is computed from the number of PDD, and the degree–day factors determine the amount of melting per PDD (Jóhannesson, 1997). Degree–day factors are different for snow and ice, because snow and ice require different amounts of energy to melt; ice is less reflective than snow, has a higher density, and so melts more per PDD. The ice flow model is based on the Shallow Ice Approximation (SIA) and vertically integrated continuity equation (Aðalgeirsdóttir *et al.*, 2004, 2006). The finite element method with triangular elements is used to solve the continuity equation (Aðalgeirsdóttir *et al.*, 2011). Different versions of the mass balance model are applied in this study. Until this study, constant vertical and horizontal precipitation gradients have been used in the mass balance model, but they do not take into account the locally complex spatial structure of the precipitation field on these glaciers. To account for that, downscaled orographic precipitation on a 1 km × 1 km grid is used as input.

3 Summary of papers

3.1 Paper I

***Hannesdóttir, H.**, Björnsson, H., Pálsson, F., Aðalgeirsdóttir, G., and Guðmundsson, Sn. (2014). Variations of SE-Vatnajökull ice cap (Iceland) 1650-1900 and reconstruction of the glacier surface geometry at the Little Ice Age maximum. Geografiska Annaler: Series A, Physical Geography. doi:10.1111/geoa.12064.*

In this paper the written accounts from the county of Austur-Skaftafellssýsla, that shed light on the variations of the outlet glaciers of SE-Vatnajökull ice cap during the time period 1650–1900, are analyzed. According to these sources, all glaciers advanced in the latter half of the 17th century and extended far out on the lowlands in the mid-18th century. From the contemporary documents it is clear that the outlet glaciers were at the terminal LIA moraines around ~1880–1890 and soon after started receding, marking the end of the LIA in Iceland. Descriptions from the 17th and 18th century do not provide the same accurate and decisive data on the terminus position as from the late 19th century, thus it can not be excluded that the glaciers had reached a similar advanced position earlier. According to lichenometric studies, the glaciers reached their LIA maximum in the late 18th or 19th century (e.g. Evans *et al.*,1999; Dabski, 2002; Bradwell, 2004; McKinzey *et al.*, 2005; Chenet *et al.*, 2010). However, due to diverse bedrock minerology and the microclimate of each valley causing variable growing conditions for the lichens, various calibration curves, different statistical analysis and field techniques, intercomparison of lichenometric dates of moraines is problematic. The importance of using the historical documents to infer glacier fluctuations is emphasized in this paper. The historical photographs of Frederick Howell in 1891 of a number of Öræfajökull´s outlet glaciers, and the photographs from the time of the surveys of the Danish General Staff in 1902–1904 provide additional evidence of the extent of the glaciers at the end of the 19th and beginning of the 20th century. The mass balance of Icelandic glaciers is governed by variations in the summer ablation (which is related to air temperature, representing variations in the incoming radiation flux), rather than winter accumulation (Björnsson *et al.*, 2013 and references therein). The long continuous temperature record from Stykkishólmur starting in 1798 (Wood *et al.*, 2010), which correlatates well with local temperature records, shows that summer temperatures started to decline ~1850, and reached a minimum around 1890. Assuming that the response time of the outlets of SE-Vatnajökull is in the range of 20–40 years, as estimated by a function of the glacier thickness and ablation at the terminus (Jóhannesson *et al.*, 1989), a late 19th century LIA maximum is more likely for the outlets, opposed to a late 18th century or early 19th century, as some lichenometric dates indicate.

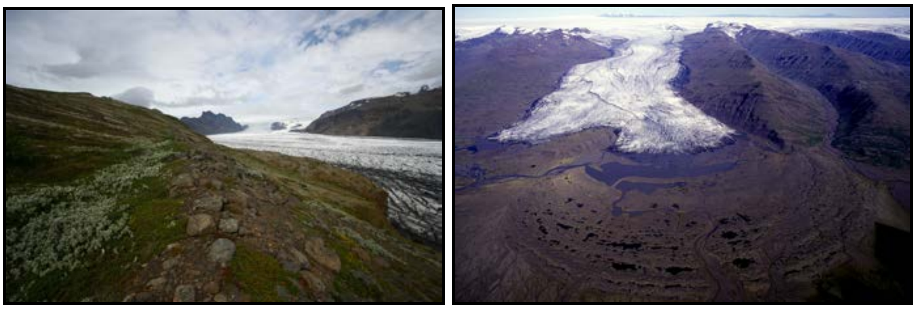

Figure 5. LIA lateral moraines west of Skaftafellsjökull in Skaftafellsheiði on the left (photo: Hrafnhildur Hannesdóttir). Fláajökull and the moraines in the forefield on the right (photo: Snævarr Guðmundsson).

Glacial geomorphological features, including lateral and terminal moraines (Fig. 5), trimlines, glacier erratics, and shorelines of former ice-dammed lakes, outlining the LIA maximum extent of SE-Vatnajökull´s outlet glaciers are well preserved and were mapped in this study. The historical (documents and photographs) and glacial geomorphological data have been combined to reconstruct the glacier surface geometry at the LIA maximum, along with information from the first reliable maps from 1904 (Danish General Staff, 1904). The LiDAR DEMs, served as a topographic reference, for example providing accurate elevation of the suite of LIA glacial geomorphological features. Quantitative estimates of the glacial extent and volume of the outlet glaciers of SE-Vatnajökull at the LIA maximum were derived. These new assessments of the ice volume and areal extent provide important information for constraining mass balance ice-flow models and global sea level rise estimates. A comparison between the altitude of the uppermost up-valley LIA lateral moraines, and the average modern snowline elevation (derived from MODIS images), both used as a proxy for the ELA, reveal an elevation difference of ~340 m of the ELA. This is in line with the estimate of Eyþórsson (1951) and Þórarinsson (1974), that the snowline of southern Vatnajökull was around 300 m lower during the LIA than during the warm decades of the mid-20th century, with average summer temperature close to the average of the period 2000–2010.

I collected and analyzed the written documents, carried out the fieldwork, and mapped the LIA glacial geomorphological features. Oblique aerial photographs were provided by Helgi Björnsson, Snævarr Guðmundsson and Víðir Reynisson. The method of reconstructing the glacier surface geometry was developed through discussions with Finnur Pálsson and Snævarr Guðmundsson. I wrote the manuscript with input from the coauthors.

3.2 Paper II

Guðmundsson, Sn., ***Hannesdóttir, H****., and Björnsson, H. (2012). Post-Little Ice Age volume loss of Kotárjökull glacier, SE-Iceland, derived from historical photography. Jökull, 62, 97–110.*

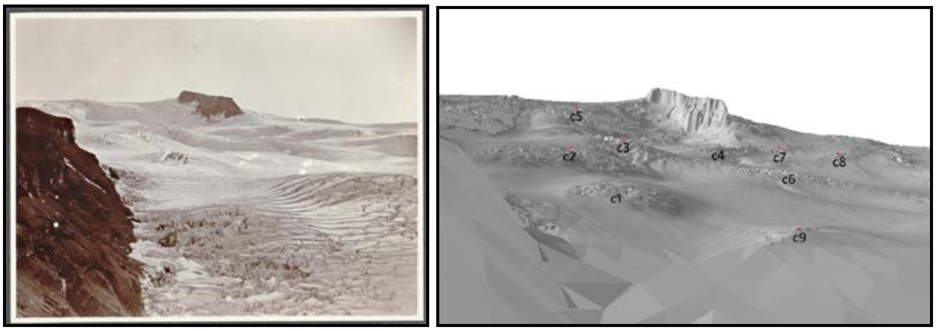

Figure 6. Rótarfjallshnúkur and the upper reaches of Kotárjökull by Howell (on the left) and a 3-D image from the 2011 LiDAR DEM of the same area (on the right). The crevassed areas (marked c1–c9) were used to calculate surface elevation changes in the accumulation area.

In this paper quantitative estimates of glacier mass change over the last 120 years of one of the smaller outlets of Öræfajökull ice cap are presented. By applying repeat photographical methods and trigonometric calculations, the glacier surface elevation changes were estimated from the unique historical oblique photographs of Kotárjökull from 1891 taken by Frederick Howell, along with modern duplicates, with topographical information from the LiDAR DEM (Fig. 6). The 11.5 km^2 outlet glacier descends from an elevation of 1800 m a.s.l., with an average slope of 20°. Surface changes 1891–2011 above 1700 m were negligible, but the surface lowering gradually increases and reaches a maximum of 180 m near the terminus in the gorge. The observed minimal surface lowering at high altitudes is supported by a comparison of the elevation of trigonometric survey points on Öræfajökull's plateau from the Danish General Staff map of 1904 and the 2011 LiDAR DEM. Nowhere else along the edge of SE-Vatnajökull, or in Iceland, are glacier surface elevation changes since the LIA maximum recorded continuously downward from the ice divide to the terminus. This dataset provides a reference for further studies of other outlet glaciers of Öræfajökull and SE-Vatnajökull.

Glacial geomorphological features delineating the maximum LIA glacier extent were mapped in the field and from high-resolution aerial images and oblique aerial photographs. The well-preserved lateral moraines are only found below the ELA, hence little field evidence attests to the former high stands of the glacier in the accumulation area at its maximum extent during the LIA. The historical oblique photographs are the only archive for surface changes in the accumulation area. A reconstruction of the glacier surface geometry is based on the photographic pairs, the geomorphological evidence and the LiDAR DEM. From the two glacier surface DEMs the ice volume and mass loss in the post-LIA period was calculated. The glacier lost 2.7 km^2, and experienced a volume loss of 0.4 km^3 equal to a geodetic mass balance of –0.22 m w.e. a^{-1}. The volume loss was however corrected to 0.5 km^3 in Guðmundsson (2014), which equals a mass balance of –0.23 m w.e. a^{-1}, and the relative mass loss since ~1890 is thus 36%.

This paper was a joint effort of Snævarr Guðmundsson and myself. Snævarr Guðmundsson made the duplicate photographs, by revisiting the two photographic locations of Frederick Howell, west of Kotárjökull. I georeferenced the 1904 map of the Danish General Staff with the LiDAR DEM to resolve possible glacier surface changes on the Öræfajökull plateau. We wrote the manuscript together, with input from Helgi Björnsson.

3.3 Paper III

Hannesdóttir, H*., Björnsson, H., Pálsson, F., Aðalgeirsdóttir, G., and Guðmundsson, Sv. (2014). Area, volume and mass changes of SE-Vatnajökull ice cap, Iceland, from the Little Ice Age maximum in the late 19th century to 2010. The Cryosphere Discussion 8, 1-55.doi:10.5194/tcd-8-1-2014.*

A series of glacier outlines and surface DEMs of the outlets of SE-Vatnajökull from various sources for the time period ~1890-2010 was compiled. The glacier outlines were delineated from maps, aerial and satellite images, and the DEMs compiled from glacial geomorphological features and historical photographs (from paper I), old maps, aerial images, DGPS and a LiDAR survey. From the multi-temporal glacier inventory, area and volume changes are derived, as well as the mass balance history by geodetic methods. From the known bedrock topography, the relative volume changes since the end of the LIA ~1890 were estimated. The glaciated area decreased by 164 km^2 in 1890–2010, and individual glaciers lost 10-30% of their ~1890 area. The glaciers lowered by 150–270 m near the terminus (Fig. 7) and collectively lost 60±8 km^3, which is equivalent to 0.15±0.02 mm of mean global sea level rise. The ice volume loss equals the estimated loss of Langjökull and Breiðamerkurjökull during the same time interval (Pálsson *et al.*, 2012; Guðmundsson, 2014). The volume loss of individual outlets of SE-Vatnajökull was in the range of 15–50% during this time period, corresponding to an average mass balance between –0.70 and –0.32 m w.e. a^{-1}. The most negative mass balance is observed in 2002–2010, when the rate of mass loss was in the range of –2.60±0.12 to –0.80±0.12 m w.e. a^{-1} for individual glaciers (Fig. 8), or on average –1.34±0.12 m w.e. a^{-1}, which is among the most negative mass balance recorded worldwide in the early 21st century (Vaughan *et al.*, 2013). The geodetic mass balance 2002–2010 is in line with the in situ measured mass balance on Breiðamerkurjökull and Hoffellsjökull.

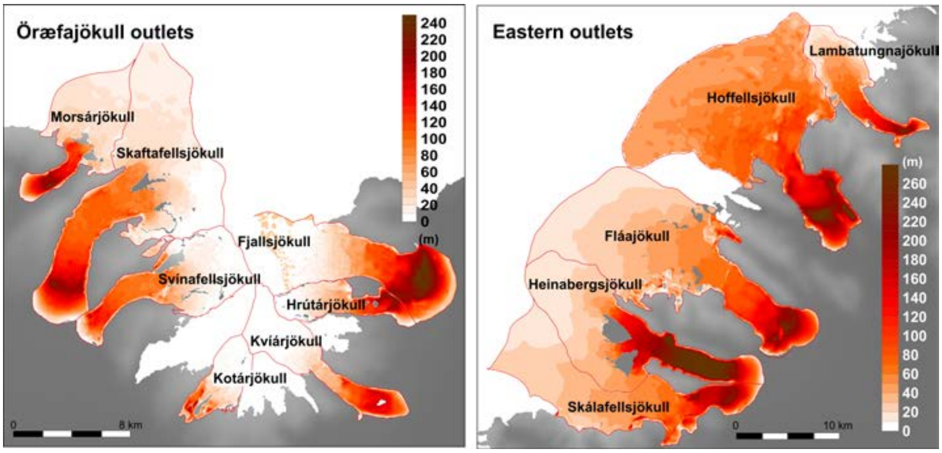

Figure 7. Surface lowering (in m) of the SE-outlet glaciers 1890-2010. Note the different scale on the two figures.

The variable dynamic response of the glaciers to the same climate forcing (changes in mass balance) is related to their different hypsometry, bedrock topography, and the presence of proglacial lakes. Their different response underlines the importance of a large sample of glaciers when interpreting the climate signal, and shows that frontal variations and aera changes only provide limited information, as some glaciers experience considerable surface lowering but little retreat.

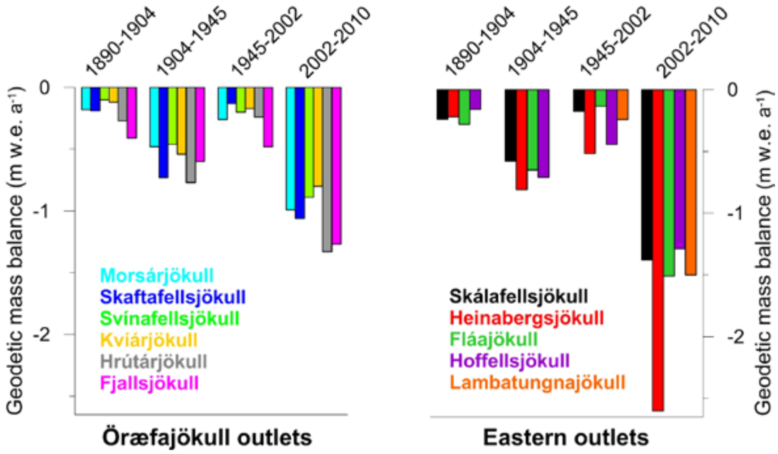

Figure 8. Geodetic mass balance of the SE-outlet glaciers during different time periods.

The scaling parameters of a power-law relationship of volume-area are evaluated from our glacier inventory, which spans the entire 120 year post-LIA period. Comparison of the ice volume calculated according to the commonly proposed constants of Bahr *et al.* (1997) and more recently coefficients derived in a modelling study by Adhikari and Marshall (2012), with our volume estimates, reveals an underestimate of the ice volume up to 50% when applying the power-law. The variable hypsometry, shape, size, and thickness of the outlets of SE-Vatnajökull, indicate that the constants of the power-law relating glacier volume and area need to be adjusted to the different glaciological parameters.

I digitized the glacier margin from maps and aerial images, constructed DEMs from the contour lines of the paper maps and the DGPS surveys. The glacier margin and contour lines of the DMA 1989 maps had previously been digitized by Finnur Pálsson and Þórdís Högnadóttir, however, the glacier surface geometry was reassessed in the accumulation area for those DEMs. I wrote the manuscript with input from the coauthors.

3.4 Paper IV

Hannesdóttir, H*., Aðalgeirsdóttir, G., Jóhannesson, T., Guðmundsson, Sv., Crochet, P., Ágústsson, H., Pálsson, F., Magnússon, E., Sigurðsson, S.Þ., Björnsson, H. Mass balance modelling and simulation of the evolution of the outlets of SE-Vatnajökull ice cap, Iceland, using downscaled orographic precipitation. To be submitted.*

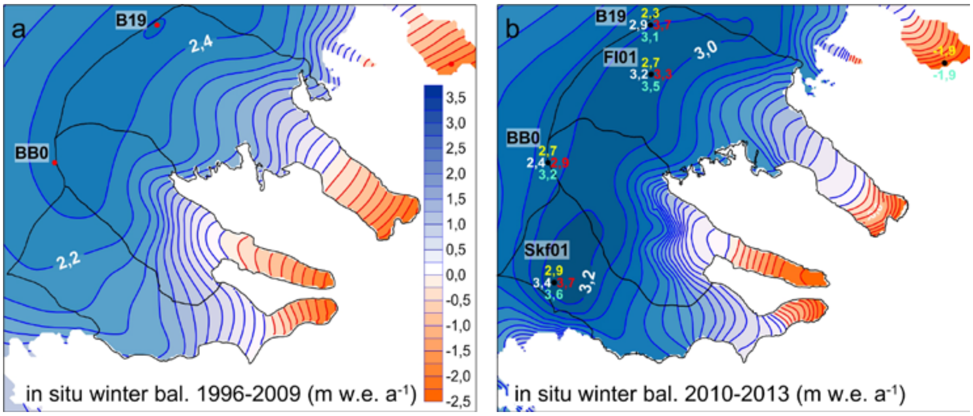

Figure 9. (a) Manually interpolated winter mass balance map showing the average of the time period 1996–2009 (b) and in 2010–2013 when the two stakes, Skf01 and Fl01, had been added to the mass balance network. The measurements of individual years are shown; 2010 (yellow), 2011 (turquoise), 2012 (white), 2013 (red).

A PDD mass balance and SIA ice flow model is applied, that uses downscaled orographic precipitation on a 1 km grid as input, to simulate the evolution of Skálafellsjökull, Heinabergsjökull and Fláajökull. The history of area and volume changes during ~1890–2010 of the three outlet glaciers of SE-Vatnajökull from paper III was used to constrain the model. For the first time downscaled precipitation is used in a mass balance modelling study of Icelandic glaciers. Model runs indicate that the spatial variations of the winter mass balance can not be realistically represented by a precipitation model based on constant horizontal and vertical precipitation gradients, as have previously been used. This was verified by adding two stakes (Skf01 and Fl01) to the mass balance network below the ice divide in 2009 (Fig. 9b) and by analysing the downscaled precipitation from the the LT-model by Crochet *et al.* (2007) and from the RÁV dataset of Rögnvaldsson *et al.* (2011). The winter balance values were approximately 1 m w.e. higher (Fig. 9b) than previously estimated by the manually interpolated mass balance maps in this location (Fig. 9a), on the southern slopes of Breiðabunga. 14 years of in situ mass balance measurements were used to calibrate the mass balance model using the downscaled precipitation data from the LT-model, indicating that the model explains 87% of the variation of the winter balance and 92% of the summer balance. Simulating the three outlets glaciers with a constant climate forcing of the baseline period 1980–2000, using a rate factor of $A=2.4\times10^{-15}$ s^{-1} kPa^{-3} resulted in an ice volume close to the 2002 observed value and the glacier surface profiles were reproduced by the model (Fig. 10).

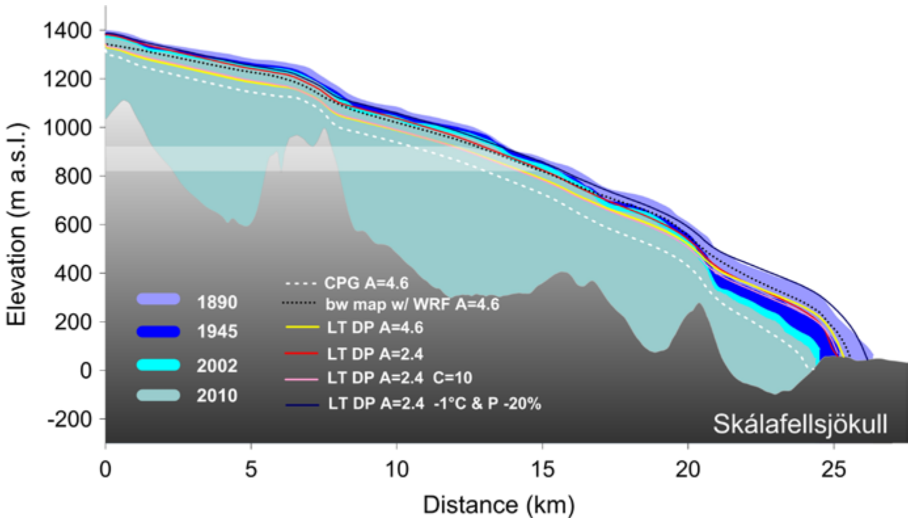

Figure 10. Longitudinal profiles down the central flowline of Skálafellsjökull showing the thickness and location of the terminus at different times according to observations (solids) and at the end of various simulations (lines). The white horizontal line indicates the elevation range of the ELA, derived from the MODIS images of 2007–2011.

Steady state experiments with step changes in temperature and precipitation were carried out to analyze the sensitivity of the modelled glaciers. The calculated sensitivity of the net mass balance to a warming of 1°C is –1.51 to –0.97 m w.e. a^{-1}, whereas +0.16 to +0.65 m w.e. a^{-1} to a 10% increase in annual precipitation, slightly varying between the outlets. Heinabergsjökull is more sensitive to changes in temperature and precipitation than the other outlets. A cooling of 1°C results in an increase in ice volume of 50%, but only 30–35% for the other two neighbouring outlets. Heinabergsjökull terminates in an overdeepened basin, where a large part of the bedrock is below sea level, and the terminus is flat and long. Simulations imply that the LIA maximum volume of the outlets is reached with temperatures 1°C lower than the average of the 1980–2000 baseline period and a decrease in annual precipitation of 20%, which is in line with data from nearby meteorological stations away from the glaciers (Figs. 10 and 11a). Future climate scenarios indicate a 2–3°C warming and precipitation increase in the range of 0–10% in Iceland by the end of the 21st century (Nawri and Björnsson, 2010). According to our model simulations, using step changes in temperature and precipitation, a 2°C warming and a 10% increase in annual precipitation would lead to a >50% ice volume loss, and 80–90% for a 3°C increase in annual temperature and same change in precipitation (Fig. 11b).

The ice flow model was developed by Guðfinna Aðalgeirsdóttir and Sven Þ. Sigurðsson, and has been used in previous studies. The mass balance model was written by Tómas Jóhannesson. I revised the mass balance maps with precipitation data from the RÁV dataset, which were provided by Hálfdán Ágústsson, and I ran the model with the updated winter balance maps with help from Sverrir Guðmundsson. The precipitation data from the LT model was provided by Philippe Crochet. I calibrated the mass balance model using the LT downscaled precipitation data, against in situ mass balance measurements. The bedrock topography was measured by Finnur Pálsson and Eyjólfur Magnússon. I ran the simulations, interpreted the results, and wrote the manuscript, with input from the coauthors.

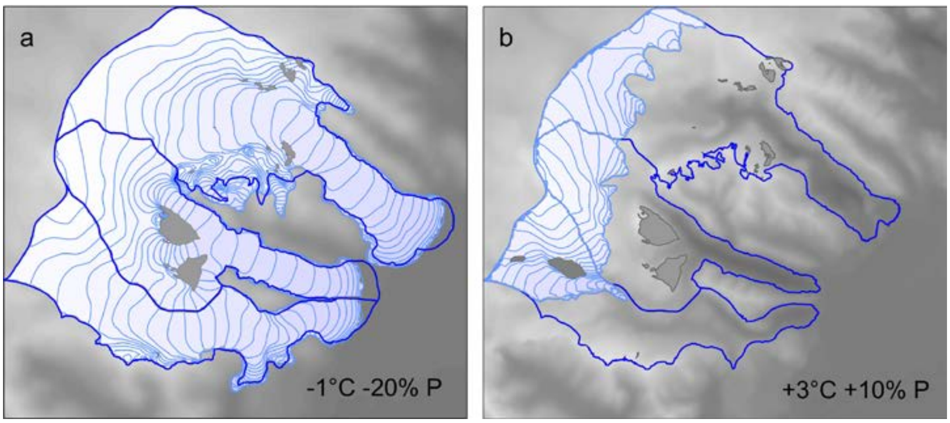

Figure 11. (a) The simulated LIA glacier geometry obtained with a step change in temperature equal to 1°C cooling and 20% decrease of annual precipitation, relative to the baseline period 1980–2000. (b) The glacier geometry at the end of a 200 year simulation forced with step change of +3°C and 10% increase in annual precipitation relative to the baseline period.

4 General conclusions and outlook

The fluctuations and timing of the LIA maximum of the SE-outlet glaciers of Vatnajökull are determined by analyzing the history of the glacier fluctuations in the 17th, 18th and 19th century as represented in historical documents. Quantitative estimates of the glacial extent and ice volume, at this advanced stage are based on LIA glacial geomorphological field evidence, historical oblique photographs, and descriptions from the written sources. The importance of using historical data is accentuated, not least considering the conflicting results of previous lichenometric dates of terminal LIA moraines in the forefield of the outlets of this study. Contemporary documents detail how the glaciers were at the outermost LIA moraines around 1880–1890, and some indicate that a few glaciers had reached similar positions in the mid-18th century, however, the earlier descriptions are not conclusive. The photographs from the end of 19th and early 20th century confirm the timing of the maximum glacier extent, at least for the recorded glaciers. The potential of using historical oblique photographs, by comparison with modern duplicates, to determine glacier surface elevation changes, has been demonstrated. In addition, the old photographs provide a striking visual impression of glacier retreat in the post-LIA time period (~1890–2010). With repeat photography important estimates of surface elevation changes in the accumulation area have been made, where geomorphological data is sparse or absent (since lateral moraines are only deposited below the ELA).

The reconstructed glacier surface geometry of Skálafellsjökull, Heinabergsjökull and Fláajökull at their advanced stage in the late 19th century, has been successfully simulated with the mass balance-ice flow model. The model was forced using constant temperatures, 1°C lower than the average of the 1980–2000 baseline period, and 80% of the annual precipitation, which is in consonance with the records from nearby lowland meteorological stations. This resemblance of the simulated and reconstructed volume gives confidence in both the method of reconstructing the glacier surface geometry and in the mass balance-ice flow model.

The record of volume and area changes of the 11 outlet glaciers of SE-Vatnajökull during the post-LIA time period, compiled in this thesis, provides an analogue for previous fluctuations of the outlets. The record illustrates close to synchronous response of the glaciers to similar climate forcing, which is inferred from the comparable temperature and precipitation fluctuations of the records from the two lowland meteorological stations in the vicinity. However, their rate of retreat and mass loss varies considerably. For example, all glaciers, except Kvíárjökull and Svínafellsjökull (which both have overdeepened basins), retreated following the warm decades of the 1930s and advanced or showed stillstands in the 1970s and 1980s. Previous mass balance measurements and modelling have demonstrated that the mass balance of Icelandic glaciers is governed by summer ablation (which is related to air temperature measured outside the glaciers), rather than winter accumulation (Björnsson *et al.*, 2013 and references therein). The temperature record of Stykkishólmur, which correlates well with the local record of Hólar in Hornafjörður, shows a decline around 1850 and reaches a minimum around 1890. Thereby, supporting a late 19th century glacier maxima of the SE-outlet glaciers, assuming the response time of 20–40 years, estimated as a function of the glacier thickness and ablation at the terminus (see Jóhannesson *et al.*, 1989).

This study has shed light on the area and volume changes of outlet glaciers of SE-Vatnajökull during the post-LIA time period ~1890–2010 and provided estimates of geodetic mass balance changes. The average mass balance has been negative during every time interval, but the likely positive mass balance period in the 1970s–1980s can not be resolved with the currently available temporal resolution. The highest rate of mass loss is observed in the first decade of the 21st century, with values ranging from –2.70 to –0.80 m w.e. a^{-1} (–1.34±0.12 m w.e. a^{-1} on average), which ranks among the most negative mass balance worldwide during this time period (Vaughan *et al.*, 2013). The difference in the magnitude of the response of the glaciers to similar changes in mass balance, highlights the need of a large dataset for interpreting the climate signal from glacier variations. It is also clear that frontal variations and area changes only provide limited information on the dynamic glacier response to climate perturbations, as some undergo considerable surface lowering, but little retreat.

The database on area and volume changes of the SE-oulets was compared to the commonly proposed power-law that relates glacier area and volume (Bahr *et al.*, 1997; Adhikari and Marshall, 2012). When applying the constants of the power-law, the calculated ice volume is underestimated by up to 50%. Accurate estimates of ice volume stored in glaciers are important for future global sea level rise projections, as melting glaciers outside the polar areas are contributing at an accelerated rate (Vaughan *et al*., 2013). It is concluded that the proposed power-law can only be used as a statistical method to infer ice volume from measured glacier area for large datasets of glaciers and the coefficients may need to be adjusted to variable glaciological parameters.

The multi-temporal glacier inventory created in this thesis serves as input for glacial unloading studies in Iceland. Hitherto a linear rate of mass loss has been assumed in modelling the uplift of the earth´s crust in response to the retreating glaciers (Árnadóttir *et al.,* 2009; Auriac *et al.*, 2013). The retreat history of some of the SE-outlet glaciers has been used in a number of biological studies, e.g. the development of freshwater systems in ponds following glacier retreat (Ólafsson, 2012), soil development (Vilmundardóttir *et al*., 2014, 2015), and vegetation succession in front of the retreating ice front (Magnúsdóttir *et al.,* 2013).

Simulations with the mass balance-ice flow model of the three outlets of Breiðabunga revealed that downscaled orographic precipitation data is necessary for the simulations in order to capture variance of the winter mass balance. A precipitation model using constant precipitation gradients, based on precipitation data from meteorological stations away from the glacier (as used in previous modelling studies), could not realistically represent this variability. The good fit between the modelled ELA and the snowline at the end of the summer (a proxy for the ELA on temperate glaciers), derived from MODIS images 2007**–**2010, provides additional validation of the calculations of the mass balance model using the downscaled precipitation data. The sensitivity of the annual balance to 1°C warming is calculated as –1.51 to –0.97 m w.e. a^{-1}, which is similar to a 40% reduction in annual precipitation. Simulations indicate, that a +3°C step change in temperature relative to the baseline period 1980–2000 (which is in line with predictions of increased temperature by the end of the 21st century), would lead to almost disappearance of the glaciers.

The recently acquired LiDAR DEMs (2010**–**2011) have revolutionized the work presented in this thesis. They have provided an accurate reference topography, simplifying the georeferencing of old maps and aerial images. Accurate elevation of the glacial geomorphological features outlining the LIA glacier extent, are obtained from the DEMs. They provide precise location, elevation and configuration of nunataks in the accumulation areas, which are used to infer glacier surface elevation changes from the original aerial photographs from 1945 and 1989, relative to the 2010 glacier surface.

The importance of field observations and measurements are emphasized. For example, the LIA glacial geomorphological features, including the lateral moraines and trimlines are not all detectable on the aerial or satellite images, thus requiring field mapping to retrieve detailed outlines of the LIA maximum extent of the outlets. The suite of LIA lateral moraines, were recognized to be of very variable composition, offering an opportunity to conduct thorough geomorphological studies of these glacial landforms, that can shed light on the various depositional processes and transportation mechanisms of these sediments. The value of the in situ mass balance measurements is evident, providing data to validate geodetic mass balance estimates and for comparison with downscaled precipitation data. The good agreement with the calculated winter mass balance using the downscaled precipitation data from the LT model, and the manually interpolated winter mass balance maps (after the addition of the two stakes on Skálafellsjökull and Fláajökull) underline this. The mass balance measurements at the new stakes also manifest the importance of strategically selecting the location of mass balance stakes.

This study provides guidelines for reconstructing the glacier surface geometry at the LIA maximum for other glaciers and ice caps in Iceland. The LIA extent of the majority of them has been mapped from a series of aerial images (Sigurðsson *et al*., 2013; Guðmundsson, unpublished data), a number of historical photographs of the glaciers are preserved from Frederick Howell taken in the late 19th century (Fiske Icelandic collection, Cornell University, http://cidc.library.cornell.edu/howell/; Ponzi, 2004), and from the early 20th century taken during the surveys of the Danish General Staff (archives of the National Land Survey of Iceland, http://atlas.lmi.is/islandskort-dana/ljosmyndir.php). The maps of the Danish General Staff from the early 20th century are available for some of the glaciers and ice caps in Iceland (http://www.lmi.is/kortasafn/). The lateral moraines in the glaciated valleys of SE-Vatnajökull conspicuously delineate the glacier surface at the LIA maximum. Their preservation potential is high, in valleys with not too steep walls, where they have been left intact by glacial meltwater. The flat lobes of western and northern Vatnajökull, for example, are not constrained by mountains, and thus their LIA fingerprint is mostly confined to terminal moraines.

The temporal resolution of the geodetic mass balance records in the time period 1945–1989/2002 could be increased by using aerial images to construct glacier surface DEMs, as has been sucessfully done on e.g. Drangajökull (Munoz-Cobo Belart et al., 2014). A series of aerial images from the National Land Survey of Iceland are available from the 1960s, 1970s and 1980s of the SE-outlet glaciers (www.lmi.is/loftmyndasafn-2), however, few of the flight lines cover the glaciers all the way from the ice divide down to the terminus. The possibly positive mass balance of the cold decades (after the mid-20th century) could be resolved, that can be inferred from the small advances of some of the SE-outlet glaciers of Vatnajökull during this time period.

Simulating the record of volume changes of the 3 outlets of Breiðabunga which is known for the whole post-LIA period (presented in paper III) would be worthwhile, given that a downscaled precipitation field for the period ~1890-1959 can be reconstructed. It may be possible to extrapolate back in time the spatial structure of the precipitation field for certain periods for which the precipitation is well reproduced during 1959-2010, based on correlations with precipitation measurements from local lowland stations since the late 19th century. Other downscaled precipitation datasets than the those of the LT and WRF models could also be used as input for the mass balance model, including HIRHAM. Furthermore, the downscaled orographic precipitation data should be applied in mass balance modelling on other ice caps and glaciers in Iceland, and preferrably starting with those that have previously been modelled, in order to compare the performance of the mass balance model using either constant precipitation gradients or downscaled precipitation data.

It would be interesting to carry out simulations with a higher-order or a full-Stokes model, and compare the results with the SIA model simulations from this study. Heinabergsjökull has a steeper bedrock slope than the other neighbouring outlets, terminates in a proglacial lake, and today its tongue is floating, making it more difficult to simulate than the other neighbouring outlets. It is therefore a good candidate for such comparison. In this work, the floating tongue was not accounted for in the SIA model, whereas the full-Stokes model could resolve the grounded and floating part of the glacier. Finally, the known history of area and volume changes of the Öræfajökull outlets, provides validation points for simulations. The question remains wheter the mass balance-ice flow model used in this study is applicable for these steeper outlets, which have very few mass balance stakes to calibrate the mass balance model.

References

Adhikari, S. and Marshall, S.J., 2012. Glacier volume-area relation for high-order mechanics and transient glacier states. *Geophysical Research Letters*, 39.doi 10.1029/2012gl052712.

Aðalgeirsdóttir, G., 2003: *Flow dynamics of Vatnajökull ice cap, Iceland*. PhD thesis. ETH Zurich, Zurich.

Aðalgeirsdóttir, G., Björnsson, H. and Jóhannesson, T., 2004. Vatnajökull ice cap, results of computations with a dynamical model coupled with a degree-day mass-balance model. Science Institute, University of Iceland, Reykjavík, 35.

Aðalgeirsdóttir, G., Guðmundsson, G.H. and Björnsson, H., 2005. Volume sensitivity of Vatnajökull Ice Cap, Iceland, to perturbations in equilibrium line altitude. *Journal of Geophysical Research-Earth Surface*, 110.doi 10.1029/2005jf000289.

Aðalgeirsdóttir, G., Guðmundsson, S., Björnsson, H., Pálsson, F., Jóhannesson, T., Hannesdóttir, H., Sigurðsson, S.P. and Berthier, E., 2011. Modelling the 20th and 21st century evolution of Hoffellsjökull glacier, SE-Vatnajökull, Iceland. *The Cryosphere*, 5, 961-975.doi 10.5194/tc-5-961-2011.

Aðalgeirsdóttir, G., Jóhannesson, T., Björnsson, H., Pálsson, F. and Sigurðsson, O., 2006. Response of Hofsjökull and southern Vatnajökull, Iceland, to climate change. *Journal of Geophysical Research-Earth Surface*, 111.doi:10.1029/2005JF000388.

Ahlmann, H.W. and Þórarinsson, S., 1943. *Vatnajökull, Scientific results of the Swedish-Icelandic investigations 1936-37-38*. Esselte, Stockholm.

Army Map Servie,, 1950-1951. *Series C762, 1:50000.* U.S. Army, Washington DC.

Auriac, A., Spaans, K.H., Sigmundsson, F., Hooper, A., Schmidt, P. and Lund, B., 2013. Iceland rising: Solid Earth response to ice retreat inferred from satellite radar interferometry and visocelastic modeling. *Journal of Geophysical Research-Solid Earth*, 118, 1331-1344.doi 10.1002/Jgrb.50082.

Árnadóttir, T., Lund, B., Jiang, W., Geirsson, H., Björnsson, H., Einarsson, P. and Sigurðsson, T., 2009. Glacial rebound and plate spreading: results from the first countrywide GPS observations in Iceland. *Geophysical Journal International*, 177, 691-716.doi 10.1111/j.1365-246X.2008.04059.x.

Bahr, D.B., 1997. Global distributions of glacier properties: A stochastic scaling paradigm. *Water Resource Research*, 3, 1669-1679.doi:10.1029/97WR00824.

Bárðarson, G., 1934. Islands Gletscher: Beiträge zur Kenntnis der Gletscherbewegungen und Schwankungen auf Grund alter Quellenschriften und neuester Forschung : nachgelassenes Manuskript. *Rit Vísindafélags Íslendinga*, 16, 60.

Benn, D.I. and Hulton, N.R.J., 2010. An Excel (TM) spreadsheet program for reconstructing the surface profile of former mountain glaciers and ice caps. *Computers & Geosciences*, 36, 605-610.doi 10.1016/j.cageo.2009.09.016.

Berthier, E., Le Bris, R., Mabileau, L., Testut, L. and Remy, F., 2009. Ice wastage on the Kerguelen Islands (49 degrees S, 69 degrees E) between 1963 and 2006. *Journal of Geophysical Research-Earth Surface*, 114.doi:10.1029/2008JF001192.

Björnsson, F., 1956. Kvíárjökull. *Jökull*, 6, 20-22.

Björnsson, F., 1993. Samtíningur um Jökulsá á Breiðamerkursandi og Jökulsárlón. *Skaftfellingur*, 9, 8-24.

Björnsson, F., 1996. Þættir um Breiðamerkursand. *Skaftfellingur,* 11, 105-125.

Björnsson, F., 1998. Samtíningur um jökla milli Fells og Staðarfjalls. *Jökull*, 46, 49-61.

Björnsson, H., 1979. Glaciers in Iceland. *Jökull*, 29, 74-80.

Björnsson, H., 1986. Surface and bedrock topography of ice caps in Iceland mapped by radio echo soundings. *Annals of Glaciology*, 8, 11-18.

Björnsson, H., 1988. Hydrology of ice caps in volcanic regions. *Societas Scientiarum Islandica*, Rit 45, 139 p., 121 maps.

Björnsson, H., 2009. *Jöklar á Íslandi*. Opna, Reykjavík.

Björnsson, H. and Eydal, G.P., 1998. Rannsóknir á stærð jökla á Íslandi síðastliðin 300 ár. Verkþáttur: Breytingar á Vatnajökli. Raunvísindastofnun Háskólans, Reykjavík.

Björnsson, H., Guðmundsson, S., Pálsson, F. and Haraldsson, H.H., 2005. Glacier winds on Vatnajökull ice cap, Iceland and their relation to temperatures of its environs. *Annals of Glaciology*, 42, 291-296.

Björnsson, H. and Pálsson, F., 2004. Jöklar í Hornafirði, rannsóknir og saga In: Björnsson, H. (Ed.), *Jöklaveröld, náttúra og mannlíf*. Skrudda, Reykjavík. 125-164.

Björnsson, H. and Pálsson, F., 2008. Icelandic glaciers. *Jökull*, 58, 365-386.

Björnsson, H., Pálsson, F., Guðmundsson, M.T. and Haraldsson, H.H., 1998. Mass balance of western and northern Vatnajökull, Iceland, 1991-1995. *Jökull*, 45, 35-58.

Björnsson, H., Pálsson, F., Guðmundsson, S., Magnússon, E., Aðalgeirsdóttir, G., Jóhannesson, T., Berthier, E., Sigurðsson, O. and Thorsteinsson, T., 2013. Contribution of Icelandic ice caps to sea level rise: Trends and variability since the Little Ice Age. *Geophysical Research Letters*, 40, 1546-1550.doi 10.1002/Grl.50278.

Björnsson, H., Pálsson, F. and Haraldsson, H.H., 2002. Mass balance of Vatnajökull (1991–2001) and Langjökull (1996–2001), Iceland. *Jökull*, 53, 75-78.

Bradwell, T., 2004. Lichenometric dating in southeast Iceland: The size-frequency approach. *Geografiska Annaler Series a-Physical Geography*, 86A, 31-41.doi: 10.1111/j.0435-3676.2004.00211.x.

Bradwell, T., Dugmore, A.J. and Sugden, D.E., 2006. The Little Ice Age glacier maximum in Iceland and the North Atlantic Oscillation: evidence from Lambatungnajokull, southeast Iceland. *Boreas*, 35, 61-80.doi 10.1080/03009480500359202.

Chenet, M., Roussel, E., Jomelli, V. and Grancher, D., 2010. Asynchronous Little Ice Age glacial maximum extent in southeast Iceland. *Geomorphology*, 114, 253-260.doi 10.1016/j.geomorph.2009.07.012.

Crochet, P., Jóhannesson, T., Jónsson, T., Sigurðsson, O., Björnsson, H., Pálsson, F. and Barstad, I., 2007. Estimating the spatial distribution of precipitation in Iceland using a linear model of orographic precipitation. *Journal of Hydrometeorology*, 8, 1285-1306.doi: 10.1175/2007JHM795.1.

Crochet, P., 2013. Gridding daily precipitation with an enhanced two-step spatial interpolation method. IMO Technical report PC/2013-01. Icelandic Meteorological Office, Reykjavík, 26.

Dabski, M., 2002. Dating of Fláajökull moraine ridges SE-Iceland, comparison of the glaciological, cartographical and lichenometric data. *Jökull*, 51, 17-24.

Danish General Staff, 1904. *Sheets: 87-NV,SV,SA, 97-NV, NA, 96-NA, 1:50000.* The topographic department of the Danish General Staff, Copenhagen.

De Woul, M. and Hock, R., 2005. Static mass-balance sensitivity of Arctic glaciers and ice caps using a degree-day approach. *Annals of Glaciology, Vol 42, 2005*, 42, 217-224.doi 10.3189/172756405781813096.

Defense Mapping Agency, 1997. *DMA series C761, 1:50,000.* National Land Survey of Iceland, Reykjavík.

Einarsson, M.Á., 1984. Climate of Iceland In: van Loon, H. (Ed.), *Climates of the Oceans*. Elsevier, Amsterdam. 673-697.

Evans, D.J.A., Archer, S. and Wilson, D.J.H., 1999. A comparison of the lichenometric and Schmidt hammer dating techniques based on data from the proglacial areas of some Icelandic glaciers. *Quaternary Science Reviews*, 18, 13-41.doi 10.1016/S0277-3791(98)00098-5.

Eyþórsson, J., 1951. Þykkt Vatnajökull. *Jökull*, 1, 1-6.

Eyþórsson, J., . 1963. Variations of glaciers 1931-1960. *Jökull*, 13, 31-33.

Flowers, G.E., Marshall, S.J., Björnsson, H. and Clarke, G.K.C., 2005. Sensitivity of Vatnajökull ice cap hydrology and dynamics to climate warming over the next 2 centuries. *Journal of Geophysical Research*, 110.doi:10.1029/2004JF000200.

Geirsdóttir, Á., Miller, G.H., Axford, Y. and Ólafsdóttir, S., 2009. Holocene and latest Pleistocene climate and glacier fluctuations in Iceland. *Quaternary Science Reviews*, 28, 2107-2118.doi 10.1016/j.quascirev.2009.03.013.

Geirsdóttir, Á., Miller, G.H., Larsen, D.J. and Ólafsdóttir, S., 2013. Abrupt Holocene climate transitions in the northern North Atlantic region recorded by synchronized lacustrine records in Iceland. *Quaternary Science Reviews*, 70, 48-62.doi 10.1016/j.quascirev.2013.03.010.

Gordon, J.E. and Sharp, M., 1983. Lichenometry in dating recent glacial landforms and deposits, southeast Iceland. *Boreas*, 12, 191-200.

Guðmundsson, H., 1998: *Holocene glacier fluctuations and tephrochronology of the Öræfi district, Iceland*. PhD thesis. University of Edinburgh, Edinburgh.

Guðmundsson, H.J., 1997. A review of the Holocene environmental history of Iceland. *Quaternary Science Reviews*, 16, p. 81-92.

Guðmundsson, M.T., 2000. Mass balance and precipitation on the summit plateau of Öræfajökull, SE-Iceland. *Jökull*, 48, 49-54.

Guðmundsson, S., 2014: *Reconstruction of late 19th century glacier extent of Kotárjökull and Breiðamerkurjökull in SE–Iceland and comparison with the current extent*. MSc. University of Iceland, Reykjavík.

Guðmundsson, S., Björnsson, H., Aðalgeirsdóttir, G., Jóhannesson, T., Pálsson, F. and Sigurðsson, O., 2006. Áhrif loftlagsbreytinga á stærð og afrennsli Langjökuls, Hofsjökuls og suður Vatnajökuls, Orkuþing 2006, Reykjavík.

Guðmundsson, S., Björnsson, H., Jóhannesson, T., Aðalgeirsdóttir, G., Pálsson, F. and Sigurðsson, O., 2009a. Similarities and differences in the response to climate warming of two ice caps in Iceland. *Hydrology Research*, 40, 495-502.doi 10.2166/Nh.2009.210.

Guðmundsson, S., Pálsson, F., Björnsson, H. and Haraldsson, H.H., 2009b. Comparison of energy balance and degree-day models of summer ablation on the Langjökull ice cap, SW-Iceland. *Jökull*, 59, 1-18.

Icelandic Meteorological Office and Institute of Earth Sciences, U.o.I., 2013. DEMs of Icelandic glaciers (dataset).

Jóhannesson, T., 1997. The response of two Icelandic glaciers to climatic warming computed with a degree-day glacier mass-balance model coupled to a dynamic glacier model. *Journal of Glaciology*, 43, 321-327.

Jóhannesson, T., Aðalgeirsdóttir, G., Björnsson, H., Crochet, P., Elíasson, E.B., Ólafsson, H., Pálsson, F., Rögnvaldsson, Ó., Sigurðsson, O., Snorrason, Á., Blöndal Sveinsson, Ó.G. and Þorsteinsson, Þ., 2007. Effect of climate change on hydrology and hydro-resources in Iceland. National Energy Authority - Hydrological Service, Reykjavík, 91.

Jóhannesson, T., Björnsson, H., Magnússon, E., Guðmundsson, S., Pálsson, F., Sigurðsson, O., Thorsteinsson, T. and Berthier, E., 2013. Ice-volume changes, bias estimation of mass-balance measurements and changes in subglacial lakes derived by lidar mapping of the surface of Icelandic glaciers. *Annals of Glaciology*, 54, 63-74.doi 10.3189/2013aog63a422.

Jóhannesson, T., Raymond, C. and Waddington, E., 1989. Time-Scale for Adjustment of Glaciers to Changes in Mass Balance. *Journal of Glaciology*, 35, 355-369.

Jóhannesson, T., Sigurdsson, O., Laumann, T. and Kennett, M., 1995. Degree-Day Glacier Mass-Balance Modeling with Applications to Glaciers in Iceland, Norway and Greenland. *Journal of Glaciology*, 41, 345-358.

Jóhannesson, T. and Sigurðsson, O., 1998. Interpretation of glacier variations in Iceland 1930-1995. *Jökull*, 45, 27-33.

Kirkbride, M.P. and Dugmore, A.J., 2008. Two millenia of glacier advances from southern Iceland dated by tephrochronology. *Quaternary Research*, 70, 398-411.doi 10.1016/j.yqres.2008.07.001.

Knudsen, K.L., Eiríksson, J. and Bartels-Jónsdóttir, H.B., 2012. Oceanographic changes through the last millennium off North Iceland: Temperature and salinity reconstructions based on foraminifera and stable isotopes. *Marine Micropaleontology*, 84-85, 54-73.doi 10.1016/j.marmicro.2011.11.002.

Larsen, D.J., Miller, G.H., Geirsdottir, A. and Thordarson, T., 2011. A 3000-year varved record of glacier activity and climate change from the proglacial lake Hvitarvatn, Iceland. *Quaternary Science Reviews*, 30, 2715-2731.doi 10.1016/j.quascirev.2011.05.026.

Magnúsdóttir, Ó.B., Þórhallsdóttir, Þ.E. and Svavarsdóttir, K., 2013. Drivers of vegetation succession in proglacial environments in SE-Iceland: Deterministic or stochastic?, Líffræðiráðstefnan 2013. Líffræðifélag Íslands, Reykjavík.

Magnússon, E., Björnsson, H. and Pálsson, F., 2007. Landslag í grennd Kvískerja í fortíð og framtíð: Niðurstöður ísjármælinga á Kvíár-, Hrútár og Fjallsjökli (Radio echo sounding on Kvíárjökull, Hútárjökull and Fjallsjökull). *Jökull*, 57, 83-89.

Magnússon, E., Pálsson, F., Björnsson, H. and Guðmundsson, S., 2012. Removing the ice cap of Öraefajokull central volcano, SE-Iceland: Mapping and interpretation of bedrock topography, ice volumes, subglacial troughs and implications for hazards assessments. *Jökull*, 62, 131-150.

Marshall, S.J., Bjornsson, H., Flowers, G.E. and Clarke, G.K.C., 2005. Simulation of Vatnajokull ice cap dynamics. *Journal of Geophysical Research-Earth Surface*, 110. doi:10.1029/2004JF000262.

McKinzey, K.M., Orwin, J.F. and Bradwell, T., 2004. Re-dating the moraines at Skálafellsjökull and Heinabergsjökull using different lichenometric methods: Implications for the timing of the Icelandic Little Ice Age maximum. *Geografiska Annaler Series a-Physical Geography*, 86A, 319-335.doi 10.1111/j.0435-3676.2004.00235.x.

McKinzey, K.M., Orwin, J.F. and Bradwell, T., 2005. A revised chronology of key Vatnajökull (Iceland) outlet glaciers during the Little Ice Age. *Annals of Glaciology*, 42, 171-179.foi10.3189/172756405781812817.

Munoz-Cobo Belart, J., Magnússon, E. and Pálsson, F., 2014. The mass balance record and surge behavior of Drangajökull Ice Cap (Iceland) from 1946 to 2011 deduced from aerial photographs and LiDAR DEM General Assembly EGU, Vienna.

Nawri, N. and Björnsson, H., 2010. Surface air temperature and precipitation trends for Iceland in the 21st century. Icelandic Meteorological Office, Reykjavík, 42.

Ogilvie, A., 2005. Local knowledge and Traveller´s tales: A selection of climatic observations in Iceland In: Caseldine, C., Russell, A.J., Harðardóttir, J., Knudsen, Ó. (Eds.), *Iceland-Modern Processes and Past Environments*. Elsevier, Amsterdam. 257-287.

Ogilvie, A.E.J. and Jónsson, T., 2001. "Little Ice Age" research: A perspective from Iceland. *Climatic Change,* 48, 9-52.doi 10.1023/A:1005625729889.

Ólafsson, H., Furger, M. and Brummer, B., 2007. The weather and climate of Iceland. *Meteorologische Zeitschrift*, 16, 5-8.doi 10.1127/0941-2948/2007/0185.

Ólafsson, J.S., 2012. Líf í tjörnum við rætur Skaftafellsjökuls, Haustráðstefna Vistfræðifélags Íslands 2012. Félag íslenskra vistfræðinga, Reykjavík.

Paterson, W.S.B., 1994. *The Physics of Glaciers*. Butterworth-Heinemann, Oxford.

Pálsson, F., Guðmundsson, S., Björnsson, H., Berthier, E., Magnússon, E., Guðmundsson, S. and Haraldsson, H.H., 2012. Mass and volume changes of Langjökull ice cap, Iceland, similar to 1890 to 2009, deduced from old maps, satellite images and in situ mass balance measurements. *Jökull,* 62, 81-96.

Ponzi, F., 2004. *Ísland Howells – Howell's Iceland*. Brennholtsútgáfa, Mosfellsbær.

Rögnvaldsson, Ó., Ágústsson, H. and Ólafsson, H., 2011. Aflræn niðurkvörðun veðurs innan LOKS verkefnisins. Technical report. Reiknistofa í veðurfræði.

Sigurðsson, O., 2005. Variations of termini of glaciers in Iceland in recent centuries and their connection with climate. In: Caseldine, C., A. Russell, O. Knudsen and J. Harðardóttir: (Ed.), *Iceland-Modern Processes and Past Environments*. Elsevier, Amsterdam. 241-256.

Sigurðsson, O., Jónsson, T. and Jóhannesson, T., 2007. Relation betwen glacier-termini variations and summer temperature in Iceland since 1930. *Annals of Glaciology,* 46, 170-176.

Sigurðsson, O., Williams, R.S. and Víkingsson, S., 2013. *Map of the glaciers of Iceland, with names, updated contour lines and coordinates, 1:500,000.* Icelandic Meteorological Office, Reykjavík.

Skamarock, W.C., Klemp, J.B., Dudhia, J., Gill, D.O., Barker, D.M., Duda, M.G., Huang, X.Y., Wang, W. and Powers, J.G., 2008. A description of the Advanced

Research WRF version 3 Tech. Rep. NCAR/TN-475+STR. National center for atmospheric research

Smith, R.B., 2003. A linear upslope-time-delay model for orographic precipitation. *Journal of Hydrology,* 282, 2-9.

Snorrason, S., 1984: *Mýrajöklar og Vatnsdalur*. Cand Real thesis. Universitetet i Oslo, Oslo.

Striberger, J., Bjorck, S., Ingolfsson, O., Kjaer, K.H., Snowball, I. and Uvo, C.B., 2010. Climate variability and glacial processes in eastern Iceland during the past 700 years based on varved lake sediments. *Boreas*, 40, 28-45.doi 10.1111/j.1502-3885.2010.00153.x.

Thompson, A., 1988. Historical development of the proglacial landforms of Svínafellsjökull and Skaftafellsjökull, southeast Iceland. *Jökull,* 38, 17-30.

Thompson, A. and Jones, A., 1986. Rates and Causes of Proglacial River Terrace Formation in Southeast Iceland - an Application of Lichenometric Dating Techniques. *Boreas*, 15, 231-246.

Vaughan, D.G., Comiso, J.C., Allison, I., Carrasco, J., Kaser, G., Kwok, R., Mote, P., Murray, T., Paul, F., Ren, J., Rignot, E., Solomina, O., Steffen, K. and Zhang, T., 2013. Observations: Cryosphere In: Stocker, T.F., Qin, D., Plattner, G.-K., Tignor, M., Allen, S.K., Boschung, J., Nauels, A., Xia, Y., Bex, V., Midgley , P.M. (Eds.), *Climate Change 2013: The Physical Science Basis. Contribution of Working Group I to the Fifth Assessment Report of the Intergovernmental Panel on Climate Change* Cambridge University Press, Cambridge, United Kingdom and New York, NY, USA.

Vilmundardóttir, O.K., Gísladóttir, G. and Lal, R., 2014. Early stage development of selected soil properties along the proglacial moraines of Skaftafellsjökull glacier, SE-Iceland. *Catena*, 121, 142-150.doi: 10.1016/j.catena.2014.04.020.

Vilmundardóttir, O.K., Gísladóttir, G. and Lal, R., 2015. Soil carbon accretion along an age chronosequence formed by the retreat of the Skaftafellsjökull glacier, SE-Iceland. *Geomorphology,* 228, 124-133. doi: 10.1016/j.geomorph.2014.08.030.

Wood, K.R., Overland, J.E., Jonsson, T. and Smoliak, B.V., 2010. Air temperature variations on the Atlantic-Arctic boundary since 1802. *Geophysical Research Letters*, 37.doi 10.1029/2010gl044176.

Þórarinsson, S., 1939. The ice dammed lakes of Iceland with particular reference to their values as indicators of glacier oscillations. *Geografiska Annaler,* 21, 216-242.

Þórarinsson, S., 1943. Oscillations of the Iceland glaciers in the last 250 years. *Geografiska Annaler*, 25 bls. 1-54.

Þórarinsson, S., 1960. Glaciological knowledge in Iceland before 1800. *Jökull*, 10, 1-17.

Þórarinsson, S., 1964. On the variations of Svínafellsjökull, Skaftafellsjökull and Kvíárjökull in Öræfi. *Jökull*, 6, 1-15.

Þórarinsson, S., 1974. Sambúð lands og lýðs í ellefu aldir In: Líndal, S. (Ed.), *Saga Íslands, 1. bindi*. Sögufélagið, Reykjavík. 29-97.

Paper I

Hannesdóttir, H., Björnsson, H., Pálsson, F., Aðalgeirsdóttir, G., Guðmundsson, Sn. Variations of southeast Vatnajökull ice cap (Iceland) 1650-1900 and reconstruction of the glacier surface geometry at the Little Ice Age maximum. Geografiska Annaler: Series A, Physical Geography. doi:10.1111/geoa.12064.

VARIATIONS OF SOUTHEAST VATNAJÖKULL ICE CAP (ICELAND) 1650–1900 AND RECONSTRUCTION OF THE GLACIER SURFACE GEOMETRY AT THE LITTLE ICE AGE MAXIMUM

HRAFNHILDUR HANNESDÓTTIR[1], HELGI BJÖRNSSON[1], FINNUR PÁLSSON[1], GUÐFINNA AÐALGEIRSDÓTTIR[1] and SNÆVARR GUÐMUNDSSON[1,2]

[1]Institute of Earth Sciences, University of Iceland, Reykjavík, Iceland
[2]Southeast Iceland Nature Center, Litlubrú 2 Höfn, Iceland

Hannesdóttir, H., Björnsson, H., Pálsson, F., Aðalgeirsdóttir, G. and Guðmundsson, S., 2014. Variations of southeast Vatnajökull ice cap (Iceland) 1650–1900 and reconstruction of the glacier surface geometry at the Little Ice Age maximum. *Geografiska Annaler: Series A, Physical Geography*, ••, ••–••. DOI:10.1111/geoa.12064

ABSTRACT. We present an overview of glacier variations of the outlet glaciers of southeast Vatnajökull ice cap, Iceland, during the time period ~1650–1900 as represented in historical archives, by geomorphological field evidence and assess the timing of the *Little Ice Age* (*LIA*) maximum. According to written documents, all glaciers advanced in the latter half of the seventeenth century and extended far out on the lowlands in the mid-eighteenth century. Contemporary documents describe how all the studied glaciers were at their LIA terminal moraines around ~1880–1890 (no descriptions found for Morsárjökull) and soon after started receding, marking the end of the LIA in Iceland. Reconstruction of the LIA maximum glacier surface geometry was based on glacial geomorphological features (including lateral and terminal moraines, trimlines and erratics), historical photographs, maps from 1904, and a 2010 LiDAR digital elevation model. The glaciers were at their LIA maximum around 150–270 m thicker near the terminus than in 2010, whereas negligible differences were observed in the upper reaches of the accumulation area. By combining the historical, glacial geomorphological and high-resolution LiDAR data, we provide quantitative estimates of the glacial extent and volume at the LIA maximum. The highest up-valley lateral moraines provided estimates of the equilibrium line altitude (ELA) during the LIA, which was on average 340 m lower than the present day ELA. Consistency was found in the spatial variability of the ELA during both time periods, with higher values on the westfacing outlets of Öræfajökull ice cap (at the southern end of Vatnajökull ice cap), than on the east flowing glaciers, and a rise in the ELA from west to east on the outlets east of Breiðamerkurjökull.

Key words: Little Ice Age, southeast Iceland, glacier variations, historical data, lateral moraines, ELA, reconstructing glacier geometry, glacier volume.

Introduction

The *Little Ice Age* (*LIA*) was characterized by cold but variable climate, and the timing and magnitude of the cold periods varied regionally (Le Roy Ladurie 1971; Jones and Briffa 2001; Ogilvie and Jónsson 2001; Grove 2004; Brázdil *et al*. 2005; Matthews and Briffa 2005; Mann *et al*. 2008; Miller *et al*. 2010; Wanner *et al*. 2011). Glaciers around the North Atlantic advanced during the LIA (e.g. Grove 2001) and many of them reached their Holocene maxima (Hagen and Liestøl 1990; Geirsdóttir *et al*. 2009; Nesje 2009; Miller *et al*. 2010). The cooler and fluctuating climate of the LIA in Iceland is clearly evidenced in written documents as early as in the thirteenth century (Þórarinsson 1960; Ogilvie 1986, 2005), and in the sea ice annals since the 1600 (Bergþórsson 1969; Ogilvie 1986, 2010; Ogilvie and Jónsson 2001). In Konungs Skuggsjá or Kings Mirror from the middle of the thirteenth century (Lárusson 1955), glaciers and glacial rivers are described, and their existence explained by their geographical location close to cold ice-covered Greenland. Þórarinsson (1960) infers that this is most likely the oldest climatological explanation of glaciers found in the literature. Permanently frozen glaciers on high mountains and sea ice filled northern harbors are mentioned in Guðmundar Saga Biskups Arasonar, written around 1350 (Kristjánsson 2002). Descriptions of advancing glaciers due to colder climate are found in the treatise of bishop Oddur Einarsson from 1590 (Einarsson 1971). But the written accounts describing the deteriorating climate and advancing glaciers in Iceland only become prolific and detailed around 1700 (e.g. Þórarinsson 1943; Ogilvie 1992, 2005). Several continuous high-

DOI:10.1111/geoa.12064

resolution lake and marine sedimentary records from around Iceland have shed light on the varying climatic and environmental conditions during the LIA and the transition into the LIA has been defined to ~1250–1300 from the terrestrial records (e.g. Geirsdóttir *et al.* 2009, 2013; Axford *et al.* 2011; Striberger *et al.* 2010, 2012; Larsen *et al.* 2011, 2013; Knudsen *et al.* 2012 and references therein). Widespread glacier advances manifest the LIA cooling in Iceland, and the majority of glaciers reached their Holocene maximum extent either in the eighteenth or nineteenth century and some advanced during both periods (e.g. Þórarinsson 1943; Guðmundsson 1997; Evans *et al.* 1999; Sigurðsson 2005; Kirkbride and Dugmore 2008; Björnsson 2009; Geirsdóttir *et al.* 2009; Larsen *et al.* 2011). However, moraine remnants are found tens of metres outside the LIA limit of some glaciers. One of them is Stóralda moraine in front of Svínafellsjökull (Fig. 1), which has been dated approximately ~2500 years old (Þórarinsson 1964). Furthermore, 100 m outside the LIA moraines of Fjallsjökull and Kvíárjökull are older moraines with dense vegetation cover (Björnsson 1998a). This illustrates that some glaciers had been larger in the Holocene than during the LIA. The LIA terminal moraines in the forefield of the outlets of southeast Vatnajökull have been dated to the eighteenth or the nineteenth century by lichenometry and a few by tephrochronology (e.g. Gordon and Sharp 1983; Snorrason 1984; Thompson and Jones 1986; Thompson 1988; Guðmundsson 1998; Evans *et al.* 1999; Dabski 2002, 2007; McKinzey *et al.* 2004, 2005a, 2005b; Bradwell 2004; Bradwell *et al.* 2006; Ómarsdóttir 2007; Chenet *et al.* 2010).

Iceland is located at major climatic and oceanographic boundaries in the North Atlantic, where the warm Irminger current meets the cold East Greenland current (Fig. 1) and is in the northern part of the storm tracks (Ólafsson *et al.* 2007). Changes in the atmospheric and ocean circulation influences the mass balance of the temperate glaciers and ice caps in Iceland. They cover about 11% of the land area (Björnsson and Pálsson 2008), and their mass balance sensitivities to climate warming are among the highest in the world (De Woul and Hock 2005) ranging from –3.0 to –0.6 m w.e. $°C^{-1}$ (Björnsson *et al.* 2013 and references therein). The highest rate of glacier meltwater input to the North Atlantic Ocean apart from Greenland comes from the Icelandic ice caps (Björnsson *et al.* 2013). The melting ice caps and glaciers outside the polar areas constitute more than half of the contribution of continental ice to the global mean sea level rise in the twentieth century (Church *et al.* 2013). Information on the volume of ice stored in glaciers at different times is essential to infer about their contribution to sea level rise (e.g. Leclercq *et al.* 2011; Grinsted 2013). Only a few studies have reconstructed the LIA glacier surface geometry from glacial geomorphological and historical evidence (e.g. Rabatel *et al.* 2006; Steiner *et al.* 2008; Knoll *et al.* 2009; Glasser *et al.* 2011; Vallis 2013).

On the narrow strip of land south of Vatnajökull, people have lived in close proximity to the glaciers for centuries and explorers of the eighteenth and nineteenth centuries had to cross the glaciers and/or the glacial rivers when passing through the lowlands, resulting in numerous contemporary descriptions of the dynamic environment. We give an overview of the fluctuations of the non-surging glaciers of southeast Vatnajökull during the time period 1650–1900, as evidenced in written historical sources, and the timing of the LIA maximum is determined from those records. Well preserved glacial geomorphological features, including lateral and terminal moraines and trimlines, delineate the LIA maximum extent of the outlet glaciers of southeast Vatnajökull. This is the first time extensive mapping of these up-valley glacial geomorphological landforms has been done to determine the LIA maximum glacier surface geometry and to obtain quantitative estimates of the glacial extent and volume during this advanced stage. From the highest up-valley lateral moraines, we assess the *equilibrium line altitude* (*ELA*) of the LIA and compare it with the present day ELA derived from satellite images.

Study area

The outlets of southeast Vatnajökull analyzed in this study are non-surging glaciers, less than 100 km apart and most of them reach down to 20–100 m a.s.l. (Fig. 1). Of the outlet glaciers of southeast Vatnajökull, only the eastern arm of Breiðamerkurjökull is recorded to have surged (Björnsson *et al.* 2003). The glaciers are located in the warmest and wettest part of Iceland. Seasonal variations in temperature on the south coast are small, average winter temperature is around 0°C and average July temperature close to 11°C (Björnsson *et al.* 2007). The climate is characterized by heavy winter precipitation in the range of 1000–2000 mm at the lowland meteorological sta-

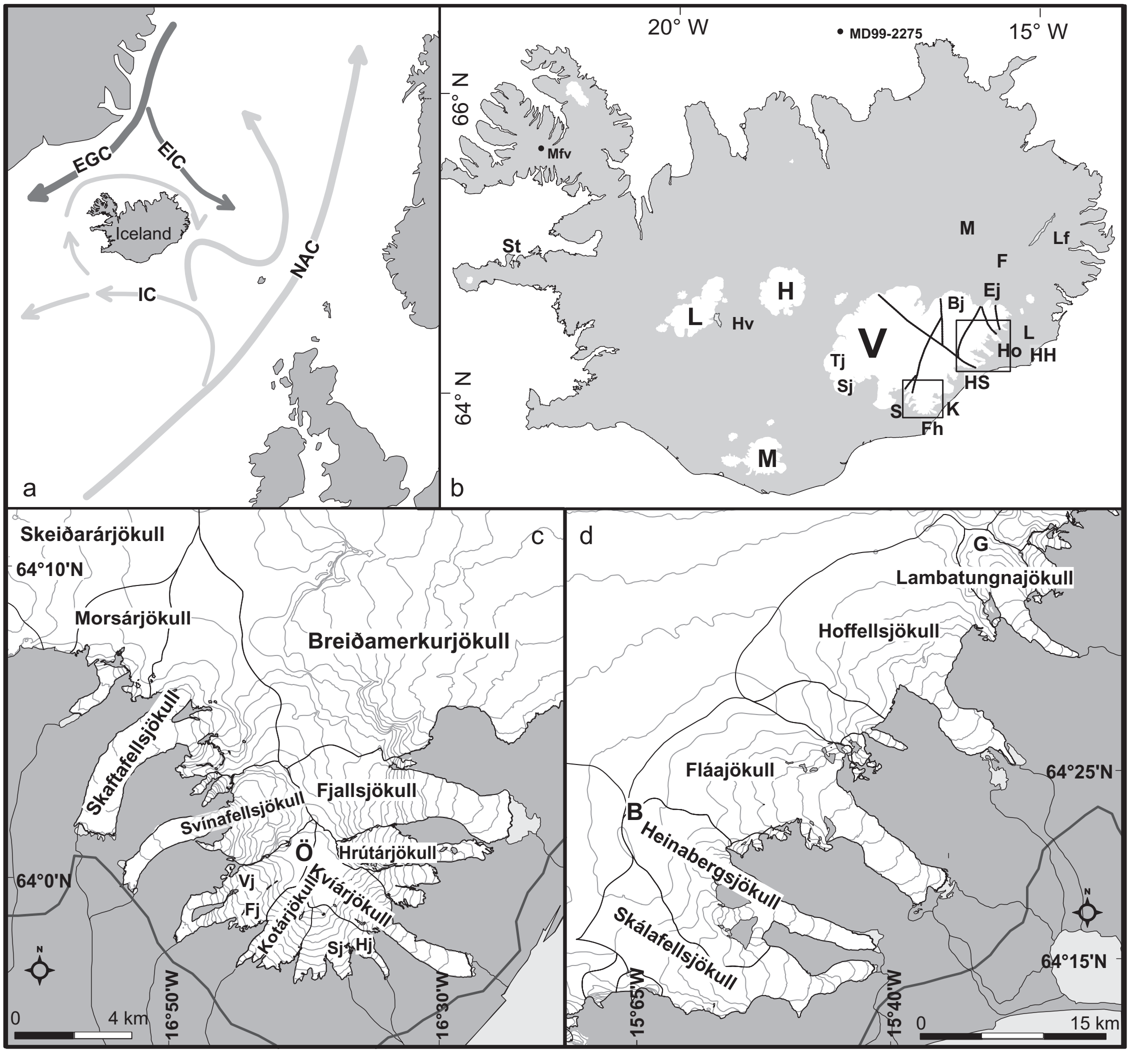

Fig. 1. (a) Iceland and modern ocean surface circulation patterns in the North Atlantic; NAC = North Atlantic Current, IC = Irminger Current, EGC = East Greenland Current, EIC = East Icelandic Current, modified from Knudsen *et al*. (2012). (b) Iceland and its ice caps, Vatnajökull (V), Langjökull (L), Hofsjökull (H), and Mýrdalsjökull (M). Meteorological stations are indicated with letters: Höfn in Hornafjörður (HH), Kvísker (K), Fagurhólsmýri (Fh), Skaftafell (S) and Stykkishólmur (St). Historical routes between northeast and southeast Iceland are indicated with dotted lines (modified from Björnsson 2009). Farms that were said to have traded before Vatnajökull closed off the routes are marked with the following letters, Möðrudalur (M), Fljótsdalur (F), Lón (L), Hoffell (Ho), Hálsatindur in Suðursveit (HS), Skaftafell (S). Other sites mentioned in the text: Hvítárvatn (Hv), Lagarfljót (Lf), Mýfluguvatn (Mfv), marine core MD99-2275, Tungnafellsjökull (Tj), Síðujökull (Sj), Brúarjökull (Bj), and Eyjabakkajökull (Ej). The insets frame the two study areas. (c, d) The studied outlets of southeast Vatnajökull in 2010. Ice divides are delineated in black, derived from the 2010 LiDAR DEM (Icelandic Meteorological Office and Institute of Earth Sciences, University of Iceland 2013). Nunataks are marked in gray, and 100 m contour lines of the LiDAR DEM are shown. Highway 1 is shown with a dark gray line, the glacial rivers in black, and ice-marginal lakes in light gray. (c) Morsárjökull and glaciers draining Öræfajökull ice cap (Ö). Only labelled glaciers are included in this study. Outlets mentioned later in the text: Virkisjökull (Vj), Falljökull (Fj), Stigárjökull (St), and Hólárjökull (Hj). (d) The outlet glaciers east of Breiðamerkurjökull (the eastern outlets), descending from the dome of Breiðabunga (B) and mountainous area of Goðahnúkar (G). Note the different scales of the two figures (c) and (d).

tions. The head of most of Öræfajökull's outlet glaciers is around 2000 m a.s.l., whereas the outlet glaciers east of Breiðamerkurjökull (hereafter referred to as the eastern outlet glaciers) descend from an elevation of approximately 1500 m a.s.l. (Fig. 1). The bedrock topography from the outlet glaciers is known from radio echo sounding measurements, and the outlets have carved into soft glacial and glaciofluvial sediments, forming depressions that are or will be occupied by ice-marginal lakes as a result of future warming (Björnsson 1996, 1998b, 2009; Magnússon *et al*. 2007, 2012; Schomacker 2010). It is unlikely that the troughs were only formed during the LIA, considering the present rate of sediment transport in the main glacial rivers of Öræfajökull (Magnússon *et al*. 2012).

Data

LIA geomorphological features

Glacial geomorphological features, including lateral and terminal moraines, trimlines, glacier erratics, and shorelines of former ice-dammed lakes, outlining the LIA maximum extent of southeast Vatnajökull's outlet glaciers are well preserved and have been mapped (Fig. 2). In many places, lateral moraines are found on both sides of the glaciers. Parts of the moraine systems in the forefield have been eroded by the glacial rivers and jökulhlaups, however, at least part of LIA terminal moraines are detectable in front of all the outlet glaciers.

Historical documents and local knowledge

Information on glacier extent and variations of southeast Vatnajökull has been retrieved from numerous historical documents (e.g. Bárðarson 1934; Þórarinsson 1939, 1943, 1956, 1964; Snorrason 1984; Björnsson 1998a, 2009; Grove 2004; McKinzey *et al*. 2005a; Sigurðsson 2005). Þórarinsson gathered local knowledge of farmers, who lived in the areas bordering the ice cap and had experienced how the glaciers advanced and had devastating impact on their livelihood. The historical sources presented here include the official county and parish reports (~1700–1900) and land registers since the early eighteenth century; travel diaries of Icelandic naturalists; descriptions of foreign travelers; and local accounts and oral tradition. A few accounts report on the complete southeast stretch of Vatnajökull, providing contemporaneous descriptions of the outlet glaciers. The proximity of the glaciers to farms and main travel routes has influenced how well they are represented in the literature. Interviews with old farmers living in the area were conducted in the summer of 2007 to collect local knowledge on glacier changes and gather historical photographs. Many of them recalled old people saying that the glaciers reached their greatest extent in the last decade of the nineteenth century.

Historical maps and photographs

A number of historical maps are preserved from the sixteenth century onwards portraying the Icelandic glaciers and their names (National and University Library of Iceland, http://islandskort.is/en/). Abraham Ortelius' Iceland map from 1590 shows many of the glaciers in Iceland, however Vatnajökull is not drawn on the map. Eiríksson and Schöning's map, that was published in Ólafsson and Pálsson's travel book from the mid-eighteenth century, shows Vatnajökull and its outlet glaciers some of which are named correctly. In Sveinn Pálsson's treatise from 1794 a map of Vatnajökull is presented, with a limited number of place names. Björn Gunnlaugson's Iceland maps of 1831–1843 show more detail than previous maps, for example how glaciers coalesced and closed off mountains; Breiðamerkurjökull and Fjallsjökull evidently merged in the forefield at that time.

A number of photographs are preserved from the last decade of the nineteenth century, and the first years of the twentieth century (Fig. 3 and Table 1). The photographs taken by Frederick W. Howell in 1891 of a number of Öræfajökull's outlet glaciers (Fiske Icelandic collection, Cornell University, http://cidc.library.cornell.edu/howell/), are the oldest known set of photographs of Icelandic glaciers. His photographs of Kotárjökull have provided information on elevation changes between 1890 and 2010 derived by repeat photography (Guðmundsson *et al*. 2012). A number of photographs are preserved from the time of the surveys of the Danish General Staff in 1902–1904 (archives of the National Land Survey of Iceland, http://atlas.lmi.is/islandskort-dana/ljosmyndir.php).

Maps from 1904

The oldest reliable maps (1:50.000) of the outlet glaciers were made by the Danish General Staff (1904), based on trigonometrical geodetic surveys conducted in the summers of 1902–1904 (Fig. 4 and Table 2). Considerable distortion was observed in the horizontal field of the maps, due to errors in the first trigonometric survey network for Iceland established by the Danish Geodetic Institute (Böðvarsson 1996; Pálsson *et al*. 2012), but fewer errors were discovered in the vertical component. Comparison of the elevation of trigonometrical

Fig. 2. Examples of lateral moraines outlining the LIA extent of southeast Vatnajökull's outlet glaciers (photos: Hrafnhildur Hannesdóttir). (a) Trimlines east of Skaftafellsjökull. (b) Lateral moraine west of Skaftafellsjökull. (c) Lateral moraine of Hrútárjökull in Ærfjall. (d) Lateral moraine of Fjallsjökull in Ærfjall. (e) Lateral moraine of Skálafellsjökull in Hafrafell. (f) Lateral moraine on the slopes of Vatnsdalur valley, representing the position of the glacier tongue damming the lake of Vatnsdalur at its maximum size. (g) Lateral moraine of Skálafellsjökull close to Sultartungnajökull. (h) Lateral moraine of Heinabergsjökull, at the col between Vatnsdalur and Heinabergsdalur. (i) Lateral moraine of Skálafellsjökull in Skálafellshnúta. (j) Lateral moraine above Lambatungnajökull, Skyndidalur valley in the background. For location of photos, see Figs 5 and 6.

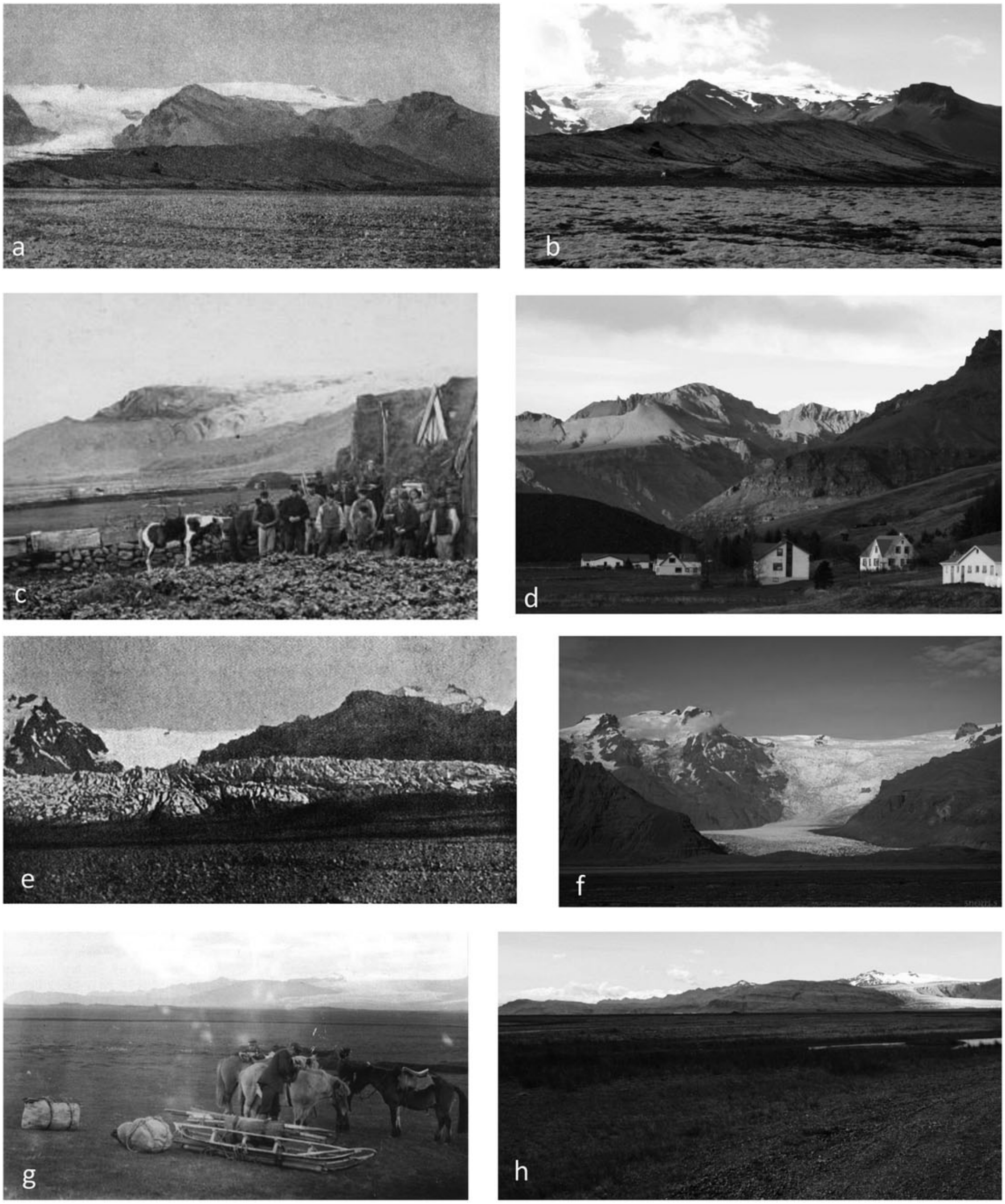

Fig. 3. Examples of historical photographs used in the reconstruction of the LIA glacier surface geometry. (a) Kvíárjökull by Frederick Howell in 1891 (Thoroddsen 1925). (b) Kvíárjökull in 2014 (photo: Hrafnhildur Hannesdóttir). (c) Svínafellsjökull in 1891 (photo: Frederick Howell). (d) the Svínafell moraines in 2010 (photo: Jóhann Helgason). (e) Svínafellsjökull by Tretow-Loof in 1902–1904 (Bruun 1928). (f) Svínafellsjökull in 2012 (photo: Snorri Sævarsson). (g) Skálafellsjökull in 1902 (photograph of the Danish General Staff, published in Jónsson 2004). (h) Skálafellsjökull in 2014 (photo: Hrafnhildur Hannesdóttir). For the location of photographs, see Figs 5 and 6.

Table 1. List of historical photographs of the outlet glaciers of southeast Vatnajökull.

Glacier	Photographer	Year	Reference
Kotárjökull	Howell	1891	Cornell University Library website
Kvíárjökull	Howell	1891	Thoroddsen (1925)
Svínafellsjökull (from farm)	Howell	1891	Cornell University Library website
Svínafellsjökull (from moraines)	Tretow Loof	1902–1904	Bruun (1928) and Thoroddsen (1925)
Svínafellsjökull (from farm)	Daniel Bruun	1902–1904	Hornafjörður cultural center
Skálafellsjökull (from the sandur)	unknown	1902–1904	National Land Survey of Iceland, Jónsson (2004)
Fláajökull/Humarkló nunatak	unknown	1902–1904	National Land Survey of Iceland

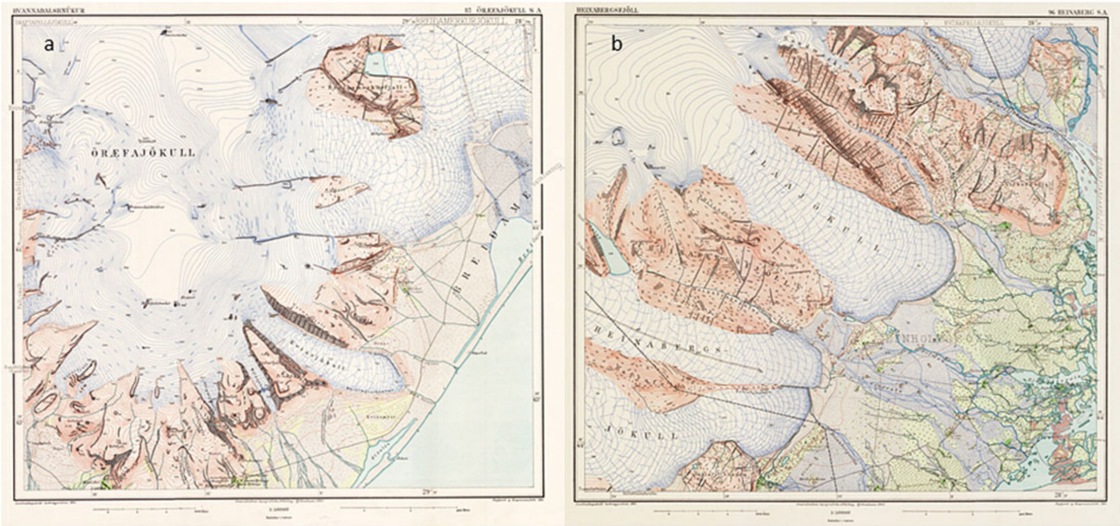

Fig. 4. Two maps from 1904. (a) Öræfajökull ice cap (Danish General Staff 1904, sheet 87-SA). (b) Skálafellsjökull, Heinabergsjökull, Fláajökull and the terminus of Hoffellsjökull (Danish General Staff 1904, sheet 96-NA).

points on the maps of definite landmarks (such as conspicuous mountain peaks) with the LiDAR *digital elevation model* (*DEM*) revealed an elevation difference of 10 m on average, the 1904 maps generally showed higher values (see also Guðmundsson *et al*. 2012). Thus, the trigonometrical points were considered to be reliable elevational signposts with an error of ±10 m, but the contour lines of the glaciers on the maps are inaccurate estimates of the surface topography. Lambatungnajökull was not surveyed at this time, and only the very front of Hoffellsjökull (Fig. 4).

LiDAR DEMs

The most accurate DEM of southeast Vatnajökull was produced with airborne laser surveys (LiDAR) in late August–September 2010 and 2011 (Jóhannesson *et al*. 2013; Icelandic Meteorological Office and Institute of Earth Sciences, University

Table 2. The Danish General maps of 1904, 1:50.000 (Danish General Staff 1904).

Map sheet	Coverage
87 SA Öræfajökull	Öræfajökull ice cap and the upper part of the acc. area of Skaftafellsjökull and Svínafellsjökull
87 SV Öræfajökull	The lower ablation area of Morsárjökull, Skaftafellsjökull and Svínafellsjökull
87 NV Öræfajökull	Morsárjökull and part of the upper accumulation area of Skaftafellsjökull
96 NA Heinaberg	Part of ablation area of Skálafellsj. and Heinabergsj., Fláaj. up to 1100 m a.s.l., the snout of Hoffellsjökull
97 NA Kálfafellsstaður	Sultartungnajökull, outlet of Skálafellsjökull
97 NV Kálfafellsstaður	Part of the western rim of Skálafellsjökull

Table 3. The images/photos used in outlining the LIA glacier extent. The resolution of the images indicated in parenthesis in the first column.

Airborne imagery	Time period	References/photographer
Aerial images (<1 m)	2001, 2002, 2003	Loftmyndir ehf
Oblique aerial photographs	2000–2012	Helgi Björnsson, Snævarr Guðmundsson, Víðir Reynisson
Aerial photographs	1945, 1960, 1982, 1989	National Land Survey of Iceland (http://www.lmi.is/loftmyndasafn-2/)
Satellite images (5 m)	2005	SPOT5 (SpotImage©)

of Iceland 2013). The vertical and horizontal accuracy of the survey is <0.5 m and DEMs with a resolution of 5×5 m have been produced. The DEMs serve as a topographical reference, covering areas bordering the glaciers, thus providing accurate elevation of the suite of geomorphological features outlining the LIA maximum glacier extent.

Airborne imagery

Airborne imagery was used to map the geomorphological features marking the ice extent of the LIA maximum (Table 3). They include oblique aerial photographs taken from airplanes, aerial photographs of the National Land Survey of Iceland, SPOT5 satellite images and the high-resolution images of Loftmyndir ehf. All images are from late summer or early fall. The color images of Loftmyndir ehf from 2001–2003 demonstrate most clearly the geomorphic fingerprint of the outlets at the LIA maximum. They cover land areas bordering the outlets in the lower reaches, however upper parts of the accumulation areas have not been surveyed.

Bedrock data

The bedrock topography of the outlet glaciers has been derived from radio echo sounding measurements in the last two decades (Björnsson and Pálsson 2004, 2008; Magnússon *et al*. 2007, 2012; Björnsson 2009; database of the Glaciology Group of the Institute of Earth Science, University of Iceland). Some of the glaciers have eroded their bed 100–200 m below sea level. Using this dataset combined with the reconstructed LIA glacier surface topography we estimate the total ice volume of the studied glaciers at the LIA maximum.

Methods

Delineating the LIA maximum glacier extent

Detailed field surveys were carried out in the summers of 2007 and 2008, mapping LIA glacial geomorphological features (Fig. 2) with a GPS. The 2010 LiDAR DEM provides precise elevation of the glacial geomorphological features and glacier surface elevation around the nunataks in the accumulation area. A laser rangefinder with accuracy of ±0.3 m was used to map lateral moraines and erratics in unreachable areas. The thin soil cover (in some places non-existing, see Fig. 2) along the glacier margin does not allow the use of tephrochronology for dating the lateral moraines. The extent of the outlet glaciers at the LIA maximum was also determined from the historical photographs, written documents and airborne images. The obvious distinction between the younger vegetation on the glacier side of the lateral moraines versus the thicker vegetation cover on the other side is also used as an indicator of the LIA glacial extent (see for example Matthews 1992). The terminal LIA moraines are shown on the 1904 maps, typically 200–300 m in front of the glacier termini. We assume that the LIA terminal moraines and highest lateral moraines are contemporary, although lateral moraines may be formed by repeated glacier advances (e.g. Small 1983; Nye 1990; Kruger 1994; Evans and Twigg 2002; Iturrizaga 2008; Curry *et al*. 2009; Sigurðardóttir 2014).

Reconstructing the glacier surface geometry at the LIA maximum

Surface elevation changes are determined from the LIA glacial geomorphological features, historical photographs and information from the 1904 maps. The crest of the LIA lateral moraines was used for determining the previous glacier surface level at their maximum extent. Nunataks depicted on the historical photographs from the turn of the nineteenth century were compared with duplicate modern photographs to estimate changes of the glacier surface (Fig. 3a, b, e–h and Table 1). The photo pairs are overlain and from the size of the nunataks the surface elevation changes were assessed. It provides estimates in the upper reaches of the glaciers where geomorphological data are sparse or absent. The elevation of the trigonometrical points on the 1904 maps were used for reference in reconstructing the LIA glacier surface. The presence or absence of present day (2010) nunataks on the 1904 maps provided information on minimum surface elevation changes in areas where LIA geomorphological features are scarce. Trimlines and lateral moraines on nunataks were delineated from the high-resolution aerial images of Loftmyndir ehf. The images also allow identification of glacially eroded bedrock and cliffs.

The 2010 glacier surface elevation of the LiDAR DEM were plotted against all data points used to reconstruct the LIA glacier surface geometry, including elevation of lateral moraines, trigonometrical points of the 1904 maps, and photographic evidence. Best-fit lines were drawn through the dataset of each glacier, and used in the reconstruction of the glacier surface. Convex contour lines were drawn by hand from the elevation of the geomorphological features. Comparison of various DEMs of the twentieth century reveals little or no change in the shape of contour lines in the accumulation area of the southeast outlet glaciers (Hannesdóttir *et al.* 2014b). The LiDAR DEMs were thus used as topographic reference and the contour lines in the accumulation area raised according to the surface elevation change data. A conservative vertical error estimate for the reconstructed LIA maximum glacier surface is ±15 m. The surface elevation reconstruction in the accumulation area of Öræfajökull's outlet glaciers (Fig. 1c) was based on more control points than the upper reaches of the eastern outlet glaciers (Fig. 1d). By assuming similar surface elevation changes in the upper reaches for the same altitude interval for all glaciers, estimates of the LIA glacier surface elevation on Öræfajökull were extrapolated to the eastern outlet glaciers. Similar downwasting in the accumulation area of all the outlet glaciers during various time periods of the twentieth century has been observed (Hannesdóttir *et al.* 2014b), supporting this approximation. Ice divides in 1890 were assumed to be the same as in 2010, which were obtained from the LiDAR DEMs. Central ice divides of the surge-type glaciers of Vatnajökull are known to have moved following surges (Björnsson *et al.* 2003). Due to lack of better data we are left with this assumption, and the area possibly affected by surges is small compared with the total area of the outlets. The surges of Skeiðarjökull 1991 and Dyngjujökull 1999 caused ice divides to shift on the order of a few hundred meters.

Estimating the ELA at the LIA maximum

Lateral moraines are only deposited below the ELA, where ice flow is emerging and the glacier transports ice and debris to the surface (e.g. Paterson 1994; Benn and Evans 2010). The maximum elevation of lateral moraines has been used to estimate the paleo-ELAs of former glaciers, assuming they correspond with the ELA at time of deposition (e.g. Hawkins 1985; Nesje 1992; Dahl *et al.* 2003; Benn *et al.* 2005). This method determines the minimum elevation of former glaciers' ELAs, especially in basins where moraines are well preserved and where the accumulation area ratio is poorly constrained (Richards *et al.* 2000; Benn *et al.* 2005). The elevation of the highest up-valley lateral moraines along the margin of the outlet glaciers of southeast Vatnajökull was used to estimate the ELA during the LIA maximum.

Results

Variations of the outlet glaciers of southeast Vatnajökull 1650–1900

In the following section historical data on the fluctuations of the outlet glaciers of southeast Vatnajökull are presented. Descriptions of advancing glaciers are more frequent than details on their retreat. The migrating glacial rivers, which made traverses more difficult and destroyed farmland, are frequently mentioned, as well as details on when historical routes and pastures became inaccessible due to advancing glaciers, and when farms were abandoned. Historical routes between farms in southeast and northeast Iceland were no longer used in the late sixteenth and early seventeenth centuries due to advancing glaciers (Þorkelsson 1918–1920; Jónsson 1945; Pálsson 1945, 2004; Björnsson 1979; Tómasson 1980; Jónsson 2004). Farmers living in northeast Iceland had until that time come to the southeast coast to fish, and cut birch in the forests of Skaftafell, whereas farmers in the southeast came to the northeast to harvest hay and collect moss (Fig. 1; Þorkelsson 1918–1920; Pálsson 1945). The caldera of Grímsvötn in central Vatnajökull (1400 m a.s.l.) was already named before 1600, thus it must have been visited before that time, and the volcanic area was in all likelihood covered with ice then (Þórarinsson 1960). Vatnajökull has in some

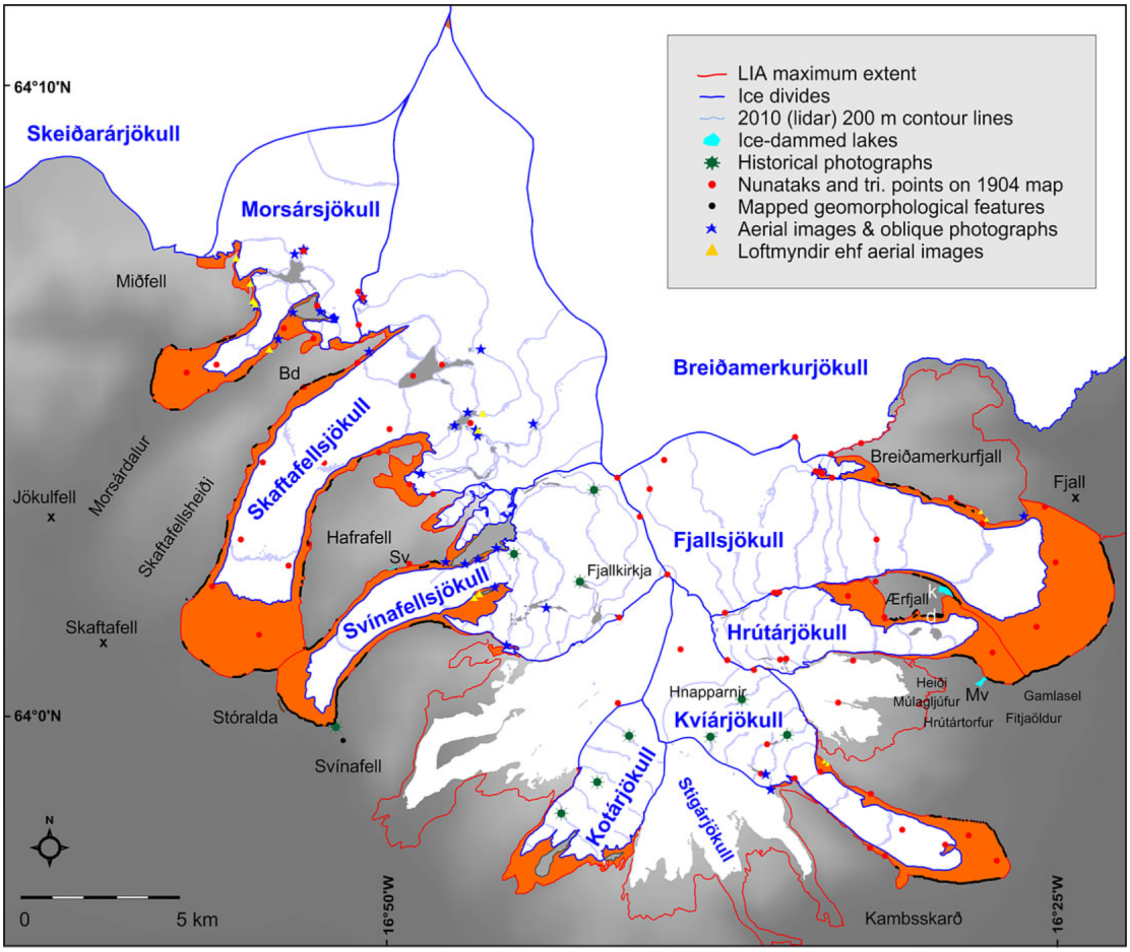

Fig. 5. The LIA maximum extent of the studied Öræfajökull outlet glaciers and Morsárjökull shown in orange. The LIA extent of other outlets (red line) is determined from the aerial images of Loftmyndir ehf (Guðmundsson unpubl.). The different archives used to determine the glacial extent and to reconstruct the LIA glacier surface are shown with different colored marks (see legend). The mapped glacial geomorphological features (in black) and that are also traceable on aerial images (in yellow) coincide in a number of sites. The 2010 surface map is derived from the LiDAR DEMs (shown here with 100 m contour lines). Location of abandoned farms is indicated with x. Remains of the historical route from Skaftafell have been observed in Birkidalur (Bd) and Miðfell. The location of photographs from Fig. 2 are shown with corresponding white letters. Ice-dammed lakes (in light blue): Sv = Svínavatn, Mv = Múlavatn and one in Ærfjall, the names are only suggested by the authors.

accounts since the eighteenth century been named Klofajökull (Olavius 1964–1965; Ólafsson and Pálsson 1981; Pálsson 2004). According to local residents the name comes from the many branches (outlets) that descended into the valleys (Pálsson 2004), but in Ólafsson and Pálsson's treatise (1981), the ice cap is said to take its name from two large glaciated areas separated by a mountain pass. The predecessors of farmers living at the foothills south of Öræfajökull around 1750 had not observed such advanced position of the nearest outlet glacier (most likely Stigárjökull, Fig. 5) as of that time (Ólafsson and Pálsson 1981).

Morsárjökull The historical route between Möðrudalur and Skaftafell (Fig. 1) was used as late as in the latter half of the sixteenth century (Thoroddsen 1958), but according to the land register from 1708 (Þorkelsson 1918–1920) it was no longer in use around 1700 due to the advancing glaciers. The farm Jökulfell in Morsárdalur had been abandoned sometime before 1708 (Þorkelsson 1918–1920). In 1756 Ólafsson and Pálsson travelled through the districts south of Vatnajökull and describe in their treatise (1981) how the glacial river had wiped away the vegetation of the valley. Thoroddsen (1911) mentioned a double series of moraines in front of the glacier in 1894, hence at that time the glacier was not at the LIA terminal moraines (dated to the late nineteenth century by Chenet *et al*. 2010), but had a similar terminus position, as in 1904.

Skaftafellsjökull and Svínafellsjökull Mt Hafrafell (Fig. 5) was used for sheep grazing, and the accessibility depended on the extent of Skaftafellsjökull and Svínafellsjökull. Around 1700 the two glaciers had merged, and the mountain was trapped in ice (Magnússon 1953; Þorkelsson 1918–1920). Birch wood, washed out from beneath Svínafellsjökull, and dated to 1690 ± 60 cal. yr BP, provides additional evidence of lesser glacial extent prior to 1700 (Ives 2007). Descriptions of the damage of pastures and hayfields caused by the glacial rivers and advancing glaciers, along with difficult access to Hafrafell, are prominent in accounts of the eighteenth century (Guðnason 1957; Pálsson 2004). The two outlet glaciers were advancing and terminated close to the two farms in 1794 (Pálsson 2004). In the early nineteenth century most outlet glaciers of Öræfajökull were advancing (Sigmundsson 1997). The Skaftafell farm was moved up to the hills of Skaftafellsheiði due to frequent jökulhlaups from Skeiðarárjökull in the first decades of the nineteenth century (Henderson 1957; Tómasson 1980). According to a local narrative, Svínafellsjökull retreated somewhat in the early nineteenth century (Ives 2007), and then advanced in the 1830s (Sigmundsson 1997), and again in the 1860s and 1870s (Paijkull 1866; Gadde 1983). Around 1870 blocks of ice broke off the glacier and rolled down the slope of the LIA terminal moraine ridge (Þórarinsson 1964). Skaftafellsjökull had been receding since about 1880 according to local knowledge (Þórarinsson 1943).

Kotárjökull Around 1702 the river Kotá had destroyed hayfields of farms south of Kotárjökull (Magnússon 1953). Thoroddsen (1896) describes how the western and eastern glacier tongues of Kotárjökull surrounded Rótarfjall and merged in the valley in the 1890s.

Kvíárjökull Kvíárjökull advanced in the seventeenth century and the river migrated and cut through the eastern moraine (Fig. 5; Björnsson 1956). The glacier probably reached the crest of the 100 m high frontal moraines in the 1750s (Björnsson 1979), and in 1794 (Pálsson 2004). According to Björnsson (1956), the glacier likely advanced until the end of the nineteenth century, when it reached its maximum extent. The moraines are formed during repeated advances according to geomorphological studies (Iturrizaga 2008; Sigurðardóttir 2014). In the time period 1870–1890, the glacier reached the moraine crests and blocks of ice rolled down the outer slopes of the moraines (Björnsson 1998a), in accordance with the photograph taken by Howell in 1891 (Fig. 3a).

Hrútárjökull and Fjallsjökull The farm Fjall (cultivated since 900), at the foothills of Breiðamerkurfjall (Fig. 5), had to be abandoned sometime before 1709 because Fjallsjökull and Breiðamerkurjökull were advancing, closing off Breiðamerkurfjall and Ærfjall (Fig. 5; cf. Þorkelsson 1918–1920; Björnsson 1979). Fjallsjökull was advancing in 1794 and merged (again) with Breiðamerkurjökull, which was pushed 'out of the way' (Pálsson 2004). Fjallsjökull must thus have retreated from its position around 1700. Most outlet glaciers of Öræfajökull were advancing in the early nineteenth century (Sigmundsson 1997). Hrútárjökull advanced between 1870 and 1877 and blocked the river of Múlagljúfur (Fig. 5; Björnsson 1958), and Fjallsjökull reached the LIA terminal moraines at Heiði and Hrútártorfur (Fig. 5), which according to local knowledge are from the mid-nineteenth century (Þórarinsson 1943; Björnsson 1998a). The recession from 1880 was interrupted by an advance in 1893–1894, when both glaciers were at the LIA terminal moraines (Thoroddsen 1911; Þórarinsson 1943; Björnsson 1998a). Ice-dammed lakes in Múlagljúfur and Ærfjall were formed as Hrútárjökull advanced (Fig. 5; Björnsson 1998a).

Skálafellsjökull and Heinabergsjökull The mountain route between Hálsatindur in Suðursveit and Möðrudalur (Fig. 1) was no longer used after 1575 (Sigmundsson 1997). The grassy pastures of Hafrafell were ~1750 enclosed in ice and Heinabergsjökull reached the fields of the farm Heinaberg (Fig. 6; Guðnason 1957; Ólafsson and Pálsson 1981). Sultartungnajökull, a small glacier tongue of Skálafellsjökull (Fig. 6), reached its maximum extent around 1750 (Þórarinsson 1943; Ólafsson and Pálsson 1981), and again in the late nineteenth century (Thoroddsen 1911). Rivers, that had since settlement followed the same course (Snorrason 1984), migrated and jökulhlaups from ice-dammed lakes spoilt farms in the forefield of the outlets, and

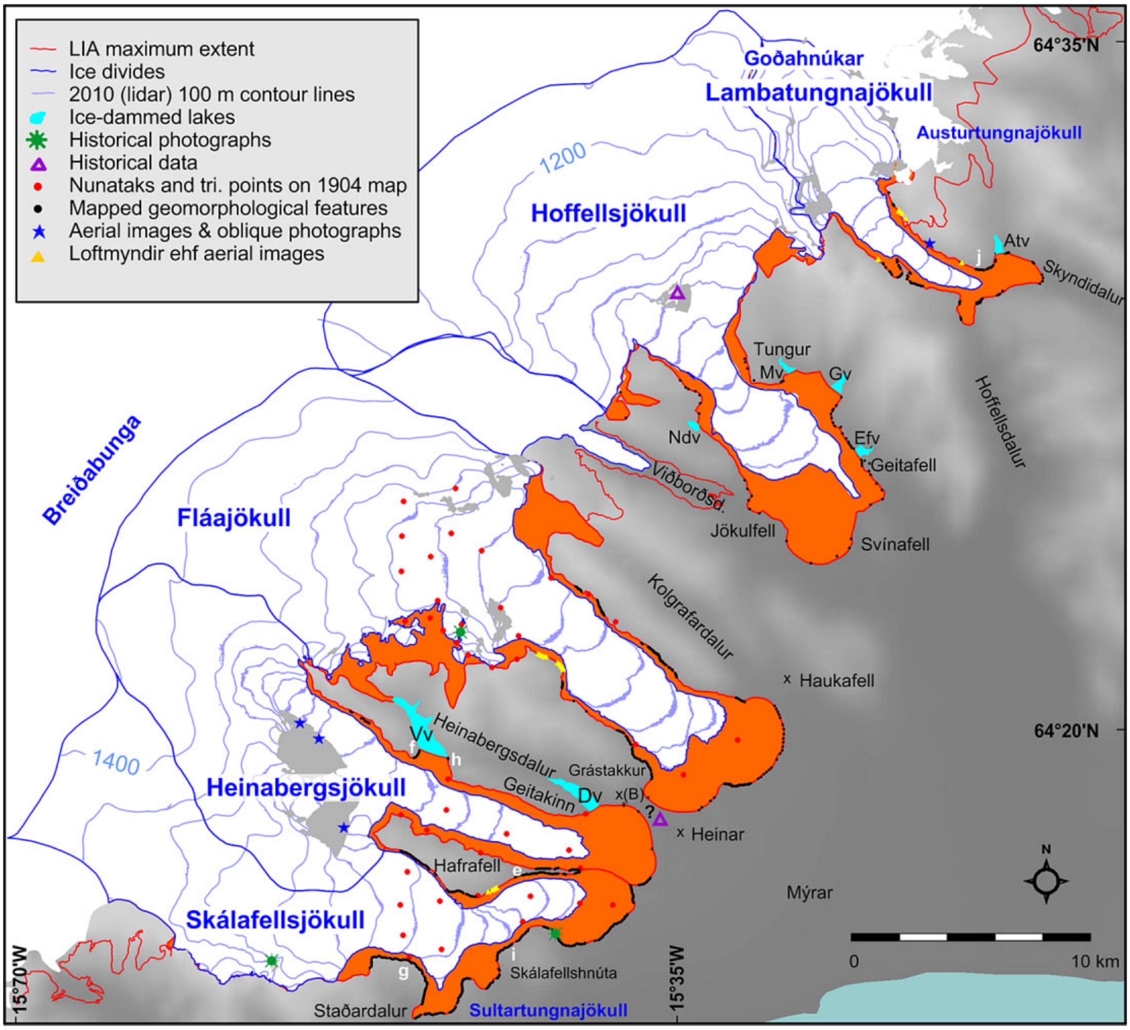

Fig. 6. The LIA maximum extent (in orange) of Skálafellsjökull, Heinabergsjökull, Fláajökull, Hoffellsjökull and Lambatungnajökull. The LIA extent of other outlets (red line) is determined from the aerial images of Loftmyndir ehf (Guðmundsson unpubl.). The different archives used to determine the glacial extent and reconstruct the LIA glacier surface geometry are shown with different colored marks (see legend). The surface map is derived from the LiDAR DEM (shown here with 100 m contour lines). The outlet glaciers dammed several lakes during their maximum extent (shown in light blue): Vv = Vatnsdalsvatn, Dv = Dalvatn, Gv = Gjávatn, Efv = Efstafellsvatn, Mv = Múlavatn, Ndv = Neðridalsvatn, Atv = Austurtungnavatn (Ndv and Atv named by the authors). Ruins of abandoned farms/houses shown with x. x(B) is a small shephards cottage (Bólstaður). Historical descriptions are not conclusive on the maximum extent of Fláajökull and Heinabergsjökull at the end of the nineteenth century (indicated with a question mark). Letters indicate the location of corresponding photographs in Fig. 2.

destroyed many of them in the 1830s (Sigmundsson 1997). In the parish descriptions from 1839 (Sigmundsson 1997) the glaciers are said to be slowly creeping forward. In 1887 the glaciers were at the LIA terminal moraines (Þórarinsson 1939), and 7 years later when Thoroddsen (1911) visited the area, the glaciers had started retreating.

Historical documents are not conclusive on whether Heinabergsjökull and Fláajökull merged during the LIA maximum, and their LIA terminal moraines have partly been eroded. A number of accounts describe how the two glaciers *almost met* at the farm Heinar in the 1860s and 1870s and were very close to the outermost moraines on the sandur (Torell 1857; Paijkull 1866; Thoroddsen 1892; Þórarinsson 1943; Fig. 6). We found the Öræfajökull 1362 tephra layer in a soil section on the slopes of Grástakkur (for location see Fig. 6) correlated with the tephra stratigraphy of Steinadalur

(Óladóttir *et al.* 2011). Close by, ruins of a small outhouse (belonging to the previous farm of Heinar) at 100 m a.s.l. are found. We found no glacial geomorphological features, confirming that Fláajökull and Heinabergsjökull had coalesced. However, Eiríksson (1932) was told by farmers that the two glaciers had met in front of Geitakinn around 1870, and flowed south of Heinar. Evans *et al.* (1999) reached the conclusion that the glaciers merged in the late nineteenth century based on tills and moraines in the forefield dated to the LIA.

Vatnsdalsvatn and Dalvatn Lakes Vatnsdalsvatn and Dalvatn (Fig. 6) were formed as Heinabergsjökull advanced and thickened in the seventeenth century (Þórarinsson 1939). Vatnsdalur was full of water up to the col in the 1860s and 1870s, and always had been as long as the oldest inhabitants could remember and drained regularly (Þórarinsson 1939). During the time period 1750–1890 Vatnsdalsvatn probably had a steady overflow to Heinabergsdalur (Fig. 6; Þórarinsson 1939; Snorrason 1984); the glacier was probably too thick to allow jökulhlaups to escape along the glacier bed. In 1898 Vatnsdalsvatn was emptied by a sudden catastrophic jökulhlaup. The lake was then emptied almost every year, but subsequent jökulhlaups were less violent (Gíslason 1954). Jökulhlaups from Dalvatn decreased in size from 1887 following the glacial retreat, and stopped in the 1920s when Heinabergsjökull no longer blocked the valley (Þórarinsson 1939). Þórarinsson (1939) and Snorrason (1984) suggested that the outlet glaciers of southeast Vatnajökull remained in their advanced stage from the middle of the eighteenth century until the end of the nineteenth century; their interpretation partly based on the record of jökulhlaups from Vatnsdalur, that did not occur until after the glacier started retreating and thinned in the late 1890s.

Fláajökull The farm Haukafell (Fig. 6) had to be abandoned around 1720 (Guðnason 1957), and the forest in the neighboring Viðborðsdalur to the east (Fig. 6) was damaged around 1700 due the advancing glacier (Þorkelsson 1918–1920). The glacier was growing in the 1830s, and jökulhlaups were released from ice-dammed lakes (Sigmundsson 1997). Fláajökull was slightly more advanced around 1880 than about 1850 (Jónsson 1945). Around 1880 the farm Haukafell was moved farther east to escape from the advancing glacier, which almost closed off Kolgrafardalur (Benediktsson 1972). Fláajökull overrode thick vegetated soil around 1880, indicating that it had not recently advanced that far (Benediktsson 1972). From 1882 to 1894 the glacier advanced and receded three times (the glacier likely advancing in late winter, and retreating during the summer months), and was at the LIA terminal moraines in 1894 (Thoroddsen 1958).

Hoffellsjökull Mountain routes between Hornafjörður and Fljótsdalur (Fig. 1) became impassable around 1640 due to advancing glaciers (Magnússon 1953). Around 1750 Hoffellsjökull had advanced to Svínafell (Fig. 6) (Guðnason 1957). However, the glacier presumably did not fill up the valley, since accounts describe how shepherds reached pastures further in the valley on flat sandy terrain (Fig. 6) in the late eighteenth century (Björnsson and Pálsson 2004). Descriptions from the late 1830s indicate that the glacier was advancing, and jökulhlaups originating from ice-dammed lakes prevented river crossings on the sandur (Sigmundsson 1997; Jónsson 2004). At that time the western arm of the glacier was close to the hill of Jökulfell (Þórarinsson 1943; Sigmundsson 1997). Svínafellsjökull reached the plains east of Svínafell in 1873 (Sigmundsson 1997). Farmers stated that the glacier was advancing slightly in the 1880s, reaching its maximum ~1890 or soon thereafter, and then started receding (Þórarinsson 1943; Jónsson 1945, 2004).

Lambatungnajökull Mountain routes between Hoffellsdalur and Möðrudalur (Fig. 1) closed off around 1650 due to advancing glaciers in Skyndidalur and Hoffellsdalur (Thoroddsen 1911; Jónsson 1945; Magnússon 1953). The river of Hoffellsdalur was in 1746 not influenced by glacial meltwater (Guðnason 1957). Descriptions from the parish letters (Sigmundsson 1997) of the nineteenth century (1841 and 1871) indicate that the glacier reached down into Hoffellsdalur, and the river was colored by the glacial meltwater. Glacial recession since the 1850s was interrupted by a number of re-advances (around 1870 and 1890), when the glacier was again close to the 1850 moraines (Þórarinsson 1943). In 1894 the outlet in Hoffellsdalur was at the LIA terminal moraines (Thoroddsen 1911; Jónsson 1945), and at the same time the main arm of Lambatungnajökull dammed the river from Austurtungnajökull (ice-dammed lake called Atv shown in Fig. 6) (Þórarinsson 1943).

The ~1890 glacier surface maps and volume

We rely on the historical accounts for dating the maximum LIA extent of the outlet glaciers of southeast Vatnajökull. From the documents it is clear that the outlets reached advanced positions in the eighteenth century, and some of them may have been as extensive then as in 1890, but the descriptions are not conclusive. Most glaciers were at their LIA terminal moraines *c*. 1880–1890, and a uniform date of ~1890 is assigned for the LIA glacier reconstruction for reference in the remainder of the text. All outlet glaciers of this study possess well defined LIA glacial geomorphological features along their margin in the ablation area, which are observed below 530–920 m a.s.l., depending on glacier (Figs 5 and 6). Below 400–500 m a.s.l. the LIA lateral moraines and trimlines are found above the glacier margin of the 1904 maps (but coincide above that elevation), indicating that downwasting in the time period ~1890–1904 was mainly confined to the glacier terminus.

Numerous photographs, from the time of maximum glacier extent show nunataks in the accumulation area (Fig. 3a, e, g). The prominent nunataks in the accumulation area of Kvíárjökull (Hnapparnir at around 1650 m a.s.l.; Fig. 5) and Svínafellsjökull (Fjallkirkja at around 1700 m a.s.l.), detectable on the old and new photographs (Fig. 2a, c), support the results of Guðmundsson *et al*. (2012) of negligible surface lowering in the upper reaches of the accumulation area in the post-LIA time period. The lower nunataks of Kvíárjökull (around 1150 m a.s.l.) were smaller in 1891 than today (approximately 10–15 m surface elevation difference). From the photograph of the terminus of Svínafellsjökull, taken by Howell in the same year (Fig. 3c), the glacier surface is calculated to be around 170 m a.s.l. Skálafellsjökull is viewed from a distance in Fig. 3(g), and the glacier margin in Skálafellshnúta (around an elevation of 350 m; Fig. 6) was in 1902–1904 at a similar altitude as the mapped LIA lateral moraines. Nunataks around 1200 m a.s.l. are visible in the background, evidently more covered in glacier ice than today; we roughly estimate a 15–20 m difference of the glacier surface elevation. This photograph is taken in the autumn, as indicated by the clear boundary between the dirty ice and white snow above; the snowline clearly lower than at present. None of these photographs have the potential for accurate calculation of glacier surface changes as was done for Kotárjökull (Guðmundsson *et al*. 2012). They are taken further away and lack the details to georeference the images with modern photographs. Poor resolution of the old images also hampers the use of accurate repeat photographical methods.

The 2010 glacier surface relative to the average glacier surface elevation difference between ~1890 and 2010 of every 20 m altitudinal interval is shown in Fig. 7. The scatter of the data, showing the different altitude of the geomorphological features on each side of individual glaciers, is related to the variable topography of the surrounding landscape. Also, the lateral moraines and trimlines may be formed at different times. The elevation difference in the accumulation area of Öræfajökull is ~30–50 m at 1000 m a.s.l., ~10–25 m around 1200 m a.s.l., diminishing linearly to negligible amounts above 1700 m a.s.l. (Fig. 7), determined from the cumulative dataset of historical photographs, the trigonometrical points, and presence and size of nunataks on the 1904 maps, Due to lack of data for the upper accumulation area on the eastern outlet glaciers, we estimate a surface change of 5–10 m on their ice divides (around 1500 m a.s.l.), based on surface elevation change for the same altitudinal range of the outlets of Öræfajökull.

The reconstructed surface maps of the LIA glaciers of southeast Vatnajökull are shown in Fig. 8. The margins of Fláajökull and Heinabergsjökull are drawn according to descriptions indicating a more limited extent, without the two adjacent glaciers merging. The area of the outlet glaciers in ~1890 is presented in Table 4. The ~1890 volume of each outlet glacier has been estimated by subtracting the bedrock DEM from the reconstructed ~1890 glacier surface DEM (Table 4). The average thickness of each glacier is also presented in the same table. The estimates of the ~1890 volume of Kotárjökull (Guðmundsson *et al.* 2012) and Hoffellsjökull (Björnsson and Pálsson 2004; Aðalgeirsdóttir *et al*. 2011), which are not included in this study, are shown in Table 4 and the LIA surface reconstruction in Fig. 8.

The maximum elevation of lateral moraines of every glacier ranges from 530 to 920 m used to infer the ELA of the LIA (Table 5 and Fig. 9). For comparison, the present day ELA, derived from the average snowline elevation during the time period 2007–2011 on MODIS images is shown in Fig. 9,

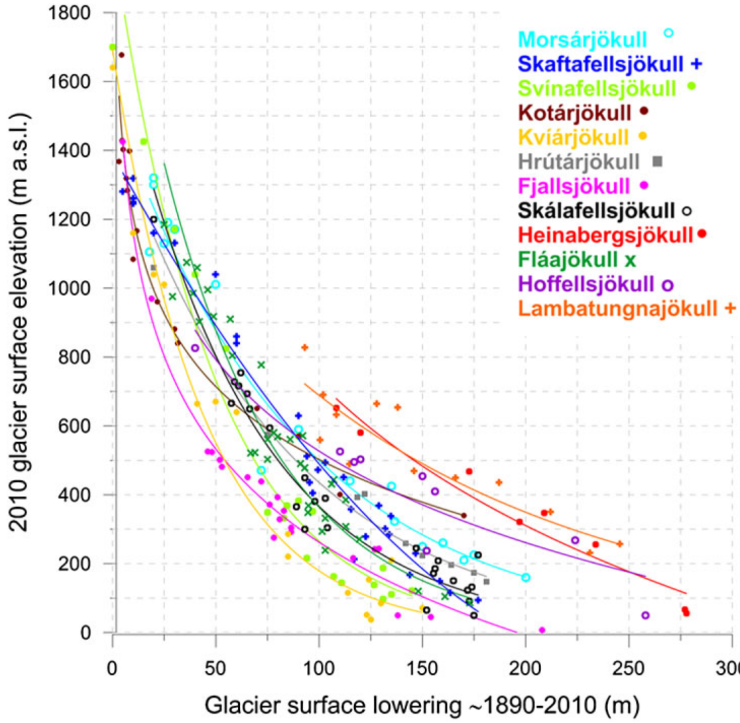

Fig. 7. The relationship between glacier surface elevation lowering ~1890–2010 of the outlet glaciers of southeast Vatnajökull and the 2010 LiDAR glacier surface. The average elevation difference for every 20 m elevation interval is plotted. No distinction is made between the type of data points, i.e. glacial geomorphological features, historical photographs, information derived from the 1904 maps and the aerial images of Loftmyndir ehf. Best fit exponential/logarithmic lines drawn through the dataset of each outlet glacier show the relation between surface elevation lowering and altitude, which was used in reconstructing the LIA maximum glacier surface geometry, with the LiDAR DEM as reference.

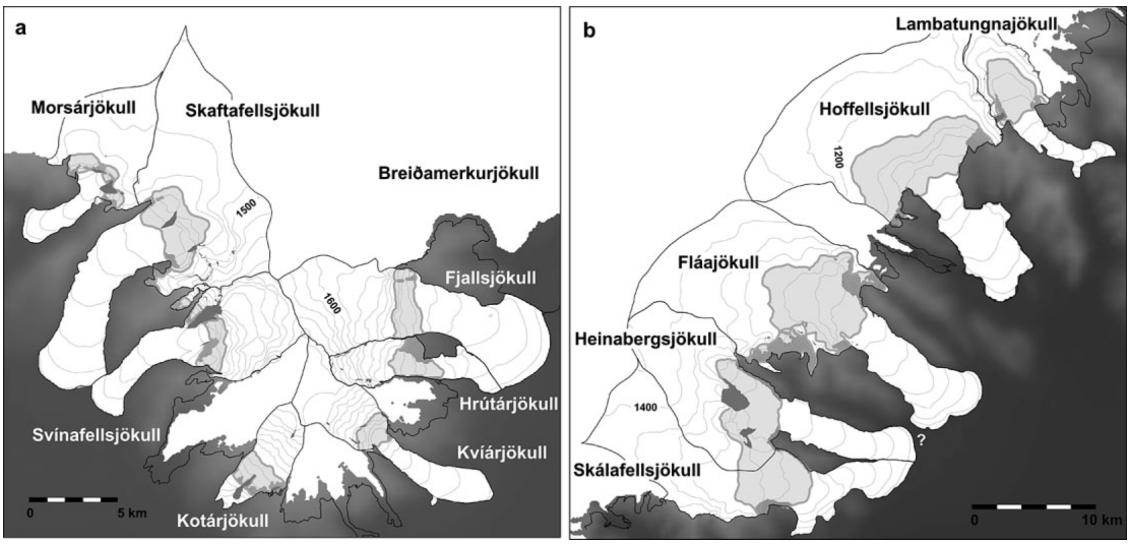

Fig. 8. The reconstructed ~1890 glacier surface map of the southeast outlet glaciers of Vatnajökull. (a) The glaciers of Öræfajökull and vicinity. The extent and LIA surface of Kotárjökull are from Guðmundsson *et al*. (2012). (b) The eastern outlet glaciers. Note the different scales of the figures. The LIA ELA and the modern ELA are shown with thick gray lines, and the area between shaded. The ~1890 glacier surface elevation in the accumulation area of Hoffellsjökull (Björnsson and Pálsson 2004), is likely overestimated due to lack of control points at the time of reconstruction.

Table 4. The ~1890 area, volume and average thickness of the outlet glaciers of southeast Vatnajökull.

Outlet glacier	Area (km^2)	Volume (km^3)	Ave. thickness (m)
Morsárjökull	35.3 ± 0.7	7.6 ± 0.4	215
Skaftafellsjökull	97.8 ± 1.3	24.8 ± 1.0	254
Svínafellsjökull	39.5 ± 0.9	5.2 ± 0.4	132
Kotárjökull	14.5 ± 0.4	2.2 ± 0.1	152
Kvíárjökull	27.9 ± 0.7	5.2 ± 0.3	187
Hrútárjökull	17.1 ± 0.5	1.9 ± 0.1	111
Fjallsjökull	57.7 ± 0.8	10.7 ± 0.6	185
Skálafellsjökull	117.9 ± 1.6	39.1 ± 1.2	332
Heinabergsjökull	120.3 ± 1.3	37.0 ± 1.2	308
Fláajökull	205.6 ± 1.9	64.3 ± 2.1	313
Hoffellsjökull*	234.0 ± 1.9	71.0 ± 2.3	303
Lambatungnajökull	46.1 ± 1.9	6.2 ± 0.5	135

* Aðalgeirsdóttir *et al*. (2011)

as well as estimates of the snowline in 1894 from Thoroddsen (1931–1935).

Discussion

Glacial variations and timing of the LIA maximum

Historical sources provide a means of assessing the timing of LIA glacier advances, and accurate age determination is possible where annually to decadally resolved records are available, as for example in the Alps (e.g. Holzhauser *et al*. 2005; Steiner *et al*. 2008; Zumbühl *et al*. 2008) and Norway (e.g. Grove 2004; Nussbaumer *et al*. 2011). The historical accounts describing the variations of the outlet glaciers of southeast Vatnajökull do not possess the same temporal resolution, and the glaciers' representation in the literature varies. Advancing glaciers in the 1830s and 1870s, are perhaps more apparent than earlier advances due to the detailed descriptions of the sheriffs and reverands of that time (Sigmundsson 1997). Björnsson (1998a) concluded that the outlets of Öræfajökull were less extensive in the eighteenth century than the nineteenth based on the descriptions of Ólafsson and Pálsson (1981) and Pálsson (2004) from the mid to late eighteenth century. Contemporary documents describe how the outlet glaciers advanced in the late eighteenth century and were at their LIA terminal moraines in the 1880s–1890s (Thoroddsen 1911; Þórarinsson 1943; Jónsson 1945; Björnsson 1998a). The older documents do not provide the same detailed conclusive information on glacier terminus position as descriptions from the late nineteenth century, and we cannot exclude that the outlets had reached as far earlier.

The historical photographs from the end of the nineteenth century and first years of the twentieth century provide additional evidence of the LIA maximum extent of the outlet glaciers. The photographs from Howell of Kotárjökull taken in 1891 demonstrate that the highest lateral moraines represent the LIA maximum glacier extent (Guðmundsson *et al*. 2012). His photograph of Kvíárjökull from the same year (Fig. 3a) shows that the glacier almost reached the crest of the moraines, in accordance with descriptions of ice-blocks rolling down the moraine wall in the 1870s to 1890s (Björnsson 1998a). Although the photograph of Skálafellsjökull (Fig. 3g) is from

Table 5. The altitude of the highest up-valley LIA lateral moraines, the average value of the average ELA elevation derived from MODIS images of 2007–2011 (Hannesdóttir *et al*. 2014b), the elevation difference between the two, and the snowline elevation as reported by Thoroddsen (1931–1935) in 1894.

Outlet glacier	max. elev. lat. mor. (m a.s.l.)	median-$ELA_{2007–2011}$ (m a.s.l.)	elev. diff. (m)	Þ. Thoroddsen (m a.s.l.)
Morsárjökull	720	1070	350	
Skaftafellsjökull	740	1080	340	
Svínafellsjökull	680	1060	380	
Kotárjökull	720	1070	350	
Kvíárjökull	710	1070	360	1020
Hrútárjökull	530	890	360	
Fjallsjökull	570	910	340	690
Skálafellsjökull	730	960	230	
Heinabergsjökull	620	1040	420	880
Fláajökull	660	1090	430	
Hoffellsjökull	640	1090	450	750
Lambatungnajökull	920	1160	240	940

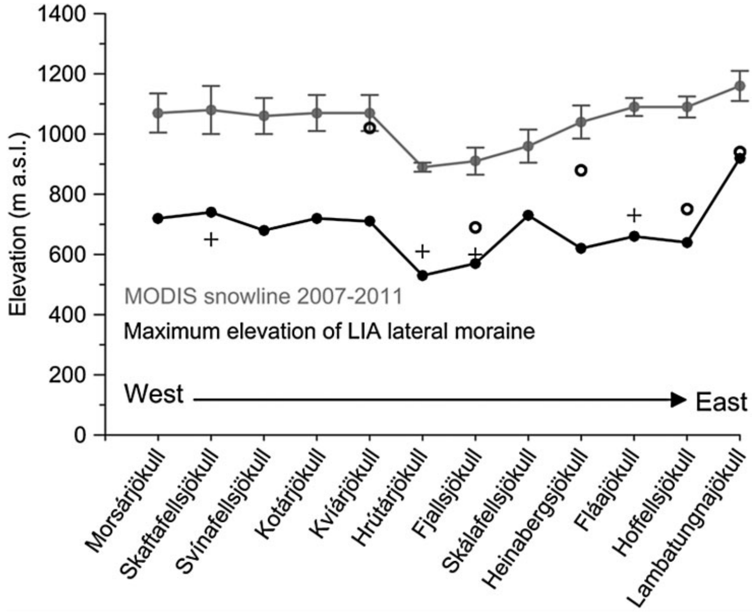

Fig. 9. The maximum elevation of the lateral moraines of the southeast outlet glaciers of Vatnajökull (black), the median value of the average ELA elevation span (gray), derived from MODIS images 2007–2011 (Hannesdóttir *et al.* 2014b) and the elevation of the snowline according to Thoroddsen in 1894 (1931–1935) with open black circles. The elevation where contour lines on the 1904 map change from being convex in the ablation area to concave in the accumulation area are shown with +.

1902 (at which time the glacier had probably been retreating for 10–15 years), it suggests that the highest lateral moraines on the southern side of the glacier in Skálafellshnúta (Fig. 6) are from the end of the nineteenth century. Other outlet glaciers of Öræfajökull (Stigárjökull, Hólárjökull, Falljökull and Virkisjökull) retreated from their LIA terminal moraines ~1880–1890 (Þórarinsson 1943). The large surging glaciers of Vatnajökull (Skeiðarárjökull, Tungnaárjökull, Síðujökull, Brúarjökull, Eyjabakkajökull, and Breiðamerkurjökull) also retreated from their LIA moraines ~1890 (Thoroddsen 1931–1935; Þórarinsson 1964; Tómasson and Vilmundardóttir 1967; Jóhannesson 1985; Björnsson 1998b).

According to lichenometric studies, the glaciers reached their LIA maximum in the late eighteenth or nineteenth century (Table 6). Different lichenometric dates are explained by various lichen calibration curves, different statistical analysis and field techniques, and asynchronous glacier advances (McKinzey *et al.* 2004; Orwin *et al.* 2008; Bradwell 2009; Dabski 2010; Jomelli *et al.* 2010; Chenet *et al.* 2011; Dabski and Tittenbrun 2013). Due to diverse bedrock minerology and different microclimate of each valley, causing different growing conditions for the lichens, intercomparison of lichenometric dates of the LIA moraines is difficult (e.g. Bradwell 2009 and references therein). Several authors have pointed out the problems of using lichenometry to date moraines in Iceland (Maizels and Dugmore 1985; Thompson and Jones 1986; Guðmundsson 1998; Kirkbride and Dugmore 2001; Kirkbride and Winkler 2012). It is beyond the scope of this paper to review the different measurement techniques and statistical methods or list the numerous biological and environmental uncertainties, and the readers are referred to the papers cited. Different lichenometric results have been reported from the exact same moraines, and some of the dates contradict information found in the detailed contemporary written sources. Different ages have been reported for the moraines of Kvíárjökull and Fláajökull (a difference of 80 years and 70 years respectively, Table 6); the older dates are inconsistent with written accounts, which explicitly state that the glaciers were at their LIA terminal moraines ~1890. The importance of using the historical documents to infer glacier fluctuations is emphasized. We rely on the historical data for timing the maximum LIA glacier extent because of the complications of using lichenometry to date moraines and the conflicting results.

Table 6. Lichenometric dates of terminal LIA moraines of the outlet glaciers of southeast Vatnajökull.

Glacier	LIA max (cal. yr. AD)	Error (–/+) yr	Reference
Morsárjökull	1888	9/15	Chenet *et al*. (2010)
Skaftafellsjökull	1878	12/14	Chenet *et al*. (2010)
Skaftafellsjökull	1870	n/a	Thompson and Jones (1986)
Skaftafellsjökull	1870	10/10	Ómarsdóttir (2007)
Svínafellsjökull	1765	14/21	Chenet *et al*. (2010)
Svínafellsjökull	1870	n/a	Thompson and Jones (1986)
Kotárjökull	1893	n/a	Thompson and Jones (1986)
Kotárjökull	1819	10/9	Chenet *et al*. (2010)
Kvíárjökull	1810	6/13	Chenet *et al*. (2010)
Kvíárjökull	1891	4/4	Evans *et al*. (1999)
Hrútárjökull	1812	16/14	Chenet *et al*. (2010)
Fjallsjökull	1812	9/11	Chenet *et al*. (2010)
Fjallsjökull	1784	n/a	Bradwell (2004)
Skálafellsjökull	1865	14/11	Chenet *et al*. (2010)
Skálafellsjökull	1820	n/a	McKinzey *et al*. (2005b)
Skálafellsjökull	1890	n/a	Evans *et al*. (1999)
Skálafellsjökull	1887	n/a	Snorrason (1984)
Heinabergsjökull	1851	16/11	Chenet *et al*. (2010)
Heinabergsjökull	1850	n/a	McKinzey *et al*. (2005b)
Heinabergsjökull	1890	n/a	Evans *et al*. (1999)
Heinabergsjökull	1887	n/a	Snorrason (1984)
Fláajökull	1821	14/10	Chenet *et al*. (2010)
Fláajökull	1894	n/a	Dabski (2002)
Fláajökull	1882	12/12	Evans *et al*. (1999)
Fláajökull	1894	n/a	Snorrason (1984)
Hoffellsjökull	1888	15/15	Chenet *et al*. (2010)
Lambatungnajökull in Skyndidalur	1835	10/10	Bradwell *et al*. (2006)
Lambatungnajökull in Hoffellsdalur	1796	12/12	Bradwell *et al*. (2006)

Various recently acquired high-resolution proxy records shed light on the climate and environmental conditions during the LIA in Iceland. Some of these datasets are shown in Fig. 10 (and site locations in Fig. 1) for comparison with the variations of the outlet glaciers of southeast Vatnajökull as evidenced in the historical documents (Fig. 10a). The lichenometric dates of the moraines of the southeast outlets are shown in Fig. 10a (references also in Table 6). All these climate data series suggest that cold but fluctuating conditions prevailed in the time period 1650–1900. Sea ice data (Fig. 10b) from historical records (Ogilvie 2010 and unpubl.) and marine sediments (Masse *et al*.

Fig. 10. Comparison of climate-proxy records, instrumental data and glacier archives in Iceland. (a) The outlet glaciers of southeast Vatnajökull from west (bottom) to east (top), right pointing filled triangles indicate when glaciers are first noted in historical accounts to be advancing, left pointing filled triangles indicate when glaciers are known to start their recession from the LIA terminal moraines. Open triangles symbolize reported advances of the glaciers. Black dots represent dated LIA terminal moraines by lichenometry (references in Table 6). (b) Sea ice around the coasts of Iceland 1601–2012 from Astrid Ogilvie (2010 and unpubl.), and relative abundances of IP25 (biomarker produced by sea ice algae) found in marine core MD99-2275 north of Iceland (Masse *et al*. 2008). (c) The average number of *ice-rafted-debris* (*IRD*) in Hvítárvatn from several sedimentary cores (Larsen *et al*. 2013), and chironomid inferred summer temperatures from lake Mýfluguvatn in northwest Iceland (black line, Langdon *et al*. 2011) with reversed *y*-axis. (d) Winter precipitation dervied from the varved sedimentary record from lake Lagarfljót east Iceland (Striberger *et al*. 2010), and the elevation of the snowline for southern Vatnajökull from Þórarinsson (1974). The average elevation of the snowline during the time period 2007–2011 (MSL = MODIS snowline, Hannesdóttir *et al.* 2014b) and average elevation of highest LIA *lateral moraine* (*LLM*) and corresponding standard deviation. (e) Summer (JJA) temperature from the composite Stykkishólmur record in gray, and the 7-year running average in black (Wood *et al*. 2010) and the 7-year running average temperature at Hólar in Hornafjörður (Icelandic Meteorological Office, Aðalgeirsdóttir *et al*. 2011) and reconstructed *northern hemisphere* (*NH*) temperatures (dark gray) calculated by combining low-resolution proxies with tree-ring data (Moberg *et al*. 2005), and a temperature reconstruction from Greenland (light gray), based on an average of uplift corrected $\delta^{18}O$ data from Agassiz and Renland (Vinther *et al*. 2009).

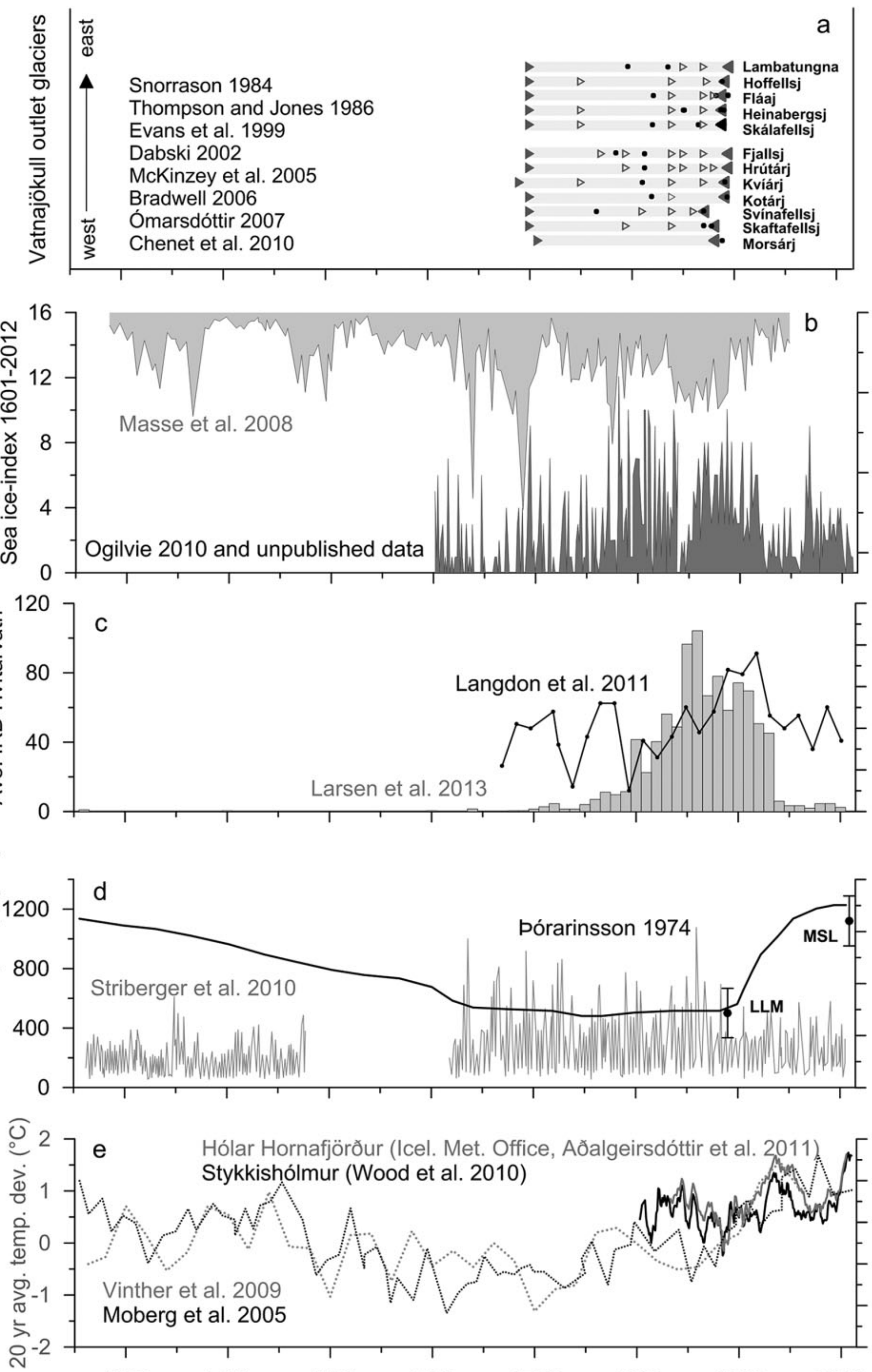
a
Vatnajökull outlet glaciers
east
west
Snorrason 1984
Thompson and Jones 1986
Evans et al. 1999
Dabski 2002
McKinzey et al. 2005
Bradwell 2006
Ómarsdóttir 2007
Chenet et al. 2010
Lambatungna
Hoffellsj
Fláaj
Heinabergsj
Skálafellsj
Fjallsj
Hrútárj
Kvíárj
Kotárj
Svínafellsj
Skaftafellsj
Morsárj
b
Sea ice-index 1601-2012
IP_{25} relative abundance
Masse et al. 2008
Ogilvie 2010 and unpublished data
c
Ave. IRD Hvítárvatn
CI summer T (1°C)
Langdon et al. 2011
Larsen et al. 2013
d
Inferred winter precip. (mm)
Snowline elev.(m a.s.l.)
Þórarinsson 1974
Striberger et al. 2010
MSL
LLM
e
Hólar Hornafjörður (Icel. Met. Office, Aðalgeirsdóttir et al. 2011)
Stykkishólmur (Wood et al. 2010)
Vinther et al. 2009
Moberg et al. 2005
NH temp anomlay (°C)
20 yr avg. temp. dev. (°C)
JJA T (°C)
1300
1400
1500
1600
1700
1800
1900
2000

2008) indicate cold but variable climate since the seventeenth century and until the end of the nineteenth century. The detailed continuous sedimentary record of Hvítárvatn (Larsen *et al.* 2013) reveals two discrete phases of expansion of Langjökull ice cap during the LIA, occurring 1400–1550 and the latter more extensive one *c.* 1680–1890 AD (Fig. 10c). Peaks in ice-rafted debris around 1840 and 1890 represent the outlet glaciers' maximum extent, similar to results of numerical ice-sheet modelling of the ice cap (Flowers *et al.* 2007). Temperature reconstruction from northwest Iceland (Fig. 10c), based on counts of chironomid head capsules in a sediment core from lake Mýfluguvatn, compare well with instrumental data of Stykkishólmur and sea surface temperature records (Langdon *et al.* 2011). Cold phases are recorded in the core in the late seventeenth and eighteenth centuries and the coldest interval between 1890 and 1917. From the varved sediments of Lagarfljót it is suggested that higher and more variable precipitation occurred between 1600 and the late 1800s, than prior to the 1600s and during the twentieth century (Fig. 10d), which may have influenced the expansion of the ice cap in the latter part of the LIA (Striberger *et al.* 2010). A northern hemisphere temperature reconstruction based on a combination of proxies (Fig. 10e; Moberg *et al.* 2005), and the ice core $\delta^{18}O$ temperature reconstruction from Greenland (Vinther *et al.* 2009) are inclined towards a LIA maximum around 1700. However, these two curves deviate from the Icelandic temperature records of Stykkishólmur (measured since 1798; Wood *et al.* 2010) and Hólar in Hornafjörður (Aðalgeirsdóttir *et al.* 2011) during most of the nineteenth century, with a closer correlation in the twentieth century (Fig. 10e).

The meteorological records from the lowland stations Hólar in Hornafjörður and Fagurhólsmýri indicate similar temperature and precipitation fluctuations at both stations during the majority of the twentieth century (data from the Icelandic Meteorological Office). The response of southeast Vatnajökull's outlets to climate perturbations in this time period provides an analogue for their LIA fluctuations; they have responded concomitantly to similar climatic forcing during the last 120 years (Hannesdóttir *et al.* 2014b). *In situ* mass balance measurements of glaciers in Iceland and degree-day mass balance models of selected glaciers indicate that the mass balance is governed by variations of the summer ablation (strongly correlated with temperature), rather than winter accumulation (Björnsson and Pálsson 2008; Guðmundsson *et al.* 2009, 2011; Pálsson *et al.* 2012; Björnsson *et al.* 2013). The rate of glacier retreat in the twentieth century is also correlated with high summer melt, and no long-term changes in precipitation measured at lowland stations have been observed in this period (Jóhannesson and Sigurðsson 1998; Björnsson and Pálsson 2008). Summer temperatures recorded at Stykkishólmur started declining *c.* 1850, and reached a minimum around 1890. Given that the response time of the outlets of southeast Vatnajökull is in the range of 20–40 years, estimated as a function of the glacier thickness and ablation at the terminus (Jóhannesson *et al.* 1989), a late nineteenth century LIA maximum is more likely for the outlets, opposed to a late eighteenth century/early nineteenth century, as some lichenometric ages of LIA moraines indicate.

The LIA maximum glacier extent and volume

We have combined historical information with the glacial geomorphological data to derive quantitative estimates of the glacial extent and volume of the outlet glaciers of southeast Vatnajökull at the LIA maximum. This is the first time extensive fieldwork has been carried out along the glacier margin up the valleys of southeast Vatnajökull to map the LIA extent and retrieve surface elevation changes. The bedrock topography of the outlets is known, allowing the total ice volume at the LIA maximum to be computed. These new estimates of the glacier surface geometry at the LIA maximum, the ice volume and areal extent provide important information, for constraining coupled mass balance ice-flow models, as well as providing input for glacial unloading studies and sea level rise estimates.

To assess the reconstructed LIA glacier surface topography we compared it with the results of two different models. A simple glacier model by Benn and Hulton (2010) provides estimates of the surface profile of former glaciers using a solution for 'perfectly plastic' ice. Negligible differences in the surface profile along a center flowline of selected glaciers were observed. Similarly the reconstructed ~1890 topography and volume of the outlets of Breiðabunga was compared with results of a coupled ice flow-positive degree day model (Hannesdóttir *et al.* 2014a), and only slight differences were observed. We are therefore confident in the quality of the surface reconstruction of the LIA glaciers, although aware of some of the limitations of the method; for example, their variable slope, ice thickness, or lateral drag, which influence the glacier surface topography, and are not accounted for especially. It should be noted that lateral moraines may be subject to erosion following glacier retreat (e.g. Schiefer and Gilbert 2007), which could lead to a slight underestimation of the glacier surface elevation. Assuming synchronous deposition of lateral moraines is perhaps a simplistic approach, but dating options are limited.

Lateral moraines indicative of the LIA ELA

Consistency is observed in the spatial variability of the LIA proxy-dervied ELA and the ELA deduced from the snowline on MODIS images from 2007 to 2011 (Fig. 9). During both time periods, the ELA of the east-facing outlet glaciers of Öræfajökull is lower than on the west-facing glaciers, and an increase in ELA is observed from Skálafellsjökull to Lambatungnajökull further east (Fig. 9 and Table 5). Thoroddsen (1931–1935) also observed a geographical variation of the snowline elevation of southeast Vatnajökull during his travels in 1894 (Table 5, Fig. 9). Westerly to southeasterly winds bring the precipitation towards south Iceland (Jónsdóttir and Uvo 2009), and the frequent passage of atmospheric lows and fronts cause orographically enhanced precipitation on mountains facing south and east on the southeast coast (Rögnvaldsson *et al*. 2004; Crochet *et al*. 2007). In comparison to Skálafellsjökull, which faces the prevailing precipitation direction and receives high precipitation, Lambatungnajökull is sheltered by mountains and is further away from the coast. The spatial variability of the snowline elevation of southeast Vatnajökull is most likely related to this variable precipitation distribution. The elevation of the snowline on Vatnajökull is dependent on weather conditions from year to year as evidenced on the MODIS images from 2007 to 2011. According to mass balance measurements, the ELA fluctuated 200–300 m during the time period 1992–2007 (Björnsson and Pálsson 2008). In the autumn of 1973 the snowline on southern Vatnajökull was below 1000 m a.s.l., reaching down to 700 m a.s.l. on Skálafellsjökull (Williams 1987), close to the elevation of the uppermost lateral moraines of that glacier. That year average summer temperature measured at Hólar in Hornafjörður was ~8.9°C, close to the average of the late nineteenth century (see below). Mass balance measurements on Vatnajökull show that 100 m change in ELA affects the net mass balance of Vatnajökull by ~0.7 m a^{-1} (Björnsson and Pálsson 2008), and modelling studies reveal similar results (Aðalgeirsdóttir *et al*. 2005). According to mass balance measurements, the average ELA of Hoffellsjökull during the time period 2001–2010 was around 1100 m a.s.l. and of Breiðamerkurjökull during the time period 1996–2010 around 1200 m a.s.l. (Aðalgeirsdóttir *et al*. 2011).

The difference between the altitude of the uppermost up-valley LIA lateral moraines and the average snowline elevation of 2007–2011 for each outlet glacier reveal an elevation difference of 340 m (Table 5). The average summer temperature during the time period 1860–1890 at Hólar in Hornafjörður (partly reconstructed from other temperature records; Aðalgeirsdóttir *et al*. 2011) was 8.5°C compared with an average of 10.5°C during the time period 2000–2010. Assuming a temperature lapse rate of 0.0065°C m^{-1}, the ELA at the time of formation of the uppermost lateral moraines would have been approximately 310 m lower on average than today. Ice-sheet modelling of the evolution of Langjökull ice cap through the Holocene indicates that the LIA maximum glacier size is reached with temperatures approximately 1.5°C lower than the 1961–1990 reference temperature (Flowers *et al*. 2008). From the chironomid-based temperature reconstruction from northwest Iceland, a 1.5–2.0°C drop in summer temperature, relative to the average of 1961–90, is observed during the coldest time periods of the LIA (Langdon *et al*. 2011).

Furthermore, the altitudinal range of the estimated ELA of the LIA is in accordance with Eyþórsson's (1951) and Þórarinsson's (1974) suggestion that the elevation of the snowline of southern Vatnajökull was approximately 300 m lower during the LIA than in the mid-twentieth century and in the first centuries after settlement (Fig. 10d). The method of approximating the ELA from the highest up-valley lateral moraines has some uncertainties, which should be kept in mind. The formation and preservation of the lateral moraines depends on the availability of sediments, which varies across the area, due to different bedrock type and steepness of the valley walls. An underestimation of the LIA ELA may occur where moraines are deposited on unstable slopes, or where moraines are reworked by subsequent processes (e.g. Hawkins 1985; Benn and Evans 2010). Furthermore, lateral moraines may not be deposited exactly at the ELA but further down the glacier, resulting in too low estimates (Nesje *et al*. 2000). The rise of the ELA since the LIA has been estimated with the same method for some glaciers in Europe and North America to be around 100–250 m (Nesje and Dahl 1993; Maisch 2000; Jiskoot *et al*. 2009; Knoll *et al*. 2009; Zasadni and Klapyta 2009).

Conclusion

Historical information and glacial geomorphological data are used to derive quantitative estimates of the glacial extent and ice volume of the outlets of southeast Vatnajökull at the LIA maximum. A reconstruction of the ~1890 glacier surface geometry of the outlets is based on geomorphological features (including lateral and terminal moraines), historical photographs, aerial images, maps from 1904, and by using the LiDAR DEMs as topographical reference. The near termini surface elevation lowering 1890–2010 is in the range of 150–270 m, and negligible downwasting is observed in the upper accumulation area. Historical records detail how the outlet glaciers advanced in the late seventeenth century and closed off grazing grounds in the mountains bordering the ice cap, and reached far out on the lowlands in the mid eighteenth century. The outlets were at the LIA terminal moraines around 1880–1890 and soon thereafter started receding according to contemporary documents. Some of them may have been as extensive in the eighteenth century as in 1890, but the descriptions are not conclusive. This complies with results of the pioneering work of Þórarinsson (1939, 1943), indicating that the outlets oscillated around an advanced stage from the middle of the eighteenth century until the end of the nineteenth century. A late nineteenth century maxima is supported by the temperature records from Hólar in Hornafjörður and Stykkishólmur (since 1798), referring to studies showing that the mass balance of Icelandic ice caps and glaciers is governed by summer ablation, which is strongly correlated with temperature. According to the elevation of the highest up-valley LIA lateral moraines, the ELA of southeast Vatnajökull during the LIA was approximately 340 m lower than the modern ELA (2007–2011). This supports previous estimates of the LIA ELA of southern Vatnajökull of Eyþórsson (1951) and Þórarinsson (1974). Comparable spatial variability of the modern and LIA ELA is observed, and an elevation difference of up to 200 m is recognized between glaciers. This study provides a baseline for reconstructing glacier surface geometry at the LIA maximum and estimating ice volume for other glaciers. Knowing the ice volume of the outlet glaciers is vital for constraining glacier models, estimating the contribution to sea level rise, and for glacial unloading studies.

Acknowledgements

This work was funded by a doctoral grant of the Research Fund of the University of Iceland to Hrafnhildur Hannesdóttir, two additional grants from the Research Fund to Guðfinna Aðalgeirsdóttir, the Icelandic Road Administration, the Kvísker Fund, the University of Iceland's Research Center in Hornafjörður, and SVALI Nordic Centre of Excellence. We thank the Icelandic Glaciological Society (JÖRFÍ), Vatnajökull National Park, Ágúst Hálfdánsson, Björn Oddsson, Þóra Karlsdóttir and Þorsteinn Jónsson for support during fieldwork. The help of Hálfdán Ágústsson, Sveinbjörn Steinþórsson, Rannveig Einarsdóttir, Jóhanna Katrín Þórhallsdóttir, Eiríkur Lárusson, Katrín Auðunardóttir, and Bergrún Arna Óladóttir during fieldwork is greatly acknowledged. Thanks to the brothers of Kvísker (Sigurður, Helgi and Hálfdán) for valuable discussions and access to their personal photo collection. We acknowledge the help of Trausti Jónsson at the Icelandic Meteorological Office with the temperature series of Stykkishólmur and Hólar in Hornafjörður. Carsten Kristinsson at the National Land Survey of Iceland is thanked for providing the aerial images. We thank Astrid Ogilvie, Darren Larsen, Johan Striberger, and Pete Langdon for access to their data. Þórdís Högnadóttir helped with drawing some of the figures. We thank Víðir Reynisson for the numerous oblique aerial photographs of Svínafellsjökull. We thank Ívar Örn Benediktsson for very helpful comments on an early draft of the manuscript, and Friðþór Sófus Sigurmundsson for discussions about the various historical sources. Careful and constructive reviews of two anonymous reviewers are gratefully acknowledged. This publication is contribution No. 37 of the Nordic Centre of Excellence SVALI, 'Stability and Variations of Arctic Land Ice', funded by the Nordic Top-level Research Initiative (TRI).

Hrafnhildur Hannesdóttir, Helgi Björnsson, Finnur Pálsson and Guðfinna Aðalgeirsdóttir, Snævarr Guðmundsson, Institute of Earth Sciences, University of Iceland, Sturlugata, 101 Reykjavík, Iceland
E-mail: hrafnha@hi.is

Snævarr Guðmundsson, Southeast Iceland Nature Center, Höfn, Iceland

References

Aðalgeirsdóttir, G., Guðmundsson, G.H. and Björnsson, H., 2005. Volume sensitivity of Vatnajökull Ice Cap, Iceland, to perturbations in equilibrium line altitude. *Journal of Geophysical Research-Earth Surface*, 110. doi: 10.1029/2005jf000289

Aðalgeirsdóttir, G., Guðmundsson, S., Björnsson, H., Pálsson, F., Jóhannesson, T., Hannesdóttir, H., Sigurðsson, S.P. and Berthier, E., 2011. Modelling the 20th and 21st century evolution of Hoffellsjökull glacier, SE-Vatnajökull, Iceland. *Cryosphere*, 5, 961–975. doi: 10.5194/tc-5-961-2011

Axford, Y., Andresen, C.S., Andrews, J.T., Belt, S.T., Geirsdóttir, Á., Masse, G., Miller, G.H., Ólafsdóttir, S. and Vare, L.L., 2011. Do paleoclimate proxies agree? A test comparing 19 late Holocene climate and sea-ice reconstructions from Icelandic marine and lake sediments. *Journal of Quaternary Science*, 26, 645–656. doi: 10.1002/Jqs.1487

Bárðarson, G., 1934. Islands Gletscher: Beiträge zur Kenntnis der Gletscherbewegungen und Schwankungen auf Grund alter Quellenschriften und neuester Forschung: nachgelassenes Manuskript. *Rit Vísindafélags Íslendinga*, 16, 60.

Benediktsson, K., 1972. Byggðasaga Mýrarhrepps [The history of the municipality of Mýrar], *Byggðasaga Austur-Skaftafellssýslu [The History of the County of Austur-Skaftafellssýsla]*. Bókaútgáfa Guðjóns Ó. Guðjónssonar, Reykjavík. 9–67. [In Icelandic]

Benn, D. and Evans, D.J.A., 2010. *Glaciers and Glaciations*. 2nd ed. Routledge, New York.

Benn, D.I. and Hulton, N.R.J., 2010. An Excel (TM) spreadsheet program for reconstructing the surface profile of former mountain glaciers and ice caps. *Computers & Geosciences*, 36, 605–610. doi: 10.1016/j.cageo.2009.09.016

Benn, D.I., Owen, L.A., Osmaston, H.A., Seltzer, G.O., Porter, S.C. and Mark, B., 2005. Reconstruction of equilibrium-line altitudes for tropical and sub-tropical glaciers. *Quaternary International*, 138, 8–21. doi: 10.1016/j.quaint.2005.02.003

Bergþórsson, P., 1969. An estimate of drift ice temperature in Iceland in 1000 years. *Jökull*, 19, 94–101.

Björnsson, F., 1956. Kvíárjökull. *Jökull*, 6, 20–22.

Björnsson, F., 1998a. Samtíningur um jökla milli Fells og Staðarfjalls [Facts about glaciers between Fell and Staðarfjall]. *Jökull [Journal of Earth Sciences]*, 46, 49–61. [In Icelandic]

Björnsson, H., 1996. Scales and rates of glacial sediment removal: a 20 km long and 300 m deep trench created beneath Breiðamerkurjökull during the Little Ice Age. *Annals of Glaciology*, 22, 141–146.

Björnsson, H., 1998b. Frá Breiðumörk til jökulsands: mótun lands í þúsund ár [From Breiðamörk to the sandur: the thousand years of land formation]. In: Árnason, G.S. (ed.), *Kvískerjabók, Rit til heiðurs systkinunum á Kvískerjum [The Book of Kvísker, in Honour of the Siblings of Kvísker]*. Sýslusafn Austur-Skaftafellssýslu, Höfn in Hornafjörður. 164–176. [In Icelandic]

Björnsson, H., 2009. *Jöklar á Íslandi [Glaciers in Iceland]*. Opna, Reykjavík. [In Icelandic]

Björnsson, H., Jónsson, T., Gylfadóttir, S.S. and Ólason, E.Ö., 2007. Mapping the annual cycle of temperature in Iceland. *Meteorologische Zeitschrift*, 16, 45–56. doi: 10.1127/0941-2948/2007/0175

Björnsson, H. and Pálsson, F., 2004. Jöklar í Hornafirði, rannsóknir og saga [Glaciers in Hornafjörður, research and history]. In: Björnsson, H. (ed.), *Jöklaveröld, náttúra og mannlíf [The World of Glaciers, Nature and Human History]*. Skrudda, Reykjavík. 125–164. [In Icelandic]

Björnsson, H. and Pálsson, F., 2008. Icelandic glaciers. *Jökull*, 58, 365–386.

Björnsson, H., Pálsson, F., Guðmundsson, S., Magnússon, E., Aðalgeirsdóttir, G., Jóhannesson, T., Berthier, E., Sigurðsson, O. and Thorsteinsson, T., 2013. Contribution of Icelandic ice caps to sea level rise: trends and variability since the Little Ice Age. *Geophysical Research Letters*, 40, 1546–1550. doi: 10.1002/Grl.50278

Björnsson, H., Pálsson, F., Sigurðsson, O. and Flowers, G.E., 2003. Surges of glaciers in Iceland. *Annals of Glaciology*, 36, 82–90.

Björnsson, S., 1958. Úr bréfum. Hrútárjökull og draumur Guðrúnar Bjarnadóttir [From letters. Hrútárjökull and the dream of Guðrún Bjarnadóttir]. *Jökull [Journal of Earth Sciences]*, 8, 36. [In Icelandic]

Björnsson, S., 1979. *Árbók Ferðafélags Íslands: Öræfasveit [The Yearbook of The Iceland Touring Association: the County of Öræfi]*. The Iceland Touring Association, Reykjavík. [In Icelandic]

Bradwell, T., 2004. Lichenometric dating in southeast Iceland: The size-frequency approach. *Geografiska Annaler Series A: Physical Geography*, 86A, 31–41. doi: 10.1111/j.0435-3676.2004.00211.x

Bradwell, T., 2009. Lichenometric dating: a commentary, in the light of some recent statistical studies. *Geografiska Annaler Series A: Physical Geography*, 91A, 61–69. doi: 10.1111/j.1468-0459.2009.00354.x

Bradwell, T., Dugmore, A.J. and Sugden, D.E., 2006. The Little Ice Age glacier maximum in Iceland and the North Atlantic Oscillation: evidence from Lambatungnajokull, southeast Iceland. *Boreas*, 35, 61–80. doi: 10.1080/03009480500359202

Brázdil, R., Pfister, C., Wanner, H., Von Storch, H. and Luterbacher, J., 2005. Historical climatology in Europe – the state of the art. *Climatic Change*, 70, 363–430. doi: 10.1007/s10584-005-5924-1

Bruun, D., 1928. *Fortidsminder og Nutidshjem paa Island [Cultural Heritage and Modern Homes in Iceland]*. Gyldendals boghandel, Copenhagen. [In Danish]

Böðvarsson, Á., 1996. *Landmælingar og kortagerð Dana á Íslandi: Upphaf landmælinga á Íslandi*. Landmælingar Íslands, Reykjavík. [In Icelandic]

Chenet, M., Roussel, E., Jomelli, V. and Grancher, D., 2010. Asynchronous Little Ice Age glacial maximum extent in southeast Iceland. *Geomorphology*, 114, 253–260. doi: 10.1016/j.geomorph.2009.07.012

Chenet, M., Roussel, E., Jomelli, V., Grancher, D. and Cooley, D., 2011. A response to the commentary of M. Dabski about the paper 'Asynchronous Little Ice Age glacial maximum extent in southeast Iceland' (Geomorphology (2010), 114, 253–260). *Geomorphology*, 128, 103–104. doi: 10.1016/j.geomorph.2010.12.024

Church, J.A., Clark, P.U., Cazenave, A., Gregory, J.M., Jevrejeva, S., Levermann, A., Merrifield, M.A., Milne, G.A., Nerem, R.S., Nunn, P.D., Payne, A.J., Pfeffer, W.T., Stammer, D. and Unnikrishnan, A.S., 2013. Sea level change In: Stocker, T.F., Qin, D., Plattner, G.-K., Tignor, M., Allen, S.K., Boschung, J., Nauels, A., Xia, Y., Bex, V. and Midgley, P.M. (eds.), *Climate Change 2013: The Physical Science Basis. Contribution of Working Group I to the Fifth Assessment Report of the Intergovernmental Panel on Climate Change*. Cambridge University Press, Cambridge, UK and New York, NY, USA. 1137–1216.

Crochet, P., Jóhannesson, T., Jónsson, T., Sigurðsson, O., Björnsson, H., Pálsson, F. and Barstad, I., 2007. Estimating the spatial distribution of precipitation in Iceland using a linear model of orographic precipitation. *Journal of Hydrometeorology*, 8, 1285–1306. doi: 10.1175/2007JHM795.1

Curry, A.M., Sands, T.B. and Porter, P.R., 2009. Geotechnical controls on a steep lateral moraine undergoing paraglacial slope adjustment In: Knight, J. and Harrison, S. (eds.), *Periglacial and Paraglacial Processes and Environments*. The Geological Society, London. 181–197.

Dabski, M., 2002. Dating of Fláajökull moraine ridges SE-Iceland, comparison of the glaciological, cartographical and lichenometric data. *Jökull*, 51, 17–24.

Dabski, M., 2007. Testing the size-frequency-based lichenometric dating curve on Fláajökull moraines (SE Iceland) and quantifying lichen population dynamics with respect to stone surface aspect. *Jökull*, 57, 21–35.

Dabski, M., 2010. A commentary to ‘Asynchronous Little Ice Age glacial maximum extent in southeast Iceland’ by Chenet et al. (Geomorphology 114 (2010) 253–260); a case of Fláajökull. *Geomorphology*, 120, 365–367. doi: 10.1016/j.geomorph.2010.03.023

Dabski, M. and Tittenbrun, A., 2013. Time-dependent surface deterioration of glacially abraded basaltic boulders by Fláajökull, SE-Iceland. *Jökull*, 63, 55–70.

Dahl, S.O., Bakke, J., Lie, O. and Nesje, A., 2003. Reconstruction of former glacier equilibrium-line altitudes based on proglacial sites: an evaluation of approaches and selection of sites. *Quaternary Science Reviews*, 22, 275–287. doi: 10.1016/S0277-3791(02)00135-X

Danish General Staff, 1904. *Sheets: 87-NV,SV,SA, 97-NV, NA, 96-NA, 1:50.000*. The topographic department of the Danish General Staff, Copenhagen.

De Woul, M. and Hock, R., 2005. Static mass-balance sensitivity of Arctic glaciers and ice caps using a degree-day approach. *Annals of Glaciology*, 42, 217–224. doi: 10.3189/172756405781813096

Einarsson, O., 1971. *Íslandslýsing/Qualiscunque descriptio Islandiae [Description of Iceland]*. Menningarsjóður, Reykjavík. [In Icelandic]

Eiríksson, H.H., 1932. *Observations and Measurements of Some Glaciers in Austur-Skaftafellssýsla*. Vísindafélag Íslendinga, Reykjavík.

Evans, D.J.A., Archer, S. and Wilson, D.J.H., 1999. A comparison of the lichenometric and Schmidt hammer dating techniques based on data from the proglacial areas of some Icelandic glaciers. *Quaternary Science Reviews*, 18, 13–41. doi: 10.1016/S0277-3791(98)00098-5

Evans, D.J.A. and Twigg, D.R., 2002. The active temperate glacial landsystem: a model based on Breiðamerkurjökull and Fjallsjökull, Iceland. *Quaternary Science Reviews*, 21, 2143–2177.

Eyþórsson, J., 1951. Þykkt Vatnajökull [The thickness of Vatnajökull]. *Jökull [Journal of Earth Sciences]*, 1, 1–6. [In Icelandic]

Flowers, G.E., Björnsson, H., Geirsdóttir, Á., Miller, G.H., Black, J.L. and Clarke, G.K.C., 2008. Holocene climate conditions and glacier variation in central Iceland from physical modelling and empirical evidence. *Quaternary Science Reviews*, 27, 797–813. doi: 10.1016/j.quascirev.2007.12.004

Flowers, G.E., Björnsson, H., Geirsdóttir, Á., Miller, G.H. and Clarke, G.K.C., 2007. Glacier fluctuation and inferred climatology of Langjokull ice cap through the Little Ice Age. *Quaternary Science Reviews*, 26, 2337–2353. doi: 10.1016/j.quascirev.2007.07.016

Gadde, N.O., 1983. *Íslandsferð sumarið 1857: úr minnisblöðum og bréfum frá Nils Ohlson Gadde [Journey through Iceland in the Summer of 1857: from Notes and Letters of Nils Ohlson Gadde]*. Hörpuútgáfan, Akranes.

Geirsdóttir, Á., Miller, G.H., Axford, Y. and Ólafsdóttir, S., 2009. Holocene and latest Pleistocene climate and glacier fluctuations in Iceland. *Quaternary Science Reviews*, 28, 2107–2118. doi: 10.1016/j.quascirev.2009.03.013

Geirsdóttir, Á., Miller, G.H., Larsen, D.J. and Ólafsdóttir, S., 2013. Abrupt Holocene climate transitions in the northern North Atlantic region recorded by synchronized lacustrine records in Iceland. *Quaternary Science Reviews*, 70, 48–62. doi: 10.1016/j.quascirev.2013.03.010

Gíslason, S., 1954. Vatnsdalshlaup [Jökulhlaups from Vatnsdalur]. *Jökull [Journal of Earth Sciences]*, 4, 41. [In Icelandic]

Glasser, N.F., Harrison, S., Jansson, K.N., Anderson, K. and Cowley, A., 2011. Global sea-level contribution from the Patagonian Icefields since the Little Ice Age maximum. *Nature Geoscience*, 4, 303–307. doi: 10.1038/Ngeo1122

Gordon, J.E. and Sharp, M., 1983. Lichenometry in dating recent glacial landforms and deposits, southeast Iceland. *Boreas*, 12, 191–200.

Grinsted, A., 2013. An estimate of global glacier volume. *Cryosphere*, 7, 141–151. doi: 10.5194/tc-7-141-2013

Grove, J.M., 2001. The initiation of the ‘Little Ice Age’ in regions round the North Atlantic. *Climatic Change*, 48, 53–82.

Grove, J.M., 2004. *Little Ice Ages: Ancient and Modern*. 2nd ed. Routledge, London and New York.

Guðmundsson, H.J., 1997. A review of the Holocene environmental history of Iceland. *Quaternary Science Reviews*, 16, 81–92.

Guðmundsson, H., 1998. *Holocene glacier fluctuations and tephrochronology of the Öræfi district, Iceland*. PhD diss. University of Edinburgh, Edinburgh.

Guðmundsson, S., Björnsson, H., Jóhannesson, T., Aðalgeirsdóttir, G., Pálsson, F. and Sigurðsson, O., 2009. Similarities and differences in the response to climate warming of two ice caps in Iceland. *Hydrology Research*, 40, 495–502. doi: 10.2166/Nh.2009.210

Guðmundsson, S., Björnsson, H., Magnússon, E., Berthier, E., Pálsson, F., Guðmundsson, M.T., Högnadottir, T. and Dall, J., 2011. Response of Eyjafjallajokull, Torfajokull and Tindfjallajokull ice caps in Iceland to regional warming, deduced by remote sensing. *Polar Research*, 30. doi: 10.3402/Polar.V30i0.7282

Guðmundsson, S., Hannesdóttir, H. and Björnsson, H., 2012. Post-Little Ice Age volume loss of Kotárjökull glacier, SE-Iceland, derived from historical photography. *Jökull*, 62, 97–110.

Guðnason, B., 1957. *Sýslulýsingar 1744–1749 [County Descriptions 1744–1749]*. Sögufélagið, Reykjavík. [In Icelandic]

Hagen, S. and Liestøl, O., 1990. Long-term glacier mass-balance investigations in Svalbard 1950–88. *Annals of Glaciology*, 14, 102–106.

Hannesdóttir, H., Björnsson, H., Aðalgeirsdóttir, G., Pálsson, F., Guðmundsson, S., Jóhannesson, T., Crochet, P., Magnússon, E., Guðmundsson, S., Sigurðsson, S.Þ. and Ágústsson, H., 2014a. Glacier variations of SE-Vatnajökull 1890–2010, International Symposium on Contribution of Glaciers and Ice Sheets to Sea-Level Change, Chamonix

Hannesdóttir, H., Björnsson, H., Pálsson, F., Aðalgeirsdóttir, G. and Guðmundsson, S., 2014b. Area, volume and mass changes of southeast Vatnajökull ice cap, Iceland, from the Little Ice Age maximum in the late 19th century to 2010. *The Cryosphere Discussion*, 8, 1–55. doi:10.5194/tcd-8-1-2014

Hawkins, F.F., 1985. Equilibrium-line altitudes and paleoenvironment in the Merchants Bay Area, Baffin Island, Nwt, Canada. *Journal of Glaciology*, 31, 205–213.

Henderson, E., 1957. *Ferðabók. Frásagnir um ferðalög um þvert og endilangt Ísland árin 1814 og 1815 með vetursetu í Reykjavík [Travel Book. Accounts on Travels in Iceland in 1814 and 1815 and a Winter Stay in Reykjavík]*. Snæbjörn Jónsson og co hf, Reykjavík. [In Icelandic]

Holzhauser, H., Magny, M. and Zumbuhl, H.J., 2005. Glacier and lake-level variations in west-central Europe over the last 3500 years. *Holocene*, 15, 789–801. doi: 10.1191/0959683605hl853ra

Iturrizaga, L., 2008. Post-sedimentary transformation of lateral moraines – the tributary tongue basins of the Kviarjokull (Iceland). *Journal of Mountain Science*, 5, 1–16.

Ives, J.D., 2007. *Skaftafell in Iceland – A Thousand Years of Change*. Ormstunga, Reykjavík.

Jiskoot, H., Curran, C.J., Tessler, D.L. and Shenton, L.R., 2009. Changes in Clemenceau Icefield and Chaba Group glaciers, Canada, related to hypsometry, tributary detachment, length-slope and area-aspect relations. *Annals of Glaciology*, 50, 133–143.

Jóhannesson, H., 1985. Þættir úr sögu Skeiðarárjökuls [Accounts on Skeiðarárjökull]. *Náttúrufræðingurinn [The Icelandic Journal of Natural Sciences]*, 54, 31–45. [In Icelandic]

Jóhannesson, T. and Sigurðsson, O., 1998. Interpretation of glacier variations in Iceland 1930–1995. *Jökull*, 45, 27–33.

Jóhannesson, T., Björnsson, H., Magnússon, E., Guðmundsson, S., Pálsson, F., Sigurðsson, O., Thorsteinsson, T. and Berthier, E., 2013. Ice-volume changes, bias estimation of mass-balance measurements and changes in subglacial lakes derived by lidar mapping of the surface of Icelandic glaciers. *Annals of Glaciology*, 54, 63–74. doi: 10.3189/2013aog63a422

Jóhannesson, T., Raymond, C. and Waddington, E., 1989. Time-scale for adjustment of glaciers to changes in mass balance. *Journal of Glaciology*, 35, 355–369.

Jomelli, V., Naveau, P., Cooley, D., Grancher, D., Brunstein, D. and Rabatel, A., 2010. A reponse to Bradwell's commentary on recent statistical studies in lichenometry. *Geografiska Annaler: Series A, Physical Geography*, 92A, 485–487. doi: 10.1111/j.1468-0459.2010.00409.x

Jones, P.D. and Briffa, K.R., 2001. The 'Little Ice Age': local and global perspectives – Preface. *Climatic Change*, 48, 5–8. doi: 10.1023/A:1005670904293

Jónsdóttir, J.F. and Uvo, C.B., 2009. Long-term variability in precipitation and streamflow in Iceland and relations to atmospheric circulation. *International Journal of Climatology*, 29, 1369–1380. doi: 10.1002/Joc.1781

Jónsson, E., 2004. Í veröld jökla, sanda og vatna [In the realm of glaciers, sands and rivers]. In: Björnsson, H., Jónsson, E. and Runólfsson, S. (eds.), *Jöklaveröld, náttúra og mannlíf [The World of Glaciers, Nature and Human History]*. Skrudda, Reykjavík. 11–86. [In Icelandic]

Jónsson, G., 1945. *Skaftfellskar þjóðsögur og sagnir [Narratives and Sayings from the County of Skaftafellssýsla]*. Bókaverzlun Guðmundar Gamalíelssonar, Reykjavík. [In Icelandic]

Kirkbride, M.P. and Dugmore, A.J., 2001. Can lichenometry be used to date the Little Ice Age glacial maximum in Iceland? *Climatic Change*, 48, 151–167. doi: 10.1023/A:1005654503481

Kirkbride, M.P. and Dugmore, A.J., 2008. Two millenia of glacier advances from southern Iceland dated by tephrochronology. *Quaternary Research*, 70, 398–411. doi: 10.1016/j.yqres.2008.07.001

Kirkbride, M.P. and Winkler, S., 2012. Correlation of Late Quaternary moraines: impact of climate variability, glacier response, and chronological resolution. *Quaternary Science Reviews*, 46, 1–29.

Knoll, C., Kerschner, H., Heller, A. and Rastner, P., 2009. A GIS-based reconstruction of Little Ice Age glacier maximum extents for South Tyrol Italy. *Transactions in GIS*, 13, 449–463. doi: 10.1111/j.1467-9671.2009.01173.x

Knudsen, K.L., Eiríksson, J. and Bartels-Jónsdóttir, H.B., 2012. Oceanographic changes through the last millennium off North Iceland: temperature and salinity reconstructions based on foraminifera and stable isotopes. *Marine Micropaleontology*, 84–85, 54–73. doi: 10.1016/j.marmicro.2011.11.002

Kristjánsson, J. (ed.), 2002. *Biskupasögur [Bishop Stories]*. Hið íslenzka fornritafélag, Reykjavík. [In Icelandic]

Kruger, J., 1994. Glacial processes, sediments, landforms and stratigraphy in the terminus region of Mýrdalsjökull, Iceland. *Folia Geographica Danica*, 21, 1–233.

Langdon, P.G., Caseldine, C.J., Croudace, I.W., Jarvis, S., Wastegård, S. and Crowford, T.C., 2011. A chironomid-based reconstruction of summer temperatures in NW Iceland since AD 1650. *Quaternary Research*, 75, 451–460. doi:10.1016/j.yqres.2010.11.007

Larsen, D.J., Miller, G.H. and Geirsdóttir, Á., 2013. Asynchronous Little Ice Age glacier fluctuations in Iceland and European Alps linked to shifts in subpolar North Atlantic circulation. *Earth and Planetary Science Letters*, 380, 52–59. doi: 10.1016/j.epsl.2013.07.028

Larsen, D.J., Miller, G.H., Geirsdóttir, Á. and Thordarson, T., 2011. A 3000-year varved record of glacier activity and climate change from the proglacial lake Hvítárvatn, Iceland. *Quaternary Science Reviews*, 30, 2715–2731. doi: 10.1016/j.quascirev.2011.05.026

Lárusson, M.M.e., 1955. *Konungs skuggsjá/Speculum regale [Kings Mirror]*. Leiftur, Reykjavík. [In Icelandic]

Leclercq, P.W., Oerlemans, J. and Cogley, J.G., 2011. Estimating the glacier contribution to sea-level rise for the period 1800–2005. *Surveys of Geophysics*, 32, 518–535. doi: 10.1007/s10712-011-9121-7

Le Roy Ladurie, E., 1971. *Times of Feast, Times of Famine: A History of Climate since the Year 1000*. Doubleday, Garden City, NY.

Magnússon, Á., 1953. Chorographica Islandica [The chorography of Iceland], *Safn til sögu Íslands og íslenzkra bókmennta að fornu og nýju [The Story of Iceland and the Icelandic literature in the past and at present]*. Hið íslenska bókmenntafélag, Reykjavík. 8–120. [In Icelandic]

Magnússon, E., Björnsson, H. and Pálsson, F., 2007. Landslag í grennd Kvískerja í fortíð og framtíð: Niðurstöður ísjármælinga á Kvíár-, Hrútár og Fjallsjökli [The landscape around Kvísker in the past and in the future: results of radio echo sounding on Kvíárjökull, Hútárjökull and Fjallsjökull]. *Jökull [Journal of Earth Sciences]*, 57, 83–89. [In Icelandic]

Magnússon, E., Pálsson, F., Björnsson, H. and Guðmundsson, S., 2012. Removing the ice cap of Öraefajokull central volcano, SE-Iceland: mapping and interpretation of bedrock topography, ice volumes, subglacial troughs and implications for hazards assessments. *Jökull [Journal of Earth Sciences]*, 62, 131–150.

Maisch, M., 2000. The longterm signal of climate change in the Swiss alps: glacier retreat since the end of the Little Ice Age and future decay scenarios. *Geografia Fisica e Dinamica Quaternaria*, 23, 139–151.

Maizels, J.K. and Dugmore, A.J., 1985. Lichenometric dating and tephrochronology of sandur deposits, Sólheimajökull area, southern Iceland. *Jökull*, 35, 69–77.

Mann, M.E., Zhang, Z.H., Hughes, M.K., Bradley, R.S., Miller, S.K., Rutherford, S. and Ni, F.B., 2008. Proxy-based reconstructions of hemispheric and global surface temperature variations over the past two millennia. *Proceedings of the National Academy of Sciences of the United States of America*, 105, 13252–13257. doi: 10.1073/pnas.0805721105

Masse, G., Rowland, S.J., Sicre, M.A., Jacob, J., Jansen, E. and Belt, S.T., 2008. Abrupt climate changes for Iceland during the last millennium: evidence from high resolution sea ice reconstructions. *Earth and Planetary Science Letters*, 269, 564–568. doi:10.1016/j.epsl.2008.03.017

Matthews, J.A., 1992. *The Ecology of Recently-Deglaciated Terrain: A Geoecological Approach to Glacier Forelands and Primary Succession*. Cambridge University Press, Cambridge.

Matthews, J.A. and Briffa, K.R., 2005. The 'Little Ice Age': re-evaluation of an evolving concept. *Geografiska Annaler Series A: Physical Geography*, 87A, 17–36. doi: 10.1111/j.0435-3676.2005.00242.x

McKinzey, K.M., Ólafsdóttir, R. and Dugmore, A.J., 2005a. Perception, history and science coherence or disparity in the timing of the Little Ice Age maximum in southeast Iceland. *Polar Record*, 41, 319–334. doi:10.1017/S0032247405004687

McKinzey, K.M., Orwin, J.F. and Bradwell, T., 2004. Re-dating the moraines at Skálafellsjökull and Heinabergsjökull using different lichenometric methods: Implications for the timing of the Icelandic Little Ice Age maximum. *Geografiska Annaler Series A: Physical Geography*, 86A, 319–335. doi: 10.1111/j.0435-3676.2004.00235.x

McKinzey, K.M., Orwin, J.F. and Bradwell, T., 2005b. A revised chronology of key Vatnajökull (Iceland) outlet glaciers during the Little Ice Age. *Annals of Glaciology*, 42, 171–179. doi: 10.3189/172756405781812817

Miller, G.H., Brigham-Grette, J., Alley, R.B., Anderson, L., Bauch, H.A., Douglas, M.S.V., Edwards, M.E., Elias, S.A., Finney, B.P., Fitzpatrick, J.J., Funder, S.V., Herbert, T.D., Hinzman, L.D., Kaufman, D.S., MacDonald, G.M., Polyak, L., Robock, A., Serreze, M.C., Smol, J.P., Spielhagen, R., White, J.W.C., Wolfe, A.P. and Wolff, E.W., 2010. Temperature and precipitation history of the Arctic. *Quaternary Science Reviews*, 29, 1679–1715. doi: 10.1016/j.quascirev.2010.03.001

Moberg, A., Sonechkin, D.M., Holmgren, K., Datsenko, N.M. and Karlén, W., 2005. Highly variable Northern Hemisphere temperatures reconstructed from low- and high-resolution proxy data. *Nature*, 433, 613–617. doi: 10.1038/Nature03265

Nesje, A., 1992. Topographical effects on the equilibrium-line-altitude on glaciers. *GeoJournal*, 27, 383–391.

Nesje, A., 2009. Latest Pleistocene and Holocene alpine glacier fluctuations in Scandinavia. *Quaternary Science Reviews*, 28, 2119–2136. doi: 10.1016/j.quascirev.2008.12.016

Nesje, A. and Dahl, S.O., 1993. Lateglacial and Holocene glacier fluctuations and climate variations in western Norway: a review. *Quaternary Science Reviews*, 12, 255–261.

Nesje, A., Lie, O. and Dahl, S.O., 2000. Is the North Atlantic Oscillation reflected in Scandinavian glacier mass balance records? *Journal of Quaternary Science*, 15, 587–601. doi: 10.1002/1099-1417(200009)15:6<587::Aid-Jqs533>3.0.Co;2-2

Nussbaumer, S.U., Nesje, A. and Zumbühl, H.J., 2011. Historical glacier fluctuations of Jostedalsbreen and Folgefonna (southern Norway) reassessed by new pictorial and written evidence. *Holocene*, 21, 455–471. doi: 10.1177/0959683610385728

Nye, J.F., 1990. Interpreting the field evience of past ice sheets: structural stability and genericity. *Annals of Glaciology*, 14, 208–210.

Ogilvie, A., 1986. The past climate and sea-ice record from Iceland, part 1: data to A.D. 1780. *Climatic Change*, 6, 131–152.

Ogilvie, A., 1992. Documentary evidence for changes in the climate of Iceland, A. D. 1500 to 1800. In: Bradley, R.S. and Jones, P.D. (eds.), *Climate Since A.D. 1500*. Routledge, London and New York. 92–117.

Ogilvie, A., 2005. Local knowledge and traveller's tales: a selection of climatic observations in Iceland. In: Caseldine, C., Russell, A.J., Harðardóttir, J. and Knudsen, Ó. (eds.), *Iceland – Modern Processes and Past Environments*. Elsevier, Amsterdam. 257–287.

Ogilvie, A., 2010. Historical climatology, climatic change, and implications for climate science in the twenty-first century. *Climatic Change*, 100, 33–47. doi: 10.1007/s10584-010-9854-1

Ogilvie, A.E.J. and Jónsson, T., 2001. 'Little Ice Age' research: a perspective from Iceland. *Climatic Change*, 48, 9–52. doi: 10.1023/A:1005625729889

Óladóttir, B.A., Larsen, G. and Sigmarsson, O., 2011. Holocene volcanic activity at Grímsvötn, Bárðarbunga and Kverkfjöll subglacial centres beneath Vatnajökull, Iceland. *Bulletin of Volcanology*, 73, 1187–1208. doi: 10.1007/s00445-011-0461-4

Ólafsson, E. and Pálsson, B., 1981. *Ferðabók Eggerts Ólafssonar og Bjarna Pálssonar: um ferðir þeirra á Íslandi árin 1752–1757 [The Travel Book of Eggert Ólafsson and Bjarni Pálsson: about their Travels in Iceland in 1752–1757]*. 2nd ed. Örn og Örlygur, Reykjavík. [In Icelandic]

Ólafsson, H., Furger, M. and Brummer, B., 2007. The weather and climate of Iceland. *Meteorologische Zeitschrift*, 16, 5–8. doi 10.1127/0941-2948/2007/0185

Olavius, Ó., 1964–1965. *Ferðabók: Landshagir í norðvestur-, norður og norðaustursýslum Íslands 1775–1777 [Travel Book: The State Economy in Northwest, North and Northeast Iceland 1775–1777]*. Bókfellsútgáfan, Reykjavík. [In Icelandic]

Ómarsdóttir, M., 2007. *Hörfunarhraði Skaftafellsjökuls eftir Litlu ísöldina [The retreat rate of Skaftafellsjökull following the end of the Little Ice Age]*. BSc diss. University of Iceland, Reykjavík. [In Icelandic]

Orwin, J.F., McKinzey, K.M., Stephens, M.A. and Dugmore, A.J., 2008. Identifying moraine surface with similar histories using lichen size distributions and the U^2 statistic, southeast Iceland. *Geografiska Annaler Series A: Physical Geography*, 90, 151–164. doi: 10.1111/j.1468-0459.2008.00168.x

Paijkull, C.W., 1866. *En sommer på Island [A Summer in Iceland]*. Albert Bonniers Förlag, Stockholm. [In Swedish]

Pálsson, F., Guðmundsson, S., Björnsson, H., Berthier, E., Magnússon, E., Guðmundsson, S. and Haraldsson, H.H., 2012. Mass and volume changes of Langjökull ice cap, Iceland, similar to 1890 to 2009, deduced from old maps, satellite images and in situ mass balance measurements. *Jökull*, 62, 81–96.

Pálsson, S., 1945. *Ferðabók Sveins Pálssonar. Dagbækur og ritgerðir 1791–1794 [The Travel Book of Sveinn Pálsson. Dairies and Essays 1791–1794]*. Snælandsútgáfan, Reykjavík. [In Icelandic]

Pálsson, S., 2004. *Draft of a physical, geographical and historical description of Icelandic ice mountains on the basis of a journey to the most prominent of them in 1792–1794 with four maps and eight perspective drawings*. The Icelandic Literary Society, Reykjavík.

Paterson, W.S.B., 1994. *The Physics of Glaciers*. Butterworth-Heinemann, Oxford.

Rabatel, A., Machaca, A., Francou, B. and Jomelli, V., 2006. Glacier recession on Cerro Charquini (16 degrees S), Bolivia, since the maximum of the Little Ice Age (17th century). *Journal of Glaciology*, 52, 110–118. doi: 10.3189/172756506781828917

Richards, B.W.M., Benn, D.I., Owen, L.A., Rhodes, E.J. and Spencer, J.Q., 2000. Timing of Late Quaternary glaciations south of Mount Everest in the Khumbu Himal. *Geological Society of America Bulletin*, 112, 1621–1632. doi: 10.1130/0016-7606(2000)112 <1621:Tolqgs>2.0.Co;2

Rögnvaldsson, L., Crochet, P. and Ólafsson, H., 2004. Mapping of precipitation in Iceland using numerical simulations and statistical modeling. *Meteorologische Zeitschrift*, 13, 209–219. doi:10.1127/0941-2948/2004/0013-0209

Schiefer, E. and Gilbert, R., 2007. Reconstructing morphometric change in a proglacial landscape using historical aerial photography and automated DEM generation. *Geomorphology*, 88, 167–178. doi: 10.1016/j.geomorph.2006.11.003

Schomacker, A., 2010. Expansion of ice-marginal lakes at the Vatnajökull ice cap, Iceland, from 1999 to 2009. *Geomorphology*, 119, 232–236. doi:10.1016/j.geomorph.2010.03.022

Sigmundsson, S., 1997. *Skaftafellssýsla. Sýslu- og sóknalýsingar Hins íslenska bókmenntafélags 1839–1873 [The County of Skaftafellssýsla. County and Parish Descriptions of the Icelandic Literature Society 1839–1873]*. Sögufélag, Reykjavík. [In Icelandic]

Sigurðardóttir, M., 2014. *The sedimentology and formation of the Gígjökull and Kvíárjökull latero-frontal moraines, Iceland*. MSc diss. University of Iceland, Reykjavík.

Sigurðsson, O., 2005. Variations of termini of glaciers in Iceland in recent centuries and their connection with climate. In: Caseldine, C., Russell, A., Knudsen, O. and Harðardóttir, J. (eds.), *Iceland – Modern Processes and Past Environments*. Elsevier, Amsterdam. 241–256.

Small, R.J., 1983. Lateral moraines of glacier Detsidjiore-Nouve – form, development, and implications. *Journal of Glaciology*, 29, 250–259.

Snorrason, S., 1984. *Mýrajöklar og Vatnsdalur [The glaciers of Mýrar district and the Vatnsdalur valley]*. Cand Real diss. Universitetet i Oslo, Oslo. [In Norwegian]

Steiner, D., Zumbuhl, H.J. and Bauder, A., 2008. Two Alpine glaciers over the past two centuries: a scientific view based on pictorial sources In: Orlove, B., Wiegandt, E., Luckman, B.H. (eds.), *Darkening Peaks: Glacier Retreat, Science, and Society*. University of California Press, Berkeley. 83–99.

Striberger, J., Björck, S., Holmgren, S. and Hamerlik, L., 2012. The sediments of Lake Lögurinn – a unique proxy record of Holocene glacial meltwater variability in eastern Iceland. *Quaternary Science Reviews*, 38, 76–88. doi: 10.1016/j.quascirev.2012.02.001

Striberger, J., Björck, S., Ingolfsson, O., Kjaer, K.H., Snowball, I. and Uvo, C.B., 2010. Climate variability and glacial processes in eastern Iceland during the past 700 years based on varved lake sediments. *Boreas*, 40, 28–45. doi: 10.1111/j.1502-3885.2010.00153.x

Thompson, A., 1988. Historical development of the proglacial landforms of Svínafellsjökull and Skaftafellsjökull, southeast Iceland. *Jökull*, 38, 17–30.

Thompson, A. and Jones, A., 1986. Rates and causes of proglacial river terrace formation in Southeast Iceland – an application of lichenometric dating techniques. *Boreas*, 15, 231–246.

Thoroddsen, Þ., 1892. Islands Jøkler i Fortid og Nutid [The glaciers of Iceland in the past and at present]. *Geografisk Tidskrift*, 1–36. [In Danish]

Thoroddsen, Þ., 1896. Ferð um Austur-Skaftafellsýslu og Múlasýslur sumarið 1894 [Travelling through the county of Austur-Skaftafellssýsla in the summer of 1894]. *Andvari [The Journal of the Association of Icelandic Allies]*, 21, 1–33. [In Icelandic]

Thoroddsen, Þ., 1911. *Lýsing Íslands II [Description of Iceland II]*. Hið íslenska bókmenntafélag, Kaupmannahöfn. [In Icelandic]
Thoroddsen, Þ., 1925. *Die Geschichte der Isländischen Vulkane: nach einem hinterlassenen Manuskript*. Høst & Søn, København.
Thoroddsen, Þ., 1931–1935. *Lýsing Íslands [Description of Iceland]*. Sjóður Þorvaldar Thoroddsen, Reykjavík. [In Icelandic]
Thoroddsen, Þ., 1958. *Ferðabók. Skýrslur og rannsóknir á Íslandi 1882–1898 [Travel Book. Reports and Research from Iceland 1882–1898]*. Snæbjörn Jónasson, Reykjavík. [In Icelandic]
Tómasson, H. and Vilmundardóttir, E.G., 1967. The lakes Stórisjór and Langisjór. *Jökull*, 17, 280–295.
Tómasson, Þ., 1980. *Skaftafell: þættir úr sögu ættarseturs og atvinnuhátta [Skaftafell: Accounts of the Family History and Farming Practices]*. Þjóðsaga, Reykjavík. [In Icelandic]
Torell, O., 1857. Bref om Island [Letters on Iceland]. *Öfersigt af Kongl.Vetenskaps-Akademiens förhandlingar [An Overview of the Proceedings of the Royal Science Academy]*. 325–335. [In Swedish]
Vallis, V.G.S., 2013. *Investigating the effects of topography on glaciers in the Purcell and Rocky Mountain Ranges during the LIA and in 2005*. MSc diss. University of Calgary, Calgary Alberta.
Vinther, B.M., Buchardt, S.L., Clausen, H.B., Dahl-Jensen, D., Johnsen, S.J., Fisher, D.A., Koerner, R.M., Raynaud, D., Lipenkov, V., Andersen, K.K., Blunier, T., Rasmussen, S.O., Steffensen, J.P. and Svensson, A.M., 2009. Holocene thinning of the Greenland ice sheet. *Nature*, 461, 385–388. doi: 10.1038/Nature08355
Wanner, H., Solomina, O., Grosjean, M., Ritz, S.P. and Jetel, M., 2011. Structure and origin of Holocene cold events. *Quaternary Science Reviews*, 30, 3109–3123. doi: 10.1016/j.quascirev.2011.07.010
Williams, R.S., 1987. Satellite remote sensing of Vatnajökull, Iceland. *Annals of Glaciology*, 9, 127–135.
Wood, K.R., Overland, J.E., Jonsson, T. and Smoliak, B.V., 2010. Air temperature variations on the Atlantic-Arctic boundary since 1802. *Geophysical Research Letters*, 37. doi: 10.1029/2010gl044176
Zasadni, J. and Klapyta, P., 2009. An attempt to assess the modern and the Little Ice Age climatic snowline altitude in the Tatra Mountains. *Landform Analysis*, 10, 124–133.
Zumbühl, H.J., Steiner, D. and Nussbaumer, S.U., 2008. 19th century glacier representations and fluctuations in the central and western European Alps: an interdisciplinary approach. *Global and Planetary Change*, 60, 42–57. doi: 10.1016/j.gloplacha.2006.08.005
Þorkelsson, J., 1918–1920. Jarðabók Ísleifs sýslumanns Einarssonar yfir Austur-Skaptafellssýslu í umboði Árna Magnússonar 1708–1709 [The book of farms in Austur-Skaftafellssýsla 1708–1709 by the county governor Ísleifur Einarsson by the commission of Árni Magnússon], *Blanda – Fróðleikur gamall og nýr [Blanda – Old and New Knowledge]*. Sögufélagið, Reykjavík. 1–38. [In Icelandic]
Þórarinsson, S., 1939. The ice dammed lakes of Iceland with particular reference to their values as indicators of glacier oscillations. *Geografiska Annaler*, 21, 216–242.
Þórarinsson, S., 1943. Oscillations of the Iceland glaciers in the last 250 years. *Geografiska Annaler*, 25 bls. 1–54.
Þórarinsson, S., 1956. The thousand years struggle In: Þórarinsson, S. (ed.), *The Thousand Years Struggle Against Ice and Fire*. Bókaútgáfa menningarsjóðs, Reykjavík. 5–33.
Þórarinsson, S., 1960. Glaciological knowledge in Iceland before 1800. *Jökull*, 10, 1–17.
Þórarinsson, S., 1964. On the variations of Svínafellsjökull, Skaftafellsjökull and Kvíárjökull in Öræfi. *Jökull*, 6, 1–15.
Þórarinsson, S., 1974. Sambúð lands og lýðs í ellefu aldir [Living in Iceland for eleven centuries]. In: Líndal, S. (ed.), *Saga Íslands, 1. bindi [The History of Iceland, 1st volume]*. Sögufélagið, Reykjavík. 29–97. [In Icelandic]

Manuscript received 12 Mar., 2014, revised and accepted 17 Jul., 2014

Paper II

Guðmundsson, S., Hannesdóttir, H., Björnsson, H. (2012). Post-Little Ice Age (1891-2011 AD) volume loss of Kotárjökull glacier, SE-Iceland, as established from historical photography. Jökull 62, 97-110.

Reviewed research article

Post-Little Ice Age volume loss of Kotárjökull glacier, SE-Iceland, derived from historical photography

Snævarr Guðmundsson, Hrafnhildur Hannesdóttir and Helgi Björnsson
Institute of Earth Sciences, University of Iceland, Sturlugata 7, 101 Reykjavík, Iceland
Corresponding author: snaevarr@mmedia.is

Abstract – *Kotárjökull is one of several outlet glaciers draining the ice-covered central volcano Öræfajökull in SE-Iceland. We estimate the average annual specific mass loss of the glacier, to be 0.22 m (water equivalent) over the post Little Ice Age period 1891–2011. The glacial recession corresponds to an areal decrease of 2.7 km^2 (20%) and a volume loss of 0.4 km^3 (30%). A surface lowering of 180 m is observed near the snout decreasing to negligible amounts above 1700 m elevation. This minimal surface lowering at high altitudes is supported by a comparison of the elevation of trigonometrical points on Öræfajökull's plateau from the Danish General Staff map of 1904 and a recent LiDAR-based digital elevation model. Our estimates are derived from a) three pairs of photographs from 1891 and 2011, b) geomorphological field evidence delineating the maximum glacier extent at the end of the Little Ice Age, and c) the high-resolution digital elevation model from 2010–2011. The historical photographs of Frederick W.W. Howell from 1891 were taken at the end of the Little Ice Age in Iceland, thus providing a reference of the maximum glacier extent.*

INTRODUCTION

The first descriptions of the Little Ice Age (LIA) glacier margins in Iceland were collected in the proximity of inhabitated regions south of Vatnajökull ice cap. Occasional reports descend from travellers passing through rural districts in the 18th and 19th centuries (e.g. Þórarinsson, 1943; Björnsson, 2009). Less attention was paid to the smaller outlet glaciers, although sparse observations were made during traverses on the glaciers. A number of photographs of Icelandic glaciers from the late 19th and early 20th century are preserved (Ponzi, 2004; Archives of the National Land Survey of Iceland; Reykjavík Museum of Photography; National Museum of Iceland). They provide valuable information on glacier extent, and can be analyzed by repeat photography to deduce glacier changes. This approach has been used world-wide, and first practiced to document glacier variations in the European Alps in the late 1880s (see e.g. Harrison, 1960; Luckman *et al.*, 1999; Molnia, 2010; Webb *et al.*, 2010; Fagre, 2011).

In this paper we present unique historical oblique photographs of Kotárjökull outlet glacier (Figures 1 and 2) from the first ascent of Hvannadalshnúkur (the highest peak in Iceland) in Öræfajökull in 1891 (Guðmundsson, 1999). They were taken by an English traveller, Frederick W. W. Howell (1857–1901), who together with two companions from the farm Svínafell (Páll Jónsson and Þorlákur Þorláksson) reached the summit on 17th of August. The photographs are among the first prints of glaciers in Iceland, and were taken during the 1890 LIA maximum stage (e.g. Þórarinsson, 1943). His photographs are used to derive the geometry of the LIA maximum glacier, by trigonometric calculations, and by including information from present-day photographs, geomorphological evidence and a detailed digital elevation model (DEM). Our findings allow quantitative estimates of

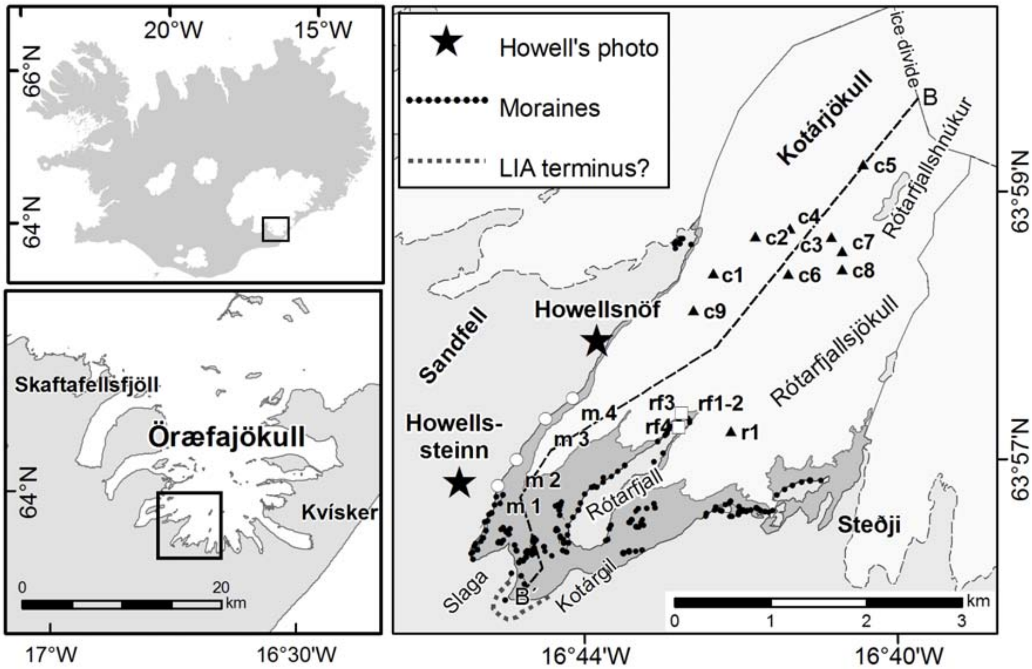

Figure 1. Kotárjökull glacier flows southwest from Öræfajökull ice cap. The eastern branch of the glacier is named Rótarfjallsjökull. The white area delineates the glacier's extent in 2011, whereas the middle-gray area indicates the glacier outline at the LIA maximum. Crevasse areas (black triangles) are used to calculate glacier surface changes between 1891 and 2011. Black dots represent lateral moraines used to reconstruct the maximum glacial extent in the gorge, and white circles and boxes indicate sites where surface changes are estimated from geomorphological and photographic evidence. Line B-B' is a longitudinal profile for later discussion. – *Kotárjökull skríður suðvestur úr Öræfajökulsöskjunni en eystri armurinn er nefndur Rótarfjallsjökull. Hvítt svæði sýnir útlínur jökulsins árið 2011 en milli-grátt markar hámarksútbreiðslu á litlu ísöld. Ísaskil liggja innan við öskjubrúnina í um 1800 m hæð. Yfirborðslækkun milli 1891 og 2011 var metin út frá gömlum ljósmyndum af sprungukollum (svartir þríhyrningar). Svartar punktraðir sýna jaðarurðir og hvítir hringir ásamt hvítum kössum sýna staði sem voru notaðir til þykktarútreikninga í Kotárgili út frá ljósmyndum Howells og rofmörkum. Línan B-B' sýnir hvar langskurðarsnið af jöklinum liggur. Howellssteinn og Howellsnöf eru ekki örnefni heldur heiti á kennileitum á Sandfelli.*

glacier mass change over the last 120 years. We also compare the 1904 map of the Danish General Staff (Herforingjaráðið, 1905) of Öræfajökull's plateau, at an altitudinal range of 1700–2100 m, with a recent DEM, to get an estimate of glacier surface changes during this time period.

RESEARCH AREA

Öræfajökull is a 2000 m high ice-covered central volcano. The ice-filled caldera is 5 km wide and 500 m deep, with an ice volume of 4.6 km^3 (Björnsson, 1988; Magnússon *et al.*, 2012). Ice flows over the caldera rim and forms several outlet glaciers. The ice thickness of Kotárjökull is on average 90 m, approx-

Figure 2. Oblique arieal photograph of Öræfajökull and Kotárjökull. The maximum LIA glacier extent is marked with a dotted line. Traces of the terminus in Kotárgil are obscure, especially east of Slaga, hence two possible extensions are presented. Photo. SG 17th of August 2006. – *Flugmynd af Kotárjökli og Rótarfjallsjökli, tekin 17. ágúst 2006 (SG). Punktalínur marka útbreiðslu jökulsins við hámark litlu ísaldar. Ummerki um stöðu sporðsins eru óljós neðst í Kotárgili og því eru tveir möguleikar sýndir.*

imated from the surface slope of the glacier (Magnússon *et al.*, 2012). The glacier plateau receives the highest amounts of annual precipitation in Iceland, 5700–7800 mm w.e., almost entirely falling as snow (Björnsson *et al.*, 1998; Guðmundsson, 2000). Comparison with observed precipitation from the nearest lowland meteorological station Kvísker (Figure 1), implies that the precipitation on the ice cap, is twice as high as on the lowlands to the southeast of Öræfajökull (Guðmundsson, 2000).

Kotárjökull covers at present about 11.5 km^2, with an average slope of 20°, and the equilibrium line lies around 1100–1200 m. Heading from an elevation of 1800 m, inside the caldera, the glacier is split into two branches by Rótarfjall mountain (946 m): the main branch terminating in 300–400 m wide gorge (Figures 1 and 2), and the eastern branch, Rótarfjallsjökull. These glaciers surrounded Rótarfjall, and merged together in Kotárgil, at the end of the 19th century (Thoroddsen, 1896). Parts of the terminal moraine northwest of Slaga mountain are obscure and may be remnants of an older stage. No dead ice is observed in the glacier's marginal area.

DATA

The photographs of Frederick W.W. Howell were taken from two locations on Sandfell mountain (Figures 1 and 2): a) one shot towards east to Rótarfjall from Howellssteinn (N63.9497°, W16.7587°, elevation 573 m a.s.l.) and b) two shots from Howellsnöf (N63.9624°, W16.7286°, elevation 1020 m), $^{1)}$northeast towards Rótarfjallshnúkur (1833 m) across the upper slopes of the Kotárjökull, and $^{2)}$east towards Rótarfjall. Howellssteinn and Howellsnöf are not geographical place names, but used as landmarks by the authors. The photographs confirm, that the highest lateral moraines, trimlines and glacial erratics in the narrow gorges of Kotárgil and Berjagil are from the 1890 LIA maximum (Figure 2) . In November 2011 the two locations were revisited, the photos reframed, and the acquired duplicates (Figures 3a-b, 4a-b and 5a-b) used to calculate the recession of the glacier between 1891 and 2011. Howell's photographs are available in the Fiske Icelandic Collection, at the Cornell University Library website.

High-resolution aerial images of Loftmyndir ehf© (2003) were used to outline the LIA maximum glacier. In situ and oblique aerial photographs of 2006 and 2010, helped derive the glacial extent.

A recent DEM, produced from airborne LiDAR measurements in August 2010 and September 2011 (data from the Icelandic Meteorological Office and the Institute of Earth Sciences, University of Iceland, 2011; Jóhannesson *et al.*, 2012); provides accurate position and elevation (Table 1). The DEM has a horizontal resolution of 5x5 m and vertical accuracy within 0.5 m. It provides precise elevation of the lateral moraines and trimlines.

METHODS

The extent of Kotárjökull at the LIA maximum, was based on photographic and geomorphological evidence, and the LiDAR DEM providing basic topographical data. The glacier margin in the ablation area, is delineated from the highest lateral moraines, glacial erratics, and trimlines. Data on elevation changes above the equilibrium line are restricted to the old photographs. The idea of obtaining quantitative estimates of glacier changes from the photographic duplicates, originates from methods used in astrometry. The movements of distant objects are measured over time from separate images, taken hours to decades apart.

Repeat photography

The three photographic pairs of Kotárjökull were collimated in GIS ArcMap (Figures 3a-b, 4a-b, 5a-b). A 3D-image, a duplication of Figure 3b, was produced from the DEM in ArcScene, to improve the accuracy of our measurements. The southeastern flank of Rótarfjallshnúkur has apparently undergone some landform changes since 1891, perhaps a landslide. The photos in Figures 3a-b were collimated, using the northern (I) and southern (II) peaks of Rótarfjallshnúkur for reference, the top of Sandfell (III), and a crevasse area (IV) on the horizon to the west of Rótarfjallshnúkur (Figure 6). The photographs in Figures 4a-b were referenced with four points, and in Figures 5a-b, with 10 points. The ease of collimating the duplicate photos, indicates minimal errors related to the older camera's focal length.

Nine crevasse areas in the accumulation area (Figures 3a-b), were used for surface elevation calculations. The lowering was measured in pixel units and converted to metres. A total of 7 measurements evenly distributed over each crevasse bulge, from center towards left (l_{1-3}) and right (r_{1-3}), were used to obtain a mean pixel value for the surface lowering (Figure 6 and Table 1). Two independent routines to calculate the glacier surface changes in metres were used.

Routine 1

The vertical glacier surface change (Δh) at any distance (d) from the site of photography was estimated by scaling in metres the pixel unit size (θ_u= H/n_m) based on a known vertical height of a mountain cliff (H spanning n_m pixels) at a known distance (D_o), in this case Rótarfjallshnúkur (Figure 6). If the measured surface lowering of a crevasse area in pixel units is n_c, the corresponding glacier surface change in metres is:

$$\Delta h = \theta_u \times (d/D_o) \times n_c$$

The northern face of Rótarfjallshnúkur is 60 m high (H_I) and n_{mI} = 30 pixels, hence θ_{uI} = 2.0 m/pixel; the distance to the face from Howellsnöf is D_I= 3.650

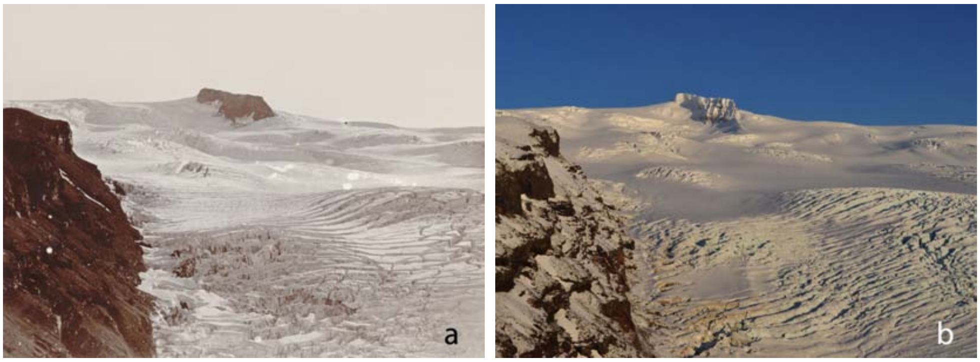

Figure 3. Kotárjökull and Rótarfjallshnúkur, view from Howellsnöf on Sandfell. – *a) Kotárjökull og Rótarfjallshnúkur, útsýni frá Howellsnöf.* Photos./*Myndir.* Howell and SG.

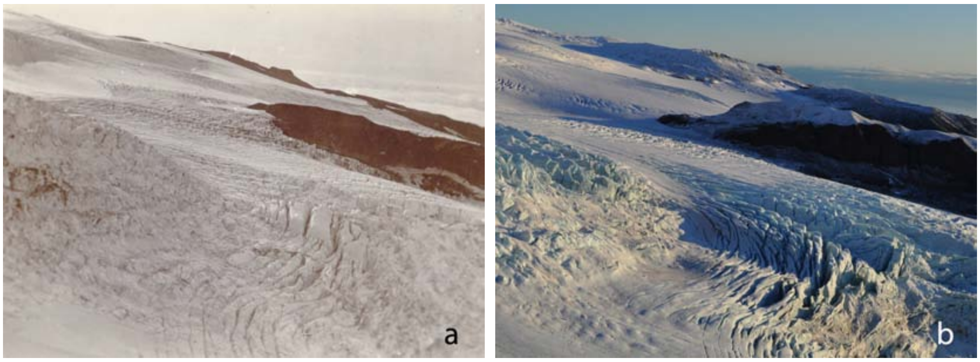

Figure 4. Kotárjökull (near) and Rótarfjallsjökull divided by Rótarfjall, view from Howellsnöf on Sandfell. Steðji ridge appears against the skyline. – *Kotárjökull og Rótarfjallsjökull, útsýni frá Howellsnöf á Sandfelli. Steðja ber við himinn.* Photos./*Myndir.* Howell and SG.

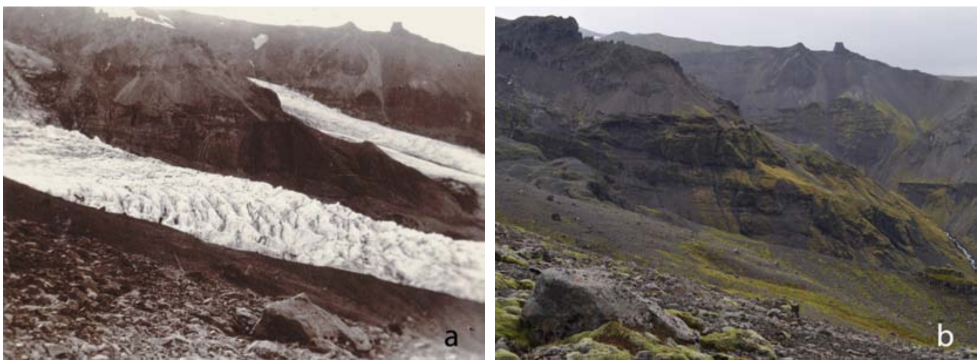

Figure 5. Kotárjökull and Rótarfjallsjökull in Kotárgil, view from Howellssteinn. – *Kotárjökull og Rótarfjallsjökull, fylltu Kotárgil 1891. Horft til austur frá Howellssteini.* Photos./*Myndir.* Howell and SG.

Table 1. Dimensions of the crevasse areas, and surface elevation change measurements in pixel units. – *Tafla 1. Grunnupplýsingar um sprungukollana (c1–c9) sem notaðar voru til þess að reikna yfirborðslækkun. Meðalhæðarbreyting (í myndeiningum) út frá 7 mælingum á hverjum sprungukolli.*

						measurements (pixels)							
area	latitude	longitude	altit. (m)	d (m)	bearing°	I_1	l_2	l_3	center	r_1	r_2	r_3	$\Delta\theta$
c1	63.9683	16.7031	1166	1405	60.2	14.36	14.92	13.40	13.2	13.25	12.83	10.02	13.14
c2	63.9716	16.6939	1319	1977	56.7	5.73	5.73	6.33	5.29	4.62	4.73	3.85	5.18
c3	63.9722	16.6865	1398	2328	59.9	5.76	5.19	4.05	5.76	5.99	5.85	5.99	5.51
c4	63.9713	16.6778	1429	2673	66.2	2.86	2.36	2.29	2.86	2.86	2.86	2.92	2.72
c5	63.9779	16.6703	1677	3335	56.60	2.36	2.29	2.36	1.81	1.81	1.81	1.81	2.04
c6	63.9680	16.6872	1283	2113	70.80	4.62	4.01	3.49	5.29	5.19	6.41	8.05	5.29
c7	63.9697	16.6790	1367	2723	70.00	1.72	1.72	1.72	1.72	1.72	2.29	1.72	1.80
c8	63.9682	16.6757	1403	2666	73.90	2.92	3.63	3.49	2.92	2.92	3.49	2.06	3.06
c9	63.9650	16.7077	1083	1058	72.50	13.78	13.88	11.70	15.5	15.59	16.60	16.07	14.73

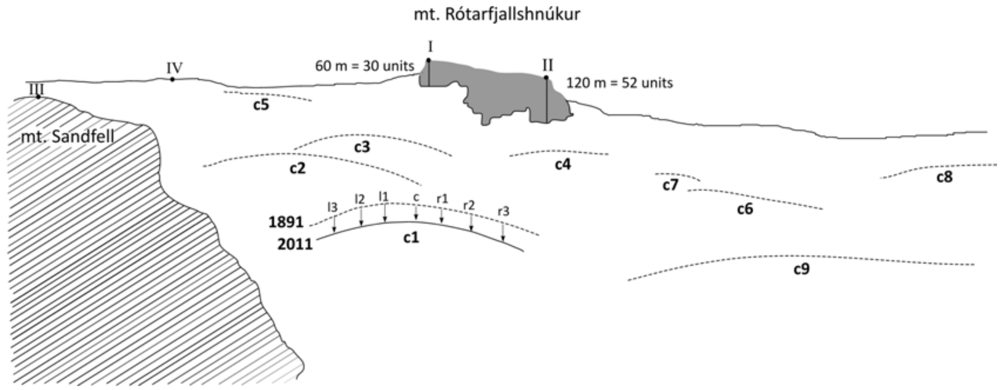

Figure 6. A sketch of the crevassed accumulation area of Kotárjökull. The edge of each crevasse area in 1891 (c1-c9) shown as a dotted line. Surface lowering of each area derived from 7 points, as illustrated for crevasse area c1. Collimation points are indicated in Roman numerals (I-IV). – *Sprungukollar (c1-c9) á safnsvæði Kotárjökuls voru notaðir í útreikninga á hæðarbreytingu milli 1891– 2011. Á sprungukolli c1 er sýnt hvernig gerðar eru 7 mælingar á þykktarbreytingu milli áranna 1891 (punktalína) og 2011 (heil lína), til þess að fá fram meðalbreytingu. Hamrarnir suðvestanmegin í Rótarfjallshnúk voru notaðir sem viðmið til þess að áætla þykktarbreytingar í aðferð 1. Ljósmyndirnar tvær voru stilltar af með fjórum punktum merktum I-IV.*

m (Figure 6). The southern face is H_{II} = 120 m and n_{mII} = 52 pixels, hence θ_{uII} = 2.3 m/pixel and the distance from Howellsnöf D_{II} = 3.320 m. To test the quality of θ_u as a satisfactorily accurate value, we calculated the size of θ_{uII} at distance D_I;

$(\theta_{uII} \times D_I)/\ D_{II} = \theta_{uII/DI}$ = 2.5 m/pixel

and then obtained an average value for θ_{uI} of 2.25 m/pixel (θ_u) at distance D_I, which was used in all calculations. Glacier surface changes were also calculated for crevasse area r_1 (Figures 1 and 4a-b), using routine 1.

Routine 2

The pixel unit size, which is used as a reference for surface elevation changes, was determined from the photographs by calculating a lateral scaling distance (a = *d tan* α) perpendicular to the line of sight from Howellsnöf to each distinct crevasse area. The distance from the site of photography is *d*, and α the angle between two crevasse areas, as seen from Howellsnöf (Figure 7). The length of the opposite side is used to find the size of the pixel unit at distance *d*. Since the measured surface lowering in pixel units

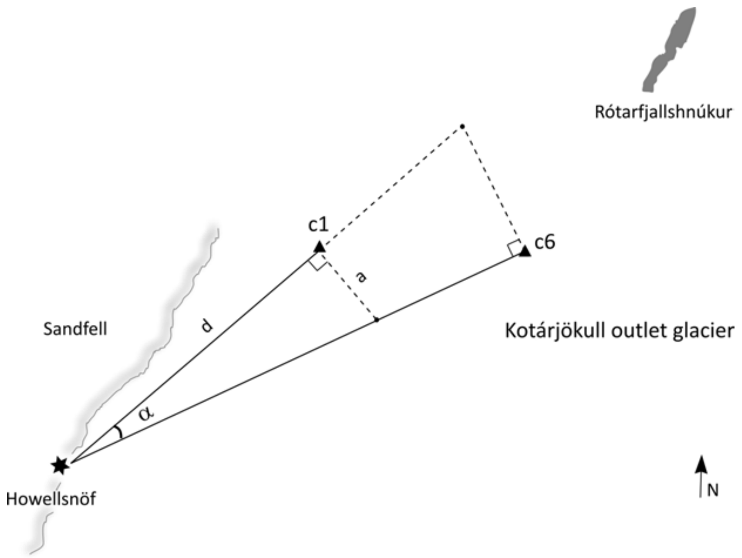

Figure 7. A schematic aerial view explaining routine 2. See text for clarification. – *Yfirlitsmynd fyrir aðferð 2. Ef fjarlægð frá Howellsnöf í hvern stakan sprungukoll (d) og hornið (α) á milli þeirra eru þekkt, fæst lengd mótlægrar hliðar (a) samkvæmt tan α=a/d og hversu stórt hornbilið er í metrum í þekktri fjarlægð. Þannig finnum við stærð myndeiningarinnar í sömu fjarlægð. Yfirborðslækkun jökulsins (Δh) er hlutfall af lengd mótlægu skammhliðarinnar. Punktalínur gefa til kynna hvernig aðlaga má hliðar þríhyrninga samkvæmt því í hvaða punkt er mælt.*

($\Delta\theta$) is a certain ratio of the opposite side, we can calculate the change in metres at a distance d from the site of photography:

$$\Delta h = \Delta\theta\ (d\ tan\alpha)/n$$

where n is the number of pixels of the corresponding angle α. This is possible since horizontal and vertical scales of the pixels are the same. We can extend the triangle's hypotenuse, depending on the point we aim at (illustrated by the dotted line in Figure 7).

The LIA glacier and volume calculations

We assume unchanged glacier geometry in the accumulation area, as seen from the photos in Figures 3a-b. Calculated elevation changes were used to raise the contour lines of the LiDAR DEM to an 1891 level. The reconstructed cross-valley profiles of the two branches, below the equilibrium line, are convex, with a maximum height of 20 m at the glacier center line. This assumption is based on the photographs in Figures 4a-b and 5a-b. Our estimate for the uncertainty limits of the reconstructed 1891 surface is $\pm$2 m. A gradual thickness changes along the longitudinal profile of Kotárjökull is assumed (Figure 1), and interpolated between data thickness points using a least-square fit to a log-linear equation. The volume loss of Kotárjökull was calculated by subtracting the glacier surface of 2011 from the reconstructed surface of 1891.

Elevation changes on Öræfajökull's plateau

The 1904 map of Öræfajökull of the Danish General Staff was georeferenced with the LiDAR DEM, and the elevation of selected trigonometrical points from the older map compared with the DEM, to resolve possible glacier surface changes. Nine geodetic points on mountain peaks or nunataks and eleven on the glacier surface were selected for this purpose, spanning an altitudinal range of 1700–2100 m.

RESULTS

Surface elevation changes

Crevasse areas were used to calculate elevation changes in the accumulation zone (Tables 1, 2 and 3). Routines 1 and 2 give similar results, showing an average difference of 1.1 m, with routine 1 always giving higher values (Table 4). Surface changes above 1700 m were negligible, and 4–11 m from there down to the equilibrium line. The lowering gradually increasing, 20–30 m north of Rótarfjall (Figures 4a-b and Table 5), and reaching a maximum of 180 m in Kotárgil (Figures 8, 9 and Table 5).

Table 2. Surface elevation changes measured by routine 1. – *Tafla 2. Yfirborðslækkun á safnsvæði Kotárjökuls samkvæmt reikniaðferð 1.*

area	$\Delta\theta(px)$	m/px	Δh (m)
c1	13.14	0.91	11.4
c2	5.18	1.28	6.3
c3	5.51	1.50	7.9
c4	2.72	1.73	4.5
c5	2.04	2.15	4.2
c6	5.29	1.36	6.9
c7	1.80	1.76	3.0
c8	3.06	1.72	5.0
c9	14.73	0.68	9.6

Area and volume changes

Glacial retreat and the volume loss of Kotárjökull is based on the inner margin in Kotárgil. The terminus of Kotárjökull has retreated 1.3 km, since the LIA maximum, from an elevation of 175 m to 350 m (Figure 9). Rótarfjallsjökull has retreated ca. 2 km, and the terminus is currently at an elevation of 660 m. The eastern branch, with a small part of the accumulation area extending up to the ice cap plateau, has on average retreated 17 m/yr, whereas the main branch shows a mean recession of 11 m/yr. Rótarfjallsjökull receives less ice from the caldera and has a smaller accumulation area. The whole glacier area has decreased from 14.5 to 11.5 km^2 (20%), and the volume loss has been approximately 0.4 $\pm$0.02 km^3, relative to the more limited glacier margin in Kotárgil (Figure 1). Given the average glacier thickness of 90 m (Magnússon *et al.*, 2012), Kotárjökull has lost approximate 30% of its volume. Evenly spread over the mean glacier area, the recession corresponds to a loss of about 0.22 $\pm$0.01 m w.e./yr.

Table 3. Surface elevation changes measured by routine 2. Three calculations for each crevasse area, and the lowering presented in the last two columns with the relevant area in parenthesis. – *Tafla 3. Yfirborðslækkun á efra svæði Kotárjökuls samkvæmt reikniaðferð 2. Þrjár mælingar gerðar fyrir hvert sprungusvæði. Í sviga í síðasta dálki er tilgreint hvaða sprungusvæði lækkunin á við.*

crev. area	α	a (px)	Δh (m)	Δh (m)
c1→c9	12.3	394	10.2 (c1)	8.6 (c9)
c1→c8	13.7	429	10.5 (c1)	3.7 (c8)
c1→c6	10.6	329	10.5 (c1)	6.4 (c6)
c2→c6	14.1	441	5.8 (c2)	6.4 (c6)
c2→c8	17.2	534	5.9 (c2)	4.7 (c8)
c2 →c4	9.5	293	5.8 (c2)	4.1 (c4)
c3→c2	3.2	101	7.1 (c3)	5.7 (c2)
c3→c7	10.1	312	7.3 (c3)	2.8 (c7)
c3→c4	6.3	194	7.3 (c3)	4.1 (c4)
c4→c7	3.8	118	4.1 (c4)	2.7 (c7)
c4→c6	4.6	152	3.8 (c4)	5.9 (c6)
c7→c8	3.9	125	2.7 (c7)	4.4 (c8)
c9→c3	12.6	429	8.1 (c9)	6.7 (c3)
c9→c2	15.8	519	8.5 (c9)	5.6 (c2)
c4→c5	9.6	308	4.0 (c4)	3.7 (c5)
c3→c5	3.3	120	6.2 (c3)	3.3 (c5)
c1→c5	3.6	187	6.2 (c1)	2.3 (c5)

Table 4. Comparing the surface elevation changes of Kotárjökull above 1100 m elevation, calculated by the two routines. Routine 2 based on average values from Table 3. – *Tafla 4. Niðurstöður og samanburður reikniaðferða á þykktarbreytingum Kotárjökuls ofan 1100 m hæðar. Gildi fyrir aðferð 2 eru meðaltöl úr Töflu 3.*

crevasse area	Δh (routine 1)	Δh (routine 2)	Δh difference
c1 (1166 m)	11.4 m	9.4 m	2.0 m
c2 (1319 m)	6.3 m	5.8 m	0.5 m
c3 (1398 m)	7.9 m	6.9 m	1.0 m
c4 (1429 m)	4.5 m	4.0 m	0.5 m
c5 (1677 m)	4.2 m	3.1 m	0.9 m
c6 (1283 m)	6.9 m	6.2 m	0.7 m
c7 (1367 m)	3.0 m	3.1 m	0.1 m
c8 (1403 m)	5.0 m	4.3 m	0.7 m
c9 (1083 m)	9.6 m	8.4 m	1.2 m

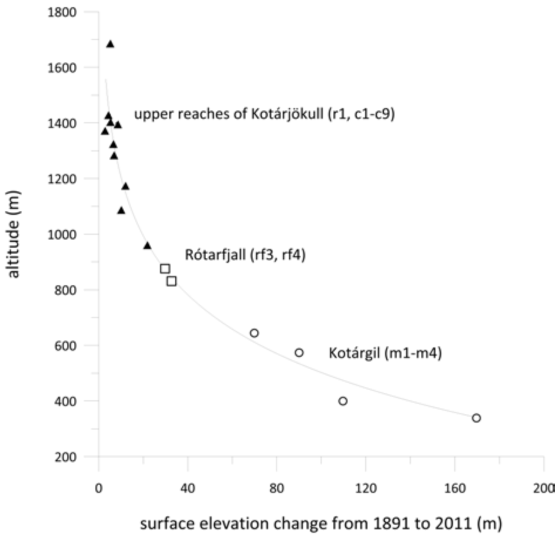

Figure 8. Surface elevation changes of Kotárjökull along profile B'B derived from photographic evidence, lateral moraines and trimlines along the edge of the glacier. Symbols in accordance to Figure 1, triangles represent the averaged thickness change by routine 1 and 2. Few lateral moraines could be used to estimate glacier thickness change in the lower parts of Kotárgil gorge due to the uneven valley floor. – *Yfirborðsbreyting Kotárjökuls, reiknuð út frá samanburði ljósmynda, urðum og rofmörkum í fjallshlíðum við jaðra jökulsins. Tákn eru í samræmi við 1. mynd og þríhyrningar meðalþykktarbreyting samkvæmt aðferð 1 og 2. Fáir staðir nýtast til þess að áætla þykktarbreytingar neðarlega í botni stórskorins Kotárgils.*

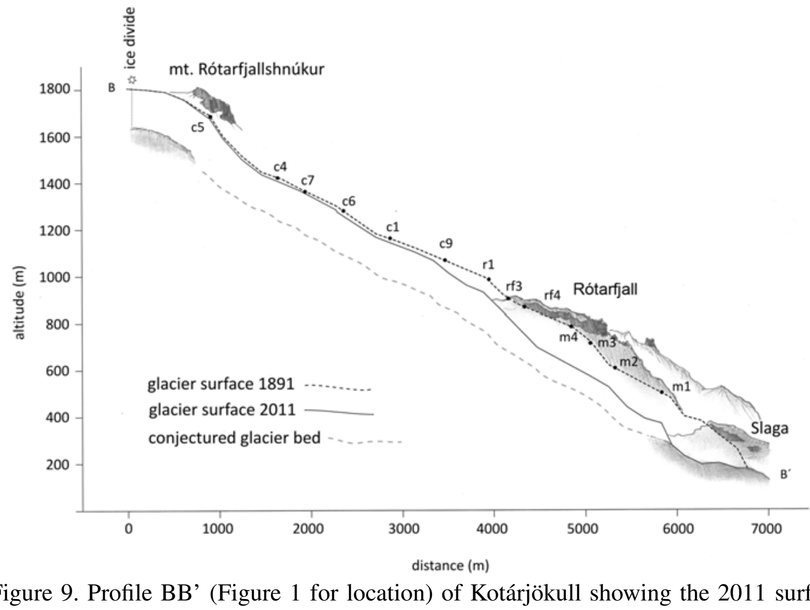

Figure 9. Profile BB' (Figure 1 for location) of Kotárjökull showing the 2011 surface and in 1891. The ice thickness on the caldera rim is known from radio-echo sounding measurements, to be approximately 150 m (Magnússon *et al.*, 2012). The glacier bed (dotted gray line) is sketched elsewhere, based on a correlation between ice thickness and surface slope (Magnússon *et al.*, 2012). – *Langskurðarmynd BB' (sjá 1. mynd) sýnir yfirborð Kotárjökuls 2011 (samkvæmt LiDAR-gögnum) og 1891 samkvæmt útreikningum okkar á hæðarbreytingum (c_1–c_9 og r_1), jaðarurðum í hlíðum Rótarfjalls (rf_3 og rf_4) og í Kotárgili (m_1–m_4). Þykkt jökulsins á öskjurimanum er 150 m samkvæmt íssjármælingum, en meðalþykkt jökulsins nálægt 90 m (sjá nánar grein Eyjólfs Magnússonar o.fl. 2012).*

Table 5. Surface elevation change in the ablation area deduced from Figures 4a-b, 5a-b and lateral moraines and other geomorphological features in Kotárgil. – *Tafla 5. Mælipunktar fyrir yfirborðsbreytingar á leysingarsvæði samkvæmt myndum 4a-b, 5a-b og jaðarurðum í Kotárgili.*

data points	description	latitude	longitude	alt. 2011 (m)	alt. 1891 (m)
r1	crevasse area	63.9536	16.7007	950	982
rf1	peak of Rótarfjall	63.9547	16.7091	946	–
rf2	N tip of Rótarfjall	63.9540	16.7118	936	–
rf3	W side of Rótarfjall	63.9554	16.7110	881	911
rf4	W side of Rótarfjall	63.9544	16.7126	840	872
steðji1	ridge	63.9420	16.6801	970	–
steðji2	ridge	63.9412	16.6810	960	–
m4	lateral moraine	63.9571	16.7341	650	720
m3	lateral moraine	63.9553	16.7400	570	660
m2	lateral moraine	63.9520	16.7466	400	510
m1	lateral moraine	63.9492	16.7507	340	520

Surface lowering on the glacier plateau?

To resolve possible elevation changes of the ice plateau of Öræfajökull, the 1904 map and the 2011 DEM were collimated (Figures 10a-b). Minor distortion was observed on the plateau, compared to the level of deviation in the lower rugged terrain of the mountain massif. The difference in elevation registered on the trigonometrical points above 1700 m is shown in Table 6. The elevation of the glacier points is on average 12.3 m higher on the 1904 map than the LiDAR DEM, and 11.9 m higher on the peaks or nunataks. This dissimilarity also applies to the ice-covered Hvannadalshnúkur. The peak was measured in 1904 at an altitude of 2119 m. The summit is 2110 m high according to the new DEM, which confirms recent measurements by the Glaciological Society of Iceland (1993 and 2004) and the National Land Survey of Iceland in 2005 (Guðmundsson, 2004; Morgunblaðið, 7th of August 2005). The surveying of the Öræfajökull ice cap by the Danish General Staff, was based on optical triangulation in several steps over long distances from the lowland through peaks in Öræfajökull and Skaftafellsfjöll (Figure 1, Koch, 1905).

DISCUSSION

Surface elevation changes of Kotárjökull are negligible at high elevations, increasing to maximum thinning of 180 m, of the former terminus in the gorge. Nowhere else along the southeastern edge of Vatnajökull, are glacier surface elevation changes since the LIA maximum recorded continuously downward from the ice divide to the terminus. The surface lowering at the glacier snout is similar to what has been observed on other outlet glaciers of Vatnajökull to the west and east of Kotárjökull (Hannesdóttir *et al.*, 2012). Comparable total volume loss over the 20th century is reported for Hoffellsjökull and its neighbouring southeastern outlet glaciers, on the order of 20–30% (Aðalgeirsdóttir *et al.*, 2011; Hannesdóttir *et al.*, 2012). The well-preserved lateral moraines are only found below the equilibrium line, hence little field evidence attests to the former high stands of the glacier in the accumulation area at its maximum extent during the LIA. The historical oblique photographs are the only archive for surface changes in the accumulation area.

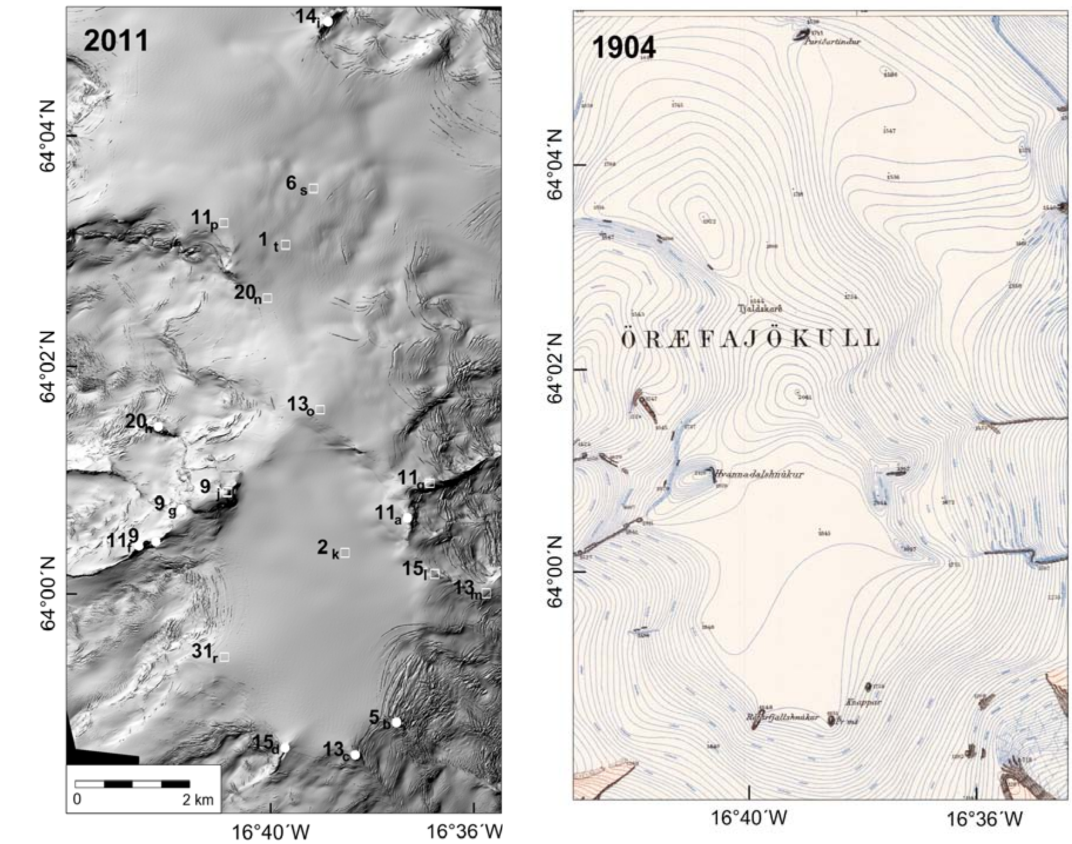

Figure 10. Elevation difference of selected trigonometrical points on the high plateau of Öræfajökull ice cap, between a) the LiDAR DEM (2011) and b) the 1904 map of the Danish General staff. Squares indicate points on the glacier, and filled circles represent points on nunataks. Each location is marked with a letter corresponding to Table 6. – *Hæðarmunur á völdum mælipunktum á Öræfajökli milli a) LiDAR-hæðargrunns og b) korts danska herforingjaráðsins frá 1904 er sýndur. Hver punktur er táknaður með bókstaf (sjá töflu 6). Kassar tákna mælistaði á jökli en fylltir hringir sýna mælipunkta á tindum eða jökulskerjum.*

No elevation change of the 5 km wide glacier plateau covering the caldera is remarkable. The ice cap has limited possibilities to expand, since any surplus in mass balance will flow straight over the caldera rim to lower elevations. The thickness change with altitude observed between the end of the 19th century and 2011 on Kotárjökull, provides a reference for further studies of other outlet glaciers of Öræfajökull and the southern edge of Vatnajökull.

The observed elevation anomaly of the trigonometrical points, along with calculated surface changes in the accumulation area, raises the question whether the geodetic survey of the plateau of Öræfajökull may have been inaccurate by about 10 m (see Table 6). We speculate whether this is due to errors, i.e. caused by light refraction, across a surface with variable reflectance and changing temperature conditions (as described in Böðvarsson, 1996). We therefore doubt,

Table 6. Selected trigonometrical points on the glacier plateau (g) and peaks (p) of Öræfajökull ice cap, used to compare their elevation (see Figure 10a-b) from the LiDAR DEM and the 1904 map. Locations from the LiDAR DEM. – *Tafla 6. Samanburður á hæð nokkurra mælipunkta innan Öræfajökulsöskjunnar milli korts danska herforingjaráðsins frá 1904 og LiDAR-hæðargrunns. Þríhyrningsmælipunktar á tindum (p) og á jökli (g) sem sýndir eru á 1904 kortinu (sjá mynd 10).*

Location	x (m)	y (m)	z_{LiDAR} (m)	$z_{1904map}$ (m)	Δ z (m)
a Sveinstindur (p)	64.0095	16.6181	2033	2044	11
b) Eystri Hnappar (p)	63.9799	16.6243	1753	1758	5
c) Vestari Hnappar (p)	63.9755	16.6382	1838	1851	13
d) Rótarfjallshnúkur (p)	63.9769	16.6613	1833	1848	15
e) Dyrhamar (p)	64.0074	16.7014	1902	1911	9
f) Hvannadalshryggur (p)	64.0068	16.7070	1830	1841	11
g) west face of Hvannadalshnúkur (p)	64.0120	16.6924	1870	1879	9
h) Tindaborg (p)	64.0240	16.6993	1727	1747	20
i) Þuríðartindur (p)	64.0817	16.6382	1727	1741	14
j) Hvannadalshnúkur (g)	64.0142	16.6771	2110	2119	9
k) center of caldera (g)	64.0048	16.6392	1843	1845	2
l) ice divide of Hrútárjökull1 (g)	64.0012	16.6098	1912	1927	15
m) ice divide of Hrútárjökull2 (g)	63.9982	16.5932	1827	1840	13
n) Tjaldskarð (g)	64.0421	16.6617	1824	1844	20
o) Snæbreið (g)	64.0256	16.6457	2028	2041	13
p) Jökulbak (g)	64.0531	16.6752	1911	1922	11
q) peak NE of Sveinstindur (g)	64.0144	16.6102	1951	1962	11
r) SW rim of caldera (g)	63.9904	16.6801	1815	1846	31
s) acc. area of Fjallsjökull1 (g)	64.0576	16.6451	1710	1716	6
t) acc. area of Fjallsjökull2(g)	64.0496	16.6550	1807	1808	1

that Hvannadalshnúkur has lowered by 9 m during the last 100 years, due to glacial melting, as a simple comparison of the 1904 map and recent measurements may indicate (Morgunblaðið, 2005).

SUMMARY

By combination of several photographic archives, a recent DEM and field inspection, we delineate the area and volume loss of Kotárjökull glacier since the LIA maximum in the late 19th century. The thinning is negligable above 1700 m and gradually increases downglacier to 180 m near the terminus. The glacier has lost a volume of 0.4 km^3 (30%) and decreased in area by 2.7 km^2 (20%). We estimate an average specific mass loss of 0.22 m w.e./yr.

Comparison of the Danish map from 1904 with the LiDAR DEM, indicates that little or no elevation changes took place during the 20th century on the Öræfajökull plateau. This also applies to the summit Hvannadalshnúkur, and we conclude whether this may be explained by surveying errors rather than surface lowering, due to reduced glacier mass balance.

Acknowledgements

We used the LiDAR-data on a processing stage with permission from the Icelandic Meteorological Office and the Institute of Earth Sciences at the University of Iceland. We thank Þorsteinn Sæmundsson, astronomer for helpful discussion on calculating glacier surface elevation changes by comparing duplicate photographs. Discussions with Eyjólfur Magnússon, Finnur Pálsson on ice thickness, ice flow, and the response of glaciers to climate change, and Magnús

Tumi Guðmundsson are acknowledged. Authors appreciate constructive comments by reviewers, Patrick Appelgate and Þorsteinn Þorsteinsson. This work was supported by the Fund of the Kvísker siblings. This publication is contribution number 17 of the Nordic Centre of Excellence SVALI, Stability and Variations of Arctic Land Ice, funded by the Nordic Top-level Research Initiative (TRI).

ÁGRIP

Rýrnun Kotárjökuls, í suðvestanverðum Öræfajökli, var metin fyrir tímabilið 1891–2011 með a) hornafallareikningum út frá þremur ljósmyndapörum, b) kortlagningu á jökulmenjum sem vitna um hámarksútbreiðslu í lok litlu ísaldar, og c) LiDAR hæðarlíkani frá 2010–2011. Sögulegar ljósmyndir sem Frederick W. W. Howell tók árið 1891, í fyrstu göngu á Hvannadalshnúk, gerðu kleift að meta yfirborðsbreytingar á þessu tímabili. Fylgdarmenn voru Páll Jónsson og Þorlákur Þorláksson frá Svínafelli og lá leið þeirra upp á Sandfell og öskjubarm Öræfajökuls. Fáar ljósmyndir eru til frá hámarki litlu ísaldar um 1890 sem sýna safnsvæði jökuls jafnskýrt og þessar myndir. Heildarrýrnun jökulsins yfir tímabilið nemur 0,4 km^3 (30%) að ísrúmmáli og nálægt 2,7 km^2 (20%) að flatarmáli, sem samsvarar meðaltalsleysingu um 0,22 m að vatnsgildi á ári. Yfirborð Kotárjökuls hefur lækkað lítið sem ekkert ofan við 1700 m, en eykst niður jökulinn og nemur um 180 m við núverandi sporð. Samanburður á hæð einstakra mælipunkta á Öræfajökli, af korti danska herforingjaráðsins frá 1904 við hæðarlíkan frá 2011, auk ljósmynda Howells, sýna að litlar yfirborðsbreytingar hafa orðið efst á safnsvæði hans. Leiða má að því líkur að Hvannadalshnúkur hafi ekki lækkað frá upphafi 20. aldar vegna rýrnunar, heldur mun hæð tindsins ávallt hafa verið nærri 2110 m eins og mælingar í upphafi 21. aldar og nýlegt LiDAR-hæðarlíkan sýna. Hæðarmuninn má hugsanlega rekja til ónákvæmni í mælingum.

REFERENCES

Aðalgeirsdóttir, G., S. Guðmundsson, H. Björnsson, F. Pálsson, T. Jóhannesson, H. Hannesdóttir, S. Þ. Sigurðsson and E. Berthier 2011. Modelling the 20th and 21st century evolution of Hoffellsjökull glacier, SE-Vatnajökull, Iceland. *The Cryosphere Discussion* 5, 961–975, doi:10.5194/tc-5-961-2011.

Björnsson, H. 1988. Hydrology of ice-caps in volcanic regions. *Soc. Sci. Isl.* 45, Reykjavík, 139 pp.

Björnsson, H., F. Pálsson, M. T. Guðmundsson and H. H. Haraldsson 1998. Mass balance of western and northern Vatnajökull, Iceland, 1991–1995. *Jökull* 45, 35–58.

Björnsson, H. 2009. *Jöklar á Íslandi*. Bókaútgáfan Opna, Reykjavík, 479 pp.

Brown, M. E., C. Trujillo and D. Rabinowitz 2004. Discovery of a candidate inner Oort cloud planetoid. *Astrophysical J. Lett.* 10, 645–649.

Böðvarsson, Á. 1996. *Landmælingar og kortagerð Dana á Íslandi – Upphaf Landmælinga Íslands*. Landmælingar Íslands, Reykjavík. 316 pp.

Fagre, D. B. and L. A. McKeon 2010. Documenting Disappearing Glaciers: Repeat Photography at Glacier National Park, Montana. In: R. H. Webb, D. E. Boyer and R. M. Turner (eds.), *Repeat Photography: Methods and Applications in the Natural Sciences,* Island press, Washington D.C., 77–88.

Guðmundsson, M. T. 2000. Mass balance and precipitation on the summit of the plateau of Öræfajökull, SE-Iceland. *Jökull* 48, 49–54.

Guðmundsson, M. T. 2004. Vorferð Jöklarannsóknafélags Íslands, 4.–12. júní 2004. *Jökull* 54, 135–138.

Guðmundsson, S. 1999. *Þar sem landið rís hæst, Öræfajökull og Öræfasveit.* Mál og menning, 183 pp.

Hannesdóttir, H., H. Björnsson, S. Guðmundsson, F. Pálsson, S. Guðmundsson, G. Aðalgeirsdóttir, S. Þ. Sigurðsson and H. Ágústsson 2012. 300 year history of glacier variations of SE Vatnajökull – a key to modelling their response to climate change. *Proc. 30th Nordic Geol. Winter Meeting,* Reykjavík, 55–56.

Harrison, A. E. 1960. *Exploring Glaciers with a Camera*. Sierra Club Books, San Francisco, CA, 71 pp.

Herforingjaráðið 1905. *Öræfajökull 87 SA*. Topographical map, 1:50.000. Kjöbenhavn, Geodætisk Inst. 1st ed.

Howell, F. W. W. 1892. The Öræfa Jökull, and its first ascent. *Proc. Royal Geographical Soc. 14*, 841–850.

(http://cidc.library.cornell.edu/howell).

Jóhannesson, T., H. Björnsson, E. Magnússon, S. Guðmundsson, F. Pálsson, O. Sigurðsson, T. Thorsteinsson and E. Berthier 2012. Ice-volume changes, bias-estimation of mass-balance measurements and changes in subglacial water-bodies derived by LiDAR- mapping of the surface of Icelandic glaciers. *Annals of Glaciology* 54 (63), in press.

Koch, J. P. 1905–1906. Fra Generalstabens topografiske Avdelings Virksomhed paa Island. *Geografisk Tidsskrift* 18, 1–14.

Luckman, B. H., TÅ. Kavanach, I. Craig and R. S. St. George 1999. Earliest photograph of Athabasca and Dome glaciers, Alberta. *Géographie physique et Quaternaire* 53(3), 401–405.

Magnússon, E., H. Björnsson, F. Pálsson and S. Guðmundsson 2012. The ice capped Öræfajökull volcano, SE-Iceland, surveyed with radio echo sounding. *Jökull* 62, this issue.

Molnia, B. F. 2010. Repeat photography of Alaskan Glaciers and Landscapes from Ground-Based Photo Stations and Airborne Platforms. In: R. H. Webb, D. E. Boyer and R. M. Turner (eds.), *Repeat Photography: Methods and Applications in the Natural Sciences,* Island press, Washington D.C, 59–76.

Morgunblaðið 2005. Hæðarbreyting á 100 ára fresti ætti engan að græta. Morgunblaðið 7th of August.

Thoroddsen, Þ. 1896. Ferð um Austur-Skaftafellssýslu og Múlasýslur sumarið 1894. *Andvari* 21, 1–33.

Webb, R. H., R. M. Turner and D. E. Boyer 2010. Introduction: A brief history of repeat photography. In: R.H. Webb, D.E. Boyer, R.M. Turner (eds.), *Repeat Photography: Methods and Applications in the Natural Sciences,* Island Press, Washington D.C., 3–11.

Þórarinsson, S. 1943. Vatnajökull; Scientific results of the Swedish-Icelandic investigations 1936-37-38. Chapter 11. Oscillations of the Icelandic Glaciers in the last 250 years. *Geografiska Annaler* 25(1–2), 1–54.

Kotárjökull viewed from Slaga. The older photo (left) was taken by Ólafur Magnússon probably in 1925, when the terminus was still in Berjagil gorge east of Mt. Sandfell, (see Figure 2). Photographer Aron Reynisson visited the same spot in the summer of 2012 (right photo). – *Sýn til Kotárjökuls ofan af Slögu. Eldri myndina (t.v.) tók Ólafur Magnússon ljósmyndari líklega um 1925, en á þeim tíma lá sporðurinn enn efst í Berjagili austan Sandfells (sjá 2. mynd hér að framan). Myndina til hægri tók Aron Reynisson ljósmyndari sumarið 2012 frá sama stað.*

Paper III

Hannesdóttir, H., Björnsson, H., Pálsson, F., Aðalgeirsdóttir, G., and Guðmundsson, Sv. (2014). Area, volume and mass changes of SE-Vatnajökull ice cap, Iceland, from the Little Ice Age maximum in the late 19th century to 2010. The Cryosphere Discussion 8, 1-55. doi:10.5194/tcd-8-1-2014.

The Cryosphere Discuss., 8, 4681–4735, 2014
www.the-cryosphere-discuss.net/8/4681/2014/
doi:10.5194/tcd-8-4681-2014

The Cryosphere
Discussions
Open Access

Area, volume and mass changes of southeast Vatnajökull ice cap, Iceland, from the Little Ice Age maximum in the late 19th century to 2010

H. Hannesdóttir, H. Björnsson, F. Pálsson, G. Aðalgeirsdóttir, and S. Guðmundsson

Institute of Earth Sciences, University of Iceland, 101 Reykjavík, Iceland

Received: 8 August 2014 – Accepted: 22 August 2014 – Published: 5 September 2014

Correspondence to: H. Hannesdóttir (hrafnha@hi.is)

Published by Copernicus Publications on behalf of the European Geosciences Union.

Abstract

Area and volume changes and the average geodetic mass balance of the non-surging outlet glaciers of southeast Vatnajökull ice cap, Iceland, during different time periods between ~1890 and 2010, are derived from a multi-temporal glacier inventory. A series of digital elevation models (DEMs) (~1890, 1904, 1936, 1945, 1989, 2002, 2010) have been compiled from glacial geomorphological features, historical photographs, maps, aerial images, DGPS measurements and a LiDAR survey. Given the mapped bedrock topography we estimate relative volume changes since the end of the Little Ice Age (LIA) ~1890. The variable dynamic response of the outlets, assumed to have experienced similar climate forcing, is related to their different hypsometry, bedrock topography, and the presence of proglacial lakes. In the post-LIA period the glacierized area decreased by 164 km^2 and the glaciers had lost 10–30 % of their ~1890 area by 2010. The glacier surface lowered by 150–270 m near the terminus and the outlet glaciers collectively lost 60 ± 8 km^3 of ice, which is equivalent to 0.154 ± 0.02 mm of sea level rise. The relative volume loss of individual glaciers was in the range of 15–50 %, corresponding to a geodetic mass balance between −0.70 and −0.32 m w.e. a^{-1}. The rate of mass loss was most negative in the period 2002–2010, on average −1.34 ± 0.12 m w.e. a^{-1}, which lists among the most negative mass balance values recorded worldwide in the early 21st century. From the data set of volume and area of the outlets, spanning the 120 years post-LIA period, we evaluate the parameters of a volume-area power law scaling relationship.

1 Introduction

Area changes and glacier retreat rates since the Little Ice Age (LIA) maximum are known from glacierized areas worldwide (e.g., Haeberli et al., 1989; WGMS, 2008). The majority of glaciers have been losing mass during the past century (Vaughan et al., 2013), and a few studies have estimated the volume loss and the mass bal-

TCD
8, 4681–4735, 2014

ance for the post-LIA period by various methods (e.g., Rabatel et al., 2006; Bauder et al., 2007; Knoll et al., 2008; Lüthi et al., 2010; Glasser et al., 2011). Knowledge about the ice volume stored in glaciers at different times is important for past, current and future estimates of sea level rise. Ice caps and glaciers outside polar areas have contributed more than half of the land ice to the global mean sea level rise in the 20th century (Church et al., 2013). Furthermore, glacier inventories are important to analyze and assess glacier changes at a regional scale, and they provide a basic data set for glaciological studies, for example to calibrate models simulating future glacier reponse to changes in climate.

Iceland is located in a climatically variable area of the North Atlantic Ocean, influenced by changes in the atmospheric circulation and warm and cold ocean currents. The temperate maritime climate of Iceland is characterized by small seasonal variations in temperature, on average close to 0 °C in the winter and 11 °C during the summer months in the lowland. The temperate glaciers and ice caps receive high amounts of snowfall, induced by the cyclonic westerlies crossing the North Atlantic and have mass turnover rates in the range of 1.5–3.0 m w.e. a^{-1} (Björnsson et al., 2013). Simulations with a coupled positive-degree-day and ice flow model reveal that Vatnajökull is one of the most sensitive ice cap in the world, and the mass balance sensitivity of southern Vatnajökull is in the range of 0.8–1.3 m w.e. a^{-1} 1 °C^{-1} (Aðalgeirsdóttir et al., 2006); among the highest in the world (De Woul and Hock, 2005). Apart from Greenland, the highest rate of meltwater input to the North Atlantic Ocean, comes from the Icelandic glaciers, that have contributed ~ 0.03 mm a^{-1} on average to sea level rise since the mid-1990s (Björnsson et al., 2013). Only a few quantitative estimates on volume and mass balance changes of the entire post-LIA period are available for Icelandic glaciers (Flowers et al., 2007; Aðalgeirsdóttir et al., 2011; Pálsson et al., 2012; Guðmundsson, 2014).

The outlet glaciers of southeast Vatnajökull (Fig. 1) are located in the warmest and wettest area of Iceland and descend down to the lowlands. Results of spatially distributed coupled models of ice dynamics and hydrology, indicate that these glaciers are the most sensitive to future warming of all outlets of Vatnajökull (Flowers et al., 2005). They are particularly vulnerable to warming climate conditions, since their beds lie even 100–300 m below the elevation of the current terminus (Björnsson and Pálsson, 2008). The surface geometry of the outlet glaciers at the LIA maximum has been reconstructed from glacial geomorphological features and historical data (Hannesdóttir et al., 2014). The outlets were at their terminal LIA moraines around ~ 1890, which marked the termination of the LIA in Iceland (Thórarinsson, 1943; Hannesdóttir et al., 2014).

To estimate the downwasting, area and volume loss and geodetic mass balance of the outlets of southeast Vatnajökull since ~ 1890, glacier outlines have been digitized from various sources, and digital elevation models (DEMs) created from contour lines of topographic maps, DGPS measurements and various airborne surveys. The equilibrium line altitude (ELA) has been estimated from a series of recent MODIS images. We consider the different response of the glaciers to similar climate forcing during the post-LIA time period, and from the constructed record of area and volume changes, the scaling parameters of a power law which relates glacier area to volume are evaluated.

2 Study area and previous work

The studied outlet glaciers of southeast Vatnajökull are non-surging, less than 100 km apart and most of them reach down to 20–100 m a.s.l. (Fig. 1). The glaciers vary in size from 10–200 km^2, their average thickness range is 80–330 m (Table 1), and the hypsometry (area distribution with altitude) differs considerably. Morsárjökull, the westernmost outlet, flows down from an ice divide of ~ 1350 m. Öræfajökull (2100 m a.s.l.) feeds several outlet glaciers: the eastern part of Skaftafellsjökull, Svínafellsjökull, Kotárjökull, Kvíárjökull, Hrútárjökull and Fjallsjökull (Fig. 1). East of Breiðamerkurjökull, three outlet glaciers descend from the 1500 m high plateau of the Breiðabunga dome, Skálafellsjökull, Heinabergsjökull, and Fláajökull. Further east is Hoffellsjökull, and its accumulation area lies between Breiðabunga and the mountainous area of Goðahnúkar (1500 m), which feeds Lambatungnajökull (Fig. 1). The outlet glaciers east of Breiðamerkurjökull are hereafter referred to as the eastern outlet glaciers. The bedrock topography of the studied outlets is known from radio echo sounding measurements (Björnsson, 2009; Magnússon et al., 2012). The glaciers terminate in glacially eroded alpine-like valleys and have carved into soft glacial and glacio-fluvial sediments. It is unlikely that the troughs were only formed during the LIA, considering the present rate of sediment transport in the main glacial rivers of Öræfajökull (Magnússon et al., 2012). Many of them presently calve into proglacial lakes, which enhances ablation, and makes them vulnerable to predicted future warming (Björnsson and Pálsson, 2008; Magnússon et al., 2012).

Mass balance measurements have been carried out on Vatnajökull since 1993, and the ice cap has lost 1 m w.e. a^{-1} on average since (Björnsson et al., 2013). The majority of the survey stakes are located on the northern and western outlet glaciers (Fig. 1), but a number of stakes are situated on Breiðamerkurjökull and the eastern outlets (Björnsson and Pálsson, 2008; Aðalgeirsdóttir et al., 2011). In the accumulation area of these last-mentioned outlets, annual mass balance has been measured 1–4 m w.e. a^{-1} in the time period 1996–2010. Losses of up to 9 m w.e. a^{-1} have been observed during summer on Breiðamerkurjökull and Hoffellsjökull, and even negative winter balances at the terminus (Björnsson and Pálsson, 2008). The mass balance at the plateau of Öræfajökull ice cap was 6–8 m w.e. a^{-1} in 1993–1998 (Guðmundsson, 2000). Based on satellite imagery, in situ mass balance measurements and model simulations, the average ELA of southeast Vatnajökull has been estimated to be around 1100–1200 m (Björnsson, 1979; Aðalgeirsdóttir et al., 2005, 2006; Björnsson and Pálsson, 2008; Aðalgeirsdóttir et al., 2011). Interannual variability of the ELA has been measured approximately 200–300 m in the time period 1992–2007 (Björnsson and Pálsson, 2008).

Regular monitoring of frontal variations of the outlets of southeast Vatnajökull started in 1932 by Jón Eyþórsson and were later carried out by volunteers of the Icelandic Glaciological Society, providing annual records of the advance and retreat of the glaciers (Eyþórsson, 1963; Sigurðsson, 2013; http://spordakost.jorfi.is). The history of

TCD
8, 4681–4735, 2014

retreat and volume changes of Hoffellsjökull since the end of the LIA has been derived from numerous archives (Aðalgeirsdóttir et al., 2011; Björnsson and Pálsson, 2004). Downwasting and volume loss of Kotárjökull (Fig. 1) in ~ 1890–2010 has been quantified by repeat photography and mapping of LIA glacial geomorphological features (Guðmundsson et al., 2012). The records of these two glaciers are integrated in our data base for comparison with the other outlets.

3 Data

3.1 Meteorological records

Long temperature and precipitation records are available from two lowland weather stations (Fig. 1) south of Vatnajökull; at Fagurhólsmýri (16 m a.s.l., 8 km south of Öræfajökull) and Hólar in Hornafjörður (16 m a.s.l., 15 km south of Hoffellsjökull). The temperature record at Hólar is available for the period 1884–1890 and since 1921, whereas, the precipitation measurements started in 1931 (Fig. 2). Temperature measurements started in 1898 at Fagurhólsmýri, and the precipitation record goes back to 1921 (Fig. 2). The temperature record has been extended back to the end of the 19th century by correlation with other temperature records from around the country, and the precipitation record by linear regression between temperature and precipitation of the local stations (see Aðalgeirsdóttir et al., 2011 for details). The mean summer temperature during the two warmest ten year periods of the measurement series at Hólar (1926–1936 and 2000–2010) was 10.3 °C and 10.5 °C respectively. For comparison the mean summer temperature for the time period 1884–1890 was 8.5 °C. Winter precipitation ranges between 800 and 1400 mm, and no long term trend is observed since start of measurements at the two stations. Precipitation has been measured at Kvísker (east of Öræfajökull) since 1963, and at Skaftafell (west of Öræfajökull) since 1964. The records from Kvísker show more than two times higher winter precipitation, and three times higher annual precipitation, than in Skaftafell (Fig. 2). This difference could be related to precipitation undercatch of the rain gauges especially during winter, but the underestimate is generally more pronounced for snow than rain (e.g., Sigurðsson, 1990).

3.2 Glacier geometry

The areal extent and the surface topography of the outlet glaciers at different times during the period ~ 1890–2010, has been derived from various data sets that are detailed in the following sub-chapters. The glacier margin has been digitized from maps and aerial images at various times for different glaciers.

3.2.1 LiDAR DEM

The most accurate DEMs of southeast Vatnajökull were produced with airborne LiDAR technology in late August–September 2010 and 2011 (Icelandic Meteorological Office and Institute of Earth Sciences, 2013). The high-resolution DEMs are 5 m × 5 m in pixel size with a < 0.5 m vertical and horizontal accuracy (Jóhannesson et al., 2013). The LiDAR DEMs provide a reference topography, used in constructing other glacier surface DEMs, for example in areas where corrections of contour lines from old paper maps have been necessary.

3.2.2 The LIA glacier surface topography

The surface topography at the LIA maximum ~ 1890 of the outlet glaciers of this study has previously been reconstructed from glacial geomorphological features (including lateral and terminal moraines, trimlines and erratics), historical photographs, and aerial images, using the LiDAR DEM as baseline topography (Hannesdóttir et al., 2014). The vertical accuracy of the ~ 1890 DEM is estimated to be around ±15–20 m.

TCD
8, 4681–4735, 2014

3.2.3 Aerial images, maps and glacier surface data

The oldest reliable maps of the outlet glaciers are from the Danish General Staff (1 : 50 000), based on a trigonometrical geodetic surveys conducted in the summers of 1902–1904 (Danish General Staff, 1904). Considerable distortion was observed in the horizontal positioning, related to errors in the survey network established by the Danish Geodetic Institute (Böðvarsson, 1996; Pálsson et al., 2012). Less errors are found in the vertical component, revealed by comparison of the elevation of trigonometric points on mountain peaks and other definite landmarks between the LiDAR DEM and the 1904 maps (see also Guðmundsson et al., 2012). The maps do not cover all glaciers up to their ice divides. Lambatungnajökull was not surveyed in the early 20th century, but a manuscript map exists from 1938, based on a trigonometric geodetic survey and oblique photographs of the Danish General Staff (archives of the National Land Survey of Iceland). Only a small part of the terminus of Hoffellsjökull was surveyed in 1904, but a map from 1936 covers the whole glacier.

The AMS 1 : 50 000 maps with 20 m contour lines (Army Map Service, 1950–1951) cover all the outlet glaciers up to the ice divides, and are based on aerial photographs taken in August–September 1945 and 1946. The geometry in the upper parts of the glaciers, above ∼ 1100 m elevation, was based on the surveys of the Danish General Staff from the 1930s and 1940s, where contour lines are only estimates, indicating shape, not accurate elevation (see also Pálsson et al., 2012). The unpublished DMA maps from 1989 (Defense Mapping Agency, 1997) include only the eastern outlet glaciers. These maps were similarly derived by standard aerial photographic methods, based on images taken in August–September, with a scale of 1 : 50 000 and 20 m contour lines.

A Landsat satellite image of 2000 and aerial photographs from 1945, 1946, 1960, 1982 and 1989 (http://www.lmi.is/loftmyndasafn) and from 2002 (www.loftmyndir.is) were used to delineate the glacier margin and to estimate surface elevation changes in the accumulation area from the appearance of nunataks (isolated rock outcrops within the glaciers). A 20 m × 20 m DEM from Loftmyndir ehf., based on late summer aerial images from 2002, covers parts of Öræfajökull's outlet glaciers with vertical accuracy of < 5 m, excluding most of the accumulation areas. DGPS surface elevation measurements (with a vertical accuracy of 1–5 m) have been carried out during repeated mass balance surveys and radio echo sounding profiling in spring during the time period 2000–2003 on southeast Vatnajökull, and are used for DEM construction.

3.2.4 Bedrock topography

The bedrock topography has been derived from radio echo sounding measurements, carried out in the last two decades (Björnsson and Pálsson, 2004, 2008; Björnsson, 2009; Magnússon et al., 2007, 2012, and the data base of the Glaciological Group of the Institute of Earth Sciences, University of Iceland). We calculate the total ice volume from the bedrock DEMs and the relative ice volume changes as a fraction of the total volume. The accuracy of the bedrock measurements is ±5–20 m, depending on location.

4 Methods

4.1 Glacier surface DEMs

Glacier surface DEMs are used to determine changes in elevation and volume, and to infer mass changes (e.g., Reinhardt and Rentsch, 1986; Kääb and Funk, 1999). Comparison of DEMs retrieved from the aerial images of Loftmyndir ehf. 2002, SPOT5 HRS images in autumn from 2008 (Korona et al., 2009), and the 2010 LiDAR, reveals that the surface geometry in the upper accumulation area has undergone negligible changes during the first decade of the 21st century, at a time of rapid changes in the ablation area (see also Björnsson and Pálsson, 2008). Minor changes in the surface geometry in the upper accumulation area of a western outlet of Vatnajökull in 1998–2010 has similarly been observed (Auriac et al., 2014). When constructing the DEMs of

TCD
8, 4681–4735, 2014

1938, 1945, 1989 and 2002, it is therefore assumed that the glacier surface geometry in the upper reaches of the accumulation area does not change, but the estimated vertical displacement is superimposed on the LiDAR DEM.

The appearance of nunataks is used to determine ice surface elevation changes in the accumulation area of the southeast outlets, as has been used to estimate downwasting elsewhere (Paul et al., 2007; Rivera et al., 2007; Berthier et al., 2009; Pelto, 2010). The LiDAR DEMs are used as reference topography; the aerial images are laid on top of and georeferenced with a shaded relief LiDAR image. This provides new estimates on surface elevation changes in the upper reaches of the glaciers. Regular 50 m × 50 m DEMs were created by digitizing the contour lines of the paper maps (1904, 1938, 1945, 1989) and interpolated using kriging method (e.g., Wise, 2000). In upper parts of the glaciers, we extrapolated surface change data headward as a linear variation between available data points.

Due to lack of accurate contour lines in the highest part of the accumulation areas, we assume that ice divides are fixed in time, which may introduce an error in the areal extent. The ice divides are determined from the LiDAR DEM and the data base of the Glaciology Group of the Institute of Earth Sciences University of Iceland. The neighbouring surging outlets have affected the location of ice divides following surges (Björnsson et al., 2003). For example, the surges of Skeiðarárjökull 1991 and Dyngjujökull 1999 (Fig. 1), caused ice divides to shift on the order of a few hundred m; however the area affected is small compared to the total area of each outlet.

We consider the average vertical bias of each DEM to be smaller than the estimated point accuracy. Uncertainties related to the DEM reconstruction based on a few data points in the accumulation area, lead to minor errors in the estimated total volume change, since main volume loss occurs in the ablation areas. Uplift rates around Vatnajökull in the last 20 years have been on the order of 10–30 mm year^{-1}, highest around the edge of the ice cap (Árnadóttir et al., 2009; Auriac et al., 2013). We do not however, account for this change of the bedrock elevation in the most recent glacier surface DEMs, as it is smaller than the vertical error estimate.

4.1.1 DEMs of 1904 and 1938

The glacier margin delineated on the 1904 maps coincides with the LIA ~ 1890 lateral moraines around an elevation of 400–500 m, thus surface lowering is assumed to only have taken place below that elevation during the cold time period ~ 1890–1904 (see Hannesdóttir et al., 2014). A 1904 DEM of the terminus below 400–500 m was reconstructed and subtracted from the ~ 1890 DEM (Hannesdóttir et al., 2014), to calculate volume changes for the time interval ~ 1890–1904. Contour lines on the 1904 map indicate shape of the glacier surface geometry, not accurate elevation. The elevation of the trigonometric survey points on the glacier surface on the 1904 maps, serve as a base for generating the DEM, with an estimated vertical accuracy of 10–15 m. The contour lines of the manuscript map of 1938 of Lambatungnajökull were digitized, and their shape was adjusted according to the contours of the AMS 1945 map.

4.1.2 DEMs of 1945

Due to the errors in the old trigonometric network for Iceland, parts of the 1945 maps are somewhat distorted horizontally. Sections of the scanned maps were thus georeferenced individually, by fitting each map segment to the surrounding valley walls, using the LiDAR as reference topography. To estimate glacier surface elevation changes in the accumulation area between 1945 and 2010, we compared the size of nunataks on the original aerial images and the LiDAR shaded relief images (an example shown in Fig. 3). No difference in surface elevation was observed above 1300–1400 m, wherefrom the LiDAR DEM was added to create a continuous 1945 DEM. The glacier margin was revised by analysing the original aerial images, for example in areas where shadows had incorrectly been interpreted as bedrock or snow-covered gullies and valley walls as glacial ice. A conservative vertical error estimate of 5–10 m is estimated for the 1945 DEM.

4.1.3 DEMs of 1989

DEMs from the contour lines of the DMA unpublished maps of the eastern outlets have previously been created at the Institute of Earth Sciences, University of Iceland. But here some adjustments were made to the glacier surface geometry in the upper accumulation area, by comparing the size of the nunataks on the original aerial images with the shaded relief image of the LiDAR DEM. The glacier outline was also reassessed from the original aerial images. A conservative vertical error of 5 m for the 1989 DEM is estimated, based on experience of interpreting the DMA maps of Icelandic glaciers (Guðmundsson et al., 2011; Pálsson et al., 2012).

4.1.4 DEMs of 2002

Negligible surface elevation changes above 1300–1400 m are observed between the aerial images of Loftmyndir ehf. from 2002 and the shaded relief of the 2010 LiDAR DEM; thus the high-resolution DEM was mosaiced (above that elevation) to create a complete 2002 DEM. Comparison of altitude in ice free areas bordering the glaciers, from the LiDAR and the Loftmyndir ehf. DEMs, reveals a vertical bias of 2–5 m. The glacier surface elevation in the accumulation area was verified by spring DGPS measurements from radio echo sounding survey transects from the same year. The glacier margins of the Öræfajökull outlet glaciers were digitized from the high-resolution aerial images of Loftmyndir ehf, whereas the glacier margin of the eastern outlets were digitized from Landsat satellite images from 2000 (http://landsat.usgs.gov).

A 2002 DEM of the eastern outlet glaciers was constructed from a series of DGPS measurements from survey transects of radio echo sounding measurements in the time period 2000–2003. The LiDAR DEM was used as topographical reference. The spring DGPS elevation measurements in the accumulation area were corrected by subtracting the difference between spring and autumn elevation from the measured surface, to retrieve an autumn DEM. Seasonal changes in glacier surface elevation amount to 5 m on average in the accumulation area, observed at mass balance stakes

TCD
8, 4681–4735, 2014

on southeast Vatnajökull every autumn and spring during the period 1996–2010. The vertical error estimate for the 2002 DEM is approximately 1–2 m.

4.2 Glacier hypsometry

The hypsometry (area distribution with altitude) of individual glaciers plays an important role in their response to climate change through its link with mass-balance elevation distribution (e.g., Furbish and Andrews, 1984; Oerlemans et al., 1998). The hypsometry is determined by bedrock topography, ice thickness, and ice volume distribution (e.g., Marshall, 2008; Jiskoot et al., 2009). One of the first people to descibe the hypsometry of glaciers and classify the hypsometric curves was Ahlmann (in Lliboutry, 1956). The hypsometric curves of the outlets of southeast Vatnajökull were generated from the LiDAR DEM and ~ 1890 DEM by creating histograms of the elevation data with 50 m elevation intervals.

4.3 ELA derived from MODIS imagery and the LiDAR DEMs

The elevation of the snowline at the end of summer provides an estimate for the ELA on temperate glaciers (e.g., Östrem, 1975; Cuffey and Paterson, 2010). In recent years satellite data have been used to estimate the ELA by this approximation in remote regions and where mass balance is not measured (e.g., Barcaza et al., 2009; Mathieu et al., 2009; Mernild et al., 2013; Rabatel et al., 2013; Shea et al., 2013). Since limited mass balance measurements exist for the outlet glaciers of this study (Fig. 1), the snowline retrieved from the MODIS images is a useful proxy for the present day ELA. The snowline was digitized and projected over the LiDAR DEMs to obtain the elevation. The average snowline elevation and standard deviation was calculated for the glaciers from each image. The accumulation area ratio (AAR) of the outlet glaciers was estimated from the average snowline elevation from all years and the glacier margin in 2010.

4.4 Volume calculations and average geodetic mass balance

Ice volume changes for the different time periods since the end of the LIA until 2010 were obtained by subtracting the DEMs from each other. Given the bedrock DEMs, the fraction of the volume loss (of the total volume) is calculated. The ice volume change is converted to average annual mass balance, bn, expressed in m of water equivalent per year (m w.e. a^{-1}) averaged over the mean glacier area

$$\mathrm{bn} = \frac{\rho \times \Delta V}{A \times \Delta t} \tag{1}$$

where ρ is the average specific density of ice, 900 kg m^3 (Sorge's law), ΔV the volume change, A the average of the initial and final glacier area and Δt the time difference in years between the two DEMs. The volume change is the average elevation change (Δh) between two years, multiplied by the area of the glacier,

$$\Delta V = \Delta h \times A \tag{2}$$

The uncertainty related to the conversion of ice volume to mass change to obtain geodetic mass balances, is small for long periods (decades) of glacier retreat, and when volume loss is mainly confined to the ablation area, mostly ice is lost (e.g., Bader, 1954; Huss, 2013). We base our estimates of the error for the geodetic mass balance on previous assessments of errors in DEM reconstruction and geodetic mass balance calculations for ice caps in Iceland (Guðmundsson et al., 2011; Pálsson et al., 2012).

5 Results

5.1 Spatial and temporal variability of the ELA

Spatial variability is observed in the ELA deduced from the 2007–2011 MODIS images. The average ELA and the standard deviation for each year is displayed in Fig. 4.

The ELA of the western outlet glaciers of Öræfajökull is approximately 170 m higher than on the eastern outlet glaciers, and the ELA rises eastward from Skálafellsjökull to Lambatungnajökull by ~ 200 m. Due to the low resolution of the MODIS images, the snowline on the narrow outlet glaciers of Öræfajökull (Morsárjökull, Svínafellsjökull, Kotárjökull, Kvíárjökull, and Hrútárjökull) is only discernible on a limited number of images. The snowline on the ~ 2 km wide Skaftafellsjökull and ~ 3.5 km wide Fjallsjökull is detectable on several images, allowing determination of the ELA in all years. The ELA range and AAR of the narrow outlet glaciers of Öræfajökull, is thus inferred by comparison with the neighbouring glaciers during overlapping years (Table 1). The ELA fluctuated by 100–150 m during this 5 years period. A similar interannual trend of the ELA is observed; the ELA in 2009 is the lowest for most of the glaciers, whereas the ELA in 2010 is usually the highest (Fig. 4). The AAR of the outlet glaciers ranges between 0.43 and 0.71, but the majority have an AAR of 0.6–0.65 (Table 1).

5.2 Frontal variations and areal change

The areal extent of the outlet glaciers at different times is shown in Figs. 5 and 6, and in Table 2. The outlets started retreating from their terminal LIA moraines ~ 1890, (Hannesdóttir et al., 2014), and had retreated 1–4 km by 2010 (Figs. 7 and 8), corresponding to an areal decrease of 164 km^2, equal to 16 % of the ~ 1890 areal extent, and in the range of 15–30 % for individual glaciers (Table 2 and Fig. 9). Main area decrease occurred in the ablation area, although small glacier tongues at higher elevation did also retreat in the 20th century (Figs. 5 and 6). Most glaciers had by 1945 lost 10 % of their ~ 1890 area (Table 2), and the rate of area loss was the highest during the time period 1904–1945 for majority of the glaciers (Fig. 10a). Hrútárjökull had by that time lost 17%, however its debris covered terminus on the 1945 aerial image prevents accurate interpretation of the glacier margin. In the following few decades glacial retreat slowed down or halted (Fig. 7). During the time period 1982/1989–2002 the areal extent of the glaciers changed little (Figs. 5, 6 and 7 and Table 2). Morsárjökull, Skaftafellsjökull, Hrútárjökull, Skálafellsjökull and Fláajökull advanced in 1970–1990, others remained stagnant (Fig. 7). The terminus position of Skálafellsjökull, Heinabergsjökull and Fláajökull was not measured during this time period, but from aerial images of 1979, it was possible to delineate the location of the termini, and infer about their slight advances based on the single year data point (Fig. 7). The majority of the glaciers started retreating just prior to the turn of the 21st century; between 2002 and 2010 the glaciers experienced high rates of area loss, the highest for Heinabergsjökull and Hoffellsjökull during the last 120 years (Fig. 10a and Table 2).

5.3 Thinning and volume changes

Between ~ 1890 and 2010 the outlet glaciers lowered by 150–270 m near the terminus, but negligible downwasting was observed above ~1500–1700 m elevation (Fig. 11a). Svínafellsjökull and Kvíárjökull underwent the smallest surface lowering during this period, whereas Heinabergsjökull, Hoffellsjökull and Lambatungnajökull experienced the greatest downwasting (Fig. 11a). Surface lowering between 1945 and 2010 is shown in Fig. 11b. The comparison of the size of nunataks in the upper reaches of the outlet glaciers, reveals negligible surface elevation change above 1300 m a.s.l. An example of the different appearance of nunataks in the 20th century is shown in Fig. 3 of the outcrops of Skaftafellsjökull called "Skerið milli skarða". Across the whole southeast part of Vatnajökull, the nunataks are smaller in area in 1989 and 1982 than in 1945 or 2002, meaning that the glacier was thicker at that time. A slight thickening in the accumulation area between 1945 and 1982/1989 is thus inferred. The similar size of the nunataks in 1945 and 2002 is evident.

In the time period ~ 1890–2010 the outlets collectively lost $60 \pm 8\,km^3$ (around 22 % of their LIA volume) and the relative volume loss of individual outlets was in the range of 15–50 % (Table 3 and Fig. 9). The rate of volume loss was highest between 2002 and 2010 and second highest in the time period 1904–1945 (Fig. 10b). All glaciers had lost at least half of their post-LIA volume loss by 1945 (Table 3). The eastern outlet glaciers (except Lambatungnajökull), experienced higher rates of volume loss than majority of the smaller and steeper outlets of Öræfajökull ice cap during every period of the last 120 years (Fig. 10b). For example between 2002 and 2010 the volume loss of the Öræfajökull outlets was in the range of −0.34 to −0.13 $km^3\,a^{-1}$ vs. −0.95 to −0.28 $km^3\,a^{-1}$ of the eastern outlets (Fig. 10b). The lack of 1980s DEMs of the Öræfajökull outlets, restricts the comparison with the eastern outlet glaciers to the time period 1945–2002.

5.4 Geodetic mass balance

The geodetic mass balance of all glaciers was negative during every time interval of the study period (Fig. 12 and Table 4). The average mass balance of the outlets ~ 1890–2010 was −0.38 m w.e. a^{-1}, and in the range of −0.70 to −0.32 m w.e. a^{-1} for individual outlets. The mass loss in ~ 1890–1904 was between −0.5 and −0.15 m w.e. a^{-1}. In the first half of the 20th century (1904–1945), the average mass balance was in the range of −1.00 to −0.50 m w.e. a^{-1}. The geodetic mass balance during the warmest decade of the 20th century (1936–1945), is only available for Hoffellsjökull and Lambatungnajökull, when they lost 1.00 and 0.75 m w.e. a^{-1}, respectively. In 1945–2002 the mass balance returned to similar values as at the turn of the 19th century. The geodetic mass balance of the eastern outlets was similar during the periods 1945–1989 and 1989–2002. The most negative balance is estimated in 2002–2010, ranging between −1.50 and −0.80 m w.e. a^{-1}, except Heinabergsjökull which lost on average −2.70 m w.e. a^{-1}.

Fjallsjökull and Hrútárjökull experienced the most negative average mass balance during the majority of the time periods of the Öræfajökull outlets (Fig. 12). Heinabergsjökull and Hoffellsjökull sustained the highest rate of mass loss of the eastern outlets during most intervals. Skálafellsjökull and Fláajökull generally had the least negative mass balance during every time period of the post-LIA interval of the eastern outlet glaciers, and Kvíárjökull and Svínafellsjökull of the Öræfajökull outlets.

5.5 Glacier hypsometry

The outlet glaciers of southeast Vatnajökull are divided into 5 hypsometric classes adopted from the categorization of De Angelis (2014), first proposed by Osmaston (1975) and also presented in Furbish and Andrews (1984):

- (A) Glaciers with a uniform hypsometry, i.e. area is constant with elevation
- (B) Glaciers where the bulk of the area lies above the ELA
- (C) Glaciers where the bulk of the area lies below the ELA
- (D) Glaciers where the bulk of the area lies at the ELA
- (E) Glaciers with bimodal hypsometric curves, where the ELA lies approximately between two peaks

The majority of the studied glaciers belong to shape class B (Table 1 and Fig. 13). Lambatungnajökull and Hrútárjökull belong to shape class D. Two glaciers have bimodal hypsometric curves (class E), Svínafellsjökull and Fjallsjökull, the latter could be classified as a piedmont glacier (class C) in its greatest extent.

6 Discussion

6.1 Glacier changes since the end of the LIA

Retreat of the outlet glaciers of southeast Vatnajökull from the LIA terminal moraines, that started in the last decade of the 19th century, was not continuous. The recession accelerated in the 1930s, as a result of the rapid warming beginning in the 1920s (Figs. 2b and 7). Glacier recession slowed down following cooler summers after 1940s, and from the 1960s to late 1980s the glaciers remained stagnant or advanced slightly (Fig. 7). A mass gain in the accumulation area during this cooler period was recognized

TCD
8, 4681–4735, 2014

on the aerial images of the 1980s, by smaller nunataks than on the 1945 aerial images (Fig. 3). The mass balance of the outlets in some years of the 1970s and 1980s may have been positive, although the geodetic mass balance of 1945–1989 (of the eastern outlets) and 1945–2002 (Öræfajökull outlets) was negative. The mass balance of the larger ice caps in Iceland was generally close to zero in 1980–2000 (e.g., Guðmundsson et al., 2009, 2011; Aðalgeirsdóttir et al., 2006, 2011). According to in situ measurements, mass balance was positive on Vatnajökull 1991–1994, but negative since then (Björnsson and Pálsson, 2008; Björnsson et al., 2013). Warmer temperatures after the mid-1990s (Fig. 2b) caused retreat of the southeast outlets, that increased after year 2000 (Björnsson and Pálsson, 2008; Björnsson et al., 2013). The rate of volume and mass loss was highest during the period 2002–2010 for almost all the southeast outlet glaciers (Figs. 10b and 12, Table 4). The geodetic mass balance is in line with the measured specific mass balance of Breiðamerkurjökull and Hoffellsjökull, which was on average $-1.4\,\mathrm{m\,w.e.\,a^{-1}}$ (Björnsson et al., 2013). Langjökull ice cap, similarly experienced high rates of mass loss in the period 1997–2009 ($-1.26\,\mathrm{m\,w.e.\,a^{-1}}$), which was however, even more negative in the warm decade of 1936–1945 (Pálsson et al., 2012).

Increasing negative mass balance in recent years from majority of ice sheets, ice caps and glaciers worldwide is reported in the latest IPCC report (Vaughan et al., 2013, and references therein). Glaciers in the Alps (Huss, 2012) and in Alaska (Luthcke et al., 2008) lost on average $1.0\,\mathrm{m\,w.e.\,a^{-1}}$ during the first decade of the 21st century, considerably smaller than the mass loss of glaciers in Iceland (Fig. 12b), which experienced among the most negative mass balance worldwide in the early 21st century (Vaughan et al., 2013). In this time period increased surface lowering on the southeast outlets of Vatnajökull is evidenced in emerging rock outcrops and expansion of nunataks up to an elevation of approximately 1200 m. The pattern of increased downwasting in accumulation areas in recent years has been observed in Alaska (Cox and March, 2004), the Alps (Paul et al., 2004), North Cascade glaciers (Pelto, 2010), and Svalbard (James et al., 2012).

The amount of ice (in km^3) lost from the outlets of southeast Vatnajökull ~ 1890–2010 equals the estimated ice loss of Langjökull and Breiðamerkurjökull during the same time interval (Pálsson et al., 2012; Guðmundsson, 2014). The average mass balance of the outlets in this time period was $-0.38\,\mathrm{m\,w.e.\,a^{-1}}$, compared to $-0.45\,\mathrm{m\,w.e.\,a^{-1}}$ of Langjökull (Pálsson et al., 2012) and $-0.64\,\mathrm{m\,w.e.\,a^{-1}}$ of Breiðamerkurjökull (Guðmundsson, 2014). For comparison glaciers in the Alps have lost on average $-0.31\,\mathrm{m\,w.e.\,a^{-1}}$ since the end of the LIA (Huss, 2012), which is 25 % less than the mass loss of the southeast outlets of Vatnajökull.

In situ mass balance measurements of glaciers in Iceland and degree-day mass balance models of selected glaciers indicate that the mass balance is governed by variation in summer ablation (which is strongly correlated with temperature), rather than winter accumulation (Björnsson and Pálsson, 2008; Guðmundsson et al., 2009, 2011; Pálsson et al., 2012; Björnsson et al., 2013). Higher than average winter precipitation at the meteorological stations south of Vatnajökull, is not correlated with more positive geodetic mass balances of the southeast outlets. However, a strong correlation ($r = 0.94$–0.98) is found between the geodetic mass balance and the average summer temperature (Table 4). Temperature records in Iceland indicate a warming of approximately 1.5 °C since the latter part of the 19th century until 2002 (Hanna et al., 2004; Jóhannesson et al., 2007). The mean annual temperature has been ~ 1 °C higher after 2000 than in the mid-1990s, which is 3–4 times higher than the average warming of the Northern Hemisphere during the same time interval (Jones et al., 2012).

The ELA of the outlets of southeast Vatnajökull has since the end of the LIA, risen by > 300 m; the ELA during the LIA maximum has been inferred from the elevation of the highest up-valley lateral LIA moraines of the studied glaciers (Hannesdóttir et al., 2014). Similar spatial differences in the ELA at both time periods have been observed, a 150–200 m difference between the western and eastern outlets of Öræfajökull, and increasing ELA from Skálafellsjökull to Lambatungnajökull. The geographical variability of the ELA is likely related to orographically enhanced precipitation on the SE coast (e.g., Crochet et al., 2007; Rögnvaldsson et al., 2007).

TCD
8, 4681–4735, 2014

6.2 Different response to similar climate forcing

The meteorological records from Hólar in Hornafjörður and Fagurhólsmýri indicate similar temperature and precipitation fluctuations during the 20th and early 21st century at both stations since start of measurements (Fig. 2). We thus infer that the studied outlets have experienced similar climate forcing since the end of the LIA. The precipitation records from the lowland stations indicate little variation during this time period. Glaciers respond to mass balance changes by adjusting their surface elevation and area. Our results show that glaciers with different hypsometry respond dynamically differently to the same climate forcing as has been reported from several studies (e.g., Kuhn et al., 1985; Oerlemans et al., 1998; Oerlemans, 2007; Jiskoot et al., 2009; Davies et al., 2012; De Angelis, 2014). Glaciers of shape class B lost the smallest percentage of their ~ 1890 volume (15–20%); except Heinabergsjökull (30%) and Hoffellsjökull (25%). Heinabergsjökull has a small peak in the area distribution in the ablation area (Fig. 13), and the peak in the area distribution of Hoffellsjökull is close to the modern average ELA. Lambatungnajökull and Hrútárjökull that are of shape class D, have lost 40 % and 50 % of their ~ 1890 volume, respectively. The two glaciers with bimodal hypsometric curves (class E), Svínafellsjökull and Fjallsjökull, have lost 30 % and 35 % of their ~ 1890 volume, respectively.

There is a noticeable difference in the response of the neighbouring outlet glaciers, Skaftafellsjökull and Svínafellsjökull. The former has retreated 2.7 km and lost 20 % of its ~ 1890 volume, whereas the latter has only retreated 0.8 km and lost 30 % of its ~ 1890 volume although part of the surface lowering may be due to excavation of the bed, creating an overdeepening in the terminus area of the glacier, as is well known for Breiðamerkurjökull (Björnsson, 1996). Similar difference is observed between Skálafellsjökull and Heinabergsjökull, where the former glacier lost 15 % of its ~ 1890 volume and retreated 2 km, and the latter lost 30 % of its ~ 1890 volume and retreated 3 km. Their bedrock topography is different (Fig. 8), and part of the surface

TCD
8, 4681–4735, 2014

lowering in the ablation area of Heinabergsjökull may likewise be attributed to excavation of the bed.

The area-altitude distribution of a glacier controls its sensitivity to a rise in the ELA. For example, a temperature rise of 0.5–1.0 °C would raise the ELA by approximately 100 m. The ablation area of the gently sloping eastern outlet glaciers will expand more than for the majority of the steeper Öræfajökull outlets following a rise in the ELA. Lambatungnajökull would almost loose its accumulation area, Hoffellsjökull and Morsárjökull would loose approximately 30 and 45 %, respectively, whereas the accumulation area of Fjallsjökull would only decrease by 7%.

A clearer distinction between the response of the Öræfajökull outlets and the eastern outlets to the post-LIA climate perturbations would perhaps be expected, as steeper glaciers generally respond faster to changes in climate (e.g., Cuffey and Paterson, 2010). The thinner Öræfajökull glaciers, with ice divides lying 400–500 m higher than on the eastern outlet glaciers and steep mass balance gradient, are suspected to have a shorter response time. The response time of a glacier, the time it takes for a glacier to adjust its geometry to a new steady state after a change in mass balance, is a function of its mean thickness and terminus ablation (Jóhannesson et al., 1989), and of its hypsometry and mass balance gradient (Cuffey and Paterson, 2010). However, the geodetic mass balance records and terminus fluctuations of the outlets of southeast Vatnajökull do not indicate a distinct difference in the response of the outlets of the two glaciated regions. But the temporal resolution of the geodetic mass balance records is lower than the supposed response time of 15–30 years, given terminus ablation of $-10\,\mathrm{m\,w.e.\,a^{-1}}$ and average ice thicknesses of 150–300 m. In order to detect mass balance changes during the colder period following the 1960s, aerial images could be used to construct surface DEMs, and thereby increase the temporal resolution of the mass balance record for the period 1945–1989/2002.

Glacier surface lowering is influenced by the geometry and hypsometry of the outlet glaciers, and the proglacial lakes. Surface lowering is generally a function of elevation (Fig. 11), but the downwasting near the terminus is highly variable. Two of the glaciers experiencing the greatest surface lowering near the termini (Heinabergsjökull and Lambatungnajökull), are constrained by valley walls on both sides, and have retreated close to 3 km in the post-LIA period (Table 1). The surface elevation changes near the terminus of Svínafellsjökull and Kvíárjökull are in the lower range (Fig. 11). The glaciers only retreated about 1 km in ~ 1890–2010 (Fig. 7), and they are both confined by steep valley walls and terminate in overdeepened basins. Their mass loss has been governed by thinning rather than retreat, which may be related to their bedrock topography. Using simplified dynamical models, Adhikari and Marshall (2013) found that valley glaciers with overdeepened beds were likely to withdraw through deflation more than marginal retreat.

6.3 Volume-area scaling

Less than 0.1 % of the world's glacier volume is known (Bahr, 1997) and observations of volume evolution are rare (e.g., Flowers and Clarke, 1999; Radic et al., 2007; Möller and Schneider, 2010). Glacier volume change estimates of the whole post-LIA time period are limited (Vaughan et al., 2013, and references therein), and results of model studies are often compared with calculations from other models, not with observations (e.g., Oerlemans, 2007). Our volume-area time series of the 12 outlets of southeast Vatnajökull starts at the end of the LIA, when most of the glaciers had reached their maximum size in historical times, some even since the end of the early Holocene deglaciation (Thórarinsson, 1943). From glacier area inventories, glacier volume has been estimated by applying scaling relations (e.g., Chen and Ohmura, 1990; Bahr, 1997) and ice-dynamical considerations (e.g., Adhikari and Marshall, 2013). Our data set provides an opportunity to evaluate the empirical and modelled volume-area scaling relation. The volume-area scaling method assumes that the volume of a glacier is proportional to its area in a power γ

$$V = c \times A^{\gamma} \tag{3}$$

where V and A are the volume and surface area of a single glacier, and c and γ are constants. Based on statistical regression of data from 63 mountain glaciers, Chen and Ohmura (1990) found γ to be close to 1.36, whereas theoretical considerations predict a value of 1.375 for valley glaciers, supported with data from 144 glaciers (Bahr et al., 1997). The volume-area evolution of the last 120 years of each studied glacier of southeast Vatnajökull is plotted in Fig. 14. The scaling constants are estimated for the years ~ 1890, 1904, 1945, 2002, 2010; γ ranging from 1.357 to 1.457, and c between 0.030 and 0.048 (Table 5).

The scaling parameters are expected to evolve over time; as the glaciers retreat, γ decreases due to the fact that glaciers thin before they undergo notable area decrease (e.g., Radic et al., 2007; Adhikari and Marshall, 2012). Adhikari and Marshall (2012) show how different topographic and climatic settings, glacier flow dynamics, and the degree of dis-equilibrium with climate systematically affect the volume-area relation. The magnitude of γ after 100 years of glacier retreat was found to be 1.377 ± 0.063, comparable with $\gamma = 1.357$ calculated for a sample of real alpine glaciers (Chen and Ohmura, 1990). The steady state exponent was however 1.46 (Adhikari and Marshall, 2012). From our data set this trend is not evident, as the volume-area data set of ~ 1890 gives $\gamma = 1.357$, compared to 1.457 in 2002 (Table 5). As seen in Fig. 14, the volume-area relation of the individual outlets varies. Glaciers with bulk of their area distribution above the ELA (shape class B) are in line with the slope of the classical volume-area relation of Bahr et al. (1997) and Adhikari and Marshall (2012) as well, with a slightly higher value for the coefficient c. The majority of the outlets belonging to other hypsometric classes (Hrútárjökull, Svínafellsjökull, Lambatungnajökull, Fjallsjökull, Hoffellsjökull and Heinabergsjökull) experienced larger relative volume loss, have a larger exponent γ (Fig. 14), and lost volume at a faster rate than the shape class B glaciers. The increase in γ from our data set can probably be explained by the variable response of individual outlet glaciers and the glaciers not being in the same transient states at each point in time. Furthermore our data set may not be not large enough to make estimates on the change of γ. Comparison of the ice volume calculated according to the exponents of Bahr et al. (1997) and Adhikari and Marshall (2012) with our volume estimates, reveals an underestimate in ice volume of up to 50 %. The variable hypsometry, shape, size, and thickness of the outlets of southeast Vatnajökull, indicate that the coefficients of the power law relating glacier volume and area need to be adjusted to variable glaciological parameters and can only be used in a statistical way on a large number of glaciers when inferring the volume from measured area.

7 Conclusions

We have compiled a series of glacier outlines and glacier surface DEMs of the outlets of southeast Vatnajökull from various sources. The multi-temporal glacier inventory of volume and area changes for the period ~1890–2010 is unique. We derive the mass balance history of one of the most sensitive glaciated areas in the world for the post-LIA period by geodetic methods. The average mass balance during the period 1890–2010 was $-0.38\,\mathrm{m\,w.e.\,a^{-1}}$. The glaciers are sensitive to climate change, with high mass turnover rates, and experienced among the highest rates of mass loss (on average $1.34\,\mathrm{m\,w.e.\,a^{-1}}$) worldwide in the early 21st century (Vaughan et al., 2013). The glaciated area decreased by $162\,\mathrm{km^2}$ in ~1890–2010, and the outlets collectively lost $60 \pm 8\,\mathrm{km^3}$ of ice, contributing $0.154 \pm 0.02\,\mathrm{mm}$ to sea level rise in the post-LIA period.

Each glacier lost between 15 and 50 % of their ~1890 volume, the difference attributed to their variable hypsometry and bedrock topography, and the presence of proglacial lakes, that enhance melting at the terminus. The different response of glaciers experiencing similar climatic forcing, underlines the importance of a large sample of glaciers when interpreting the climate signal, and highlights once more the effect of glacier hypsometry and geometry on the dynamic response of glaciers to changes in mass balance. The dynamically different response of the glaciers show, that frontal variations and aera changes only provide limited information on the glacier response to climate perturbations, as some experience rapid downwasting but little retreat.

TCD
8, 4681–4735, 2014

A ~200 m difference of the ELA of the outlets glaciers was observed during the time period 2007–2011, presumably due to spatial differences in orographically enhanced precipitation, associated with atmospheric fronts and cyclones. The ELA has risen > 300 m since the end of the 19th century. The steep Öræfajökull outlet glaciers are more likely to survive future warming, since their ice divides are 400–500 m higher than the eastern outlets. Furthermore, proglacial lakes will increase in size and new will form as the glaciers retreat, and enhance melting.

From the data set of the variations of the outlets of southeast Vatnajökull we have assessed the power-law relation between glacier area and volume. A comparison of the ice volume between our measurements and the estimates based on the constants used by Bahr et al. (1997) and Adhikari and Marshall (2012), shows that the relation could underestimate the ice volume up to 50%. This needs to be taken into account, since glaciers outside the polar areas are contributing to sea level rise at an accelerated rate. Furthermore, the glacier inventory provides information that can be used to calibrate mass balance-ice flow models that simulate future glacier response to climate scenarios. Work is already underway to simulate the 20th century evolution of three of the eastern outlets.

Acknowledgements. This work was funded by a doctoral grant of the Research Fund of the University of Iceland to Hrafnhildur Hannesdóttir, two additional grants from the Research Fund to Guðfinna Aðalgeirsdóttir, the Icelandic Road Administration, The Nordic Centre of Excellence SVALI, the Kvísker Fund, the University of Iceland's Research Centre in Hornafjörður, and the Directorate of Labour. We thank Trausti Jónsson at the Icelandic Meteorological Office for access to the temperature and precipitation records. The 2010 LiDAR DEM was acquired as a part of an ongoing collective effort between the Icelandic Meteorological Office and the Institute of Earth Sciences of the University of Iceland, to map the surface topography of Icelandic ice caps, initiated in the International Polar Year 2007–2009. We thank Tómas Jóhannesson for very helpful comments on an early draft of the manuscript. This publication is contribution No. 42 of the Nordic Centre of Excellence SVALI, "Stability and Variations of Arctic Land Ice", funded by the Nordic Top-level Research Initiative (TRI).

References

Aðalgeirsdóttir, G., Guðmundsson, G. H., and Björnsson, H.: Volume sensitivity of Vatnajökull Ice Cap, Iceland, to perturbations in equilibrium line altitude, J. Geophys. Res.-Earth, 110, F04001, doi:10.1029/2005jf000289, 2005. 4685

Aðalgeirsdóttir, G., Jóhannesson, T., Björnsson, H., Pálsson, F., and Sigurðsson, O.: Response of Hofsjökull and southern Vatnajökull, Iceland, to climate change, J. Geophys. Res.-Earth, 111, F03001, doi:10.1029/2005JF000388, 2006. 4683, 4685, 4699

Aðalgeirsdóttir, G., Guðmundsson, S., Björnsson, H., Pálsson, F., Jóhannesson, T., Hannesdóttir, H., Sigurðsson, S. Þ., and Berthier, E.: Modelling the 20th and 21st century evolution of Hoffellsjökull glacier, SE-Vatnajökull, Iceland, The Cryosphere, 5, 961–975, doi:10.5194/tc-5-961-2011, 2011. 4683, 4685, 4686, 4699, 4717, 4722

Adhikari, S. and Marshall, S. J.: Glacier volume-area relation for high-order mechanics and transient glacier states, Geophys. Res. Lett., 39, doi:10.1029/2012gl052712, 2012. 4704, 4705, 4706, 4735

Adhikari, S. and Marshall, S. J.: Influence of high-order mechanics on simulation of glacier response to climate change: insights from Haig Glacier, Canadian Rocky Mountains, The Cryosphere, 7, 1527–1541, doi:10.5194/tc-7-1527-2013, 2013. 4703

Army Map Service, C. o. E.: Series C762, sheets: 6018-I,IV, 6019-I,II,III,IV, 6020-I,II,III, 611IV, 6120-I,II,III, US Army, Washington D.C., 1950–1951. 4688

Árnadóttir, T., Lund, B., Jiang, W., Geirsson, H., Björnsson, H., Einarsson, P., and Sigurðsson, T.: Glacial rebound and plate spreading: results from the first countrywide GPS observations in Iceland, Geophys. J. Int., 177, 691–716, doi:10.1111/j.1365-246X.2008.04059.x, 2009. 4690

Auriac, A., Spaans, K. H., Sigmundsson, F., Hooper, A., Schmidt, P., and Lund, B.: Iceland rising: Solid Earth response to ice retreat inferred from satellite radar interferometry and visocelastic modeling, J. Geophys. Res.-Sol. Ea., 118, 1331–1344, doi:10.1002/Jgrb.50082, 2013. 4690

Auriac, A., Sigmundsson, F., Hooper, A., Spaans, K. H., Björnsson, H., Pálsson, F., Pinel, V., and Feigl, K. L.: InSAR observations and models of crustal deformation due to glacial surge in Iceland, Geophys. J. Int., 198, 1329–1341, 2014. 4689

Bader, H.: Sorge's Law of densification of snow on high polar glaciers, J. Glaciol., 2, 319–323, 1954. 4694

TCD
8, 4681–4735, 2014

Area, volume and mass changes of southeast Vatnajökull ice cap

Hannesdóttir et al.

Bahr, D. B.: Global distributions of glacier properties: A stochastic scaling paradigm, Water Resour. Res., 3, 1669–1679, doi:10.1029/97WR00824, 1997. 4703, 4735
Bahr, D. B., Meier, M. F., and Peckham, S. D.: The physical basis of glacier volume-area scaling, J. Geophys. Res.-Sol. Ea., 102, 20355–20362, doi:10.1029/97jb01696, 1997. 4704, 4705, 4706
Barcaza, G., Aniya, M., Matsumoto, T., and Aoki, T.: Satellite-Derived Equilibrium Lines in Northern Patagonia Icefield, Chile, and Their Implications to Glacier Variations, Arct. Antarct. Alp. Res., 41, 174–182, doi:10.1657/1938-4246-41.2.174, 2009. 4693
Bauder, A., Funk, M., and Huss, M.: Ice-volume changes of selected glaciers in the Swiss Alps since the end of the 19th century, Ann. Glaciol., 46, 145–149, 2007. 4683
Berthier, E., Le Bris, R., Mabileau, L., Testut, L., and Remy, F.: Ice wastage on the Kerguelen Islands (49 degrees S, 69 degrees E) between 1963 and 2006, J. Geophys. Res.-Earth, 114, doi:10.1029/2008JF001192, 2009. 4690
Björnsson, H.: Glaciers in Iceland, Jökull, 29, 74–80, 1979. 4685
Björnsson, H.: Scales and rates of glacial sediment removal: a 20 km long and 300 m deep trench created beneath Breiðamerkurjökull during the Little Ice Age, Ann. Glaciol., 22, 141–146, 1996. 4701
Björnsson, H.: Jöklar á Íslandi, Opna, Reykjavík, 2009. 4685, 4689
Björnsson, H., and Pálsson, F.: Jöklar í Hornafirði, rannsóknir og saga, in: Jöklaveröld, Náttúra og Mannlíf, edited by: Björnsson, H., 125–164, Skrudda, Reykjavík, 2004. 4686, 4689
Björnsson, H., and Pálsson, F.: Icelandic glaciers, Jökull, 58, 365–386, 2008. 4684, 4685, 4689, 4699, 4700
Björnsson, H., Pálsson, F., Sigurðsson, O., and Flowers, G. E.: Surges of glaciers in Iceland, Ann. Glaciol., 36, 82–90, 2003. 4690
Björnsson, H., Pálsson, F., Guðmundsson, S., Magnússon, E., Aðalgeirsdóttir, G., Jóhannesson, T., Berthier, E., Sigurðsson, O., and Thorsteinsson, T.: Contribution of Icelandic ice caps to sea level rise: Trends and variability since the Little Ice Age, Geophys. Res. Lett., 40, 1546–1550, doi:10.1002/Grl.50278, 2013. 4683, 4685, 4699, 4700
Böðvarsson, A.: Landmælingar og kortagerð Dana á Íslandi: Upphaf landmælinga á Íslandi, Landmælingar Íslands, Reykjavík, 1996. 4688
Chen, J. and Ohmura, A.: Estimation of Alpine glacier water resources and their change since the 1870s, IAHS (International Association of Hydrological Sciences), 193, 127–135, 1990. 4703, 4704

Church, J. A., Clark, P. U., Cazenave, A., Gregory, J. M., Jevrejeva, S., Levermann, A., Merrifield, M. A., Milne, G. A., Nerem, R. S., Nunn, P. D., Payne, A. J., Pfeffer, W. T., Stammer, D., and Unnikrishnan, A. S.: Sea level change, in: Climate Change 2013: The Physical Science Basis. Contribution of Working Group I to the Fifth Assessment Report of the Intergovernmental Panel on Climate Change, edited by: Stocker, T. F., Qin, D., Plattner, G.-K., Tignor, M., Allen, S. K., Boschung, J., Nauels, A., Xia, Y., Bex, V., and Midgley, P. M.: Cambridge University Press, Cambridge, UK and New York, NY, USA, 2013. 4683

Cox, L. H. and March, R. S.: Comparison of geodetic and glaciological mass-balance techniques, Gulkana Glacier, Alaska, USA, J. Glaciol., 50, 363–370, doi:10.3189/172756504781829855, 2004. 4699

Crochet, P., Jóhannesson, T., Jónsson, T., Sigurðsson, O., Björnsson, H., Pálsson, F., and Barstad, I.: Estimating the spatial distribution of precipitation in Iceland using a linear model of orographic precipitation, J. Hydrometeorol., 2007. 4700

Cuffey, K. M. and Paterson, W. S. B.: The Physics of Glaciers, Elsevier, Burlington, 4th edn., 2010. 4693, 4702

Danish General Staff: Sheets: 87-NV,SV,SA, 97-NV, NA, 96-NA, Generalstabens Topografiske Afdeling, Copenhagen, 1904. 4688

Davies, B. J., Carrivick, J. L., Glasser, N. F., Hambrey, M. J., and Smellie, J. L.: Variable glacier response to atmospheric warming, northern Antarctic Peninsula, 1988–2009, The Cryosphere, 6, 1031–1048, doi:10.5194/tc-6-1031-2012, 2012. 4701

De Angelis, H.: Hypsometry and sensitivity of the mass balance to changes in equilibrium-line-altitude: the case of the Southern Patagonia Icefield, J. Glaciol., 60, 14–28, doi:10.3189/2014JoG13J127, 2014. 4698, 4701

De Woul, M., and Hock, R.: Static mass-balance sensitivity of Arctic glaciers and ice caps using a degree-day approach, Ann. Glaciol., 42, 217–224, doi:10.3189/172756405781813096, 2005. 4683

Defense Mapping Agency, H. C.: Series C761, sheets: 2113-I,2213-I,III,IV,2214-II,III, National LAnd Survey of Iceland, Reykjavík, 1997. 4688

Flowers, G. E. and Clarke, G. K. C.: Surface and bed topography of Trapridge Glacier, Yukon Territory, Canada: digital elevation models and derived hydraulic geometry, J. Glaciol., 45, 165–174, 1999. 4703

Flowers, G. E., Marshall, S. J., Björnsson, and Clarke, G. K. C.: Sensitivity of Vatnajökull ice cap hydrology and dynamics to climate warming over the next 2 centuries, J. Geophys. Res., 110, F02011, doi:10.1029/2004JF000200, 2005. 4684

Flowers, G. E., Björnsson, H., Geirsdóttir, A., Miller, G. H., and Clarke, G. K. C.: Glacier fluctuation and inferred climatology of Langjökull ice cap through the Little Ice Age, Quaternary Sci. Rev., 26, 2337–2353, 2007. 4683

Furbish, D. J. and Andrews, J. T.: The use of hypsometry to indicate long-term stability and response of valley glaciers to changes in mass transfer, J. Glaciol., 30, 199–211, 1984. 4693, 4698

Glasser, N. F., Harrison, S., Jansson, K. N., Anderson, K., and Cowley, A.: Global sea-level contribution from the Patagonian Icefields since the Little Ice Age maximum, Nat. Geosci., 4, 303–307, doi:10.1038/Ngeo1122, 2011. 4683

Guðmundsson, S.: Reconstruction of late 19th century glacier extent of Kotárjökull and Breiðamerkurjökull in SE–Iceland and comparison with the current extent, M.Sc. thesis, University of Iceland, Reykjavík, 2014. 4683, 4700

Guðmundsson, S., Pálsson, F., Björnsson, H., and Haraldsson, H. H.: Comparison of energy balance and degree-day models of summer ablation on the Langjökull ice cap, SW-Iceland, Jökull, 59, 1–18, 2009. 4699, 4700

Guðmundsson, S., Björnsson, H., Magnússon, E., Berthier, E., Pálsson, F., Guðmundsson, M. T., Högnadottir, T., and Dall, J.: Response of Eyjafjallajökull, Torfajökull and Tindfjallajökull ice caps in Iceland to regional warming, deduced by remote sensing, Polar Res., 30, doi:10.3402/Polar.V30i0.7282, 2011. 4692, 4694, 4699, 4700, 4733

Guðmundsson, S., Hannesdóttir, H., and Björnsson, H.: Post-Little Ice Age volume loss of Kotárjökull glacier, SE-Iceland, derived from historical photography, Jökull, 62, 97–110, 2012. 4688

Haeberli, W., Muller, P., Alean, P., and Bösch, H.: Glacier changes following the Little Ice Age-a survey of the international data basis and its perspectives, in: Glacier Fluctuations and Climatic Change, edited by: Oerlemans, J., Kluwer Academic Publishers, Utrecht, 1989. 4682

Hanna, E., Jonsson, T., and Box, J. E.: An analysis of icelandic climate since the nineteenth century, Int., 24, 1193–1210, 2004. 4700

Hannesdóttir, H., Björnsson, H., Pálsson, F., Aðalgeirsdóttir, G., and Guðmundsson, S.: Variations of southeast Vatnajökull ice cap (Iceland) 1650–1900 and reconstruction of the glacier surface geometry at the Little Ice Age maximum, Geografiska Annaler, in press. 4684, 4687, 4691, 4695, 4725, 4726, 4727, 4732, 4734

Huss, M.: Extrapolating glacier mass balance to the mountain-range scale: the European Alps 1900–2100, The Cryosphere, 6, 713–727, doi:10.5194/tc-6-713-2012, 2012. 4699, 4700

Huss, M.: Density assumptions for converting geodetic glacier volume change to mass change, The Cryosphere, 7, 877–887, doi:10.5194/tc-7-877-2013, 2013. 4694

Icelandic Meteorological Office and Institute of Earth Sciences, University of Iceland: DEMs of Icelandic glaciers (data set), The Icelandic Meteorological Office, Reykjavík, 2013. 4687

James, T. D., Murray, T., Barrand, N. E., Sykes, H. J., Fox, A. J., and King, M. A.: Observations of enhanced thinning in the upper reaches of Svalbard glaciers, The Cryosphere, 6, 1369–1381, doi:10.5194/tc-6-1369-2012, 2012. 4699

Jiskoot, H., Curran, C. J., Tessler, D. L., and Shenton, L. R.: Changes in Clemenceau Icefield and Chaba Group glaciers, Canada, related to hypsometry, tributary detachment, length-slope and area-aspect relations, Ann. Glaciol., 50, 133–143, 2009. 4693, 4701

Jóhannesson, T., Raymond, C., and Waddington, E.: Time-Scale for Adjustment of Glaciers to Changes in Mass Balance, J. Glaciol., 35, 355–369, 1989. 4702

Jóhannesson, T., Aðalgeirsdóttir, G., Björnsson, H., Crochet, P., Elíasson, E. B., Ólafsson, H., Pálsson, F., Rögnvaldsson, O., Sigurðsson, O., Snorrason, A., Blöndal Sveinsson, Ó. G., and Þorsteinsson, Þ: Effect of climate change on hydrology and hydro-resources in Iceland, Tech. Rep. OS-2007/011, Reykjavík, 2007. 4700

Jóhannesson, T., Björnsson, H., Pálsson, F., Sigurðsson, O., and Thorsteinsson, T.: LiDAR mapping of the Snæfellsjökull ice cap, western Iceland, Jökull, 61, 19–32, 2011. 4733

Jóhannesson, T., Björnsson, H., Magnússon, E., Guðmundsson, S., Pálsson, F., Sigurðsson, O., Thorsteinsson, T., and Berthier, E.: Ice-volume changes, bias estimation of mass-balance measurements and changes in subglacial lakes derived by lidar mapping of the surface of Icelandic glaciers, Ann. Glaciol., 54, 63–74, doi:10.3189/2013aog63a422, 2013. 4687, 4733

Jones, P. D., Lister, D. H., Osborn, T. J., Harpham, C., Salmon, M., and Morice, C. P.: Hemispheric and large-scale land surface air temperature variations: An extensive revision and an update to 2010, J. Geophys. Res., 35, L19502, doi:10.1029/2008GL034470, 2012. 4700

Kääb, A., and Funk, M.: Modelling mass balance using photogrammetric and geophysical data: a pilot study at Griesgletscher, Swiss Alps, J. Glaciol., 45, 575–583, 1999. 4689

Knoll, C., Kerschner, H., and Abermann, J.: Development of area, altitude and volume of South Tyrolean glaciers since the Little Ice Age maximum, Zeitschrift für Gletscherkunde und Glazialgeologie, 42, 19–36, 2008. 4683

Korona, J., Berthier, E., Bernard, M., Remy, F., and Thouvenot, E.: SPIRI T. SPOT 5 stereoscopic survey of Polar Ice: Reference Images and Topographies during the fourth International Polar Year (2007-2009), Int. Soc. Photogramme., 64, 204–212, doi:10.1016/j.isprsjprs.2008.10.005, 2009. 4689

Kuhn, M., Markel, G., Kaser, G., Nickus, U., Obleitner, F., and Schneider, H.: Fluctuations of climate and mass balances: different responses of two adjacent glaciers, Zeitschrift für Gletscherkunde und Glazialgeologie, 21, 409–416, 1985. 4701

Lliboutry, L.: Nieves y Glaciares de Chile: Fundamentos de glaciología, University of Chile, Santiago, 1956. 4693

Luthcke, S. B., Arendt, A. A., Rowlands, D. D., McCarthy, J. J., and Larsen, C. F.: Recent glacier mass changes in the Gulf of Alaska region from GRACE mascon solutions, J. Glaciol., 54, 767–777, doi:10.3189/002214308787779933, 2008. 4699

Lüthi, M. P., Bauder, A., and Funk, M.: Volume change reconstruction of Swiss glaciers from length change data, J. Geophys. Res.-Earth, 115, F04022, doi:10.1029/2010jf001695, 2010. 4683

Magnússon, E., Björnsson, H., and Pálsson, F.: Landslag í grennd Kvískerja í fortíð og framtíð: Niðurstöður ísjármælinga á Kvíár-, Hrútár og Fjallsjökli (Radio echo sounding on Kvíárjökull, Hútárjökull and Fjallsjökull)., Jökull, 57, 83–89, 2007. 4689

Magnússon, E., Pálsson, F., Björnsson, H., and Guðmundsson, S.: Removing the ice cap of Öraefajokull central volcano, SE-Iceland: Mapping and interpretation of bedrock topography, ice volumes, subglacial troughs and implications for hazards assessments, Jökull, 62, 131–150, 2012. 4685, 4689

Marshall, S. J.: Modelling glacier response to climate change, in: Glacier Science and Environmental Change, edited by: Knight, P. G., Blackwell Publishing, Malden, USA, 275–292, 2008. 4693

Mathieu, R., Chinn, T., and Fitzharris, B.: Detecting the equilibrium-line altitudes of New Zealand glaciers using ASTER satellite images, New Zealand J. Geol. Geophys., 52, 209–222, 2009. 4693

Mernild, S. H., Pelto, M., Malmros, J. K., Yde, J. C., Knudsen, N. T., and Hanna, E.: Identification of snow ablation rate, ELA, AAR and net mass balance using transient snowline variations on two Arctic glaciers, J. Glaciol., 59, 649–659, doi:10.3189/2013jog12j221, 2013. 4693

Möller, M., and Schneider, C.: Calibration of glacier volume-area relations from surface extent fluctuations and application to future glacier change, J. Glaciol., 56, 33–40, 2010. 4703

Nawri, N., and Björnsson, H.: Surface Air Temperature and Precipitation Trends for Iceland in the 21st Century, Tech. Rep. VÍ 2010-005, The Icelandic Meteorological Office, Reykjavík, 2010.

Oerlemans, J.: Estimating the reponse times of Vadret da Morteratsch, Vadret da Palu, Briksdalsbreen and Nigardsbreen from their length records, J. Glaciol., 53, 357–362, 2007. 4701, 4703

Oerlemans, J., Anderson, B., Hubbard, A., Huybrechts, P., Johannesson, T., Knap, W. H., Schmeits, M., Stroeven, A. P., van de Wal, R. S. W., Wallinga, J., and Zuo, Z.: Modelling the response of glaciers to climate warming, Clim. Dynam., 14, 267–274, 1998. 4693, 4701

Osmaston, H. A.: Models for the estimation of firnlines of present and Pleistocene glaciers, in: Processes in physical and human geography: Bristol essays, edited by: PeeL, R. F., Chisholm, M. D. I., and Haggart, P., 218–245, Heinemann Educational Books Ltd, London, 1975. 4698

Östrem, G.: ERTS data in glaciology- an effort to monitor glacier mass balance from satellite imagery, J. Glaciol., 15, 403–415, 1975. 4693

Pálsson, F., Guðmundsson, S., Björnsson, H., Berthier, E., Magnússon, E., Guðmundsson, S., and Haraldsson, H. H.: Mass and volume changes of Langjokull ice cap, Iceland, similar to ~ 1890 to 2009, deduced from old maps, satellite images and in situ mass balance measurements, Jökull, 62, 81–96, 2012. 4683, 4688, 4692, 4694, 4699, 4700, 4733

Paul, F., Kääb, A., Maisch, M., Kellenberger, T., and Haeberli, W.: Rapid disintegration of Alpine glaciers observed with satellite data, Geophys. Res. Lett., 31, doi:10.1029/2004gl020816, 2004. 4699

Paul, F., Kääb, A., and Haeberli, W.: Recent glacier changes in the Alps observed by satellite: Consequences for future monitoring strategies, Global Planet. Change, 56, 111–122, doi:10.1016/j.gloplacha.2006.07.007, 2007. 4690

Pelto, M. S.: Forecasting temperate alpine glacier survival from accumulation zone observations, The Cryosphere, 4, 67–75, doi:10.5194/tc-4-67-2010, 2010. 4690, 4699

Rabatel, A., Machaca, A., Francou, B., and Jomelli, V.: Glacier recession on Cerro Charquini (16 degrees S), Bolivia, since the maximum of the Little Ice Age (17th century), J. Glaciol., 52, 110–118, doi:10.3189/172756506781828917, 2006. 4683

Rabatel, A., Francou, B., Soruco, A., Gomez, J., Cáceres, B., Ceballos, J. L., Basantes, R., Vuille, M., Sicart, J.-E., Huggel, C., Scheel, M., Lejeune, Y., Arnaud, Y., Collet, M., Condom, T., Consoli, G., Favier, V., Jomelli, V., Galarraga, R., Ginot, P., Maisincho, L., Mendoza, J., Ménégoz, M., Ramirez, E., Ribstein, P., Suarez, W., Villacis, M., and Wagnon, P.: Current state of glaciers in the tropical Andes: a multi-century perspective on glacier evolution and climate change, The Cryosphere, 7, 81–102, doi:10.5194/tc-7-81-2013, 2013. 4693

Radic, V., Hock, R., and Oerlemans, J.: Volume-area scaling vs flowline modelling in glacier volume projections, Ann. Glaciol., 46, 234–240, 2007. 4703, 4704

Reinhardt, W. and Rentsch, H.: Determination of chnages in volume and elevation of glaciers using digital elevation models for the Veragtferner, Ötztal Alps, Austria, Ann. Glaciol., 8, 151–155, 1986. 4689

Rivera, A., Benham, T., Casassa, G., Bamber, J., and Dowdeswell, J. A.: Ice elevation and areal changes of glaciers from the Northern Patagonia Icefield, Chile, Global Planet. Change, 59, 126–137, doi:10.1016/j.gloplacha.2006.11.037, 2007. 4690

Rögnvaldsson, O., Jónsdóttir, J. F., and Ólafsson, H.: Numerical simulations of precipitation in the complex terrain of Iceland- Comparison with glaciological and hydrological data, Meterol. Z., 16, 71–85, 2007. 4700

Shea, J. M., Menounos, B., Moore, R. D., and Tennant, C.: An approach to derive regional snow lines and glacier mass change from MODIS imagery, western North America, The Cryosphere, 7, 667–680, doi:10.5194/tc-7-667-2013, 2013. 4693

Sigurðsson, F.: Vandamál við úrkomumælingar á Íslandi, in: Vatnið og landið. Vatnafræðiráðstefna, Október 1987, edited by: Sigbjarnarson, G., Orkustofnun, Reykjavík, 307, 101–110, 1990. 4687

Thórarinsson, S.: Oscillations of the Iceland glaciers in the last 250 years, Geogr. Ann. A, 25, 1–54, 1943. 4684, 4703

Vaughan, D. G., Comiso, J. C., Allison, I., Carrasco, J., Kaser, G., Kwok, R., Mote, P., Murray, T., Paul, F., Ren, J., Rignot, E., Solomina, O., Steffen, K., and Zhang, T.: Observations: Cryosphere, in: Climate Change 2013: The Physical Science Basis. Contribution of Working Group I to the Fifth Assessment Report of the Intergovernmental Panel on Climate Change, edited by: Stocker, T. F., Qin, D., Plattner, G.-K., Tignor, M., Allen, S. K., Boschung, J.,

TCD
8, 4681–4735, 2014

Area, volume and mass changes of southeast Vatnajökull ice cap

Hannesdóttir et al.

Title Page
Abstract | Introduction
Conclusions | References
Tables | Figures
◀| |▶
◀ ▶
Back | Close
Full Screen / Esc
Printer-friendly Version
Interactive Discussion

Nauels, A., Xia, Y., Bex, V., and Midgley, P. M.: Cambridge University Press, Cambridge, UK and New York, NY, USA, 317–382, 2013. 4682, 4699, 4703, 4705

WGMS: Global Glacier Changes: Facts and Figures, Tech. rep., Zurich, Switzerland, 2008. 4682

Wise, S.: Assessing the quality for hydrological applications of digital elevation models derived from contours, Hydrol. Process., 14, 1909–1929, doi:10.1002/1099-1085(20000815/30)14:11/12<1909::Aid-Hyp45>3.0.Co;2-6, 2000. 4690

Table 1. Characteristics of the southeast outlet glaciers. Some glaciers have gently sloping accumulation and ablation areas, which are connected by ice falls, thus the mean slope is not representative for the entire profile. The ELA is presented as the range of the averages of all years. Average ice thickness and terminus elevation are presented in ~ 1890 and 2010.

glacier	slope (°)	ice divide (m a.s.l.)	area (km^2)	volume (km^3)	thickness (m)	AAR	ELA (m a.s.l.)	length (km)	term. elev. (m a.s.l.)	retreat (km)	hypsom.
Morsárj.	6.3	1350	28.9	6.0	215/208	0.64	1000–1130	10.8	150/170	1.8	B
Skaftafellsj.	3.8	1880	84.1	20.3	254/241	0.66	1000–1160	19.3	80/95	2.5	B
Svínafellsj.	9.0	2030	33.2	3.6	132/108	0.66	1000–1120	12.0	90/100	0.8	E
Kotárj.	13.3	1820	11.5	1.7	152/148	0.71	1000–1130	6.2	220/400	1.3	B/D
Kvíárj.	6.0	2010	23.2	4.1	187/177	0.64	1010–1130	14.1	30/30	1.5	E
Hrútárj.	12.4	1980	12.2	0.9	111/74	0.58	880–910	8.6	50/60	2.0	A/C
Fjallsj.	7.9	2030	44.6	7.0	185/157	0.6	870–960	12.9	20/30	2.2	E/C
Skálafellsj.	3.1	1490	100.6	33.3	332/331	0.68	910–1020	24.4	40/50	2.0	B
Heinabergsj.	3.7	1490	99.7	26.7	308/268	0.61	990–1100	22.7	60/70	2.9	B/C
Fláaj.	3.1	1480	169.8	53.9	313/317	0.59	1060–1120	25.1	40/70	2.7	B
Hoffellsj.	3.4	1470	206.0	54.3	303/264	0.63	1050–1120	23.6	30/50	4.0*	B/D
Lambatungnaj.	5.0	1480	36.3	3.6	135/99	0.43	1110–1210	19.3	180/250	2.7	D

*The retreat applies to the western arm of Hoffellsjökull (named Svínafellsjökull).

TCD
8, 4681–4735, 2014

Area, volume and mass changes of southeast Vatnajökull ice cap

Hannesdóttir et al.

Table 2. Area of the outlet glaciers at different times in km^2. The estimated error of the glacier margin is shown in parenthesis in the top row. The DMA aerial photographs of Öræfajökull are from 1982, and of the eastern outlet glaciers from 1989. Glacier outlines from 2002 for Öræfajökull (obtained from images of Loftmyndir ehf.), and from 2000 for Skálafellsjökull, Heinabergsjökull, Fláajökull, Hoffellsjökull and Lambatungnajökull (digitized from Landsat satellite images). Ice divides are assumed to remain constant throughout the time period. The numbers for Hoffellsjökull are from Aðalgeirsdóttir et al. (2011). Percentages are relative to the ~ 1890 area. *The area of Lambatungnajökull in 1904 is estimated from the relative extent of the neighbouring outlets in that year (99 %). Kotárjökull is not included in the sum of the Öræfajökull outlets, since its area is only known in ~ 1890 and 2010.

glacier	~ 1890 (20 m)	1904 (15 m)	1945 (10 m)	1982/1989 (10 m)	2002 (5 m)	2010 (2 m)
Morsárj.	35.3 ± 0.7	34.5 ± 0.6 (98 %)	31.6 ± 0.3 (90 %)	30.9 ± 0.4 (87 %)	30.0 ± 0.2 (85 %)	28.9 ± 0.1 (82 %)
Skaftafellsj.	97.8 ± 1.3	96.7 ± 1.0 (99 %)	90.1 ± 0.6(92 %)	89.4 ± 0.6 (91 %)	86.4 ± 0.3 (88 %)	84.1 ± 0.1 (86 %)
Svínafellsj.	39.5 ± 0.9	38.9 ± 0.7 (98 %)	36.1 ± 0.5 (91 %)	35.5 ± 0.5 (90 %)	34.8 ± 0.3 (88 %)	33.2 ± 0.1 (84 %)
Kotárj.	14.5 ± 0.4		12.3 ± 0.5 (85 %)			11.5 ± 0.04 (79 %)
Kvíárj.	27.9 ± 0.7	27.4 ± 0.5 (98 %)	25.4 ± 0.4 (91 %)	25.1 ± 0.3 (90 %)	24.4 ± 0.2 (88 %)	23.2 ± 0.1 (83 %)
Hrútárj.	17.1 ± 0.5	16.7 ± 0.4 (98 %)	14.1 ± 0.2 (83 %)	13.9 ± 0.2 (81 %)	13.2 ± 0.1 (77 %)	12.2 ± 0.04 (71 %)
Fjallsj.	57.7 ± 0.8	56.1 ± 0.6 (97 %)	51.7 ± 0.4 90 %)	49.4 ± 0.4 (86 %)	47.3 ± 0.2 (82 %)	44.6 ± 0.1 (77 %)
Öræfaj.	275.3 ± 5.3	270.3 ± 3.8	249.0 ± 2.4	244.1 ± 2.4	236.1 ± 1.3	181.6 ± 0.58
Skálafellsj.	117.9 ± 1.6	116.4 ± 1.2 (99 %)	106.6 ± 0.7 (90 %)	104.0 ± 0.7 (88 %)	102.8 ± 0.3 (87 %)	100.6 ± 0.1 (85 %)
Heinabergsj.	120.3 ± 1.3	118.2 ± 1.0 (98 %)	109.0 ± 0.6 (91 %)	102.5 ± 0.6 (85 %)	101.8 ± 0.3 (85 %)	100.6 ± 0.1 (83 %)
Fláaj.	205.6 ± 1.9	202.1 ± 1.4 (98 %)	184.1 ± 1.0 (90 %)	181.9 ± 0.9 (88 %)	177.4 ± 0.5 (86 %)	169.7 ± 0.2 (83 %)
Hoffellsj.	234.5 ± 1.9	232.3 ± 1.4 (99 %)	224.5 ± 1.1 (96 %)	215.9 ± 1.0 (92 %)	212.7 ± 0.5 (91 %)	207.5 ± 0.2 (88 %)
Lambatungnaj.	46.1 ± 0.9	45.1 ± 0.9*	40.9 ± 0.4 (89 %)	39.4 ± 0.4 (86 %)	38.8 ± 0.2 (84 %)	36.3 ± 0.1 (79 %)
Eastern	723.9 ± 7.6	714.2 ± 5.9	664.6 ± 3.8	643.8 ± 3.6	632.8 ± 1.8	612.3 ± 0.7

1936 area: Hoffellsjökull 227.7 ± 1.5 (97%), Lambatungnajökull 41.9 ± 0.7 (91%).

TCD
8, 4681–4735, 2014

Area, volume and mass changes of southeast Vatnajökull ice cap

Hannesdóttir et al.

Table 3. Volume of the southeast outlet glaciers derived from glacier surface DEMs and the bedrock DEM at different times in km^3. Percentage is relative to the ~ 1890 volume. The estimated point accuracy of the elevation is in parenthesis. * The volume of Lambatungnajökull in 1904 is estimated from the relative size of the neighbouring outlets in that year (99%). Kotárjökull is not included in the sum of the Öræfajökull outlets, since its volume is only known in ~ 1890 and 2010.

glacier	~ 1890 (15–20 m)	1904 (10–15 m)	1945 (5–10 m)	1989 (5 m)	2002 (2 m)	2010 (0.5 m)
Morsárj.	7.6 ± 0.5	7.5 ± 0.4 (99 %)	6.8 ± 0.2 (89 %)		6.3 ± 0.1 (82 %)	6 ± 0.01 (79 %)
Skaftafellsj.	24.8 ± 1.5	24.5 ± 1.0 (99 %)	21.4 ± 0.6 (86 %)		20.7 ± 0.2 (83 %)	19.9 ± 0.04 (80 %)
Svínafellsj.	5.2 ± 0.6	5.1 ± 0.4 (99 %)	4.4 ± 0.3 (84 %)		4.1 ± 0.1 (78 %)	3.6 ± 0.02 (70 %)
Kotárjökull	2.2 ± 0.2					1.7 ± 0.01 (77 %)
Kvíárjökull	5.2 ± 0.4	5.15 ± 0.3 (99 %)	4.5 ± 0.2 (87 %)		4.2 ± 0.05 (81 %)	4.1 ± 0.01 (79 %)
Hrútárjökull	1.9 ± 0.3	1.8 ± 0.2 (96 %)	1.3 ± 0.1 (68 %)		1.08 ± 0.03 (57 %)	0.93 ± 0.01 (49 %)
Fjallsjökull	10.7 ± 0.9	10.3 ± 0.6 (97 %)	8.9 ± 0.4 (83 %)		7.3 ± 0.1 (69 %)	7 ± 0.02 (65 %)
Öræfajökull	55.4 ± 4.4	54.5 ± 2.9	47.2 ± 1.8		43.5 ± 0.58	41.3 ± 0.12
Skálafellsj.	39.1 ± 1.8	38.7 ± 1.2 (99 %)	35.7 ± 0.8 (91 %)	34.9 ± 0.5 (89 %)	34.6 ± 0.2 (88 %)	33.3 ± 0.05 (85 %)
Heinabergsj.	37 ± 1.8	36.6 ± 1.2 (99 %)	32.4 ± 0.8 (88 %)	29.4 ± 0.5 (80 %)	29.1 ± 0.2 (79 %)	26.7 ± 0.05 (72 %)
Fláajökull	64.3 ± 3.1	63.4 ± 2.0 (99 %)	57.7 ± 1.3 (90 %)	57.2 ± 0.9 (89 %)	56.2 ± 0.4 (87 %)	53.9 ± 0.09 (84 %)
Hoffellsj.	71 ± 4	70.4 ± 2.3 (99 %)	63 ± 2 (89 %)	57.6 ± 1.1 (81 %)	57 ± 0.4 (80 %)	54.3 ± 0.1 (76 %)
Lambatungnaj.	6.2 ± 0.7	6.1 ± 0.7 (99 %)	4.7 ± 0.3 (76 %)	4.4 ± 0.2 (76 %)	4.1 ± 0.1 (66 %)	3.6 ± 0.02(58 %)
Eastern outlets	217.6 ± 11.4	215.2 ± 7.4	193.5 ± 5.2	183.6 ± 3.2	180.9 ± 1.3	171.8 ± 0.31

1936 volume: Hoffellsjökull 65 ± 3 (92%), Lambatungnajökull 4.9 ± 0.4 (79%).

TCD

8, 4681–4735, 2014

Area, volume and mass changes of southeast Vatnajökull ice cap

Hannesdóttir et al.

Table 4. Geodetic mass balance in m w.e. a^{-1} for outlets of Öræfajökull (upper panel) and the eastern outlet glaciers (lower panel) for different time intervals. The correlation of the average summer (JJA) temperature measured at Hólar in Hornafjörður (shown as ave. T) with geodetic mass balance estimates during the same time intervals is shown in the last column.

Öræfaj.	~ 1890–1904	1904–1945	1945–2002	2002–2010	~ 1890–2010	corr. T (r)
Morsárj.	−0.18 ± 0.63	−0.48 ± 0.15	−0.26 ± 0.06	−0.99 ± 0.12	−0.37 ± 0.96	0.98
Skaftaf.	−0.19 ± 0.63	−0.73 ± 0.15	−0.13 ± 0.06	−1.06 ± 0.12	−0.40 ± 0.96	0.94
Svínaf.	−0.1 ± 0.63	−0.46 ± 0.15	−0.2 ± 0.06	−0.89 ± 0.12	−0.32 ± 0.96	0.98
Kvíárj.	−0.12 ± 0.63	−0.54 ± 0.15	−0.17 ± 0.06	−0.8 ± 0.12	−0.34 ± 0.96	0.96
Hrútárj.	−0.27 ± 0.63	−0.77 ± 0.15	−0.24 ± 0.06	−1.33 ± 0.12	−0.5 ± 0.96	0.96
Fjallsj.	−0.41 ± 0.63	−0.6 ± 0.15	−0.48 ± 0.06	−1-.27 ± 0.12	−0.57 ± 0.96	0.96
ave. T	9.2	9.9	9.7	10.6		

Eastern	~ 1890–1904	1904–1945	1936–1945	1945–1989	1989–2002	2002–2010	~ 1890–2010	corr. T (r)
Skálaf.	−0.24 ± 0.63	−0.58 ± 0.15		−0.27 ± 0.08	−0.25 ± 0.19	−1.38 ± 0.12	−0.40 ± 0.96	0.96
Heinab.	−0.22 ± 0.63	−0.81 ± 0.15		−0.56 ± 0.08	−0.36 ± 0.19	−2.6 ± 0.12	−0.70 ± 0.96	0.97
Fláaj.	−0.28 ± 0.63	−0.65 ± 0.15		−0.42 ± 0.08	−0.4 ± 0.19	−1.51 ± 0.12	−0.42 ± 0.96	0.97
Hoff.	−0.16 ± 0.63	−0.71 ± 0.15	−0.88 ± 0.39	−0.46 ± 0.08	−0.35 ± 0.19	−1.45 ± 0.12	−0.57 ± 0.96	0.94
Lambat.	−0.14 ± 0.63	−0.6 ± 0.15	−0.68 ± 0.39	−0.17 ± 0.08	−0.48 ± 0.19	−1.5 ± 0.12	−0.47 ± 0.96	0.94
ave. T	9.2	9.9	10.4	9.7	9.7	10.6		

1904–1936 mb: Hoffellsjökull −0.66 ± 0.39, Lambatungnajökull −0.51 ± 0.39.

TCD
8, 4681–4735, 2014

Area, volume and mass changes of southeast Vatnajökull ice cap

Hannesdóttir et al.

Table 5. The scaling exponent γ and coefficient c derived from the best fit line of every year.

year	γ	c
all	1.405	0.038
1890	1.357	0.048
1904	1.387	0.043
1945	1.430	0.034
2002	1.457	0.030
2010	1.391	0.040

TCD
8, 4681–4735, 2014

Area, volume and mass changes of southeast Vatnajökull ice cap

Hannesdóttir et al.

TCD
8, 4681–4735, 2014

Area, volume and mass changes of southeast Vatnajökull ice cap

Hannesdóttir et al.

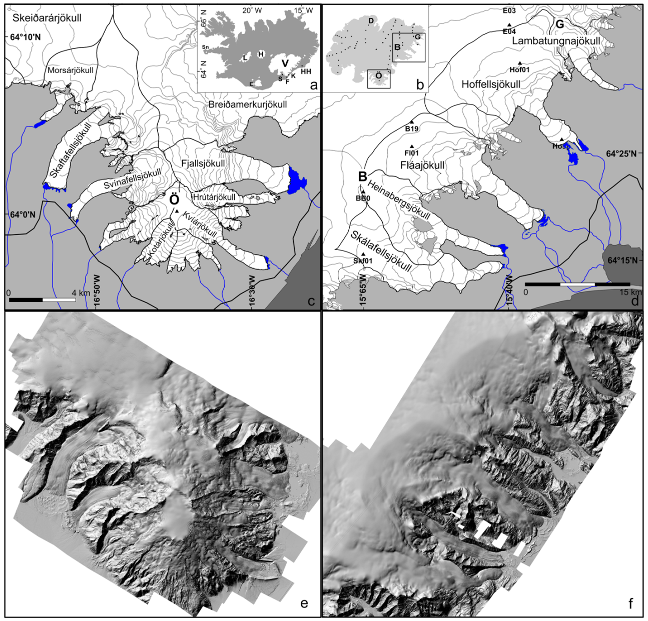

Figure 1. (a) Iceland and Vatnajökull (V) and other ice caps and glaciers mentioned in the text, Hofsjökull (H), Langjökull (L), Eyjafjallajökull (E), and Snæfellsjökull (Sn). Weather stations in Skaftafell (S), Fagurhólsmýri (F), Kvísker (K) and Hólar in Hornafjörður (HH). **(b)** Vatnajökull and mass balance stakes (black dots), the insets show the outline of figures **(c)** the outlet glaciers descending from Öræfajökull ice cap (Ö) and Morsárjökull and **(d)** the outlet glaciers east of Breiðamerkurjökull, descending from the Breiðabunga dome (B), and Goðahnúkar (G), D = Dyngjujökull (mentioned later in the text). The surface topography is from the 2010 LiDAR DEMs, with 100 m contour lines, and ice divides are delineated in black. The location of mass balance measurements is indicated with triangles. Note the different scale of the two figures. Proglacial lakes and rivers are shown in blue and highway 1 in black. (**e** and **f**) Topographic relief shading of the LiDAR DEMs of the same area as in **(a)** and **(b)**. The LIA terminal moraines are clearly visible in front of the glaciers and a number of ice-marginal lakes.

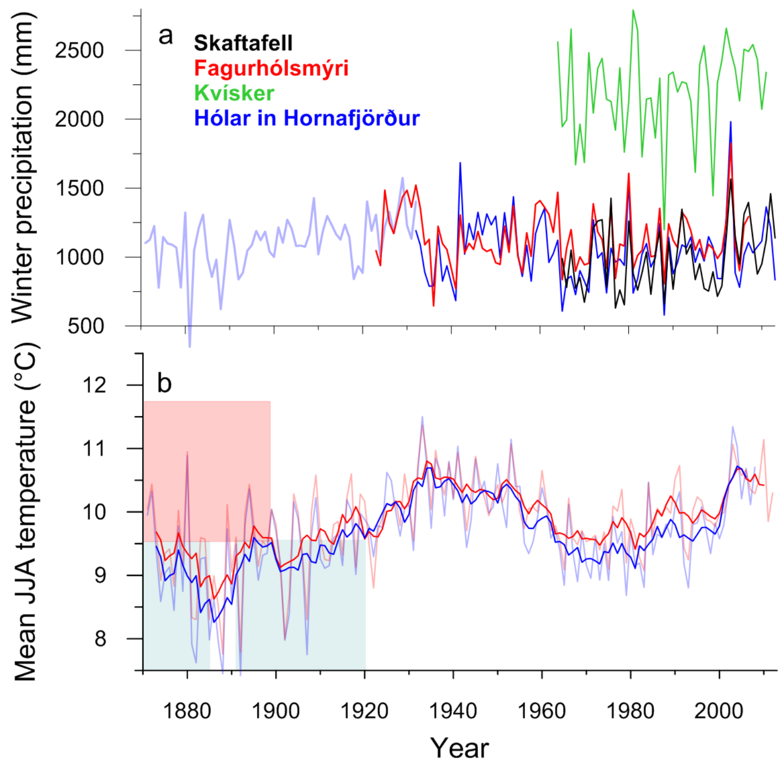

Figure 2. (a) Winter precipitation (October–April in mm) at Skaftafell (black), Fagurhólsmýri (red), Kvísker (green) and Hólar in Hornafjörður (blue), see Fig. 1a for location of stations. Reconstructed precipitation indicated with a light blue line (from Aðalgeirsdóttir et al., 2011). **(b)** Mean summer (JJA) temperature at Fagurhólsmýri (red) and Höfn in Hornafjörður (blue) and 5 years running average. Light blue and light red boxes indicate time period of reconstructed temperature (from Aðalgeirsdóttir et al., 2011).

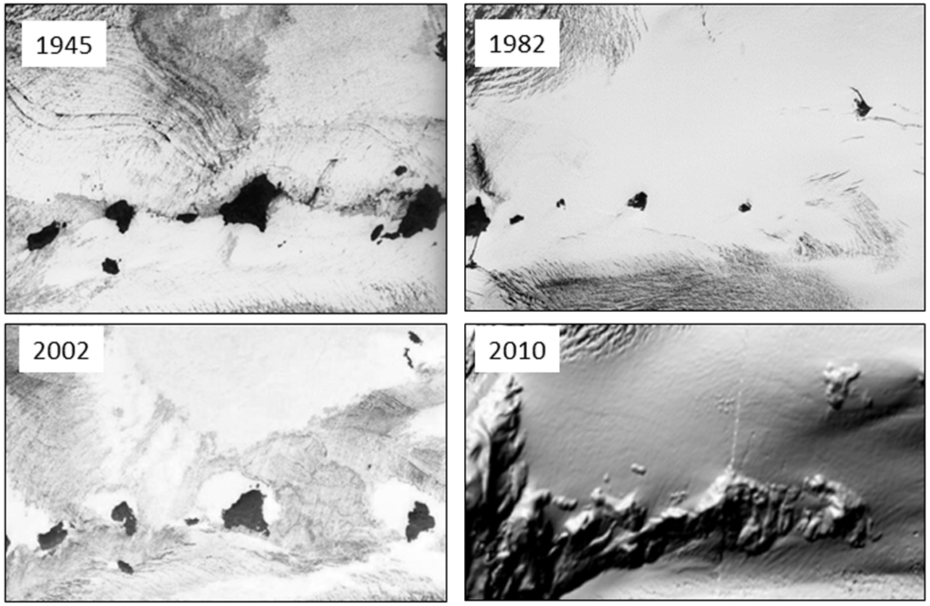

Figure 3. Small nunataks at an elevation of 950–1050 m, east of the mountain “Skerið milli skarða”, which divides the main branch of Skaftafellsjökull (see Fig. 5), at different times. Aerial photograph of National Land Survey of Iceland 1945 and 1982, aerial image of Loftmyndir ehf. from 2002, LiDAR shaded relief map from 2010. Only the largest mid nuntak is visible on the 1904 map (not shown).

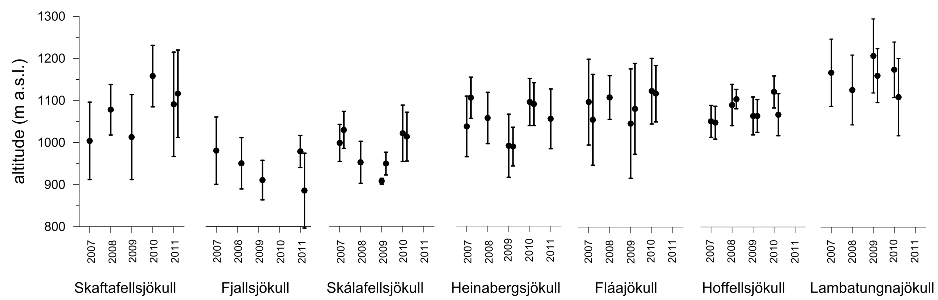

Figure 4. The elevation range (average and standard deviation) of the snowline for each glacier deduced from MODIS images (2007–2011); the elevation obtained from the LiDAR DEM.

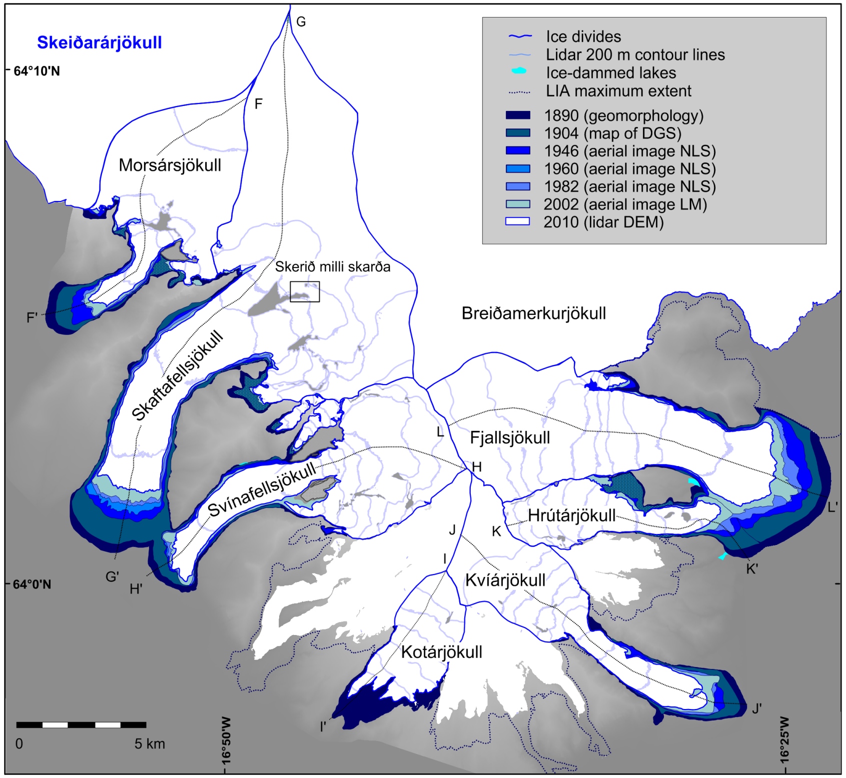

Figure 5. The extent of Öræfajökull's outlet glaciers and Morsárjökull at different times. The surface map is derived from the LiDAR DEM, showing 200 m contour lines. The locations of longitudinal profiles shown in Fig. 8 are indicated with capital letters F-F′, G-G′, etc. The area covering the nunataks east of “Skerið milli skarða”, shown in Fig. 3 is outlined. The ice extent in 1904 is uncertain in the mountains surrounding Morsárjökull and Skaftafellsjökull, due to distorted topography on the old map. DGS = Danish General Staff, NLS = National Land Survey of Iceland, LM = Loftmyndir ehf. The ~ 1890 glacier extent is from Hannesdóttir et al. (2014).

TCD
8, 4681–4735, 2014

Area, volume and mass changes of southeast Vatnajökull ice cap

Hannesdóttir et al.

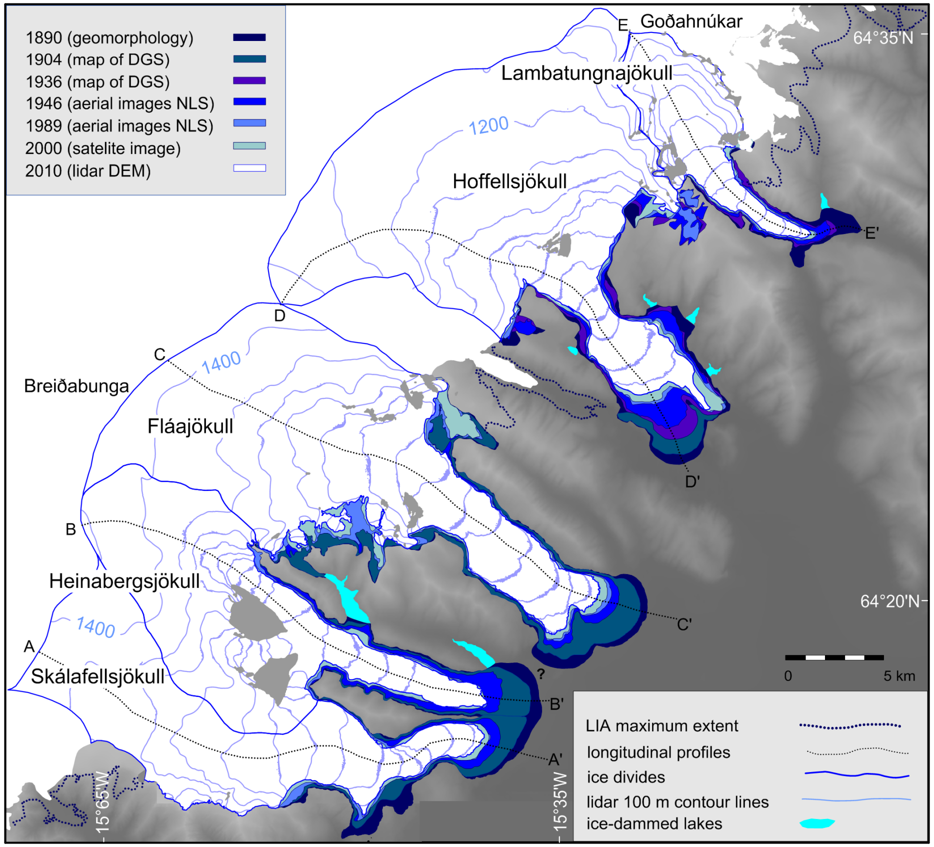

Figure 6. The extent of Skálafellsjökull, Heinabergsjökull, Fláajökull, Hoffellsjökull and Lambatungnajökull at different times. The locations of longitudinal profiles shown in Fig. 8 are indicated with capital letters (A-A′, B-B′ etc.). Surface map is derived from the LiDAR DEM, showing 100 m contour lines. (DGS = Danish General Staff, NLS = National Land Survey of Iceland). The ~ 1890 glacier extent is from Hannesdóttir et al. (2014).

TCD
8, 4681–4735, 2014

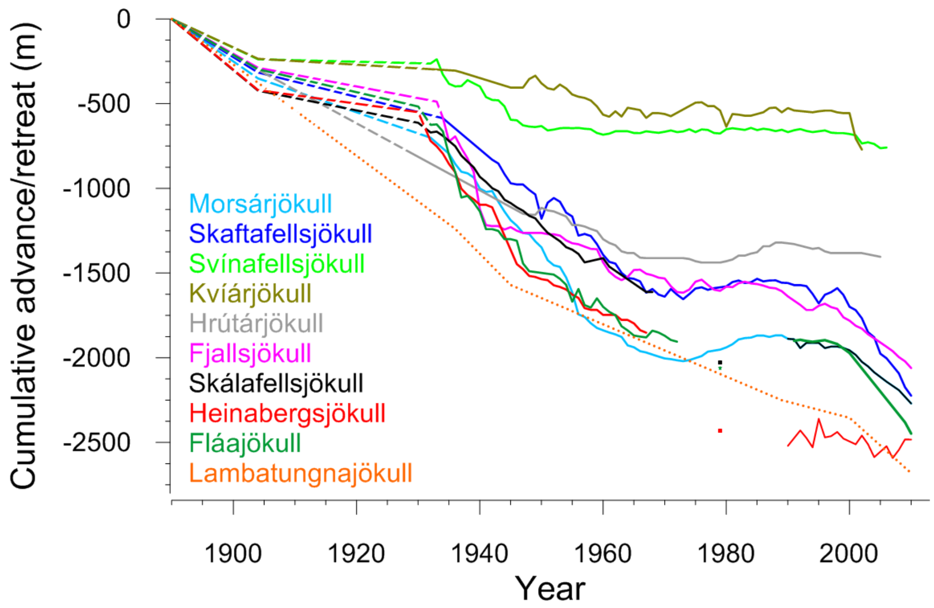

Figure 7. Cumulative frontal variations of the southeast outlet glaciers relative to the ~ 1890 terminus position determined from the terminal LIA moraines (Hannesdóttir et al., 2014). The retreat until 1932, when measurements of volunteers of the Icelandic Glaciological Society started, is indicated by broken lines; the position in 1904 is known from the maps of the Danish General Staff; note that a linear recession is not expected in ~ 1890–1904 or 1904–1932. Annual measurements are shown with an unbroken line (http://spordakost.jorfi.is). Skálafellsjökull, Heinabergsjökull and Fláajökull were not measured in the 1970s and 1980s, but their terminus position in 1979 is determined from aerial images of the National Land Survey of Iceland (indicated by dots). The terminus of Lambatungnajökull (dotted line) has not been measured, but its recession is retrieved from maps, aerial photographs and satellite images.

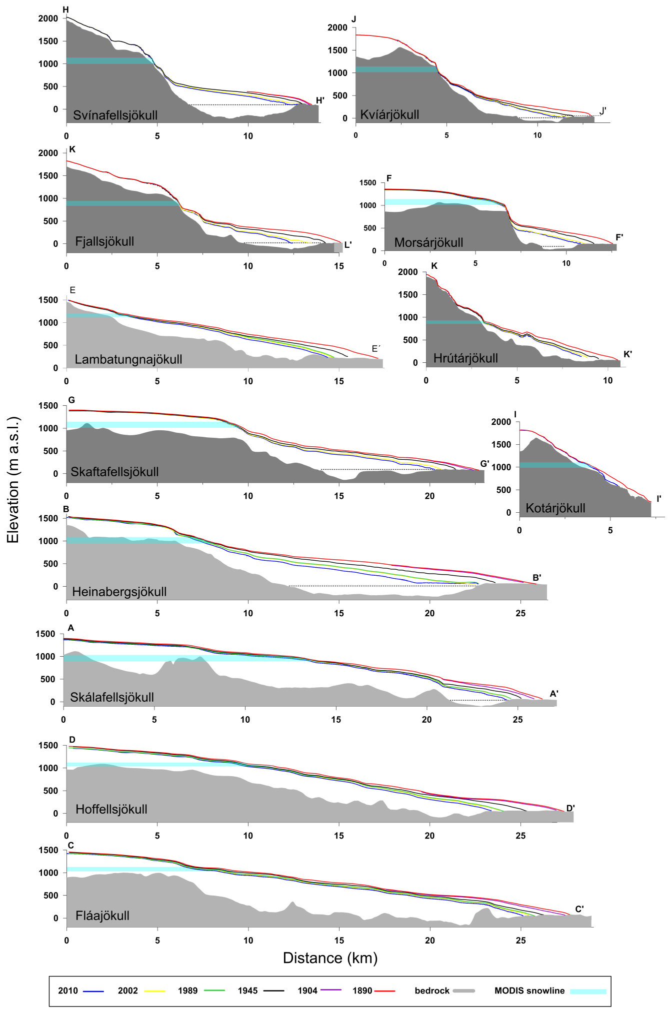

TCD
8, 4681–4735, 2014

Area, volume and mass changes of southeast Vatnajökull ice cap

Hannesdóttir et al.

Figure 8. Longitudinal profiles of the southeast outlet glaciers, showing ice thickness and location of the termini at different times. The average ELA derived from the MODIS images is shown with a light blue horizontal line. Öræfajökull outlets with dark gray colored bedrock and the eastern outlets with light gray colored bedrock.

TCD
8, 4681–4735, 2014

TCD
8, 4681–4735, 2014

Area, volume and mass changes of southeast Vatnajökull ice cap

Hannesdóttir et al.

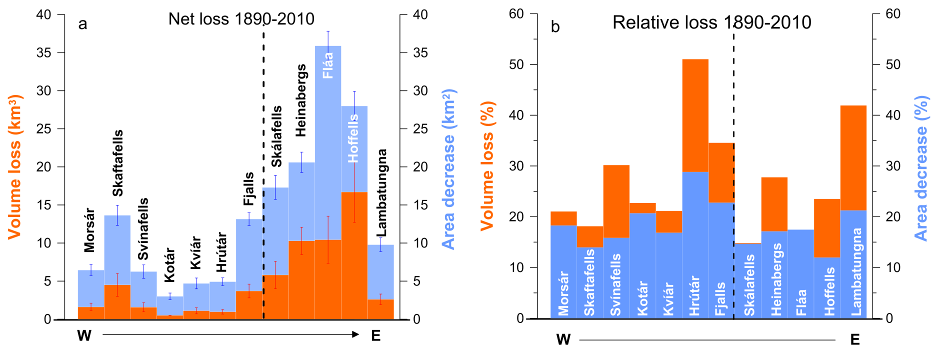

Figure 9. Total area decrease (light blue) and volume loss (orange) during the time period ~1890–2010 **(a)** absolute values, and **(b)** relative to the LIA maximum size. Glaciers represented in geographical order and the dotted line separates the outlets of Öræfajökull and the eastern outlets.

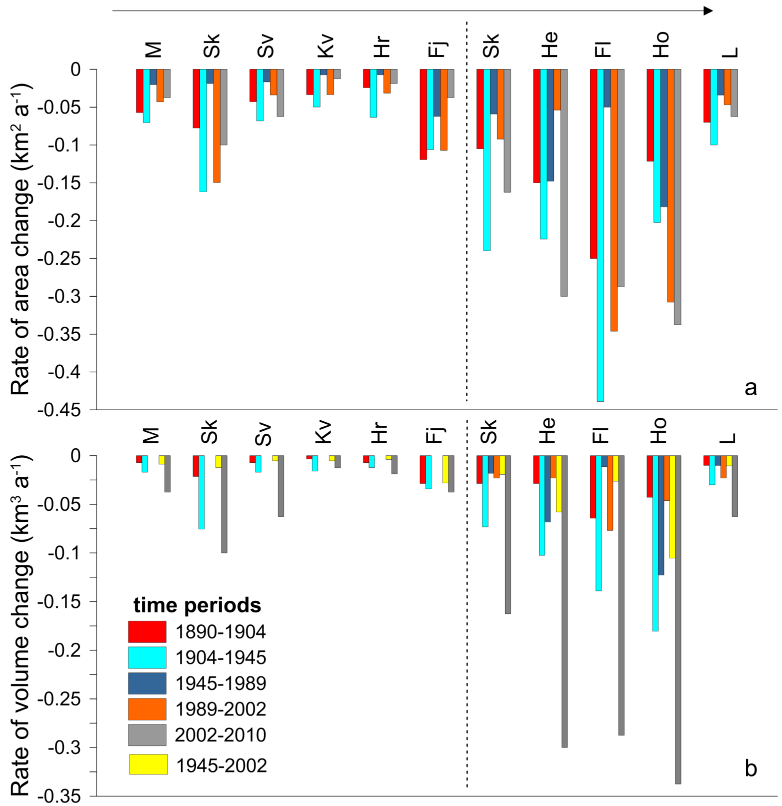

Figure 10. Rate of area **(a)** and volume **(b)** change of the outlet glaciers (from west to east) during different time periods of the last 120 years. The first few letters of each glacier name are shown at the top, glaciers represented in geographical order, from west to east. The dotted line separates the outlets of Öræfajökull and the eastern outlets.

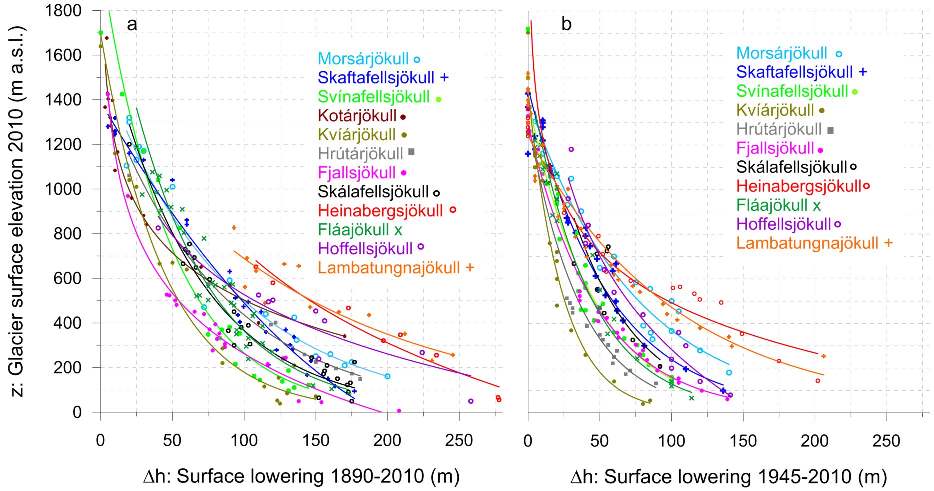

Figure 11. Average surface lowering of every 20 m altitudinal interval of the outlets of southeast Vatnajökull. **(a)** Between ~ 1890 and 2010 (modified from Hannesdóttir et al., 2014). The ~ 1890 glacier surface elevation in the accumulation area is derived from historical photographs, survey elevation points on the 1904 maps and the aerial images of Loftmyndir ehf., and in the ablation area it is mainly deduced from glacial geomorphological features. **(b)** Between 1945 and 2010. The glacier surface lowering in the accumulation area is based on comparison of the size of nunataks as observed on the original aerial images of 1945 and the LiDAR DEMs. No 1945 DEM is available for Kotárjökull.

TCD
8, 4681–4735, 2014

Area, volume and mass changes of southeast Vatnajökull ice cap

Hannesdóttir et al.

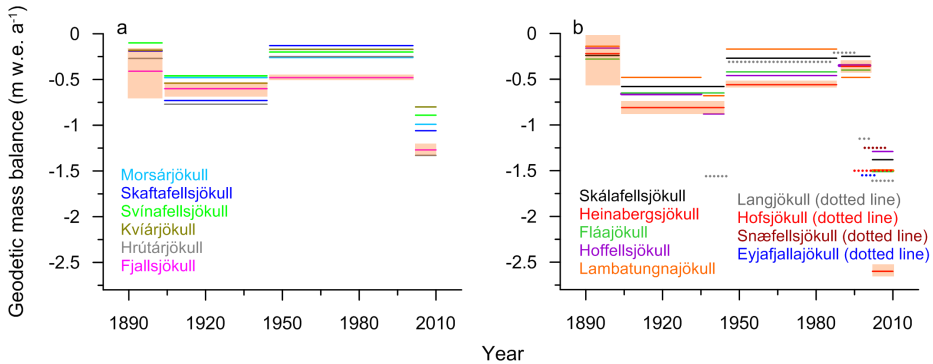

Figure 12. Geodetic mass balance rates during different time periods of the last 120 years. **(a)** The outlet glaciers of Öræfajökull and Morsárjökull. **(b)** The eastern outlet glaciers. For comparison, the geodetic mass balance of Langjökull (Pálsson et al., 2012), Eyjafjallajökull 1998–2004 (Guðmundsson et al., 2011), Snæfellsjökull 1999–2008 (Jóhannesson et al., 2011), and Hofsjökull 1995–2010 (Jóhannesson et al., 2013) is presented with dotted lines in **(b)**. The two latest time periods of Langjökull (1997–2002 and 2002–2010) are based on surface mass balance measurements (data base Glaciological group Institute of Earth Sciences, University of Iceland). For error estimates of the geodetic mass balance see Table 4, only the error bars for Fjallsjökull and Heinabergsjökull are shown here.

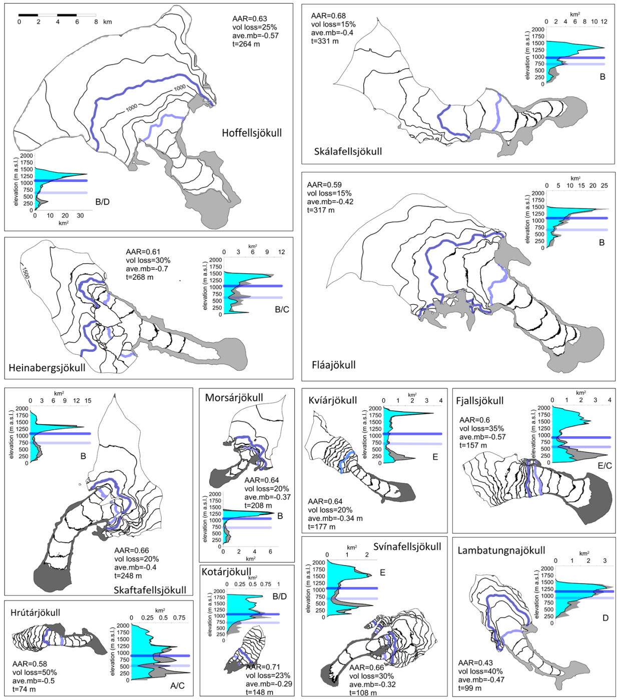

Figure 13. The topography of the outlet glaciers in 2010 with 100 m contour lines of the LiDAR DEM. The ~ 1890 areal extent is shown in dark gray for the Öræfajökull outlets and in light gray for the eastern outlets. The average MODIS-derived ELA (2007–2011) is drawn in dark blue on the map, and the inferred ELA of the maximum LIA in light blue (Hannesdóttir et al., 2014). Inset graphs show the 2010 area-altitude distribution of the glaciers (hypsometry) in 2010 (cyan) and ~ 1890 (gray), with the average ELA for 2010 and ~ 1890 shown in dark blue and light blue, respectively. The AAR, the relative volume loss of their ~ 1890 size, the average geodetic mass balance ~1890–2010 is shown in m w.e. a^{-1}, as well as the average ice thickness (t) in 2010, for every glacier.

TCD
8, 4681–4735, 2014

Area, volume and mass changes of southeast Vatnajökull ice cap

Hannesdóttir et al.

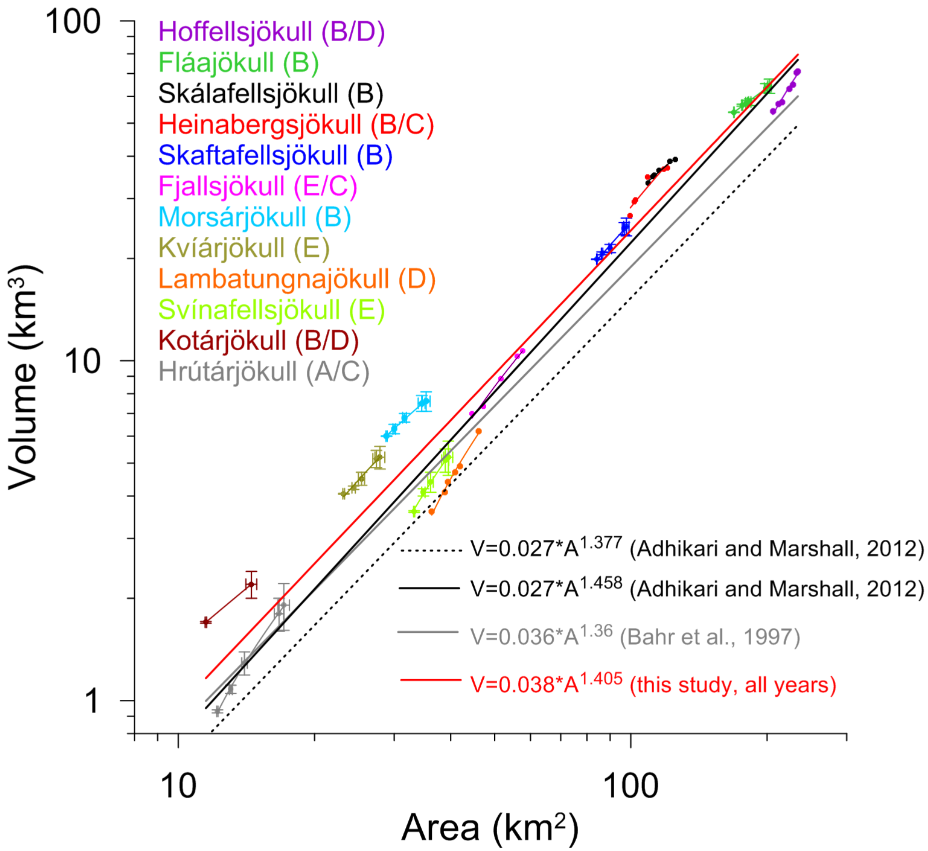

Figure 14. Volume-Area evolution of the individual outlet glaciers at ~ 1890, 1904, 1937, 1945, 1989, 2002, and 2010. The solid red line shows a least-squares fit to all the data points of this study, the solid gray line the corresponding least-squares line derived by Bahr (1997) for 144 glaciers, the solid black line the least-squares line dervied by Adhikari and Marshall (2012) for synthetic glaciers in steady state, and the dashed black line for the same glaciers after 100 years of retreat.

TCD
8, 4681–4735, 2014

Paper IV

Hannesdóttir, H., Aðalgeirsdóttir, G., Jóhannesson, T., Guðmundsson, Sv., Crochet, P., Ágústsson, H., Pálsson, F., Magnússon, E., Sigurðsson, S.Þ., Björnsson, H. Mass balance modelling and simulation of the evolution of the outlets of SE-Vatnajökull ice cap, Iceland, using downscaled orographic precipitation.

To be submitted .

To be submitted

Mass balance modelling and simulation of the evolution of the outlets of SE-Vatnajökull ice cap, Iceland, using downscaled orographic precipitation

Hrafnhildur HANNESDÓTTIR[1], Guðfinna AÐALGEIRSDÓTTIR [1], Tómas JÓHANNESSON [2], Sverrir GUÐMUNDSSON [1], Philippe CROCHET [2], Hálfdán ÁGÚSTSSON [2,3], Finnur PÁLSSON[1], Eyjólfur MAGNÚSSON [1], Sven Þ. SIGURÐSSON[4], Helgi BJÖRNSSON [1]

1 *Institute of Earth Sciences, University of Iceland, Sturlugata 7, IS-101 Reykjavík, Iceland*
2 *Icelandic Meteorological Office, Bústaðavegi 7-9, IS-150 Reykjavík, Iceland*
3 *Institute for Meteorological Research, Grensásvegi 9, IS-108 Reykjavík, Iceland*
4 *Department of Computer Science, University of Iceland, Dunhaga 5, IS-107 Reykjavík, Iceland*

ABSTRACT

Simulations of the evolution of three outlet glaciers of SE-Vatnajökull, Skálafellsjökull, Heinabergsjökull and Fláajökull, are presented. A coupled Shallow-Ice-Approximation ice flow and degree–day mass balance model is applied, that uses downscaled orographic precipitation on a 1 km grid as input. For the first time downscaled precipitationis used in mass balance modelling of Icelandic glaciers. It is necessary to use high-resolution precipitation fields for the simulations, in order to capture the spatial variations of the winter mass balance, which can not be realistically represented by a precipitation model based on constant horizontal and vertical precipitation gradients. 14 years of in-situ mass balance measurements are used to calibrate the mass balance model, which explains 87% of the variance of the winter balance and 92% of the summer balance. The modelled equilibrium line altitude compares well with the observed snowline at the end of the summer, derived from MODIS images 2007–2010. The sensitivity of each glacier´s annual balance to 1°C warming is –1.51 to –0.97 m w.e. a^{-1} and +0.16 to +0.65 m w.e. a^{-1} for a 10% increase in precipitation, relative to the baseline climate period 1980–2000. Known area and volume changes since the end of the Little Ice Age (LIA) ~1890 to 2010 is used to constrain the model. The observed ice volume at the end of the LIA (15–30% larger than in 2000) is simulated with a 1°C cooling and 20% reduction in the annual precipitation, compared with the baseline period, which is in line with temperature records from the end of the 19th century at nearby lowland stations and estimates of precipitation at that time. Applying a step increase in temperature of 2°C, and precipitation increase of 10%, results in >50% decrease in ice volume and terminus retreat up to 10 km according to our model runs. A warming of 3°C and same precipitation increase would lead to a volume loss of 80–90% or almost disappearance of the outlets.

INTRODUCTION

The climate in Iceland is influenced by the atmospheric circulation of the North Atlantic and the oceanic boundaries defined by the warm Irminger current and the cold East Greenland current (e.g. Einarsson, 1984; Ólafsson and others, 2007). Iceland is located in the northern part of the North Atlantic stormtrack and high amounts of precipitation are delivered to the temperate glaciers in Iceland, which have mass turnover rates on the order of 1.5–3.0 m w.e.

a^{-1} (Björnsson and others, 2013). The mass balance sensitivity of the glaciers and ice caps is in the range of –3.0 to –0.6 m w.e. °C^{-1} (Guðmundsson and others, 2011; Pálsson and others, 2012; Jóhannesson and others, 2013), which is among the highest in the world (De Woul and Hock, 2005). Due to the high spatial variability of the precipitation and relative sparseness and low realiability of precipitation observations, which are mostly confined to lowland areas, numerical atmospheric models, rather than statistical methods, have been used to simulate the spatial and temporal structure of the precipitation fields (Rögnvaldsson and others, 2004, 2007; Crochet and others, 2007 Jóhannesson and others, 2007 and references therein). Undercatch of rain gauges is a known problem, especially during winter (e.g. Sigurðsson, 1990; Crochet, 2007). Thus, estimates of precipitation by observations of snow accumulation and runoff available in the vicinity of the area of interest may be more suitable for estimates on precipitation at high elevation and in complex terrain, than conventional precipitation measurements (e.g. Rögnvaldsson and others, 2004). Precipitation observations from lowland stations can not be reliably extrapolated in complex topography and may not be representative for glaciers and can cause errors in mass balance modelling (e.g. Stahl and others, 2006; Huss and others, 2008). However, it is common practice to extrapolate precipitation from meteorological stations outside the glaciers in most mass balance models (e.g. Andreassen and Oerlemans, 2009; Aðalgeirsdóttir and others, 2011). Mass balance models are of varying complexity, ranging from simple temperature-index models or positive degree-day (PDD) models (e.g. Laumann and Reeh, 1993; Jóhannesson and others, 1995; Braithwaite and Zhang, 2000) to surface energy-balance models (e.g. Hock 2005 and references therein). A number of studies have used data from distant weather stations to produce precipitation grids for the glaciers (e.g. Auer and others, 2007; Huss and others, 2012; Marzeion and others, 2012; Engelhardt and others, 2013; Radic and others, 2014) or use data from atmospheric models providing input for mass balance modelling (e.g. Rasmussen, 2007; Machguth and others, 2009; Paul and Kotlarski, 2010; Andreassen and others, 2012; Jarosch and others, 2012; van Pelt and others, 2012).

Ice dynamical models are based on Stokes equations or approximations; from zeroth order Shallow Ice Approximation (SIA) to higher order models where the flow equations are fully considered, including the longitudinal stress gradients (e.g. Hindmarsh, 2004; LeMeur and others, 2004). A number of comparative studies indicate that numerical models of reduced complexity and full system models, give similar length and volume changes for valley glaciers (Leysinger-Vieli and Guðmundsson, 2004; Oerlemans, 2008; Lüthi, 2009). Numerical ice-flow models simulating the larger ice caps in Iceland and their response to changes in mass balance have been developed in recent years (Aðalgeirsdóttir and others, 2004; Flowers and others, 2005; Marshall and others, 2005). A vertically integrated SIA ice-flow model coupled with a PDD surface mass balance model (Jóhannesson, 1997; Jóhannesson and others, 1995) has been used to simulate the evolution of ice caps in Iceland (Aðalgeirsdóttir and others 2004, 2006; Jóhannesson and others, 2007; Guðmundsson and others, 2009a). Air temperature measured outside the glaciers represents variations in the incoming radiation flux (better than the dampened temperature of the boundary layer above the melting glacier surface), and thus can the ablation of the glaciers be described with PDD models (e.g., Guðmundsson and others, 2009b). Furthermore, simulations for the period 1600–2300 indicate that air temperature is the dominant control on the volume and area evolution of Vatnajökull (Marshall and others, 2005). The variations of the outlet glacier Hoffellsjökull (Fig. 1) during whole post-Little Ice Age (LIA) period ~1890-2010 were simulated with the same coupled model (except that it used the finite element method for solving the equations, rather than finite difference) allowing variable spatial resolution (Aðalgeirsdóttir and others, 2011). The coupled model successfully reproduced the timing and magnitude of ice volume changes in this period.

In this paper we use the PDD mass balance model coupled with the vertically integrated SIA ice flow model, solved with the finite element method, to simulate the evolution of three outlet glaciers of SE-Vatnajökull and their sensitivity to climate change. The first part of the paper describes how three different datasets were used to simulate the mass balance in the coupled model runs as input for the PDD model; (1) precipitation model based on constant vertical and horizontal precipitation gradients, using data from meteorological stations outside the glacier (as has been used in previous modelling studies on Icelandic glaciers), (2) constant winter mass balance grid (manually interpolated from in situ balance measurements) revised with downscaled precipitation data from a numerical atmospheric model (Skamarock and others, 2008), (3) downscaled orographic precipitation from a linear model which simulates physical precipitation processes (Crochet and others, 2007). In the second part of the paper a series of model simulations, using the downscaled precipitation data from the linear model, with step changes in precipitation and temperature, are described. The simulations were carried out to assess the sensitivity of the modelled glaciers to perturbations in the climate. Observations of area and volume changes since the LIA maximum around 1890 until 2010 are available for the outlet glaciers of SE-Vatnajökull (Hannesdóttir and others, 2014a), and provide validation data for the model simulations. We simulate the LIA maximum glacier geometry and the evolution of the glaciers during time period when distributed precipitation data are available (1959-2010).

STUDY AREA

The three outlet glaciers of SE-Vatnajökull are located in one of the warmest and wettest area of Iceland (e.g. Ólafsson and others, 2007). These non-surging outlets are 300 m thick on average, descend from the 1500 m high plateau of the Breiðabunga dome towards the lowlands, and their termini are at an elevation of 30–60 m a.s.l. (Fig. 1 and Table 1). The outlet glaciers are 23-25 km long and have an average slope of 3–4°. They range in area from 100 to 170 km^2 and have a volume of 30–55 km^3 (Table 1). The ice divides are derived from LiDAR DEMs surveyed in 2010 and 2011 (Icelandic Meteorological Office and Institute of Earth Sciences, 2013). The snowline at the end of summer, which is used as a proxy for the equilibrium line altitude (ELA), has been derived from a series of MODIS images during the period 2007–2011 (Hannesdóttir and others, 2014a), and is in the range of 900-11000 m on the three outlets. (Table 1). The present day accumulation area ratio (AAR) of the glaciers is determined from the MODIS derived snowline and the 2010 area (Table 1). Proglacial lakes formed in front of the outlet glaciers around the middle of the 20th century (detected on aerial images from the database of the National Land Survey of Iceland, www.lmi.is/loftmyndasafn-2). Skálafellsjökull has a long and narrow accumulation area, and funnels down an ice fall, where the elevation drops by 200 m over a distance of 1 km. A small proglacial lake was formed in the 1960s and has remained of similar size throughout the period. Heinabergsjökull is divided into three branches by two mountains, Snjófjall and Litla-Fell (Fig. 1), and has a long and flat ablation area. The glacier terminates in a proglacial lake, that was formed in the 1940s and has increased in size since then. The glacier tongue broke up in the autumn of 2013 and the terminus shortened by 1 km (Sigurðsson, 2014). Fláajökull has a wide accumulation area and a gently sloping 4 km wide tongue that terminates in a lake that formed during or prior to the 1940s.

DATA

Bedrock topography

The three outlet glaciers were surveyed with a radio echo sounder (RES) and Differential Global Positioning System (DGPS) equipment in the period 2000–2005 (for details of the method see e.g. Magnússon and others, 2012). Point measurements were carried out in the ablation area, whereas continuous profiles were surveyed in the accumulation area (Fig. 2a). The vertical accuracy of the bedrock measurements is 5–20 m, depending on the location. The glaciers have excavated deep troughs that reach below sea level into glacial and glacio-fluvial sediments. A small depression below the terminus of Skálafellsjökull reaches 100 m below sea level. Heinabergsjökull has excavated a 10 km long trench, which underlies the majority of its ablation area, reaching maximum depths of 220 m below sea level. The bedrock of Fláajökull is 200 m below sea level in the ablation area (Fig. 2a). In some areas the RES lines are spaced some km apart (Fig. 2a), and the bedrock topography may be inaccurately estimated, which may affect the accuracy of the ice flow model. Previous model simulations on the neighbouring Hoffellsjökull show that, using a filled trench or the current bedrock topography, had negligible effects on the simulations (Aðalgeirsdóttir and others, 2011). We thus use the measured bedrock DEM (unfilled trench) in all model runs.

Glacier area and volume changes 1890-2010

The evolution of area and volume of the three outlet glaciers 1890–2010 (Fig. 2b and Table 2) has been derived from a multi-temporal glacier inventory. DEMs of 1890 were created from glacial geomorphological features and historical data from the time of the LIA maximum (Hannesdóttir and others, 2014b), whereas DEMs from 1904, 1945, 1989, 2002 and 2010, were generated from maps, aerial images, DGPS-surveys, and a LiDAR survey (Hannesdóttir and others, 2014a). The most accurate DEMs were produced with airborne LiDAR technology in late August–September of 2010 and 2011 (Icelandic Meteorological Office and the Institute of Earth Sciences, 2013), with a 5 m × 5 m horizontal resolution and a vertical and horizontal accuracy of <0.5 m (Jóhannesson and others, 2013). The glaciers started retreating from their terminal LIA moraines after 1890, and retreated during most of the 20th century. The retreat accelerated in the 1930s and slowed down after the 1940s following cooler summers. The glaciers halted or advanced slightly in the 1960s to 1980s due to colder temperatures, but the retreat accelerated again after ~2000. During the first decade of the 21st century, the glaciers experienced the highest rate of mass loss in the post-LIA period (Hannesdóttir and others, 2014a).

Mass balance observations

Mass balance measurements have been carried out on Vatnajökull since 1991, and today the network consists of ~60 stakes (Björnsson and Pálsson, 2008). The net annual balance has been negative after 1995, and the ice cap has lost on average 1 m w.e. a^{-1} since then (Björnsson and others, 2013). The majority of the stakes are located on the northern and western part of the ice cap, but six stakes are on a profile from the terminus up to the ice divide on Breiðamerkurjökull and a few survey sites are located in the accumulation area of the studied glaciers (Fig. 1, Björnsson and Pálsson, 2008). Three stakes are measured on Hoffellsjökull, at the ice divide, around the ELA and in the ablation area (Aðalgeirsdóttir and others, 2011). The elevation dependency of mass balance of SE-Vatnajökull is shown in Fig. 3a. Ablation of up to 9 m w.e. a^{-1} is observed during summers on Breiðamerkurjökull and Hoffellsjökull, and negative winter balances at the terminus (Björnsson and Pálsson, 2008).

Two new stakes were added to the mass balance survey network in 2009 in the accumulation area of Skálafellsjökull and Fláajökull. Digital mass balance maps, for every year since 1996, have been manually interpolated (for method details see e.g. Björnsson and others, 2002), using the in situ mass balance measurements and the observed mass balance gradient on SE-Vatnajökull (Fig. 3a). The resulting maps are integrated over the whole glacier area to calculate the mean specific mass balance shown in Fig. 3b for the three outlets of this study.

Temperature and precipitation data from meteorological stations

Long temperature and precipitation records are available from two lowland meteorological stations south of Vatnajökull (Fig. 1), at Fagurhólsmýri (16 m a.s.l., 8 km south of Öræfajökull) and Hólar in Hornafjörður (16 m a.s.l., 15 km south of Hoffellsjökull). The temperature record at Hólar is available for the period 1884–1890 and since 1921 (Fig. 4), whereas precipitation measurements started in 1931. The temperature record from Fagurhólsmýri goes back to 1898, and precipitation has been measured since 1921 and until 2008 (Fig. 4). Temperature records from other stations around the country were used to extend the local records back to 1860 and fill in gaps by an iterative expectation maximization algorithm (described in Aðalgeirsdóttir and others, 2011). To extend the precipitation record of Fagurhólsmýri back to 1860, Aðalgeirsdóttir and others (2011) applied a linear regression between the monthly values of temperature (Hólar) and precipitation (Fagurhólsmýri) and tuned with the available precipitation record. The mean summer temperature during the time period 1980–2000 was 9.6 °C, when the mass balance of most glaciers in Iceland was close to zero (Sigurðsson, 2005; Aðalgeirsdóttir and others, 2006; Guðmundsson and others, 2009a, 2011) compared to 8.5°C in 1884–1890 (Table 3). The average climate of the period 1980–2000 is used as a reference climate for the model simulations in this study.

DOWNSCALED PRECIPITATION DATA

Two different downscaled precipitation datasets are available for Iceland and used in this study. Based on data from the RÁV project (Rögnvaldsson and others, 2011), dynamically downscaled precipitation in Iceland is available on a 3 km grid since 1995 and 9 km resolution from 1958, and with a 3 hour temporal resolution. The atmospheric data was produced with the state-of-the-art non-hydrostatic atmospheric model WRF (Weather Research Forecasting, Skamarock and others, 2008). The model takes full account of atmospheric physics and dynamics, with atmospheric moisture and precipitation proceesses parameterized with the scheme of Thompson and others (2004). The high-resolution is needed to adequately simulate the flow in the complex topography of Iceland. The model is forced by atmospheric analyses from the European Centre for Medium Range Weather Forecasts (ECMWF). The model has been extensively used for atmospheric research in Iceland, and the performance in simulating the precipitation on the Mýrdalsjökull ice cap in S-Iceland is good (Ágústsson and others, 2013).

A linear theory (LT) model of orographic precipitation (Smith, 2003), which includes airflow dynamics, condensed water advection, and downslope evaporation was used to create 1 km resolution precipitation dataset for Iceland for the time period 1958–2006 (Crochet and others, 2007). The model was revised during the Climate and Energy Systems project (Jóhannesson and others, 2007). The model is similarly driven by coarse-resolution 40 year reanalysis data from ECMWF until 2001 and from 2002, using available ECMWF analysis. The simulated precipitation is in good agreement with precipitation observations accumulated over various time scales (from wind-loss corrected rain gauge data and glacier mass balance measurements), both in terms of magnitude and distribution. The results suggest that the model captures the main physical processes governing orographic generation of precipitation in the mountains of Iceland (Crochet and others, 2007). The model allows simulations of the distribution of snow accumulation on glaciers in more detail than has been possible in previous glacier mass balance studies in Iceland (Crochet and others, 2007). A new daily precipitation dataset for the time period 2007–2010 was made by combining rain gauge data and monthly climatic precipitation maps derived from the LT-model (Crochet and others, 2007; Jóhannesson and others, 2007) through anomaly interpolation (Crochet, 2013). The rain gauge network used in the construction of the daily precipitation maps is composed of manual and automatic stations. The data have been quality controlled and corrected to account for measurement errors such as due to wind-loss, wetting and evaporation. For the sake of simplicity, this dataset will also be referred to as the downscaled orographic precipitation from the LT model (LT-DP).

MODELS

The mass balance model

The mass balance model used in this study is a PDD (temperature index) model that has been developed for temperate glaciers (called MBT-model) in Iceland and the Nordic countries (Jóhannesson and others, 1995; Jóhannesson 1997) and has previously been used in several glaciological studies in Iceland (Aðalgeirsdóttir and others, 2006, 2011; Jóhannesson and others, 2007; Guðmundsson and others, 2009a). Glacier accumulation and ablation are computed from daily precipitation and temperature values from meteorological stations outside the glacier or distributed fields of daily temperature and precipitation. Melting of snow and ice is computed from the number of PDD, using different degree–day factors (amount of melting per PDD) for snow and ice and a constant snow/rain threshold (1°C) is applied (Jóhannesson, 1997). Previously, constant horizontal and vertical precipitation gradients have been used to represent spatial precipitation variations when forced with data from meteorological stations away from the glaciers.

The in situ mass balance data from SE-Vatnajökull were used to calibrate the mass balance model using the LT-DP (Fig. 5). The precipitation model extends to 2010, and mass balance measurements started in 1996, resulting in a 14 year long calibration period. The new mass balance stakes on the southern slopes of Breiðabunga (Skf01 and Fl01, Fig. 1) were not used in the calibration of the mass balance model, since the data from the LT model is only available until 2010. The mass balance model calculates the mass balance for each day, but the model output is defined for summer (May 1–September 30), winter (October 1–April 30) and annual balance for every balance year.

The modelled winter mass balance is overestimated at BB0 on average by 0.8 m (compared to in situ measurements), whereas the winter mass balance on other stakes in the accumulation area is better represented by the model, on average 0.1–0.4 m higher (Fig. 5). This may be due to snowdrift at the highest survey points, which is not taken into account in the mass balance model. The model generally underestimates the winter balance at stakes in the ablation area, on average by 1.5 m at Hosp for example. This difference would be even greater if the LT-model would account for surface lowering that has occurred during the 14 year long calibration period, which is as high as 70 m for stakes at the lowest elevation. The degree–day scaling factors for snow (ddf_s) and ice (ddf_i), are determined by minimizing the root mean square (RMS) between measured and modelled mass balance. The ddf_s is derived from 7 points in the accumulation area, whereas the ddf_i from 6 points in the ablation area (Fig. 1). The best fit (lowest RMS value) was found when using ddf_s =3.7 mm w.e. °C^{-1} d^{-1}, and ddf_i =5.5 mm w.e. °C^{-1} d^{-1} (Table 4). This is in the range of previously estimated degree–

day factors from studies on Langjökull and Vatnajökull (Guðmundsson and others, 2003; Flowers and others, 2007; Jóhannesson and others, 2007; Aðalgeirsdóttir and others, 2011). The mass balance model explains 87% of the variance of the winter balance and 92% of the variance of the summer balance in the period 1996–2010 (Fig. 6).

The ice flow model

The ice flow model used in this study is based on the SIA and vertically integrated continuity equation, neglecting longitudinal stress gradients, bed isostatic adjustments and seasonal variations in sliding (e.g. Aðalgeirsdóttir, 2003; Aðalgeirsdóttir and others, 2006). Glen's flow law with an exponent n=3 is assumed as a constitutive equation for ice (Cuffey and Paterson, 2010). In terms of numerical implementation, this version of the model uses the finite element method with triangular elements, and has previously been applied to simulate the evolution of Hoffellsjökull (Aðalgeirsdóttir and others, 2011). Comparison of the modelled velocity and SPOT derived surface velocity on Hoffellsjökull, indicated that the model captures the large-scale flow pattern (Aðalgeirsdóttir and others, 2011). The average slope of the studied outlet glaciers is in the range of 3–4° and the aspect ratio (typical thickness to characteristic length for the ice body) is on the order of 10^{-3}, which is acceptable for application of the SIA method (e.g. Aðalgeirsdóttir and others, 2000; LeMeur and others, 2004).

Several values for the rate factor (A) are applied to select one that best simulates the observed glacier geometry. In previous studies (Aðalgeirsdóttir and others, 2006; Guðmundsson and others, 2009a) the rate factor was 6.8×10^{-15} s^{-1} kPa^{-3}, and in the more recent study of Aðalgeirsdóttir and others (2011), the rate factor $A=4.6\times10^{-15}$ s^{-1} kPa^{-3} was determined from a series of model runs for Hoffellsjökull to best fit the observed velocity field. Based on the results of several ice flow model studies, the recommendation of the rate factor for temperate ice is $A=2.4\times10^{-15}$ s^{-1} kPa^{-3} (Cuffey and Paterson, 2010). Model runs that include explicit basal sliding were made, applying a Weertman type sliding law (Paterson, 1994); where the sliding velocity (V_s) is assumed to be proportional to the basal shear stress, τ_b, to a power of m ($V_s=C\times\tau_b^m$). C is the sliding parameter and the exponent m is assumed equal to 3 in our model runs. We do not have data to determine the relative contributions of deformation and sliding velocities to the glacier flow. The horizontal resolution of the input files (bedrock and surface topography, mass balance data) is 200 m , and similarly the size of the triangular elements of the model mesh is ~200 m. The ice divides are kept at a fixed location in the model and no flow occurs across them, and thus we ignore that ice divides can shift due to mass balance changes. The ice flow model is run both coupled and uncoupled with the mass balance model using LT-DP in the time-dependent simulations. When coupled, the changing glacier surface elevation is updated each year, which affects the calculated mass balance, whereas in uncoupled runs the mass balance is computed on the same topography throughout.

I. SIMULATIONS WITH VARIABLE MASS BALANCE

In this section we describe the different model results emerging from using constant precipitation gradients in the mass balance model, an average winter mass balance grid based on in situ measurements revised with precipitation from the WRF-model, and using LT-DP as input for the mass balance model. In all the simulations constant temperature and precipitation forcing is applied, using the averages of the baseline period 1980–2000. The model simulation all start with a smoothed measured 2000 glacier surface DEM (obtained by running the model for 2 years), and use a rate factor of $A=4.6\times10^{-15}$ s^{-1} kPa^{-3}.

Constant precipitation gradients and new stake data

A simulation with the mass balance-ice flow model was carried out using constant horizontal and vertical precipitation gradients; 0.5 per 100 m in vertical, 0.0005 and -0.0008 per 100 m in horizontal east and north direction, respectively. Temperature at Hólar in Hornafjörður and precipitation at Fagurhólsmýri was used to force the mass balance model, with the same degree–day factors for snow and ice as in previous studies on S-Vatnajökull (Aðalgeirsdóttir and others, 2006). These simulations revealed a surface lowering in the accumulation area of >90 m and a volume reduction of 20–30% between the start and end of the simulation (Fig. 7a and Table 5). The results indicate that the mass balance is underestimated in the accumulation area of the glaciers.

Experience from fieldwork led us to suspect that winter accumulation on the southern slopes of Breiðabunga is higher than on the ice divide as measured at BB0 and B19 (Fig. 8a). Two new stakes (Sk01 and Fl01, Fig. 8b), were therefore added to the mass balance network in the fall of 2009 located south of the ice divide, which confirmed this. Measurements from 4 years at the new stakes show that higher winter balance values are found south of the ice divide, than at BB0 and B19, and the values are around 1 m higher than previously estimated with the manual interpolation of the in-situ mass balance data at this location (Fig. 8b). It is clear that the 2 stakes on the ice divides (BB0 and B19) do not adequately represent the winter mass balance variance of the studied outlets (Fig. 8a).

Winter mass balance map from in situ measurements revised with downscaled precipitation from the WRF-model

In order to explore the possible deficit of the winter mass balance in the accumulation area of the three glaciers, as found when using the constant precipitation gradient in the mass balance model, two independent modelled precipitation datasets were analyzed; the downscaled winter precipitation fields dervied from the WRF-model and from the the LT-model (Figs. 8c and d). Both datasets indicate that the winter precipitation distribution is more complex in this area than can be accounted for by constant precipitation gradients. The greatest snow accumulation is to the south of the Breiðabunga plateau according to both model results; maximum values are approximately 5.0 m in the WRF modelled winter precipitation (Fig. 8c) and around 3.5 m according in the LT modelled winter precipitation (Fig. 8d).

The manually interpolated winter mass balance maps of the time period 1996–2006 were revised with downscaled precipitation data from the WRF-model, by overlaying the two grids. Summer melting was deduced from the degree–day model, using the average temperature from Hólar in Hornafjörður in the time period 1980–2000. Forcing the model with the interpolated mass balance maps lead to an improvement of the simulated glacier geometry. Less surface lowering occurred in the accumulation area and the glaciers reached equilibrium without loosing the same ice volume as forcing it with the constant precipitation gradients (Figs. 7a and b, Table 5). The outlets advanced beyond the 2000 margin (Fig. 7b), resulting in a 5–14% increase in area (Table 5).

LT-DP and tuning of the rate factor

To create mass balance grids to force the ice flow model with, we first ran the mass balance model with the LT-DP for every year, which produced 1x1 km mass balance grids and averaged over the 20 year baseline period. They were interpolated on to a grid size of 200 m resolution, to match the resolution of the flow model. In Figure 7c the elevation difference between the start and end of the simulation is shown. The surface lowering in the accumulation area is similar as when using the revised mass balance maps with WRF data, but thickening in the ablation area is less (Figs. 7b and c). The volume loss is on the order of 2–12%, and the simulated areal extent is slightly larger than the observed area (Fig. 7c and Table 5). In view of the good agreement between observed and simulated glacier geometry a series of simulations with various rate factors and adding explicit sliding were carried out (see Table 5). The best fit is obtained with a rate factor of $A=2.4\times10^{-15}$ s^{-1} kPa^{-3}, representing stiffer ice (Fig. 7d). The glaciers undergo less surface lowering in the accumulation area than in earlier simulations (Figs. 7a–c), and the modelled volume and area are closer to the observations, the difference being within 3% (Table 5). Adding sliding ($C=10\times10^{-15}$ ma^{-1} Pa^{-3}) gives the same results as having softer ice ($A=4.6\times10^{-15}$ s^{-1} kPa^{-3}) (Table 5).

Summary of simulations using various precipitation data for the mass balance model

A further comparison of the simulations described above is shown in Figure 9, where longitudinal surface profiles from the ice divide to the terminus are shown, and compared with a number of observed surface profiles. The substantial lowering of the glacier surface using constant precipitation gradients in the mass balance model is evident on the modelled surface profiles on all three outlets. The simulations using the revised winter mass balance map with precipitation from the WRF-model indicate an overestimation of the winter mass balance, as all three outlets advance ~1 km beyond the observed margin, and thickenin the ablation zone by up to 100 m Fig. 7b). Simulations using the LT-DP show a good fit with the observed surface profiles (Fig. 9). An average thickening of 100 m in the accumulation area of Fláajökull occurs in all simulations (see Figs. 7a–d). As the RES survey lines in the eastern accumulation area of Fláajökull are further apart than in other areas, the lack of details in the bedrock topography may be the cause for this arbitrary thickening in the simulations (Figs. 7a–d).

In Figures 10a and b, the modelled winter mass balance and the manually interpolated winter mass balance map, based on the in situ measurements (including the new stakes), are shown, respectively. There is good agreement between the two maps, both showing the highest winter mass balance values south of the ice divide in the upper parts of the accumulation area of Skálafellsjökull. The modelled and measured specific winter balance is given for each outlet on the figures, showing comparable values. The mass balance model was not able to reproduce the abnormally low summer balance of 2010 (see Fig. 3b), which was affected by the tephra from the Eyjafjallajökull eruption deposited on the ice cap (Guðmundsson and others, 2012) and caused increased radiative forcing and glacier melt (see e.g. Björnsson and others, 2013). For further validation of the mass balance model using the LT-DP, the end of the summer snowline, which is used as a proxy for the ELA, derived from a set of MODIS images from 2007 to 2010 (from Hannesdóttir and others, 2014a), is plotted on the modelled net mass balance maps in Figures 10 c–f. The location of the MODIS snowline agrees well the modelled ELA in all four years, providing further validation of the results of the mass balance model using the LT-DP.

II. SIMULATIONS WITH LT-DP

Step changes in temperature and precipitation

Steady state experiments were performed to analyze the sensitivity of the model to step changes in temperature and precipitation. In reality, glaciers are constantly responding to climate variations and are never in a steady state, but such simulations provide insight to the sensitivity of glaciers to climate changes. All simulations start with a geometry that has been run into a steady state. A series of simulations with step changes in temperature and/or precipitation relative to the baseline period 1980–2000 were carried out (Table 6). Each model simulation is forced with constant mass balance grids, that were produced by the mass balance model, interpolated to a 200 m horizontal resolution and the average of the 20 years calculated. The applied step changes in temperature are in the range of the observed temperature difference since the late 19th century until 2010 observed at Hólar in Hornafjörður (Table 3), and possible future climate scenarios. Figure 11 shows that the modelled glaciers respond to step changes in precipitation and temperature by increasing or decreasing their volume and extent. The mass balance sensitivity to a 1°C temperature decrease is in line with a 40% increase in annual precipitation (Table 6). The mass balance sensitivity to +1°C is –1.51 to –0.97 m w.e. a^{-1}, similar to a 40% decrease in annual precipitation or in the range of –1.29 to –0.86 m w.e. a^{-1} (Table 6), and this forcing leads to a volume loss of up to 40% (Fig. 11).

Simulations were made to assess the sensitivity of the glaciers to possible future temperature and precipitation changes, according to climate change predictions for the 21st century in Iceland (e.g. Jóhannesson and others, 2007; Nawri and Björnsson, 2010). Climate scenarios for Iceland indicate less seasonal temperature variations, and the future warming is projected to be concentrated in the spring and autumn (Jóhannesson and others, 2007). Temperature is predicted to increase at a rate close to 0.3°C per decade until 2050, and 0.2°C per decade until 2100, with superimposed decadal variations determined by natural climate variability (Nawri and Björnsson, 2010). Changes in precipitation are projected to be moderate, increase in annual precipitation from 1961–1990 to 2071–2100 is likely to be in the range of 0–10% in most regions (Jóhannesson and others, 2007; Nawri and Björnsson, 2010).
A 2°C warming and a 10% increase in annual precipitation would lead to > 50% volume loss and 8–10 km termini retreat and up to 35% area loss (Fig 12b and Table 6). A temperature increase of 3°C and 10% increase in annual precipitation, could lead to 80–90% volume loss (Table 6 and Fig. 12d). The glaciers undergo similar volume loss if the annual precipitation is unchanged, i.e. kept the same as in 1980–2000 (Table 6).

Simulating the LIA maximum volume

We ran simulations to reproduce the reconstructed LIA maximum glacier geometry and volume of the three outlets (as described in Hannesdóttir and others, 2014b). Temperature measurements, from the late 19th century are available from Hólar in Hornafjörður (Table 3), indicate a 1°C cooling relative to the baseline period. We tried three different precipitation variants (90%, 85%, 80% of the average annual precipitation of 1980–2000) accompanied with the 1°C lower temperature (Fig. 11). The simulation that best resembles the reconstructed LIA glacier geometry was obtained using 20% reduction of annual precipitation, which is in accordance with the precipitation estimates for the time period 1860–1890 (from Aðalgeirsdóttir and others, 2011, see Table 3). A simulation with 1°C decrease and unchanged annual precipitation, relative to the baseline period, resulted in an ice volume that is 20-30% larger than the observed LIA volume (Table 6).

The simulated LIA maximum volume is within the error estimates of the observed volume (Table 2). The simulated LIA areal extent is slightly smaller than the observed, except for Fláajökull. The disagreement between its observed and simulated area can be explained by the small tongues on the west side of Fláajökull, reaching beyond the mapped 1890 glacier margin in the simulations, (Fig. 12a). However the main terminus of Fláajökull is fairly well represented in the simulations (Fig. 12a). The ELA of the simulated LIA glaciers is around 800 m on Skálafellsjökull, 750 m on Heinabergsjökull and 800 m on Fláajökull, which is in good agreement with the estimated LIA ELA, which is based on the elevation of the uppermost lateral moraines (Hannesdóttir and others, 2014b). This is a known method, where lateral moraines are used as a proxy for the ELA, since moraines are only deposited below the ELA, where glacier flow is emerging (e.g. Benn and Evans, 2010).

Simulating the 1959-2010 evolution

The time-dependent simulations for the time period 1959–2010 were initialized with a steady state glacier geometry, and run both with coupled and uncoupled mass balance ice flow models (Fig. 13). The model simulates the observed volume changes well (Fig. 13). The simulations show a slight mass gain in the 1990s, which has also been observed as slight advances of the termini and gain in the glacier surface elevation in the accumulation area (Hannesdóttir and others, 2014a). The observed volume decrease from 2002 to 2010 is not entirely captured by the model, and this is especially noticeable for Heinabergsjökull. The difference between the observed and simulated volume in 2010 is 2.3 km^3 (or 9% of the observed 2010 volume). This is a larger difference than the 1.5% and 3.2%, for Skálafellsjökull and Fláajökull, respectively. There is a 1–2% difference in volume between the coupled and uncoupled simulations in these model runs; all glaciers experience greater volume loss in the coupled runs when the mass balance is computed on a lowering surface (Fig. 13 and Table 2). This emphasizes the importance of using coupled models for future simulations, when the glaciers will undergo increased surface lowering and retreat, as a result of a warmer climate.

DISCUSSION

The importance of using downscaled precipitation in the simulations

Skálafellsjökull, Heinabergsjökull and Fláajökull face the prevailing precipitation direction on the SE-coast and receive high amounts of precipitation, associated with the frequent passage of atmospheric fronts and lows. From model simulations it is evident that the precipitation is not adequately described by constant horizontal and vertical precipitation gradients. Orographically enhanced precipitation and snowdrift complicates the pattern of snow distribution in the accumulation area of the three outlet glaciers. For comparison, the variance of the winter mass balance of Langjökull was neither captured with constant precipitation gradients in mass balance simulations (Guðmundsson and others, 2009b). Guðmundsson and others (2009a) found discrepancies between modelled and observed winter balance at Langjökull and Hofsjökull (Fig. 1 for location), which they attributed to snowdrift.

The two new mass balance stakes (Skf01 and Fl01) confirm the modelled winter mass balance pattern of the LT-DP and WRF simulations. The good agreement between the modelled and measured winter balance during the one overlapping year (2010) on the three outlets (Figs. 10a and b) and between the MODIS derived and modelled ELA (Figs. 10c–f), indicates that the 1 km model resolution is adequate to simulate the precipitation distribution in the complex topography. The LT-DP has previously been found to be in good agreement with glacier mass balance measurements on Langjökull, Hofsjökull and Vatnajökull (Crochet and others, 2007). Downscaled precipitation from the RÁV dataset has previously been successfully used to estimate the measured winter mass balance of 2007–2012 in the accumulation area of Mýrdalsjökul ice cap (Ágústsson and others, 2013). The horizontal resolution of 3 km is sufficient to adequately simulate the atmospheric flow and the spatial structure of the precipitation field on the relatively flat ice cap. This may not be the case for the outlet glaciers of SE-Vatnajökull as they are in more complex terrain than the accumulation area of Mýrdalsjökull. The LT model of Crochet and others (2007) has a higher horizontal resolution than the RÁV data and may therefore perform better in those locations.

The higher resolution of the LT-model, may counterbalance its simplified parameterization of airflow and moisture physics compared to the more complex parameterizations employed in the lower resolution RÁV data.

The constant precipitation gradients may work better when simulating one outlet glacier, as Hoffellsjökull (with well constrained mass balance model), than modelling a group of outlets, separated by steep mountains, which influences the orographically enhanced precipitation. Also a wealth of data are available for Hoffellsjökull, which are not applicable for the outlet glaciers of this study. These include a denser network of mass balance measurements, glacier velocity fields from GPS surveys and satellite data, and energy balance measurements from automatic weather stations, which were used in the calibration of the mass balance model (Aðalgeirsdóttir and others, 2011).

Sensitivity of the outlet glaciers to climate perturbations

The importance of precipitation variations for the growth and presence of these outlet glaciers is clear when comparing the results of simulations forced with and without a change in the precipitation. For example a 1°C cooling versus a 1°C cooling and 20% less annual precipitation, relative to the baseline period 1980–2000, results in a 30–50% increase in ice volume versus a 10–18% increase, respectively (Table 6). To counterbalance a volume increase due to a 1°C cooling, the precipitation would need to decrease by ~40% (Table 6). This is similar to previous results of mass balance modelling studies where increases in precipitation of 20–50% and 30–40% respectively, were required to balance increased ablation due to temeprature rise in a variety of climate regimes (Oerlemans and others, 1998; Braithwaite and Raper, 2002). The average temperature at Hólar in Hornafjörður in the period 2000–2010 was 10.5°C, versus 9.6°C during the baseline period 1980–2000 (Table 3). A +1°C step change, relative to the period 1980–2000, results in a volume loss of 23–34%, whereas adding 10% of the annual precipitation to that warming, the glaciers would lose 7–8% less of their ice volume. However, simulations using the average temperature and precipitation of the period 2000–2010 results in volume loss of 7–12% (Table 6), less than the volume loss due to a 1°C warming relative to the baseline period. This implies that considerably more precipitation fell in the mountains and on the outlet glaciers of SE-Vatnajökull, even though a similar change is not seen at the lowland meteorological stations. However, recent experiments with numerical weather models indicate that changes in precipitation in the mountains are not necessarily correlated with changes in precipitation at the lowlands, implying that care must be taken when observed precipitation is extrapolated into complex topography (Ágústsson, 2014). Unfortunantly, as the mass balance measurements started in 1996, they have limited use in a further analysis of the baseline period.

The three outlets respond differently to warming and cooling scenarios (Fig. 11 and Table 6). Considerable deviations are observed between the modelled and observed surface profiles for Heinabergsjökull in most simulations (Fig. 9), whereas there is better agreement between modelled and observed surface profiles for the two other outlets. Heinabergsjökull is more sensitive to changes in temperature and precipitation; a cooling of 1°C results in a 50% increase in ice volume but only 30–35% for the other two neighbouring outlets. In general Heinabergsjökull´s increase or decrease in volume in response to changes in precipitation and/or temperature is nearly twofold that of Skálafellsjökull for example (Table 6). The hypsometry (area distribution with elevation) and bedrock topography of these outlets differs. Heinabergsjökull terminates in an overdeepened basin, where a large part of the bedrock is below sea level (Fig. 2a) and its terminus is at low elevation. The AAR of Skálafellsjökull is 0.68 (Table 1), which is close to 10% higher than the AAR of the other two outlets, and usually has a more positive winter balance (Figs. 3b and 10b). The proglacial lake of Heinabergsjökull probably affects the mass balance and enhances the ablation by melting and calving, as has been observed and calculated for Hoffellsjökull (see Aðalgeirsdóttir and others, 2011). This additional mass loss is not taken into account in the flow model, as no calving mechanism is included. The lake area has been estimated from an aerial image from 2002 (www.loftmyndir.is) and a LiDAR shaded relief from 2010, and has not increased in size during the 8 year long period. However, the surface topography of the terminus has changed in this time period, indicating that the tongue is now floating.

Future simulations

Our results from the steady state model simulations assuming a warming of 2°C together with a 10% increase in precipitation (relative to 1980–2000), indicate a >50% volume loss loss. A warming of 3°C would cause almost disappearance of the outlets, which is in line with previous studies (Aðalgeirsdóttir and others, 2006 and 2011). Very little difference is found between forcing the model with only higher temperatures or adding 10% to the annual precipitation, as the precipitation will fall as rain at higher temperatures. Previous glacier modelling studies project that downwasting of S-Vatnajökull will intensify during the coming decades, leading to its almost complete disappearance within the next 150–200 years (Aðalgeirsdóttir and others, 2006; 2011).

Small or negligible trends in the precipitation in Iceland have been observed on lowland meteorological stations since beginning of measurements (e.g. Hanna and others, 2004; Jóhannesson and others, 2007), but that may not neccessarily apply to the mountainous areas. Although trends or temporal variability in temperature can be reasonably extrapolated from lowland stations to other locations within the same region, including complex orography and to higher altitudes, the same is not true for precipitation. Results of model simulations of precipitation emphasize the limitation of precipitation observations in the lowlands as a proxy for precipitation in the mountains (Rögnvaldsson and others, 2007). In recent numerical simulations of a large orographic precipitation event in SE-Iceland, a change in air temperature of 2°C introduced dramatic changes in the spatial distribution of precipitation and in maximum precipitation amounts, compared to a control run (Ágústsson, 2014). These changes were most pronounced on the glaciers and the mountains, and only to a small degree, or even not at all seen, at many lowland locations, including where some of the meteorlogical stations in the region are found. Downscaled precipitation fields will be necessary for future simulations. Indeed, the WRF model has been used to scale down simulations of future climate in Iceland until 2050 (Thorsteinsson and Björnsson, 2012; Rögnvaldsson, 2013), that result should be considered for future simulations of the three studied oulets.

It would be worthwhile to simulate the known history of volume changes of the 3 outlets since the LIA maximum in the late 19th century to 1959, given that a distributed precipitation field for the period can be produced. It may be possible to extrapolate back in time the spatial structure of the precipitation field for certain periods for which the precipitation is well reproduced (1959–2010), based on correlations with precipitation observations from lowland meteorological stations since the late 19th century.

CONCLUSION

A numerical mass balance-ice flow model has been used to simulate the evolution of three outlet glaciers of SE-Vatnajökull. The history of area and volume changes 1890–2010 of the three outlet glaciers of SE-Vatnajökull (Hannesdóttir and others, 2014a) was used to constrain the model. For the first time downscaled precipitation is used in mass balance modelling of

Icelandic glaciers, obtained from an orographic precipitation model. The results indicate that the 1 km resolution of the LT model is adequate to simulate the precipitation fields on the glaciers, and demonstrate that downscaled precipitation data is necessary for mass balance modeling of glaciers in complex mountain topography. When forcing the mass balance model with constant horizontal and vertical precipitation gradients as has been done previously, the mass balance model does not successfully represent the winter mass balance variance in this area. Two new mass balance stakes were added to the survey network of Vatnajökull on Skálafellsjökull and Fláajökull, which show higher winter accumulation on the slopes south of the ice divide, than on the plateau, close to modelled winter precipitation maximum. Simulations of the three SE-outlets imply that their LIA maximum volume is reached with temperatures 1°C lower than the average of the 1980–2000 baseline period and a decrease in annual precipitation of 20%, which is in line with data from nearby meteorological stations outside the glaciers. Calculated sensitivity of annual balance to 1°C warming is on the order of –1.51 to –0.97 m w.e. a^{-1} (similar to results of Aðalgeirsdóttir and others, 2006) and +0.16 to +0.65 m w.e. a^{-1} for a 10% increase in precipitation. The calculated sensitivity to 1°C cooling is similar to a 40% increase in annual precipitation in the range of 1.06–1.47 m w.e. a^{-1}. Climate scenarios for Iceland predict a 2–3°C warming by 2100, and precipitation increase in the range of 0–10%. The model indicates that these changes will result in >50–80% decrease in ice volume, relative to the baseline period 1980–2000.

ACKNOWLEDGEMENTS

This work was funded by a doctoral grant of the Research Fund of the University of Iceland, the Icelandic Road Administration, SVALI Nordic Centre of Excellence, the University of Iceland Research Fund and the Directorate of Labour. We thank Trausti Jónsson at the Icelandic Meteorological Office for access to the temperature and precipitation records. The 2010 LiDAR DEM was acquired as a part of a collective effort of the Icelandic Meteorological Office and the Institute of Earth Sciences of the University of Iceland among others, to map the surface topography of Icelandic ice caps, initiated in the International Polar Year 2007–2009.

REFERENCES

Aðalgeirsdóttir, G., 2003: *Flow dynamics of Vatnajökull ice cap, Iceland*. PhD thesis. ETH Zurich, Zurich.

Aðalgeirsdóttir, G., Björnsson, H. and Jóhannesson, T., 2004. Vatnajökull ice cap, results of computations with a dynamical model coupled with a degree-day mass-balance model. Science Institute, University of Iceland, Reykjavík, 35.

Aðalgeirsdóttir, G., Guðmundsson, G.H. and Björnsson, H., 2000. The response of a glacier to a surface disturbance: a case study on Vatnajökull ice cap, Iceland. *Annals of Glaciology*, 31, 104-110.

Aðalgeirsdóttir, G., Guðmundsson, S., Björnsson, H., Pálsson, F., Jóhannesson, T., Hannesdóttir, H., Sigurðsson, S.P. and Berthier, E., 2011. Modelling the 20th and 21st century evolution of Hoffellsjökull glacier, SE-Vatnajökull, Iceland. *The Cryosphere*, 5, 961-975.doi 10.5194/tc-5-961-2011.

Aðalgeirsdóttir, G., Jóhannesson, T., Björnsson, H., Pálsson, F. and Sigurðsson, O., 2006. Response of Hofsjökull and southern Vatnajökull, Iceland, to climate change. *Journal of Geophysical Research-Earth Surface*, 111.doi:10.1029/2005JF000388.

Andreassen, L.M., Kjollmoen, B., Rasmussen, A., Melvold, K. and Nordli, O., 2012. Langfjordjokelen, a rapidly shrinking glacier in northern Norway. *Journal of Glaciology*, 58, 581-593.

Andreassen, L.M. and Oerlemans, J., 2009. Modelling Long-Term Summer and Winter Balances and the Climate Sensitivity of Storbreen, Norway. *Geografiska Annaler Series a-Physical Geography*, 91A, 233-251.

Auer, I., Bohm, R., Jurkovic, A., Lipa, W., Orlik, A., Potzmann, R., Schoner, W., Ungersbock, M., Matulla, C., Briffa, K., Jones, P., Efthymiadis, D., Brunetti, M., Nanni, T., Maugeri, M., Mercalli, L., Mestre, O., Moisselin, J.M., Begert, M., Muller-Westermeier, G., Kveton, V., Bochnicek, O., Stastny, P., Lapin, M., Szalai, S., Szentimrey, T., Cegnar, T., Dolinar, M., Gajic-Capka, M., Zaninovic, K., Majstorovic, Z. and Nieplova, E., 2007. HISTALP - historical instrumental climatological surface time series of the Greater Alpine Region. *International Journal of Climatology*, 27, 17-46.doi: 10.1002/joc.1377.

Ágústsson, H., 2014. Kortlagning úrkomu við Öræfajökul. Report. Belgingur, Institute for Meteorological Research, Reykjavík, 68.

Ágústsson, H., Hannesdóttir, H., Thorsteinsson, T., Pálsson, B. and Oddsson, B., 2013. Mass balance of Mýrdalsjökull ice cap accumulation area and comparison of observed winter balance with simulated precipitation. *Jökull*, 63, 91-104.

Benn, D. and Evans, D.J.A., 2010. *Glaciers and Glaciations*, 2nd ed. Routledge, New York.

Björnsson, H., Pálsson, F. and Haraldsson, H.H., 2002. Mass balance of Vatnajökull (1991-2001) and Langjökull (1996-2001), Iceland. *Jökull*, 51, 75-78.

Björnsson, H. and Pálsson, F., 2008. Icelandic glaciers. *Jökull*, 58, 365-386.

Björnsson, H., Pálsson, F., Guðmundsson, S., Magnússon, E., Aðalgeirsdóttir, G., Jóhannesson, T., Berthier, E., Sigurðsson, O. and Thorsteinsson, T., 2013. Contribution of Icelandic ice caps to sea level rise: Trends and variability since the Little Ice Age. *Geophysical Research Letters*, 40, 1546-1550.doi 10.1002/Grl.50278.

Braithwaite, R.J. and Zhang, Y., 2000. Sensitivity of mass balance of five Swiss glaciers to temperature changes assessed by tuning a degree-day model. *Journal of Glaciology*, 46, 7-14.

Braithwaite, R.J. and Raper, S.C.B., 2002. Glaciers and their contribution to sea level change. *Physics and Chemistry of the Earth*, 27, 1445-1454.

Crochet, P., 2007. A study of regional precipitation trends in Iceland using a high-quality gauge network and ERA-40. *Journal of Climate*, 20, 4659-4677.doi 10.1175/Jcli4255.1.

Crochet, P., 2013. Gridding daily precipitation with an enhanced two-step spatial interpolation method. IMO Technical report PC/2013-01. Icelandic Meteorological Office, Reykjavík, 26.

Crochet, P., Jóhannesson, T., Jónsson, T., Sigurðsson, O., Björnsson, H., Pálsson, F. and Barstad, I., 2007. Estimating the spatial distribution of precipitation in Iceland using a linear model of orographic precipitation. *Journal of Hydrometeorology*, 8, 1285-1306.doi: 10.1175/2007JHM795.1.

Cuffey, K.M. and Paterson, W.S.B., 2010. *The Physics of Glaciers*, 4th edition ed. Elsevier, Burlington.

De Woul, M. and Hock, R., 2005. Static mass-balance sensitivity of Arctic glaciers and ice caps using a degree-day approach. *Annals of Glaciology, Vol 42, 2005*, 42, 217-224.doi 10.3189/172756405781813096.

Einarsson, M.Á., 1984. Climate of Iceland In: van Loon, H. (Ed.), *Climates of the Oceans*. Elsevier, Amsterdam. 673-697.

Engelhardt, M., Schuler, T.V. and Andreassen, L.M., 2012. Evaluation of Gridded Precipitation for Norway Using Glacier Mass-Balance Measurements. *Geografiska Annaler Series a-Physical Geography*, 94A, 501-509.doi 10.1111/j.1468-0459.2012.00473.x.

Flowers, G.E., Björnsson, H., Geirsdóttir, Á., Miller, G.H. and Clarke, G.K.C., 2007. Glacier fluctuation and inferred climatology of Langjokull ice cap through the Little Ice Age. *Quaternary Science Reviews*, 26, 2337-2353.doi:10.1016/j.quascirev.2007.07.016.

Flowers, G.E., Marshall, S.J., Björnsson, H. and Clarke, G.K.C., 2005. Sensitivity of Vatnajökull ice cap hydrology and dynamics to climate warming over the next 2 centuries. *Journal of Geophysical Research*, 110.doi:10.1029/2004JF000200.

Guðmundsson, M.T., Thordarson, T., Höskuldsson, A., Larsen, G., Björnsson, H., Prata, F.J., Oddsson, B., Magnússon, E., Högnadóttir, T., Petersen, G.N., Hayward, C.L., Stevenson, J.A. and Jónsdóttir, I., 2012. Ash generation and distribution from the April-May 2010 eruption of Eyjafjallajokull, Iceland. *Scientific Reports*, 2

Guðmundsson, S., Björnsson, H., Jóhannesson, T., Aðalgeirsdóttir, G., Pálsson, F. and Sigurðsson, O., 2009a. Similarities and differences in the response to climate warming of two ice caps in Iceland. *Hydrology Research*, 40, 495-502.doi 10.2166/Nh.2009.210.

Guðmundsson, S., Björnsson, H., Magnússon, E., Berthier, E., Pálsson, F., Guðmundsson, M.T., Högnadottir, T. and Dall, J., 2011. Response of Eyjafjallajokull, Torfajokull and Tindfjallajokull ice caps in Iceland to regional warming, deduced by remote sensing. *Polar Research*, 30.doi 10.3402/Polar.V30i0.7282.

Guðmundsson, S., Björnsson, H., Pálsson, F. and Haraldsson, H.H., 2003. Physical energy balance and degree-day models of summer ablation on Langjökull ice cap, SW-Iceland. Technical Report RH-20-2003. Science Institute, University of Iceland, Reykjavík, 20

Guðmundsson, S., Pálsson, F., Björnsson, H. and Haraldsson, H.H., 2009b. Comparison of energy balance and degree-day models of summer ablation on the Langjökull ice cap, SW-Iceland. *Jökull*, 59, 1-18.

Hanna, E., Jonsson, T. and Box, J.E., 2004. An analysis of icelandic climate since the nineteenth century. *International Journal of Climatology*, 24, 1193-1210.

Hannesdóttir, H., Björnsson, H., Pálsson, F., Aðalgeirsdóttir, G. and Guðmundsson, S., 2014a. Area, volume and mass changes of southeast Vatnajökull ice cap, Iceland, from the Little Ice Age maximum in the late 19th century to 2010. *The Cryosphere Discussion*, 8, 1-55.doi:10.5194/tcd-8-1-2014.

Hannesdóttir, H., Björnsson, H., Pálsson, F., Aðalgeirsdóttir, G. and Guðmundsson, S., 2014b. Variations of southeast Vatnajökull ice cap (Iceland) 1650-1900 and reconstruction of the Little Ice Extent. *Geografiska Annaler*.doi:10.1111/geoa.12064.

Hindmarsh, R.C.A., 2004. A numerical comparison of approximations to the Stokes equations used in ice sheet and glacier modeling. *Journal of Geophysical Research-Earth Surface*, 109.doi:10.1029/2003JF000065.

Hock, R., 2005. Glacier melt: a review of processes and their modelling. *Progress in Physical Geography*, 29, 362-391.

Huss, M., Bauder, A., Funk, M. and Hock, R., 2008. Determination of the seasonal mass balance of four Alpine glaciers since 1865. *Journal of Geophysical Research-Earth Surface*, 113.doi 10.1029/2007jf000803.

Huss, M., Hock, R., Bauder, A. and Funk, M., 2012. Conventional versus reference-surface mass balance. *Journal of Glaciology*, 58, 278-286.doi 10.3189/2012jog11j216.

Icelandic Meteorological Office and Institute of Earth Sciences, U.o.I., 2013. DEMs of Icelandic glaciers (dataset).

Jarosch, A.H., Anslow, F.S. and Clarke, G.K.C., 2012. High-resolution precipitation and temperature downscaling for glacier models. *Climate Dynamics*, 38, 391-409.doi 10.1007/s00382-010-0949-1.

Jóhannesson, T., 1997. The response of two Icelandic glaciers to climatic warming computed with a degree-day glacier mass-balance model coupled to a dynamic glacier model. *Journal of Glaciology*, 43, 321-327.

Jóhannesson, T., Aðalgeirsdóttir, G., Björnsson, H., Crochet, P., Elíasson, E.B., Ólafsson, H., Pálsson, F., Rögnvaldsson, Ó., Sigurðsson, O., Snorrason, Á., Blöndal Sveinsson, Ó.G. and Þorsteinsson, Þ., 2007. Effect of climate change on hydrology and hydro-resources in Iceland. National Energy Authority - Hydrological Service, Reykjavík, 91.

Jóhannesson, T., Björnsson, H., Magnússon, E., Guðmundsson, S., Pálsson, F., Sigurðsson, O., Thorsteinsson, T. and Berthier, E., 2013. Ice-volume changes, bias estimation of mass-balance measurements and changes in subglacial lakes derived by lidar mapping of the surface of Icelandic glaciers. *Annals of Glaciology*, 54, 63-74.doi 10.3189/2013aog63a422.

Jóhannesson, T., Sigurdsson, O., Laumann, T. and Kennett, M., 1995. Degree-Day Glacier Mass-Balance Modeling with Applications to Glaciers in Iceland, Norway and Greenland. *Journal of Glaciology*, 41, 345-358.

Laumann, T. and Reeh, N., 1993. Sensitivity to climate change of the mass balance of glaciers in southern Norway. *Journal of Glaciology*, 39, 656-665.

Le Meur, E., Gagliardini, O., Zwinger, T. and Ruokolainen, J., 2004. Glacier flow modelling: a comparison of the Shallow Ice Approximation and the full-Stokes solution. *Comptes Rendus Physique*, 5, 709-722.doi:10.1016/j.crhy.2004.10.001.

Leysinger Vieli, G.J.M.C. and Gudmundsson, G.H., 2004. On estimating length fluctuations of glaciers caused by changes in climatic forcing. *Journal of Geophysical Research*, 109.doi: 10.1029/2003JF000027.

Lüthi, M.P., 2009. Transient response of idealized glaciers to climate variations. *Journal of Glaciology*, 55, 918-930.

Machguth, H., Paul, F., Kotlarski, S. and Hoelzle, M., 2009. Calculating distributed glacier mass balance for the Swiss Alps from regional climate model output: A methodical description and interpretation of the results. *Journal of Geophysical Research-Atmospheres*, 114.doi: 10.1029/2009JD011775.

Magnússon, E., Pálsson, F., Björnsson, H. and Guðmundsson, S., 2012. Removing the ice cap of Öraefajokull central volcano, SE-Iceland: Mapping and interpretation of bedrock topography, ice volumes, subglacial troughs and implications for hazards assessments. *Jökull*, 62, 131-150.

Marshall, S.J., Bjornsson, H., Flowers, G.E. and Clarke, G.K.C., 2005. Simulation of Vatnajokull ice cap dynamics. *Journal of Geophysical Research-Earth Surface*, 110. doi:10.1029/2004JF000262.

Marzeion, B., Hofer, M., Jarosch, A.H., Kaser, G. and Molg, T., 2012. A minimal model for reconstructing interannual mass balance variability of glaciers in the European Alps. *Cryosphere*, 6, 71-84.

Nawri, N. and Björnsson, H., 2010. Surface air temperature and precipitation trends for Iceland in the 21st century. Icelandic Meteorological Office, Reykjavík, 42.

Oerlemans, J., 2008. *Minimal Glacier Models*. Igitur, Utrecht University.

Oerlemans, J., Anderson, B., Hubbard, A., Huybrechts, P., Johannesson, T., Knap, W.H., Schmeits, M., Stroeven, A.P., van de Wal, R.S.W., Wallinga, J. and Zuo, Z., 1998. Modelling the response of glaciers to climate warming. *Climate Dynamics*, 14, 267-274.

Ólafsson, H., Furger, M. and Brummer, B., 2007. The weather and climate of Iceland. *Meteorologische Zeitschrift*, 16, 5-8.doi 10.1127/0941-2948/2007/0185.

Paterson, W.S.B., 1994. *The Physics of Glaciers*. Butterworth-Heinemann, Oxford.

Paul, F. and Kotlarski, S., 2010. Forcing a Distributed Glacier Mass Balance Model with the Regional Climate Model REMO. Part II: Downscaling Strategy and Results for Two Swiss Glaciers. *Journal of Climate*, 23, 1607-1620.doi: 10.1175/2009JCLI3345.1.

Pálsson, F., Guðmundsson, S., Björnsson, H., Berthier, E., Magnússon, E., Guðmundsson, S. and Haraldsson, H.H., 2012. Mass and volume changes of Langjökull ice cap, Iceland, similar to 1890 to 2009, deduced from old maps, satellite images and in situ mass balance measurements. *Jökull*, 62, 81-96.

Radic, V., Bliss, A., Beedlow, A.C., Hock, R., Miles, E. and Cogley, J.G., 2014. Regional and global projections of twenty-first century glacier mass changes in response to climate scenarios from global climate models. *Climate Dynamics*, 42, 37-58.doi 10.1007/s00382-013-1719-7.

Rasmussen, S.O., Andrews, J.T. and Conway, H., 2007. Reconstruction of mass balance of glaciers in southern Norway back to 1948. *Annals of Glaciology*, 46, 255-260.

Rögnvaldsson, L., Crochet, P. and Ólafsson, H., 2004. Mapping of precipitation in Iceland using numerical simulations and statistical modeling. *Meteorologische Zeitschrift*, 13, 209-219.doi:10.1127/0941-2948/2004/0013-0209.

Rögnvaldsson, Ó., Ágústsson, H. and Ólafsson, H., 2011. Aflræn niðurkvörðun veðurs innan LOKS verkefnisins. Technical report. Reiknistofa í veðurfræði.

Rögnvaldsson, Ó., Jónsdóttir, J.F. and Ólafsson, H., 2007. Numerical simulations of precipitation in the complex terrain of Iceland- Comparison with glaciological and hydrological data. *Meterologische Zeitschrift* 16, 71-85.doi: 10.1127/0941-2948/2007/0181.

Rögnvaldsson, Ó., 2013: *Numerical simulations of winds and precipitation in Iceland*. PhD thesis. University of Bergen, Bergen.

Sigurðsson, F., 1990. Vandamál við úrkomumælingar á Íslandi In: Sigbjarnarson, G. (Ed.), *Vatnið og landið. Vatnafræðiráðstefna, október 1987*. Orkustofnun, Reykjavík. 101-110.

Sigurðsson, O., 2005. Variations of termini of glaciers in Iceland in recent centuries and their connection with climate. In: Caseldine, C., A. Russell, O. Knudsen and J. Harðardóttir: (Ed.), *Iceland-Modern Processes and Past Environments*. Elsevier, Amsterdam. 241-256.

Sigurðsson, O., 2014. Sporðamælingar haustið 2013, Newsletter of the Icelandic Glaciological Society. The Icelandic Glaciological Society, Reykjavík, 5-6.

Skamarock, W.C., Klemp, J.B., Dudhia, J., Gill, D.O., Barker, D.M., Duda, M.G., Huang, X.Y., Wang, W. and Powers, J.G., 2008. A description of the Advanced Research WRF version 3 Tech. Rep. NCAR/TN-475+STR. National center for atmospheric research.

Smith, R.B., 2003. A linear upslope-time-delay model for orographic precipitation. *Journal of Hydrology*, 282, 2-9.

Smith, W.H.F. and Wessel, P., 1990. Gridding with continuous curvature splines in tension. *Geophysics*, 55, 293-305.

Stahl, K., Moore, R.D., Floyer, J.A., Asplin, M.G. and McKendry, I.G., 2006. Comparison of approaches for spatial interpolation of daily air temperature in a large region with complex topography and highly variable station density. *Agricultural and Forest Meteorology*, 139, 224-236.doi: 10.1016/j.agrformet.2006.07.004.

Thorsteinsson, T. and Björnsson, H.(editors), 2012. Climate Change and Energy Systems: Impacts, Risks and Adaptation in the Nordic and Baltic countries. Nordic Council of Ministers, Copenhagen.

van Pelt, W.J.J., Oerlemans, J., Reijmer, C.H., Pohjola, V.A., Pettersson, R. and van Angelen, J.H., 2012. Simulating melt, runoff and refreezing on Nordenskioldbreen, Svalbard, using a coupled snow and energy balance model. *Cryosphere*, 6, 641-659.doi:10.5194/tc-6-641-2012.

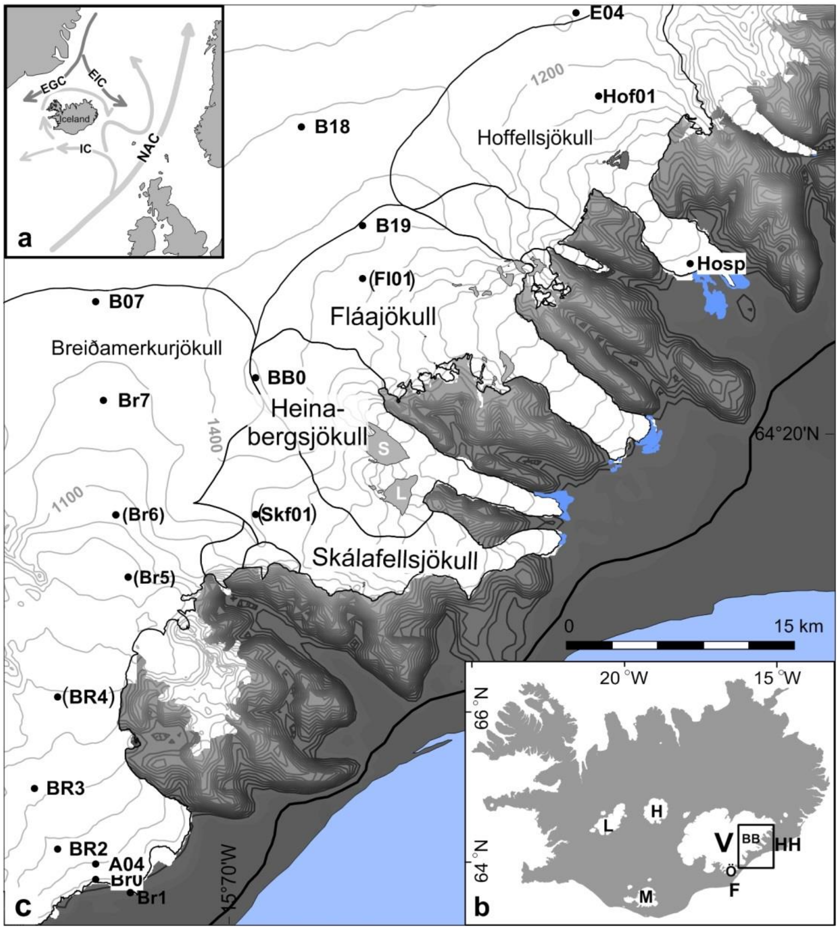

Figure 1. (a) Iceland in the North Atlantic Ocean and major ocean surface currents; East Greenland Current (EGC), East Iceland Current (EIC), Irminger Current (IC) and North Atlantic Current (NAC). (b) Iceland and the larger ice caps; Vatnajökull (V), Langjökull (L), Hofsjökull (H), Mýrdalsjökull (M). Öræfajökull (Ö), the plateau of Breiðabunga (BB) and the locations of the meteorological stations at Fagurhólsmýri (F) and Hólar in Hornafjörður (HH). The box outlines (c) eastern Breiðamerkurjökull, Skálafellsjökull, Heinabergsjökull, Fláajökull, and Hoffellsjökull. The surface topography is from the 2010 LiDAR DEM with 100 m contour lines shown in gray, and ice divides in black. The locations of mass balance stakes are indicated by black dots, stakes that are not used for the calibration of the mass balance model are in parenthesis. Nunataks are shown in light gray, including Snjófjall (S) and Litlafell (L) in Heinabergsjökull. Proglacial lakes are shown in blue and the road delineated in black.

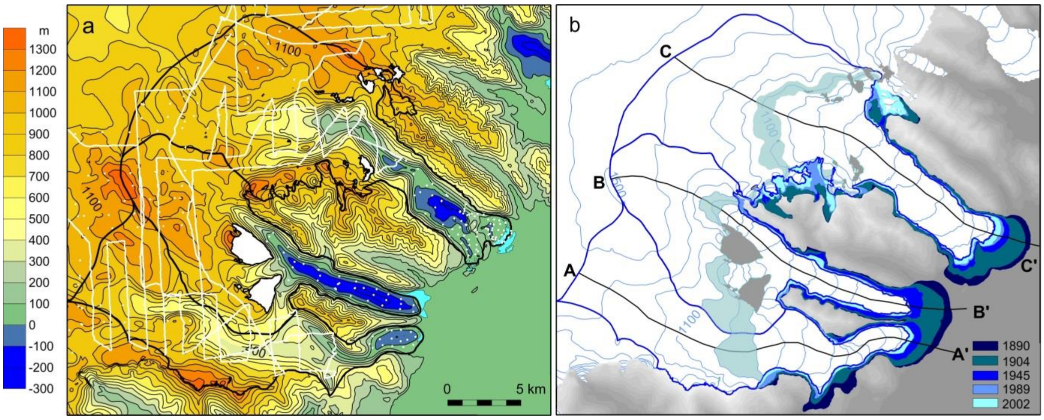

Figure 2. (a) The bedrock topography derived from radio echo sounding measurements (shown with white lines and dots) of Skálafellsjökull, Heinabergsjökull and Fláajökull. Glacier margin in 2000 is shown. Proglacial lakes are shown with light blue colour and nunataks with white. (b) The surface topography from the 2010 LiDAR DEM shown with 100 m contour lines and glacier outlines at different times from Hannesdóttir and others (2014a). The location of the MODIS derived snowline in the period 2007–2011 is shown with light blue colour.

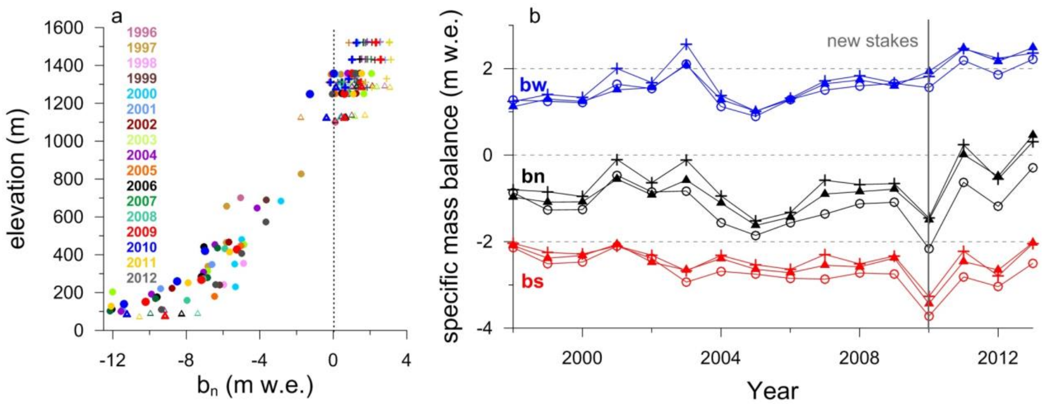

Figure 3. (a) The annual mass balance (b_n) measured at stakes on Breiðamerkurjökull (circles), Skálafellsjökull and Fláajökull (crosses) and Hoffellsjökull (triangles) in the period 1996–2012. (b) Specific winter (b_w, blue), summer (b_s, red) and net balance (b_n, black) for Skálafellsjökull (triangles), Heinabergsjökull (circles) and Fláajökull (crosses) for the period 1996–2013. New mass balance stakes were added to the network in 2009 (the timing is shown with a vertical line).

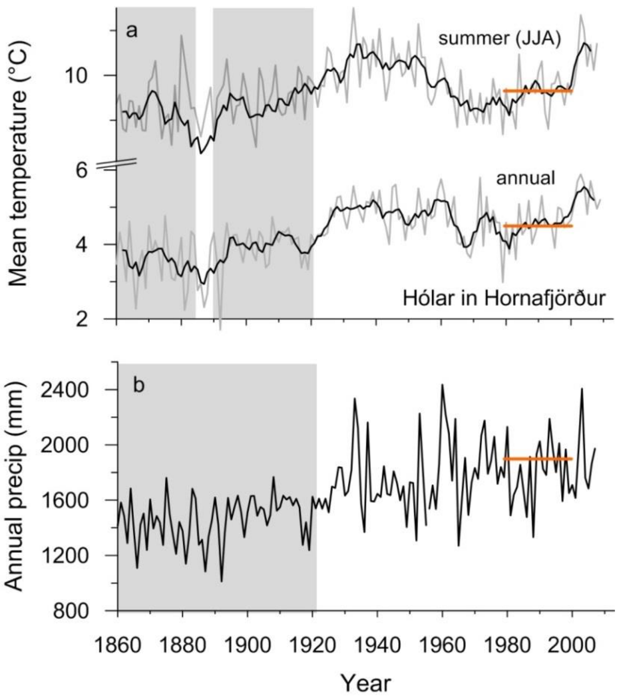

Figure 4. (a) Mean summer (June–August) and annual temperature (gray lines) at Hólar in Hornafjörður and 5 year running average (black lines). (b) Annual precipitation at Fagurhólsmýri. Gray boxes indicate the time period of reconstructed temperature and precipitation (for details see Aðalgeirsdóttir and others, 2011). The baseline period 1980–2000 used for reference in the computations is shown with orange lines.

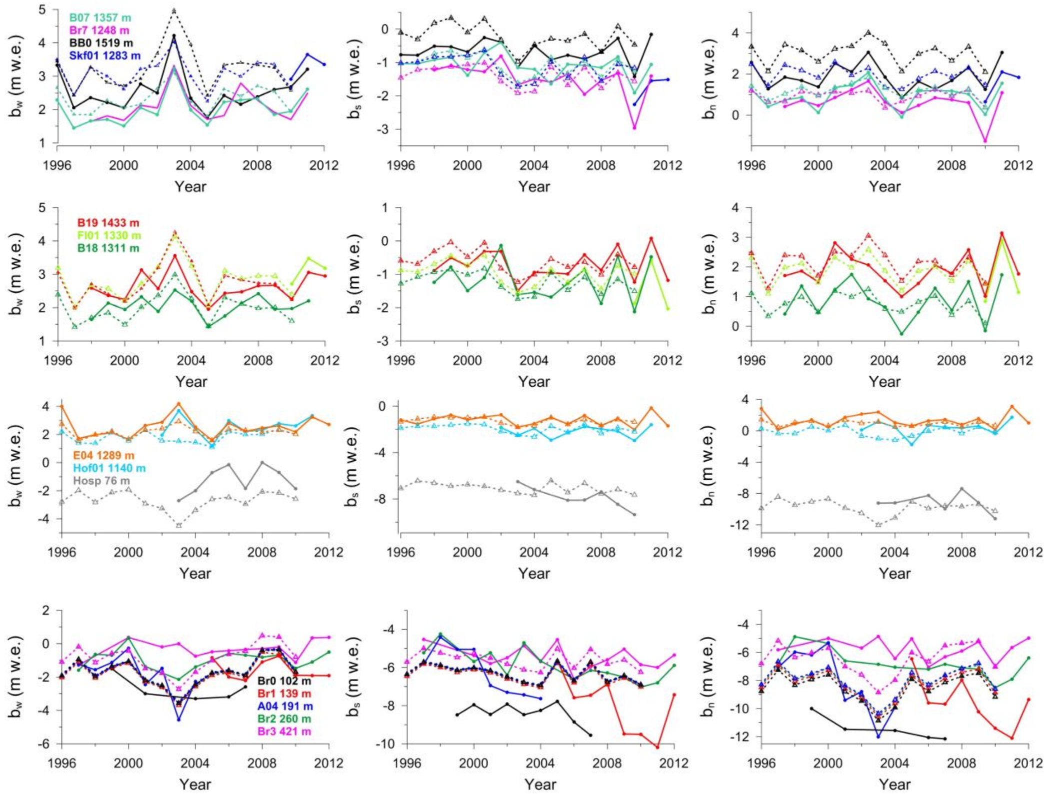

Figure 5. Comparison of measured (solid lines) and modelled (using LT-DP and best fitting ddf, ddf_i= 5.5 mm w.e. C^{-1} d^{-1} and ddf_s=3.7 mm w.e. C^{-1} d^{-1}, dotted line) winter mass balance (b_w, left column), summer mass balance (b_s, middle column), and annual mass balance (b_n, right column) in m w.e. for the period 1996–2010 for individual stakes (location is shown in Fig 1). The legend shows the elevation of each stake in 2010, or in the year of the last measurement.

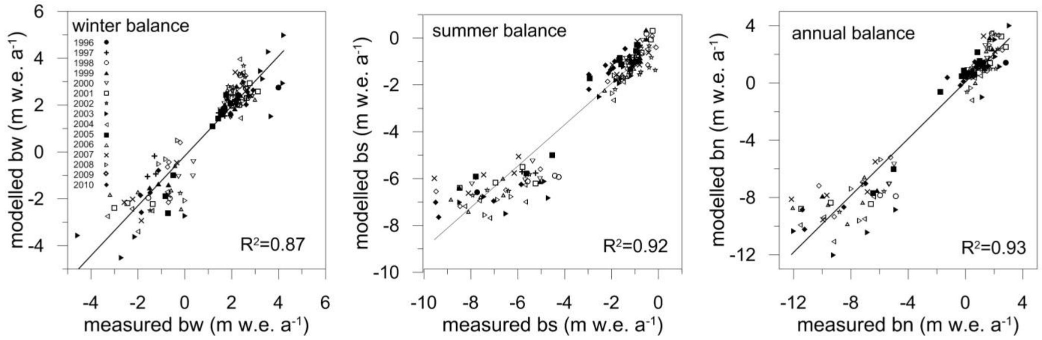

Figure 6. Measured vs. modelled (using LT-DP and ddf_i= 5.5 mm w.e. C^{-1} d^{-1} and ddf_s=3.7 mm w.e. C^{-1} d^{-1}) winter, summer and annual net balance of SE-Vatnajökull in the period 1996–2010. The linear relationship is shown and the R^2 value indicates the linear regression coefficient.

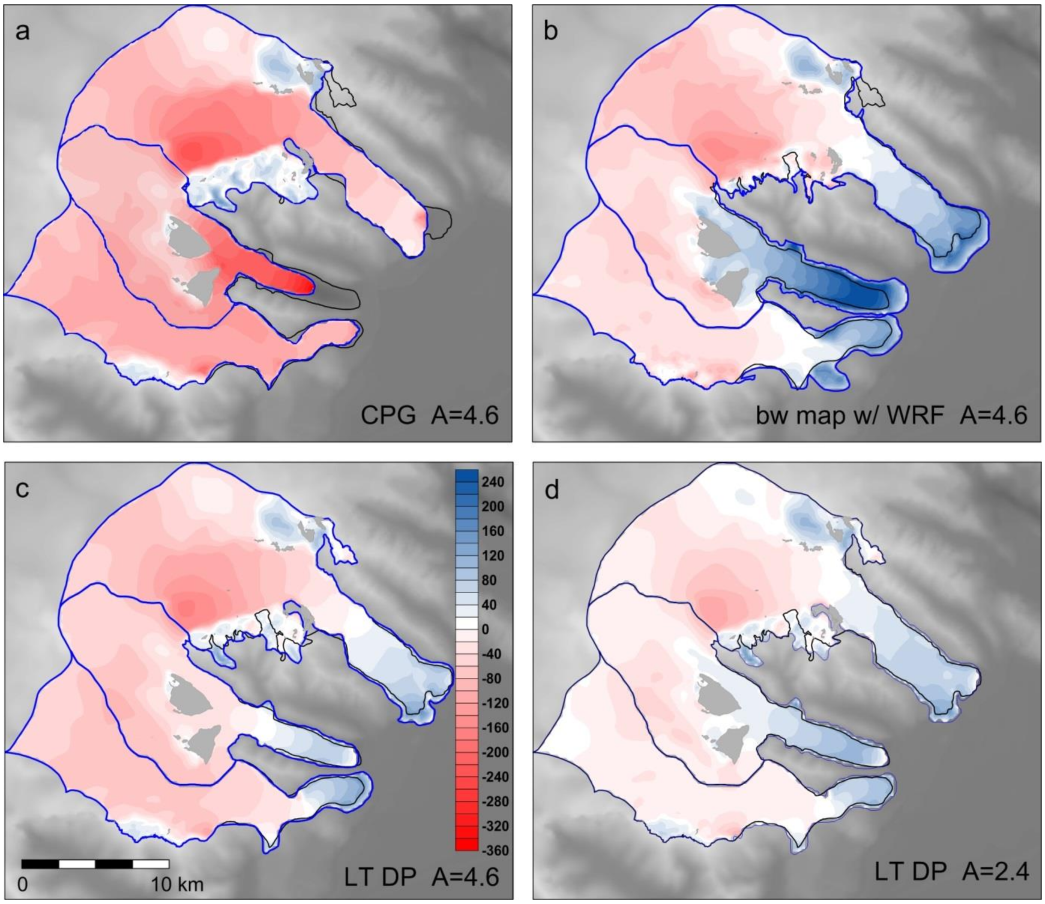

Figure 7. The elevation difference between the initial measured and the final simulated glacier surface using constant temperature and precipitation forcing of the baseline period 1980–2000. (a) The mass balance model using a constant precipitation gradient (CPG). (b) Interpolated mean winter mass balance grid for the period 1996–2006 revised with the downscaled winter precipitation from the WRF model (c) and (d) mass balance model using downscaled precipitation from the LT model (LT-DP). In the simulations in figures (a) – (c) a rate factor of A=4.6 $\times 10^{-15}$ s^{-1} kPa^{-3} is used in the flow model and the simulation shown in (d) a rate factor A=2.4 $\times 10^{-15}$ s^{-1} kPa^{-3} is applied.

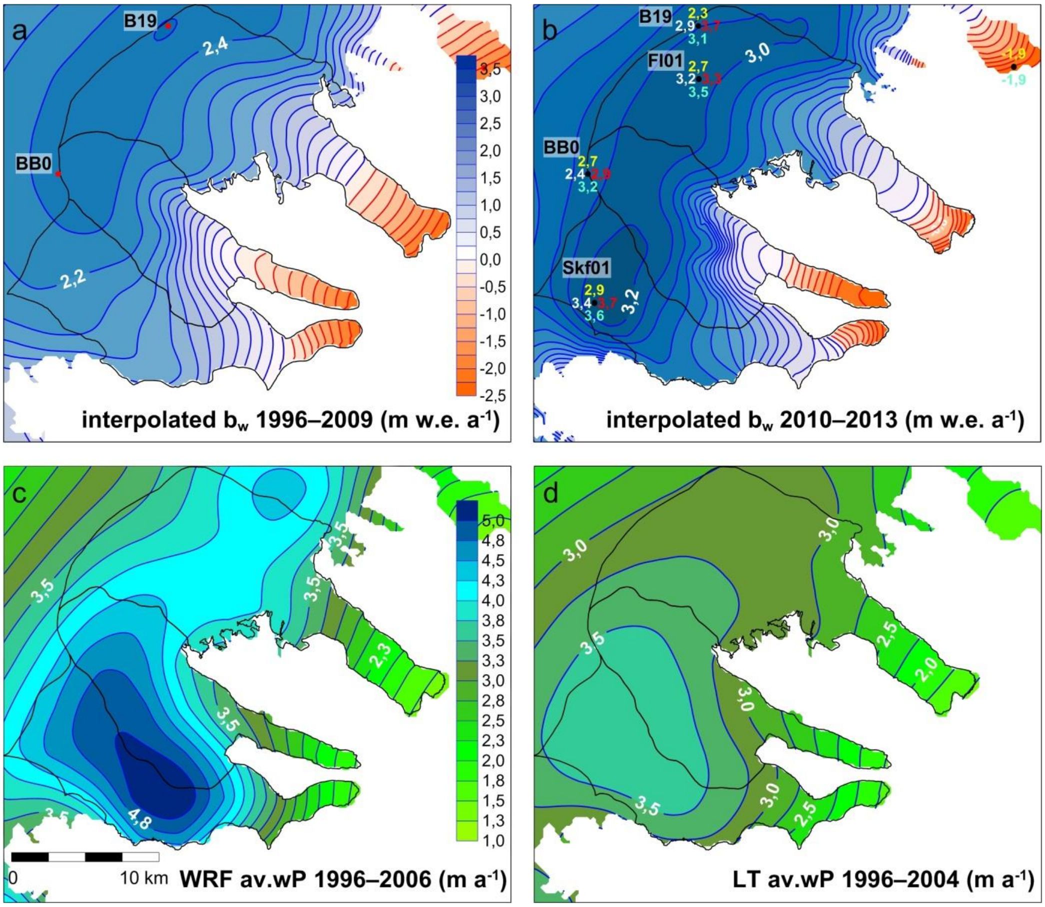

Figure 8. (a) Manually interpolated average winter balance (b_w) maps for the period 1996–2009, based on in situ measurements, (b) for the period 2010–2013, when stakes Skf01 and Fl01 have been added to the mass balance network. The measurements of the individual years are shown by each stake; 2010 (yellow), 2011 (turquoise), 2012 (white), 2013 (red). (c) Average winter precipitation (av.wP) in the period 1996–2006 simulated with the WRF-model. (d) Average winter precipitation in the period 1996–2004 simulated with the LT-model.

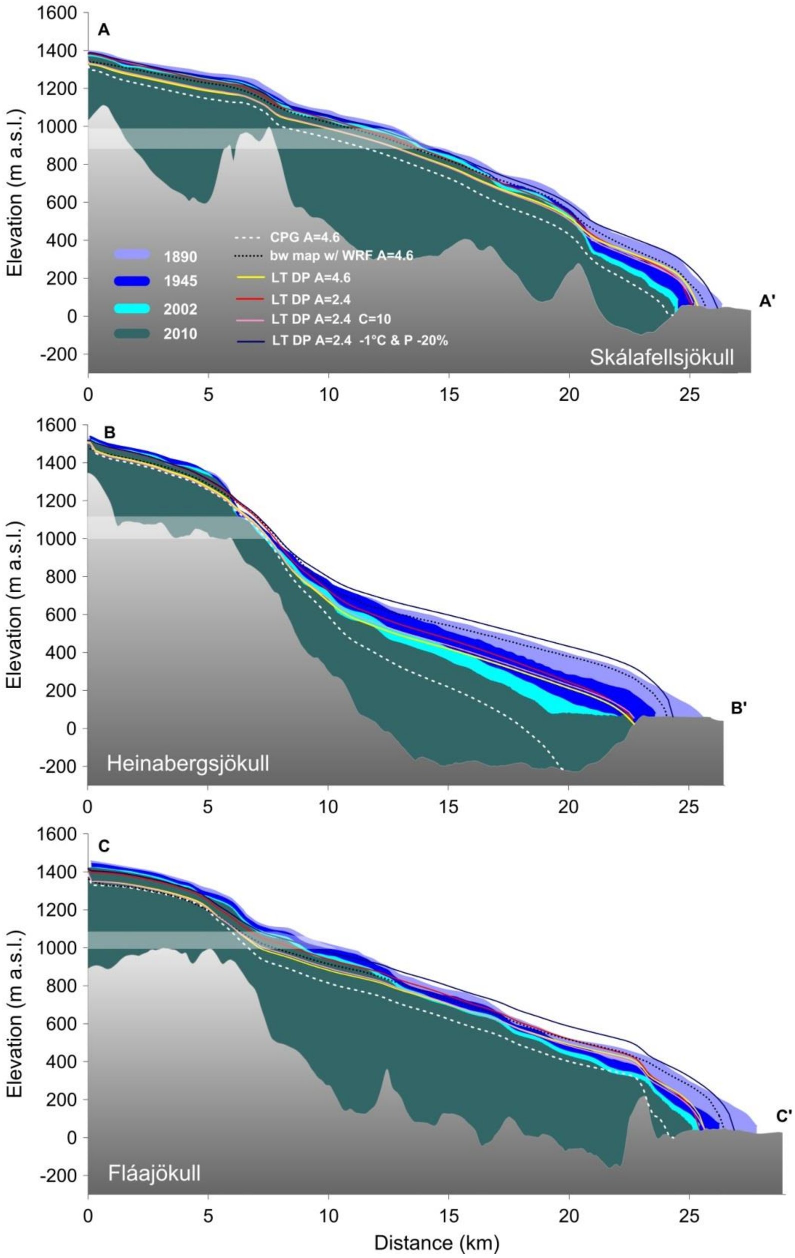

Figure 9. Longitudinal profiles (locations shown in Fig. 2b) showing the glacier thickness and extent af different times according to observations (solids, from Hannesdóttir and others, 2014a) and the various simulations (lines) using constant temperature and precipitation forcing (average of the baseline period 1980–2000), except the dark blue surface profile (–1°C and –20% precipitation). Two different rate factors applied ($A=4.6\times10^{-15}$ s^{-1} kPa^{-3} and $A=2.4\times10^{-15}$ s^{-1} kPa^{-3}). Three different precipitation distributions are applied; CPG=constant precipitation gradient, winter mass balance (b_w) map revised with downscaled precipitation from the WRF-model, and LT-DP. The white shaded horizontal bands indicate the elevation range of the snowline, derived from the MODIS images.

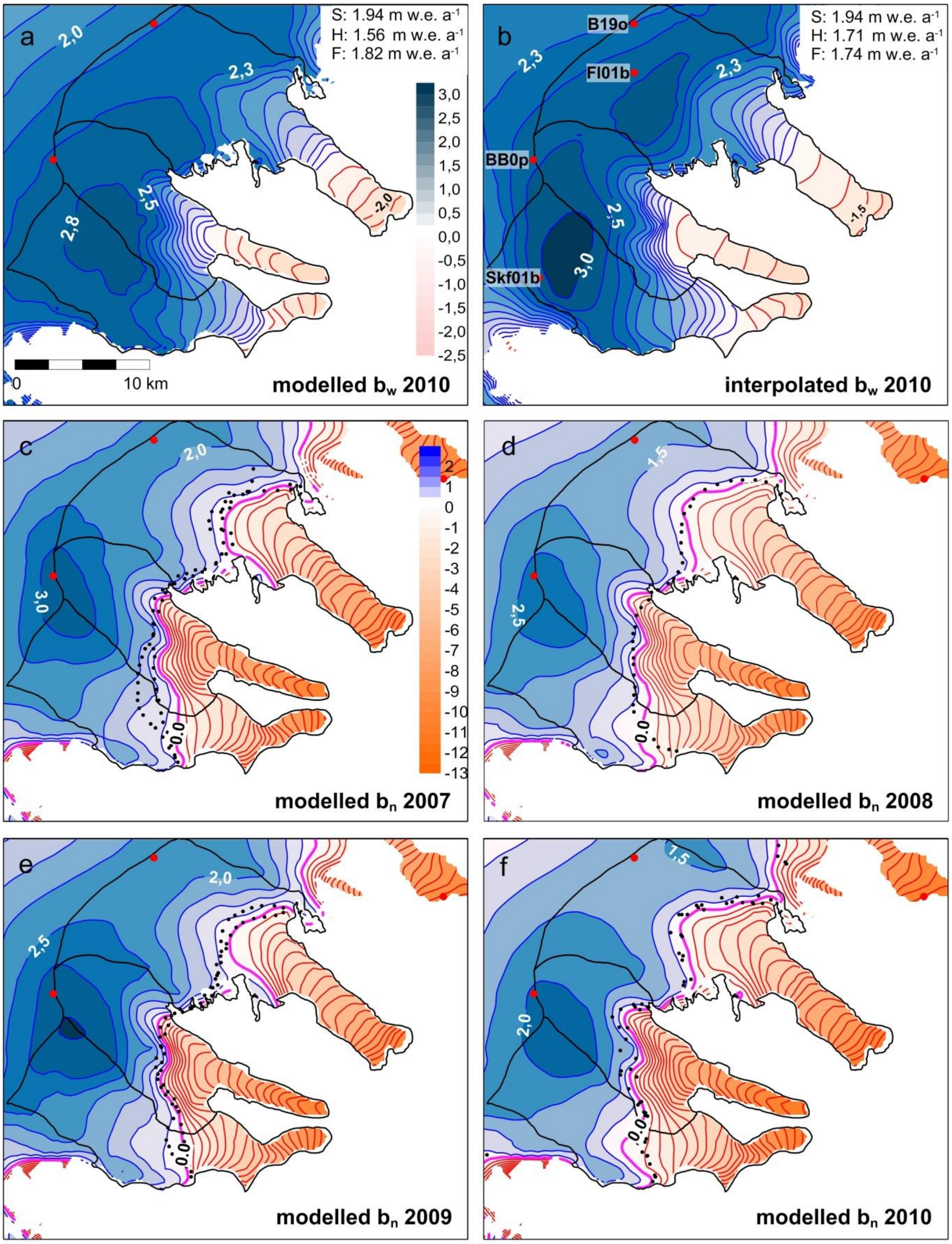

Figure 10. The winter mass balance (b_w) in 2010 (a) modelled using LT-DP and (b) manually interpolated b_w (based on in situ measurements) in m w.e. a^{-1}. The specific winter balance is shown for each glacier, Skálafellsjökull (S), Heinabergsjökull (H), Fláajökull (F) in (a) and (b). (c–f) Modelled net balance (b_n) in m w.e. a^{-1} in 2007, 2008, 2009, 2010, and the ELA (b_n=0) drawn in pink. The MODIS end of summer snowline (a proxy for the ELA), is shown with black dots (from Hannesdóttir and others, 2014a).

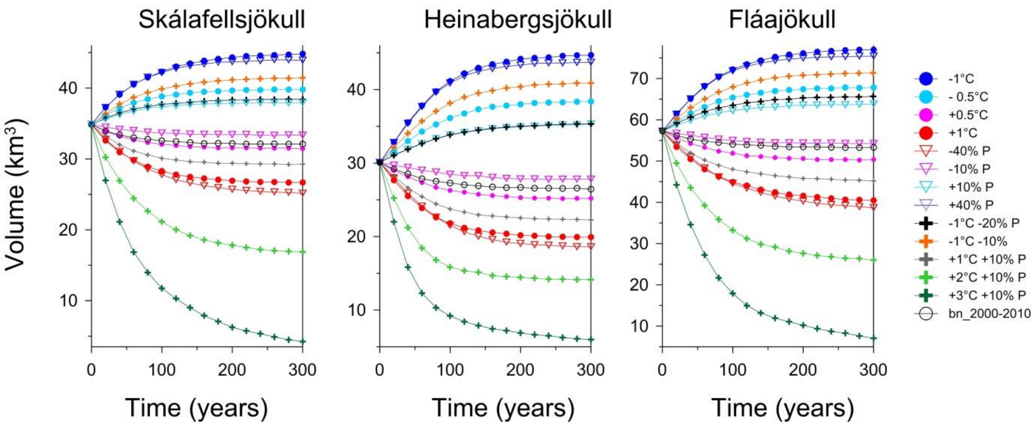

Figure 11. Volume evolution due to step changes in temperature (filled circles) and precipitation (triangles) and temperature+precipitation (crosses) changes relative to the baseline period of 1980–2000, starting with the simulated steady state surface aquired using $A=2.4 \times 10^{-15}\ s^{-1}\ kPa^{-3}$ and average temperature and precipitation of the period 1980–2000 (see also Table 6).

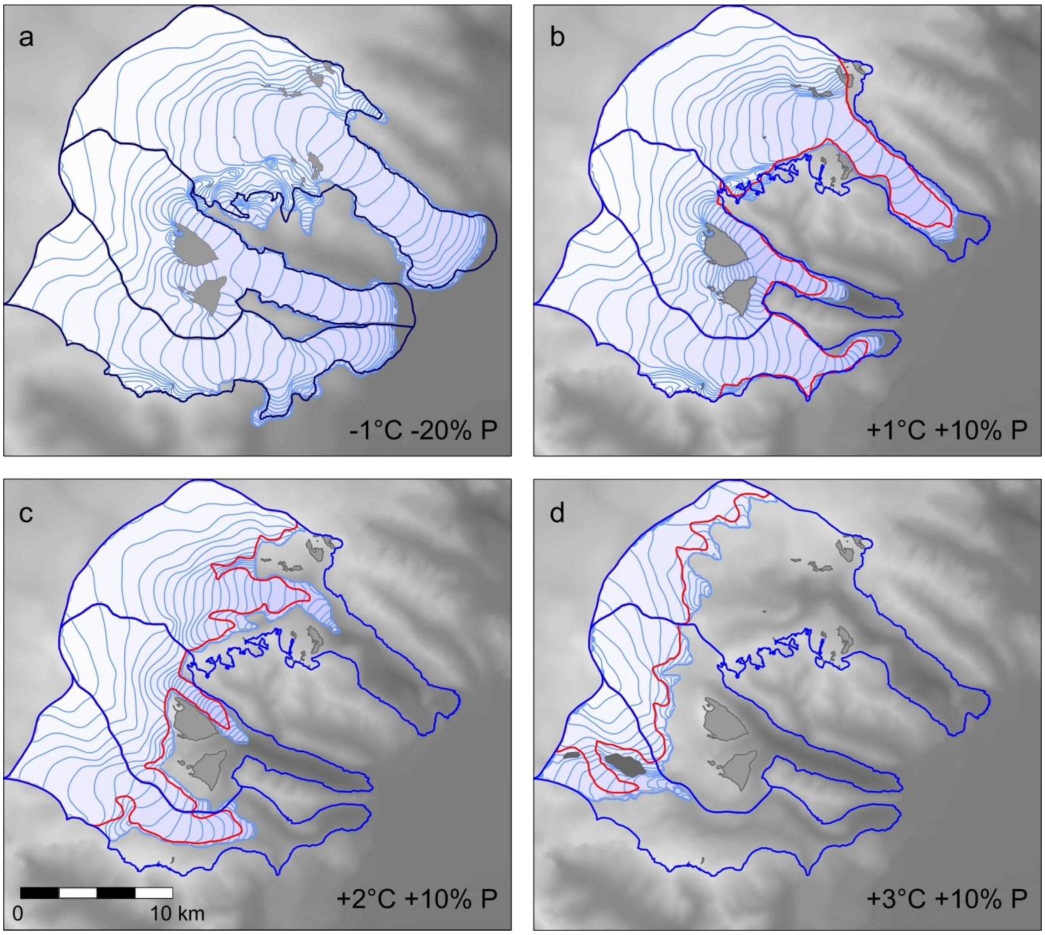

Figure 12. (a) The simulated LIA glacier geometry obtained with a constant 1°C cooling and 20% decrease in annual precipitation, relative to the baseline period 1980–2000, and the reconstructed LIA extent in dark blue (Hannesdóttir and others, 2014b). (b) – (d) The glacier geometry at the end of simulations forced with 10% step increase in annual precipitation and step increase in temperature (b) 1°C (c) 2°C (d) 3°C, relative to the baseline period. The red glacier margin is the result of simulations without any change in annual precipitation, only increase in the temperature, and the LiDAR margin of 2010 is shown with blue colour.

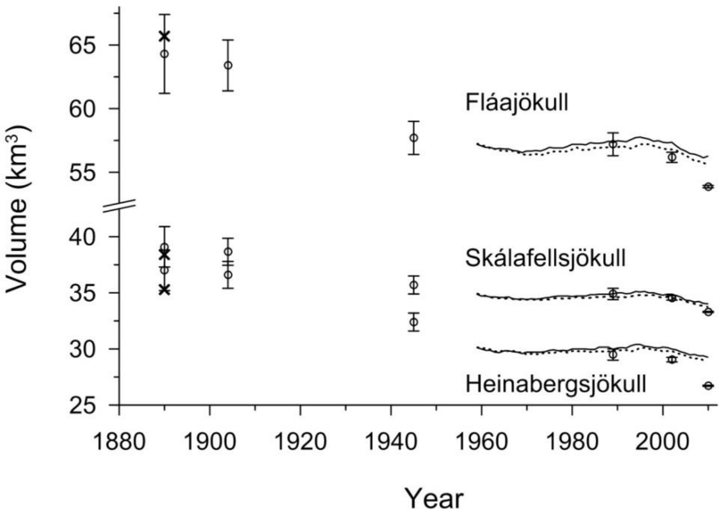

Figure 13. The volume evolution of the time-dependent simulations, from coupled (dotted lines) and uncoupled (solid lines) runs using the temperature from Hólar in Hornafjörður and LT-DP during the time period 1959–2010. The observed volumes of 1890, 1904, 1945, 1989, 2002 and 2010 are shown with open circles (from Hannesdóttir and others, 2014a). The simulated volume of 1890 is shown with x, assuming that temperatures were 1°C colder than during the baseline period 1980–2000 and the annual precipitation 20% less (see Fig. 12a for glacier extent).

Table 1. Characteristics of the three outlet glaciers in year 2010, and Hoffellsjökull for comparison.

glacier	ice divide (m a.s.l.)	volume (km^3)	area (km^2)	mean thickness (m)	AAR_{2010} (%)	snowline range 2007─2011 (m)	glacier length (km)	glacier slope (°)
Skálafellsjökull	1490	33.3	100.6	331	0.68	910─1020	24.4	3.1
Heinabergsjökull	1490	26.7	99.7	268	0.61	990─1100	22.7	3.7
Fláajökull	1480	53.9	169.8	317	0.59	1060─1120	25.1	3.1
Hoffellsjökull*	1280	54.3	206.0	264	0.63	1050─1120	23.6	3.4

* from (Aðalgeirsdóttir and others, 2011)

Table 2. Observed area (A, in km^2) and volume (V, in km^3) (from Hannesdóttir and others, 2014a) and simulated (using temperature from Hólar and LT-DP). Uncoupled/coupled simulated area and volume in 1989, 2002 and 2010 is presented (see Fig. 13).

Observed A	A_{1890}	A_{1904}	A_{1945}	A_{1989}	A_{2002}	A_{2010}
Skálafellsjökull	117.9±1.6	116.4±1.2	106.6±0.7	104.0±0.7	102.8±0.3	100.6±0.1
Heinabergsjökull	120.3±1.3	118.2±1.0	109.0±0.6	102.5±0.6	101.8±0.3	99.7±0.1
Fláajökull	205.6±1.9	202.1±1.4	184.1±1.0	181.9±0.9	177.4±0.5	169.8±0.2

Observed V	V_{1890}	V_{1904}	V_{1945}	V_{1989}	V_{2002}	V_{2010}
Skálafellsjökull	39.1±1.8	38.7±1.2	36.3±0.8	35.2±0.5	34.9±0.2	33.3±0.05
Heinabergsjökull	37.0±1.8	36.6±1.2	34.7±0.8	29.7±0.5	29.3±0.2	26.7±0.05
Fláajökull	64.4±3.1	63.5±2.0	57.1±1.3	57.4±0.9	56.5±0.4	53.9±0.09

Simulated A	A_{1890} (─1°C ─10%P)	A_{1890} (─1°C ─15%P)	A_{1890} (─1°C ─20%P)	A_{1989}	A_{2002}	A_{2010}
Skálafellsjökull	122.7	119.5	115.6	104.6/104.7	104.6/104.5	104.6/104.2
Heinabergsjökull	123.0	120.2	116.2	101.8/101.7	101.9/101.6	101.1/100.7
Fláajökull	223.2	217.5	210.5	181.5/181.8	181.2/180.9	180.7/180.0

Simulated V	V_{1890} (─1°C ─10%P)	V_{1890} (─1°C ─15%P)	V_{1890} (─1°C ─20%P)	V_{1989}	V_{2002}	V_{2010}
Skálafellsjökull	41.4	40.0	38.4	34.9/34.7	34.9/34.6	34.0/33.8
Heinabergsjökull	40.9	38.8	35.3	30.0/29.9	30.0/29.8	29.3/29.0
Fláajökull	71.3	68.5	65.7	57.3/57.0	57.4/56.8	56.3/55.6

Table 3. Mean summer (JJA) temperature (T) at Hólar in Hornafjörður and annual precipitation (P) at Fagurhólsmýri averaged over the respective time periods. The precipitation and temperature during the time priod 1860–1890 is estimated by Aðalgeirsdóttir and others (2011).

period	summer T	annual T	P (annual)
1860-1890	~8.5°C	3.5°C	~1.43 m
1884-1890	8.5°C	3.3°C	
1926-1936	10.3°C	5.0°C	2.00 m
1980-2000	9.6°C	4.5°C	1.79 m
2000-2010	10.5°C	5.3°C	1.90 m

Table 4. Degree–day factors for snow and ice used in mass balance modelling studies on Vatnajökull, determined by minimizing RMS between observed and modelled mass balance

glaciers	ddf_s (mm w.e. C^{-1} d^{-1})	ddf_i (mm w.e. C^{-1} d^{-1})	reference
S-Vatnajökull	4.5	5.3	Aðalgeirsdóttir and others, 2006
Hoffellsjökull	4.0	5.3	Aðalgeirsdóttir and others, 2011
Breiðabunga outlets	3.7	5.5	this study

Table 5. The % difference between the volume and area at the start and end of simulations using the mass balance model with constant precipitation gradient (CPG), the winter mass balance (b_w) revised with downscaled precipitation data from the WRF-model and the mass balance model using LT-DP, with rate factors between A=4.6×10^{-15} s^{-1} kPa^{-3} and A=2.4×10^{-15} s^{-1} kPa^{-3}, and including basal sliding (C=10×10^{-15} ma^{-1} P^{-3}).Constant temperature and precipitation forcing applied, the average of the baseline period 1980–2000, and starting with the smoothed 2000 glacier surface DEM. See also Figs. 7 and 9.

Glacier/mass balance model	Volume	Area
Fláajökull CPG (A=4.6)	–22%	0%
Fláajökull b_w w/WRF (A=4.6)	–7%	5%
Fláajökull LT-DP (A=4.6)	–11%	3%
Fláajökull LT-DP (A=3.5)	–7%	3%
Fláajökull LT-DP (A=3.0)	–4%	3%
Fláajökull LT-DP (A=2.4)	1%	3%
Fláajökull LT-DP (A=2.4 and C=10)	–12%	4%
Skálafellsjökull CPG (A=4.6)	–23%	-5%
Skálafellsjökull b_w w/WRF (A=4.6)	–2%	9%
Skálafellsjökull LT-DP (A=4.6)	–11%	3%
Skálafellsjökull LT-DP (A=3.5)	–7%	2%
Skálafellsjökull LT-DP (A=3.0)	–4%	2%
Skálafellsjökull LT-DP (A=2.4)	0%	2%
Skálafellsjökull LT-DP (A=2.4 and C=10)	–12%	2%
Heinabergsjökull CPG (A=4.6)	–29%	-10%
Heinabergsjökull b_w w/WRF (A=4.6)	10%	14%
Heinabergsjökull LT-DP (A=4.6)	–12%	1%
Heinabergsjökull LT-DP (A=3.5)	–7%	2%
Heinabergsjökull LT-DP (A=3.0)	–3%	2%
Heinabergsjökull LT-DP (A=2.4)	2%	3%
Heinabergsjökull LT-DP (A=2.4 and C=10)	–11%	2%

Table 6. The mass balance sensitivity of the three outlet glaciers to given deviations from the climate of the baseline period 1980–2000 (first 3 columns). The % difference between the volume (middle columns) and area (last 3 columns) at the start and end of steady state simulations, using step changes in temperature and precipitation, relative to the average of the baseline period. The last line shows the results of using the average precipitation and temperature of the period 2000–2010.

	b_n sensitivity (m w.e. a^{-1})			ΔVolume (%)			ΔArea (%)		
forcing	Skála	Heina	Fláa	Skála	Heina	Fláa	Skála	Heina	Fláa
–1°C	1.47	1.04	1.10	29	49	35	25	25	30
–0.5°C	0.95	0.46	0.55	14	28	19	10	15	17
+0.5°C	–0.30	–0.80	–0.61	-9	–16	–12	–5	–9	–9
+1°C	–0.97	–1.51	–1.29	–23	–34	–29	–12	–21	–18
+2°C	–2.59	–3.07	–2.82	–59	–59	–62	–34	–39	–36
+3°C	–4.34	–4.79	–4.54	–92	–85	–92	–60	–61	–59
P +40%	1.45	0.98	1.06	26	46	28	19	22	24
P +10%	0.65	0.16	0.27	9	18	12	6	8	10
P -10%	0.01	–0.45	–0.27	–4	–7	–5	–2	–4	–2
P -40%	–0.86	–1.29	–1.07	–28	–38	–32	–12	–22	–18
+0.5°C P+10%	–0.01	–0.50	–0.33	–3	–6	–4	–2	–4	–3
+1°C P+10%	–0.70	–1.23	–1.01	–16	–26	–21	–9	–16	–14
+2°C P+10%	–2.27	–2.78	–2.50	–51	–53	–55	–29	–35	–31
+3°C P+10%	–4.05	–4.52	–4.29	–88	–80	–88	–52	–56	–55
–1°C P-10%	1.17	0.71	0.78	19	36	25	17	20	23
–1°C P-15%	0.98	0.54	0.63	15	29	20	14	17	21
–1°C P-20%	0.81	0.35	0.47	10	18	15	10	13	16
b_n 2000-2010	–0.26	–0.68	–0.49	–8	–12	–7	–5	–7	–6